

1 STEPHANIE OSLER HASTINGS, Bar No. 186716
2 MACKENZIE W. CARLSON, Bar No. 323850
3 BROWNSTEIN HYATT FARBER SCHRECK, LLP
4 1021 Anacapa Street, 2nd Floor
5 Santa Barbara, California 93101
6 Telephone: 805.963.7000
7 Email: SHastings@bhfs.com; Mcarlson@bhfs.com

8 Attorneys for Plaintiff
9 GOLDEN STATE WATER COMPANY

10
11 SUPERIOR COURT OF THE STATE OF CALIFORNIA
12 COUNTY OF RIVERSIDE

13 Coordination Proceeding Special Title
14 (Cal. Rules of Court, rule 3.550)
15 MOJAVE BASIN AREA WATER CASES

JCCP NO.: 5265

Lead Case No. CIV 208568

Assigned for All Purposes to the
Honorable Harold W. Hopp, Dept. 1

Honorable Craig G. Reimer, Judge Presiding
by assignment of the Chief Justice

**GOLDEN STATE WATER
COMPANY'S EVIDENCE IN SUPPORT
OF MOTION TO ENFORCE
JUDGMENT – VOLUME 3
(Pages GSWC 0801 - GSWC 0987)**

16
17 CITY OF BARSTOW, et al.,
18 Plaintiff,

19 v.

20 CITY OF ADELANTO, et al.,
21 Defendant.

Date: October 2, 2024
Time: 8:30 am
Dept.: 1
Judge: Hon. Craig G. Reimer

Reservation ID: 562595011427

1
2
3
4
5
6
7
8
9
10
11
12
13
14
15
16
17
18
19
20
21
22
23
24
25
26
27
28

INDEX OF EXHIBITS

EXHIBIT	DESCRIPTION	PAGE(S)
1.	aquilogic, Inc., Expert Report of Anthony Brown, Hydrologic Conditions and Water Flow Between the Alto Subarea and the Centro Subarea of the Mojave Basin, San Bernardino County, California (Sep. 5, 2024)	GSWC 0001 – GSWC 0161
Court Orders		
2.	Order (1) Discharging Order to Show Cause Why the FPA of Alto Should Not Be Reduced by Another 4.5% of BAP, (2) Reducing the FPA in Alto by Another 0.1 % of BAP, and (3) Directing the Watermaster to Re-Evaluate PSY for the Entire Basin, <i>City of Barstow v. City of Adelanto</i> , Riverside Sup. Ct. Case No. CIV208568 (Sep. 16, 2022)	GSWC 0162 – GSWC 0171
3.	Ruling on the Watermaster’s Annual Motion to Adjust Free Production Allowance for Water Year 2024–2025, <i>City of Barstow v. City of Adelanto</i> , Riverside Sup. Ct. Case No. CIV208568 (Jul. 3, 2024)	GSWC 0172 – GSWC 0184
Watermaster Reports, Studies, and Presentations		
4.	Wagner & Bonsignore, Consulting Civil Engineers, Production Safe Yield & Consumptive Use Update (Feb. 28, 2024).	GSWC 0185 - GSWC 0292
5.	Watermaster, Thirtieth Annual Report of the Mojave Basin Area Watermaster, Water Year 2022–23 (May 1, 2024) https://www.mojavewater.org/wp-content/uploads/2024/04/30AR2223.pdf .	GSWC 0293 - GSWC 0484
6.	Watermaster, Thirtieth Annual Report of The Mojave Basin Area Watermaster Water Year 2022–23, Appendix L (May 1, 2024) https://www.mojavewater.org/wp-content/uploads/2024/04/30AppL2223.pdf .	GSWC 0485 - GSWC 0837
General Hydrologic Resources		
7.	Cha, M., Li, M., Wang, X. (2020). Estimation of Seasonal Evapotranspiration for Crops in Arid Regions Using Multisource Remote Sensing Images. July 21. https://doi.org/10.3390/rs12152398 .	GSWC 0838 - GSWC 0859
8.	Gleason, C.J. and Durand, M.T., Remote Sensing of River Discharge: A Review and a Framing for the Discipline, Remote Sensing Vol. 12, No. 1107 (Mar. 31, 2020) https://doi.org/10.3390/rs12071107 .	GSWC 0860 – GSWC 0888
9.	Masafu, C., Williams, R., and Hurst, M.D., Satellite Video Remote Sensing for Estimation of River Discharge, Geophysical Research Letters, 50, e2023GL105839 (Mar. 31, 2020) https://doi.org/10.1029/2023GL105839 .	GSWC 0889 - GSWC 0900

30883973.2

10.	Conaway, J., Eggleston, J., Legleiter, C.J., Jones, J.W., Kinzel, P.J., Fulton, J.W., Remote Sensing of Streamflow in Alaska Rivers—New Technology to Improve Safety and Expand Coverage of USGS Streamgaging, U.S. Geological Survey Fact Sheet 2019–3024. (Apr. 2019) https://doi.org/10.3133/fs20193024 .	GSWC 0901 – GSWC 0905
11.	Holmes, T.R.H. (2019). Chapter 5 – Remote sensing techniques for estimating evapotranspiration. In: Extreme Hydroclimatic Events and Multivariate Hazards in a Changing Environment. June 6. https://ntrs.nasa.gov/api/citations/20210011848/downloads/26861.pdf	GSWC 0906 - GSWC 0921
12.	Kustas, W.P., Norman, J.M. (2009). Use of remote sensing for evapotranspiration monitoring over land surfaces. December 24. https://doi.org/10.1080/02626669609491522	GSWC 0922 - GSWC 0945
Correspondence		
13.	Brownstein Hyatt Farber Schreck, LLP corresp. To Watermaster, Agenda Item 7 - Comments on Watermaster’s Production Safe Yield Update (REVISED) (Feb. 28, 2024).	GSWC 0946 – GSWC 0965
14.	Brownstein Hyatt Farber Schreck, LLP corresp. to Watermaster, Agenda Items 7 & 9 - Comments on Watermaster’s Production Safe Yield Update (February 2024), proposed recommendation for Free Production Allowance for Water Year 2024–25, Watermaster Annual Report for Water Year 2022-23 (Mar. 27, 2024).	GSWC 0966 – GSWC 0968
15.	Wagner & Bonsignore, Consulting Civil Engineers memo to Mojave Basin Area Watermaster Attorney, Response to comments on Transition Zone Water Balance memorandum, dated February 28, 2024 (Apr. 12, 2024).	GSWC 0969 - GSWC 0985
Data		
16.	Golden State Water Company Centro Well Data, available at https://bhfs.sharefile.com/share/view/sc4bbae97dcb44d288d59e7da82922368	GSWC 0986 - GSWC 0987

Dated: September 5, 2024

BROWNSTEIN HYATT FARBER
SCHRECK, LLP

By: 

Stephanie Osler Hastings
Mackenzie W. Carlson

Attorneys for Plaintiff
GOLDEN STATE WATER COMPANY

**TABLE 9
MOJAVE BASIN AREA
FACILITY TRANSFERS REPORTED TO WATERMASTER
OCTOBER 1, 1993 THROUGH SEPTEMBER 30, 2023**

TRANSFER NUMBER	TRANSFEROR	TRANSFeree	STATE WELL NUMBER	DATE OF CHANGE	SUBAREA
186	ROGERS, ROY - ORO GRANDE RANCH	ELISABELLA, LLC	07N/05W-36R05	06/26/02	ALTO
186	ROGERS, ROY - ORO GRANDE RANCH	ELISABELLA, LLC	07N/05W-36R07	06/26/02	ALTO
187	WEBER, F. R. & JUNELL	SAWYERS MOTOR SPORTS GROUP	09N/04E-20D02	06/26/02	BAJA
189	ROGERS, ROY	GABRYCH, EUGENE	04N/01W-02A01	07/24/02	ESTE
189	ROGERS, ROY	GABRYCH, EUGENE	04N/01W-02B01	07/24/02	ESTE
189	ROGERS, ROY	GABRYCH, EUGENE	04N/01W-02F01	07/24/02	ESTE
189	ROGERS, ROY	GABRYCH, EUGENE	04N/01W-02H01	07/24/02	ESTE
189	ROGERS, ROY	GABRYCH, EUGENE	04N/01W-02J01	07/24/02	ESTE
189	ROGERS, ROY	GABRYCH, EUGENE	04N/01W-02P01	07/24/02	ESTE
189	ROGERS, ROY	GABRYCH, EUGENE	04N/01W-02R04	07/24/02	ESTE
189	ROGERS, ROY	GABRYCH, EUGENE	04N/01W-03H01	07/24/02	ESTE
190	BARSTOW, CITY OF	ODESSA WATER DISTRICT	09N/02W-19G01	08/28/02	CENTRO
190	BARSTOW, CITY OF	ODESSA WATER DISTRICT	09N/02W-19P01	08/28/02	CENTRO
190	BARSTOW, CITY OF	ODESSA WATER DISTRICT	09N/02W-19P02	08/28/02	CENTRO
191	DALJO CORPORATION	RUBSCH FAMILY TRUST, G. A. & M. A.	09N/04E-31J01	08/28/02	BAJA
191	DALJO CORPORATION	RUBSCH FAMILY TRUST, G. A. & M. A.	09N/04E-31J02	08/28/02	BAJA
194	ARROWHEAD SERVICE CORPORATION	KEMPER, WALTER R. & JONNA S.	10N/01W-32F01	09/25/02	CENTRO
194	ARROWHEAD SERVICE CORPORATION	KEMPER, WALTER R. & JONNA S.	10N/01W-32F12	09/25/02	CENTRO
196	DURAN, FRANK T. & DURAN, GLENDA K.	EYGNOR, ROBERT E. & PATSY C.	08N/04W-14M01	09/25/02	CENTRO
196	DURAN, FRANK T. & DURAN, GLENDA K.	EYGNOR, ROBERT E. & PATSY C.	08N/04W-15R03	09/25/02	CENTRO
197	HILARIDES, FRANK	CDFG - CAMP CADY	10N/03E-27K01	09/25/02	BAJA
197	HILARIDES, FRANK	CDFG - CAMP CADY	10N/03E-27Q01	09/25/02	BAJA
198	HOLLIDAY, FREDRICK	BROWN, JENNIFER	04N/04W-13K01	09/25/02	ALTO
198	HOLLIDAY, FREDRICK	BROWN, JENNIFER	04N/04W-13K02	09/25/02	ALTO
198	HOLLIDAY, FREDRICK	BROWN, JENNIFER	04N/04W-13K04	09/25/02	ALTO

**TABLE 9
MOJAVE BASIN AREA
FACILITY TRANSFERS REPORTED TO WATERMASTER
OCTOBER 1, 1993 THROUGH SEPTEMBER 30, 2023**

TRANSFER NUMBER	TRANSFEROR	TRANSFeree	STATE WELL NUMBER	DATE OF CHANGE	SUBAREA
199	KIM, ET AL.	JO, MYUNG HYUN	04N/02E-17J02	09/25/02	ESTE
200	MITCHELL, CHARLOTTE	MITCHELL, CHARLES THOMAS	09N/02E-03F02	09/25/02	BAJA
201	SANFORD, WILBUR CLARENCE	BROOKLIER, NANCY L.	07N/05W-25G04	09/25/02	ALTO
201	SANFORD, WILBUR CLARENCE	BROOKLIER, NANCY L.	07N/05W-25G09	09/25/02	ALTO
202	VANNI, MIKE	WESTLAND INDUSTRIES, INC.	05N/03W-35P01	09/25/02	ALTO
202	VANNI, MIKE	WESTLAND INDUSTRIES, INC.	05N/03W-35P02	09/25/02	ALTO
204	PARKER, GEORGE R.	RIGGS, JOHN H. & MILLICENT L.	09N/04E-32D01	10/23/02	BAJA
204	PARKER, GEORGE R.	RIGGS, JOHN H. & MILLICENT L.	09N/04E-32E01	10/23/02	BAJA
205	PITTS, JOE & STELLA	CALLAHAN, BERNERD J.	09N/03E-08P02	10/23/02	BAJA
205	PITTS, JOE & STELLA	CALLAHAN, BERNERD J.	09N/03E-08P03	10/23/02	BAJA
206	SOUTHDOWN CALIFORNIA CEMENT, L.L.C.	SERVICE ROCK PRODUCTS CORPORATION	06N/04W-33N06	10/23/02	ALTO
209	BODINE, ET AL.	PEARCE, CRAIG L.	08N/04E-07E01	01/22/03	BAJA
209	BODINE, ET AL.	PEARCE, CRAIG L.	08N/04E-07E03	01/22/03	BAJA
210	CARTER, JOHN THOMAS	DE JONG FAMILY TRUST	09N/03E-17A02	01/22/03	BAJA
211	HAIGH, WHILLDYN & MARGARET	LEM, HOY	09N/03E-26H03	01/22/03	BAJA
211	HAIGH, WHILLDYN & MARGARET	LEM, HOY	09N/03E-26H04	01/22/03	BAJA
213/214	OROPEZA, JOSE M. & CONCEPCION	KIM, JIN S. & HYUN H.	09N/03W-28A02	01/22/03	CENTRO
213/214	OROPEZA, JOSE M. & CONCEPCION	KIM, JIN S. & HYUN H.	09N/03W-28A03	01/22/03	CENTRO
215	STEIMLE FAMILY TRUST, A.B. & Y.O.	BENDER, MARLENE	11N/03E-33M01	01/22/03	BAJA
216	STEIMLE FAMILY TRUST, A.B. & Y.O.	BORJA, LEONIL T. & TITAL L.	11N/03E-33N01	01/22/03	BAJA
217	TRIPLE H PARTNERSHIP	KASNER FAMILY LIMITED PARTNERSHIP	08N/03E-12R01	01/22/03	BAJA
218	PARKER REVOCABLE TRUST, D. E. & G. J.	ADES, JOHN & DEVON	05N/03W-19P03	02/26/03	ALTO
219	PETERSEN KINDRED IRREVOCABLE TRUST	HACKBARTH, EDWARD E.	09N/03E-09A01	02/26/03	BAJA
219	PETERSEN KINDRED IRREVOCABLE TRUST	HACKBARTH, EDWARD E.	09N/03E-09F01	02/26/03	BAJA

**TABLE 9
MOJAVE BASIN AREA
FACILITY TRANSFERS REPORTED TO WATERMASTER
OCTOBER 1, 1993 THROUGH SEPTEMBER 30, 2023**

TRANSFER NUMBER	TRANSFEROR	TRANSFeree	STATE WELL NUMBER	DATE OF CHANGE	SUBAREA
220	SAN BERNARDINO COUNTY SERVICE AREA 70G	SAN BERNARDINO COUNTY SERVICE AREA 70L	04N/07W-33J02	02/26/03	OESTE
220	SAN BERNARDINO COUNTY SERVICE AREA 70G	SAN BERNARDINO COUNTY SERVICE AREA 70L	04N/07W-33J04	02/26/03	OESTE
221	FELIX, ALAN E. & CAROL L.	PRUETT, ANDREA	09N/04E-18K01	03/26/03	BAJA
221	FELIX, ALAN E. & CAROL L.	PRUETT, ANDREA	09N/04E-18K02	03/26/03	BAJA
----	DOLCH, ROBERT & JUDY	JAMBOREE HOUSING CORPORATION	05N/04W-10F02	05/28/03	ALTO
----	DOLCH, ROBERT & JUDY	JAMBOREE HOUSING CORPORATION	05N/04W-10F08	05/28/03	ALTO
227	LITTLE, DON & MUSTAFA, ED	MOUNTAIN VIEW, L.L.C.	10N/03W-34A02	06/25/03	CENTRO
227	LITTLE, DON & MUSTAFA, ED	MOUNTAIN VIEW, L.L.C.	10N/03W-34A03	06/25/03	CENTRO
227	LITTLE, DON & MUSTAFA, ED	MOUNTAIN VIEW, L.L.C.	10N/03W-34A04	06/25/03	CENTRO
227	LITTLE, DON & MUSTAFA, ED	MOUNTAIN VIEW, L.L.C.	10N/03W-34A05	06/25/03	CENTRO
227	LITTLE, DON & MUSTAFA, ED	MOUNTAIN VIEW, L.L.C.	10N/03W-34A07	06/25/03	CENTRO
227	LITTLE, DON & MUSTAFA, ED	MOUNTAIN VIEW, L.L.C.	10N/03W-34B01	06/25/03	CENTRO
227	LITTLE, DON & MUSTAFA, ED	MOUNTAIN VIEW, L.L.C.	10N/03W-34B03	06/25/03	CENTRO
230	BAUR, KARL & RITA	BARON, SUSAN & PALMER, CURTIS	09N/02E-11R07	07/23/03	BAJA
230	BAUR, KARL & RITA	BARON, SUSAN & PALMER, CURTIS	09N/02E-11R08	07/23/03	BAJA
237	HP DEVELOPMENT COMPANY	PETELSKI, RICHARD A.	05N/03W-30E02	09/24/03	ALTO
237	HP DEVELOPMENT COMPANY	PETELSKI, RICHARD A.	05N/03W-30N05	09/24/03	ALTO
237	HP DEVELOPMENT COMPANY	PETELSKI, RICHARD A.	05N/03W-30N06	09/24/03	ALTO
238	LUA, ANTONIO	LUA, MICHAEL T. & DONNA S.	05N/01E-29N04	09/24/03	ESTE
240	PETTIGREW, DAN	HARVEY, JEFFREY W. & LISA M.	05N/01E-29R01	09/24/03	ESTE
240	PETTIGREW, DAN	HARVEY, JEFFREY W. & LISA M.	05N/01E-29R02	09/24/03	ESTE
245	TORRADO, JESUS & AIDA	FARLEY, GREGGORY J.	10N/04E-31M01	10/22/03	BAJA
245	TORRADO, JESUS & AIDA	FARLEY, GREGGORY J.	10N/04E-31M02	10/22/03	BAJA
----	ODESSA WATER DISTRICT	DELANO ENTERPRISES, INC.	09N/02W-19G01	12/03/03	CENTRO
----	ODESSA WATER DISTRICT	DELANO ENTERPRISES, INC.	09N/02W-19P01	12/03/03	CENTRO

**TABLE 9
MOJAVE BASIN AREA
FACILITY TRANSFERS REPORTED TO WATERMASTER
OCTOBER 1, 1993 THROUGH SEPTEMBER 30, 2023**

TRANSFER NUMBER	TRANSFEROR	TRANSFeree	STATE WELL NUMBER	DATE OF CHANGE	SUBAREA
----	ODESSA WATER DISTRICT	DELANO ENTERPRISES, INC.	09N/02W-19P02	12/03/03	CENTRO
248	CHANNELL, KATHRYNE J.	CHANNELL, DALE E.	09N/02E-24R01	01/28/04	BAJA
248	CHANNELL, KATHRYNE J.	CHANNELL, DALE E.	09N/02E-24R02	01/28/04	BAJA
250	ALVA, THOMAS G.	HASS, PAULINE L.	09N/03E-36B04	02/25/04	BAJA
251	STEIMLE FAMILY TRUST, A.B. & Y.O.	CRANDALL, ESTHER	11N/03E-29J02	02/25/04	BAJA
251	STEIMLE FAMILY TRUST, A.B. & Y.O.	CRANDALL, ESTHER	11N/03E-29P01	02/25/04	BAJA
251	STEIMLE FAMILY TRUST, A.B. & Y.O.	CRANDALL, ESTHER	11N/03E-29Q01	02/25/04	BAJA
252	BRYANT, JERRY & DONNA	HARRISON, CONNIE & HAROLD	07N/04W-31E01	03/24/04	ALTO
252	BRYANT, JERRY & DONNA	HARRISON, CONNIE & HAROLD	07N/04W-31E03	03/24/04	ALTO
252	BRYANT, JERRY & DONNA	HARRISON, CONNIE & HAROLD	07N/04W-31E06	03/24/04	ALTO
253	DOSSEY, D. A.	HANDRINOS, NICOLE A.	06N/07W-29P02	03/24/04	OESTE
254	KING, GENEVIEVE E.	LOVE, CHARLES & DEANNA	09N/03W-27L03	03/24/04	CENTRO
254	KING, GENEVIEVE E.	LOVE, CHARLES & DEANNA	09N/03W-27L05	03/24/04	CENTRO
254	KING, GENEVIEVE E.	LOVE, CHARLES & DEANNA	09N/03W-27L06	03/24/04	CENTRO
254	KING, GENEVIEVE E.	LOVE, CHARLES & DEANNA	09N/03W-27L07	03/24/04	CENTRO
256	SULLIVAN, ELLEN M.	SHINTAKU, RICHARD & CHERYL	09N/02E-14N07	03/24/04	BAJA
----	VAN VLIET, HUGO NICHOLAAS & GERI	DESERT VIEW DAIRY	11N/04W-32A02	05/25/04	CENTRO
258	FRANCO, ALFONSO & ELISA	M.B. LANDSCAPING & NURSERY, INC.	05N/01E-29Q02	05/26/04	ESTE
258	FRANCO, ALFONSO & ELISA	M.B. LANDSCAPING & NURSERY, INC.	05N/01E-29Q03	05/26/04	ESTE
258	FRANCO, ALFONSO & ELISA	M.B. LANDSCAPING & NURSERY, INC.	05N/01E-32B02	05/26/04	ESTE
258	FRANCO, ALFONSO & ELISA	M.B. LANDSCAPING & NURSERY, INC.	05N/01E-32G02	05/26/04	ESTE
259	SEALS, ELIZABETH A. & BOTHWELL, TINA	BRACHT, WILLIAM F. & ALEXANDER, ALICIA M.	04N/01W-14F03	05/26/04	ESTE
260	VAN VLIET, HENDRIKA	RYKEN, PAUL, ET AL.	10N/03W-27M01	05/26/04	CENTRO
260	VAN VLIET, HENDRIKA	RYKEN, PAUL, ET AL.	10N/03W-27M02	05/26/04	CENTRO
260	VAN VLIET, HENDRIKA	RYKEN, PAUL, ET AL.	10N/03W-27M03	05/26/04	CENTRO

**TABLE 9
MOJAVE BASIN AREA
FACILITY TRANSFERS REPORTED TO WATERMASTER
OCTOBER 1, 1993 THROUGH SEPTEMBER 30, 2023**

TRANSFER NUMBER	TRANSFEROR	TRANSFeree	STATE WELL NUMBER	DATE OF CHANGE	SUBAREA
261	POHL, ANDREAS & CATHLYN	KERNEK, KEITH & PRISCILLA	09N/01W-03Q01	06/23/04	CENTRO
264	REYNOLDS, ARDEN & MARY	BAILEY, RICHARD N.	09N/04E-21R01	07/28/04	BAJA
264	REYNOLDS, ARDEN & MARY	BAILEY, RICHARD N.	09N/04E-21R02	07/28/04	BAJA
265	AVDEEF, THOMAS & LUCILLE	MUNN AND THURSTON FAMILY TRUST	09N/01W-04G06	09/22/04	CENTRO
265	AVDEEF, THOMAS & LUCILLE	MUNN AND THURSTON FAMILY TRUST	09N/01W-04G08	09/22/04	CENTRO
265	AVDEEF, THOMAS & LUCILLE	MUNN AND THURSTON FAMILY TRUST	09N/01W-04G09	09/22/04	CENTRO
265	AVDEEF, THOMAS & LUCILLE	MUNN AND THURSTON FAMILY TRUST	09N/01W-04G10	09/22/04	CENTRO
266	BAILEY, RICHARD N.	HOWSER, HUELL B.	09N/04E-21R01	09/22/04	BAJA
266	BAILEY, RICHARD N.	HOWSER, HUELL B.	09N/04E-21R02	09/22/04	BAJA
267	BERG, TERRY & SHARON	GREENHOUSE FAMILY TRUST	07N/04W-19M04	09/22/04	ALTO
267	BERG, TERRY & SHARON	GREENHOUSE FAMILY TRUST	07N/05W-24J05	09/22/04	ALTO
267	BERG, TERRY & SHARON	GREENHOUSE FAMILY TRUST	07N/05W-24J06	09/22/04	ALTO
267	BERG, TERRY & SHARON	GREENHOUSE FAMILY TRUST	07N/05W-24J07	09/22/04	ALTO
268	MARTIN, LENDELL	FAHIM, ASHRAF & MIKHAIL, MERVAT W.	09N/02W-17G01	09/22/04	CENTRO
270	ROZELL, JAMES ROBERT	CAMPBELL, BRYAN M.	10N/01W-31J01	09/22/04	CENTRO
270	ROZELL, JAMES ROBERT	CAMPBELL, BRYAN M.	10N/01W-31J02	09/22/04	CENTRO
272	STRINGER, EDWARD & SANDRA	AVILA, ANGEL & EVALIA	04N/01E-06C01	09/22/04	ESTE
273	TAYLOR, CAROLE	KASNER, ROBERT	10N/03E-14J01	09/22/04	BAJA
273	TAYLOR, CAROLE	KASNER, ROBERT	10N/03E-14J02	09/22/04	BAJA
273	TAYLOR, CAROLE	KASNER, ROBERT	10N/03E-14K01	09/22/04	BAJA
274	VAUGHT, ROBERT E. & KAREN M.	SHAW, ROBERT M. & LORI A. SLATER-SHAW	09N/03E-13M02	09/22/04	BAJA
275	WEST, CAROLYN & SMITH, RICHARD	BUNNELL, DICK	07N/04W-06G05	09/22/04	ALTO
275	WEST, CAROLYN & SMITH, RICHARD	BUNNELL, DICK	07N/04W-06G06	09/22/04	ALTO
275	WEST, CAROLYN & SMITH, RICHARD	BUNNELL, DICK	07N/04W-06G07	09/22/04	ALTO
275	WEST, CAROLYN & SMITH, RICHARD	BUNNELL, DICK	07N/04W-06G09	09/22/04	ALTO

**TABLE 9
MOJAVE BASIN AREA
FACILITY TRANSFERS REPORTED TO WATERMASTER
OCTOBER 1, 1993 THROUGH SEPTEMBER 30, 2023**

TRANSFER NUMBER	TRANSFEROR	TRANSFeree	STATE WELL NUMBER	DATE OF CHANGE	SUBAREA
277	J. V. A. AIR, INC.	D'SILVA, MELANIE	10N/01E-35N03	10/27/04	BAJA
277	J. V. A. AIR, INC.	D'SILVA, MELANIE	10N/01E-35P02	10/27/04	BAJA
277	J. V. A. AIR, INC.	D'SILVA, MELANIE	10N/01E-35P12	10/27/04	BAJA
278	MITCHELL, JAMES L. & CHERYL A.	CARLTON, SUSAN	09N/02E-03L04	10/27/04	BAJA
278	MITCHELL, JAMES L. & CHERYL A.	CARLTON, SUSAN	09N/02E-03M01	10/27/04	BAJA
278	MITCHELL, JAMES L. & CHERYL A.	CARLTON, SUSAN	09N/02E-03M02	10/27/04	BAJA
279	ORLOSKY FAMILY TRUST	HARPER LAKE, LLC	11N/04W-29J01	10/27/04	CENTRO
279	ORLOSKY FAMILY TRUST	HARPER LAKE, LLC	11N/04W-29P01	10/27/04	CENTRO
279	ORLOSKY FAMILY TRUST	HARPER LAKE, LLC	11N/04W-30B01	10/27/04	CENTRO
279	ORLOSKY FAMILY TRUST	HARPER LAKE, LLC	11N/04W-30D01	10/27/04	CENTRO
279	ORLOSKY FAMILY TRUST	HARPER LAKE, LLC	11N/04W-30E01	10/27/04	CENTRO
279	ORLOSKY FAMILY TRUST	HARPER LAKE, LLC	11N/04W-30M01	10/27/04	CENTRO
279	ORLOSKY FAMILY TRUST	HARPER LAKE, LLC	11N/04W-30N06	10/27/04	CENTRO
279	ORLOSKY FAMILY TRUST	HARPER LAKE, LLC	11N/04W-30N07	10/27/04	CENTRO
279	ORLOSKY FAMILY TRUST	HARPER LAKE, LLC	11N/04W-30P02	10/27/04	CENTRO
279	ORLOSKY FAMILY TRUST	HARPER LAKE, LLC	11N/04W-30Q03	10/27/04	CENTRO
279	ORLOSKY FAMILY TRUST	HARPER LAKE, LLC	11N/04W-33B02	10/27/04	CENTRO
279	ORLOSKY FAMILY TRUST	HARPER LAKE, LLC	11N/04W-33C02	10/27/04	CENTRO
279	ORLOSKY FAMILY TRUST	HARPER LAKE, LLC	11N/04W-33G04	10/27/04	CENTRO
279	ORLOSKY FAMILY TRUST	HARPER LAKE, LLC	11N/04W-33J01	10/27/04	CENTRO
280	THOMAS FARMS	DESERT WIND LLC	08N/04W-20L01	10/27/04	ALTO
280	THOMAS FARMS	DESERT WIND LLC	08N/04W-20L02	10/27/04	ALTO
280	THOMAS FARMS	DESERT WIND LLC	08N/04W-20P01	10/27/04	ALTO
280	THOMAS FARMS	DESERT WIND LLC	08N/04W-20P02	10/27/04	ALTO
280	THOMAS FARMS	DESERT WIND LLC	08N/04W-20P03	10/27/04	ALTO
281	VAN VLIET, HENDRIKA	P G & E	10N/03W-26C01	10/27/04	CENTRO

**TABLE 9
MOJAVE BASIN AREA
FACILITY TRANSFERS REPORTED TO WATERMASTER
OCTOBER 1, 1993 THROUGH SEPTEMBER 30, 2023**

TRANSFER NUMBER	TRANSFEROR	TRANSFEE	STATE WELL NUMBER	DATE OF CHANGE	SUBAREA
281	VAN VLIET, HENDRIKA	P G & E	10N/03W-26F08	10/27/04	CENTRO
281	VAN VLIET, HENDRIKA	P G & E	10N/03W-26F09	10/27/04	CENTRO
281	VAN VLIET, HENDRIKA	P G & E	10N/03W-26F11	10/27/04	CENTRO
281	VAN VLIET, HENDRIKA	P G & E	10N/03W-26F12	10/27/04	CENTRO
281	VAN VLIET, HENDRIKA	P G & E	10N/03W-26F13	10/27/04	CENTRO
281	VAN VLIET, HENDRIKA	P G & E	10N/03W-26F14	10/27/04	CENTRO
281	VAN VLIET, HENDRIKA	P G & E	10N/03W-26F15	10/27/04	CENTRO
281	VAN VLIET, HENDRIKA	P G & E	10N/03W-26F16	10/27/04	CENTRO
282	WESTERN WATER COMPANY	MORCK, GREGORY M. & LISA A.	07N/04W-07F01	10/27/04	ALTO
282	WESTERN WATER COMPANY	MORCK, GREGORY M. & LISA A.	07N/04W-07G01	10/27/04	ALTO
282	WESTERN WATER COMPANY	MORCK, GREGORY M. & LISA A.	07N/04W-07K01	10/27/04	ALTO
282	WESTERN WATER COMPANY	MORCK, GREGORY M. & LISA A.	07N/04W-07L01	10/27/04	ALTO
282	WESTERN WATER COMPANY	MORCK, GREGORY M. & LISA A.	07N/04W-07N01	10/27/04	ALTO
282	WESTERN WATER COMPANY	MORCK, GREGORY M. & LISA A.	07N/04W-07P01	10/27/04	ALTO
282	WESTERN WATER COMPANY	MORCK, GREGORY M. & LISA A.	07N/04W-07P02	10/27/04	ALTO
285	SPINK, WALTHALL	HUNTBACH, DAVID J.	10N/01W-33M01	01/26/05	CENTRO
285	SPINK, WALTHALL	HUNTBACH, DAVID J.	10N/01W-33M05	01/26/05	CENTRO
286	PARK, HEA JA & JEONG IL	GARDENA MISSION CHURCH, INC.	05N/01E-34N01	02/23/05	ESTE
286	PARK, HEA JA & JEONG IL	GARDENA MISSION CHURCH, INC.	05N/01E-34N02	02/23/05	ESTE
286	PARK, HEA JA & JEONG IL	GARDENA MISSION CHURCH, INC.	05N/01E-34N04	02/23/05	ESTE
287	CHUANG, MARSHAL	KARIMI, HOOSHANG	09N/03E-35K01	03/23/05	BAJA
289	BAKER, GLORIA L.	KOROGHLIAN, TED & NAJWA	09N/03E-19Q03	05/25/05	BAJA
289	BAKER, GLORIA L.	KOROGHLIAN, TED & NAJWA	09N/03E-19Q04	05/25/05	BAJA
290	PETTIGREW, HOWARD L.	GAETA, MIGUEL & MARIA	05N/01E-30H01	05/25/05	ESTE
290	PETTIGREW, HOWARD L.	GAETA, MIGUEL & MARIA	05N/01E-30R02	05/25/05	ESTE
291	RAMIREZ, JAIME & ALICIA	RIVERO, FIDEL V.	09N/02W-06H01	05/25/05	CENTRO

**TABLE 9
MOJAVE BASIN AREA
FACILITY TRANSFERS REPORTED TO WATERMASTER
OCTOBER 1, 1993 THROUGH SEPTEMBER 30, 2023**

TRANSFER NUMBER	TRANSFEROR	TRANSFeree	STATE WELL NUMBER	DATE OF CHANGE	SUBAREA
293	THE 160 NEWBERRY RANCH CALIFORNIA, LTD.	ROCK FOUNDATION, LLC	09N/03E-28J02	05/25/05	BAJA
293	THE 160 NEWBERRY RANCH CALIFORNIA, LTD.	ROCK FOUNDATION, LLC	09N/03E-28R02	05/25/05	BAJA
293	THE 160 NEWBERRY RANCH CALIFORNIA, LTD.	ROCK FOUNDATION, LLC	09N/03E-28R03	05/25/05	BAJA
294	WARD, ET AL.	EIRICH FAMILY TRUST	10N/03E-16Q04	05/25/05	BAJA
----	HART, MERRILL W.	M.B. LANDSCAPING & NURSERY, INC.	05N/01E-32H01	06/29/05	ESTE
296	ARTINYAN, LUDVIK & LUCY	S&B BROTHERS, LLC	09N/04E-18A01	07/27/05	BAJA
296	ARTINYAN, LUDVIK & LUCY	S&B BROTHERS, LLC	09N/04E-18A02	07/27/05	BAJA
296	ARTINYAN, LUDVIK & LUCY	S&B BROTHERS, LLC	09N/04E-18A03	07/27/05	BAJA
297	COOL WATER RANCH	LEVINE, DAVID & MARGARET	09N/01E-15N01	07/27/05	BAJA
297	COOL WATER RANCH	LEVINE, DAVID & MARGARET	09N/01E-15N02	07/27/05	BAJA
297	COOL WATER RANCH	LEVINE, DAVID & MARGARET	09N/01E-15N06	07/27/05	BAJA
297	COOL WATER RANCH	LEVINE, DAVID & MARGARET	09N/01E-15N07	07/27/05	BAJA
297	COOL WATER RANCH	LEVINE, DAVID & MARGARET	09N/01E-15P01	07/27/05	BAJA
298	CRYSTAL HILLS WATER COMPANY	ABDUL, HARRY & ANITA	03N/01W-01R01	07/27/05	ESTE
298	CRYSTAL HILLS WATER COMPANY	ABDUL, HARRY & ANITA	03N/01W-01R02	07/27/05	ESTE
298	CRYSTAL HILLS WATER COMPANY	ABDUL, HARRY & ANITA	03N/01W-12A01	07/27/05	ESTE
299	MIZRAHIE, ET AL.	KIM, SEON JA	09N/03E-08E03	07/27/05	BAJA
303	CHIAO MEI DEVELOPMENT	LIN, KUAN JUNG & CHUNG, DER-BING	09N/03E-23M02	09/28/05	BAJA
303	CHIAO MEI DEVELOPMENT	LIN, KUAN JUNG & CHUNG, DER-BING	09N/03E-26D01	09/28/05	BAJA
304	FISHER, DOLORES	RUBENDALL LIVING TRUST, GERALD L. & JUDITH A.	03N/05W-12G01	09/28/05	ALTO
304	FISHER, DOLORES	RUBENDALL LIVING TRUST, GERALD L. & JUDITH A.	03N/05W-12G02	09/28/05	ALTO
304	FISHER, DOLORES	RUBENDALL LIVING TRUST, GERALD L. & JUDITH A.	03N/05W-12K03	09/28/05	ALTO
306	HONG, PAUL B. & MAY	WANG, LARRY T. AND LOW, JANNETTE Y.	08N/04E-07C03	09/28/05	BAJA
306	HONG, PAUL B. & MAY	WANG, LARRY T. AND LOW, JANNETTE Y.	08N/04E-07D04	09/28/05	BAJA
306	HONG, PAUL B. & MAY	WANG, LARRY T. AND LOW, JANNETTE Y.	08N/04E-07F02	09/28/05	BAJA

**TABLE 9
MOJAVE BASIN AREA
FACILITY TRANSFERS REPORTED TO WATERMASTER
OCTOBER 1, 1993 THROUGH SEPTEMBER 30, 2023**

TRANSFER NUMBER	TRANSFEROR	TRANSFeree	STATE WELL NUMBER	DATE OF CHANGE	SUBAREA
308	MIZRAHIE, ET AL.	PAK, EDWIN H.	09N/03E-14E01	09/28/05	BAJA
308	MIZRAHIE, ET AL.	PAK, EDWIN H.	09N/03E-14E02	09/28/05	BAJA
309	PAYAN, PAUL & FELIMA	CORBRIDGE, LINDA S.	10N/03E-15Q02	09/28/05	BAJA
309	PAYAN, PAUL & FELIMA	CORBRIDGE, LINDA S.	10N/03E-15Q03	09/28/05	BAJA
309	PAYAN, PAUL & FELIMA	CORBRIDGE, LINDA S.	10N/03E-15R01	09/28/05	BAJA
310	VAN DIEST, CORNELIUS	VAN LEEUWEN, JOHN	09N/03E-11K02	09/28/05	BAJA
311	WARD, ERNEST & LAURA	QUIROS, FRANSISCO J. & HERMANN, RONALD	09N/03E-03C04	09/28/05	BAJA
313	YARD, WILLIAM & BETTY	KOEGLER, RONALD R. & CAROLYN V.	10N/03E-04F02	09/28/05	BAJA
----	PETTIS FAMILY TRUST	SUMMERS FAMILY TRUST	04N/03W-06B01	10/26/05	ALTO
----	PETTIS FAMILY TRUST	SUMMERS FAMILY TRUST	04N/03W-06B08	10/26/05	ALTO
317	VERNOLA TRUST, PAT AND MARY ANN	KASNER, ROBERT	09N/03E-27Q02	10/26/05	BAJA
317	VERNOLA TRUST, PAT AND MARY ANN	KASNER, ROBERT	09N/03E-27Q03	10/26/05	BAJA
317	VERNOLA TRUST, PAT AND MARY ANN	KASNER, ROBERT	09N/03E-27Q04	10/26/05	BAJA
317	VERNOLA TRUST, PAT AND MARY ANN	KASNER, ROBERT	10N/03E-35H02	10/26/05	BAJA
317	VERNOLA TRUST, PAT AND MARY ANN	KASNER, ROBERT	10N/03E-35J01	10/26/05	BAJA
----	FRIENDS OF HARPER LAKE, INC.	HARPER LAKE COMPANY VIII	11N/04W-28R01	12/15/05	CENTRO
----	SON OF CADUCEUS	APPLE VALLEY RANCHOS WATER COMPANY	05N/03W-31H01	01/01/06	ALTO
318	LEE, CHUN HWA & MYUNG SOOK	KLADSTRUP, KITTY L.	09N/03E-01F01	01/25/06	BAJA
318	LEE, CHUN HWA & MYUNG SOOK	KLADSTRUP, KITTY L.	09N/03E-01F03	01/25/06	BAJA
319	MCCALL, VIVIAN E.	BELL, THOMAS	07N/05W-24J02	01/25/06	ALTO
319	MCCALL, VIVIAN E.	BELL, THOMAS	07N/05W-24J03	01/25/06	ALTO
321	SNYDER, KRYL K. & ROUTH, RICHARD J.	BREDELIS, RONALD C. & JEAN	10N/03E-28N01	01/25/06	BAJA
321	SNYDER, KRYL K. & ROUTH, RICHARD J.	BREDELIS, RONALD C. & JEAN	10N/03E-28N03	01/25/06	BAJA
321	SNYDER, KRYL K. & ROUTH, RICHARD J.	BREDELIS, RONALD C. & JEAN	10N/03E-28N07	01/25/06	BAJA
322	LEE, MOONYOUNG & OKHEA	THOMAS, STEPHEN & LORI	09N/03E-22D01	02/22/06	BAJA

**TABLE 9
MOJAVE BASIN AREA
FACILITY TRANSFERS REPORTED TO WATERMASTER
OCTOBER 1, 1993 THROUGH SEPTEMBER 30, 2023**

TRANSFER NUMBER	TRANSFEROR	TRANSFeree	STATE WELL NUMBER	DATE OF CHANGE	SUBAREA
322	LEE, MOONYOUNG & OKHEA	THOMAS, STEPHEN & LORI	09N/03E-22D02	02/22/06	BAJA
324	BALL, DAVID P.	BANK OF AMERICA, NT & SA	10N/03E-23L01	03/22/06	BAJA
325	BANK OF AMERICA, NT & SA	QUIGG AND COMPANY, INC.	10N/03E-23L01	03/22/06	BAJA
327	LUTH, KEN	UDDERLY GOLD FARMS, LLC	07N/04W-19P06	03/22/06	ALTO
328	MALIN, ANDY & SOLOMON, PAULA	JACKSON, JAMES N. JR REVOCABLE LIVING TRUST	09N/04E-06J01	03/22/06	BAJA
329	MITCHELL, ROBIN & JUDITH	TRAHAN, ELAINE	05N/03W-11E02	03/22/06	ALTO
329	MITCHELL, ROBIN & JUDITH	TRAHAN, ELAINE	05N/03W-11E04	03/22/06	ALTO
329	MITCHELL, ROBIN & JUDITH	TRAHAN, ELAINE	05N/03W-11E05	03/22/06	ALTO
330	MORCK, GREGORY M. & LISA A.	DORA LAND, INC.	07N/04W-07F01	03/22/06	ALTO
330	MORCK, GREGORY M. & LISA A.	DORA LAND, INC.	07N/04W-07G01	03/22/06	ALTO
330	MORCK, GREGORY M. & LISA A.	DORA LAND, INC.	07N/04W-07K01	03/22/06	ALTO
330	MORCK, GREGORY M. & LISA A.	DORA LAND, INC.	07N/04W-07L01	03/22/06	ALTO
330	MORCK, GREGORY M. & LISA A.	DORA LAND, INC.	07N/04W-07N01	03/22/06	ALTO
330	MORCK, GREGORY M. & LISA A.	DORA LAND, INC.	07N/04W-07P01	03/22/06	ALTO
330	MORCK, GREGORY M. & LISA A.	DORA LAND, INC.	07N/04W-07P02	03/22/06	ALTO
331	PURCIO, THOMAS R. & PATRICIA A.	HAAS, BRYAN C. AND HINKLE, MARY H.	09N/03E-01B01	03/22/06	BAJA
331	PURCIO, THOMAS R. & PATRICIA A.	HAAS, BRYAN C. AND HINKLE, MARY H.	09N/03E-01B02	03/22/06	BAJA
332	TRAHAN, ELAINE	TRAHAN, ET AL.	05N/03W-11E02	03/22/06	ALTO
332	TRAHAN, ELAINE	TRAHAN, ET AL.	05N/03W-11E04	03/22/06	ALTO
332	TRAHAN, ELAINE	TRAHAN, ET AL.	05N/03W-11E05	03/22/06	ALTO
333	WARD, RAYMOND	SMITH, PORTER AND ANITA	09N/04E-06K03	03/22/06	BAJA
333	WARD, RAYMOND	SMITH, PORTER AND ANITA	09N/04E-06K06	03/22/06	BAJA
337	SCOGGINS, RONALD & KIMBERLY	SAPP, ROBERT D. & LEE, TERESA J.	04N/03W-17L04	05/25/06	ALTO
338	GESIRIECH, WAYNE D.	HERMANAS MISIONERAS SERVIDORAS DE LA PALABRA	09N/03W-01F01	07/26/06	CENTRO

**TABLE 9
MOJAVE BASIN AREA
FACILITY TRANSFERS REPORTED TO WATERMASTER
OCTOBER 1, 1993 THROUGH SEPTEMBER 30, 2023**

TRANSFER NUMBER	TRANSFEROR	TRANSFeree	STATE WELL NUMBER	DATE OF CHANGE	SUBAREA
339	HUTCHISON TRUST, WILLIAM O.	CF PROPERTIES, LLC	09N/03E-22L01	07/26/06	BAJA
340	KAPLAN, ABRAHAM M.	WALA & WALA COMPANY, LLC	09N/03E-01M01	07/26/06	BAJA
340	KAPLAN, ABRAHAM M.	WALA & WALA COMPANY, LLC	09N/03E-01N01	07/26/06	BAJA
341	KERNEK, KEITH & PRISCILLA	VALENTINE, VITO	09N/01W-03Q01	07/26/06	CENTRO
342	VAN LEEUWEN FAMILY TRUST	AQUA CAPITAL MANAGEMENT, LP-AGRICULTURE	07N/05W-25Q01	07/26/06	ALTO
342	VAN LEEUWEN FAMILY TRUST	AQUA CAPITAL MANAGEMENT, LP-AGRICULTURE	07N/05W-25Q02	07/26/06	ALTO
342	VAN LEEUWEN FAMILY TRUST	AQUA CAPITAL MANAGEMENT, LP-AGRICULTURE	07N/05W-25R03	07/26/06	ALTO
342	VAN LEEUWEN FAMILY TRUST	AQUA CAPITAL MANAGEMENT, LP-AGRICULTURE	07N/05W-25R04	07/26/06	ALTO
343	DORMAN, DUDLEY D. & BILLIE B.	WEEMS, LIZZIE	09N/02E-27E02	09/27/06	BAJA
343	DORMAN, DUDLEY D. & BILLIE B.	WEEMS, LIZZIE	09N/02E-27E04	09/27/06	BAJA
346	YEAGER CONSTRUCTION COMPANY, INC., E. L.	AQUA CAPITAL MANAGEMENT, LP-INDUSTRIAL	07N/04W-18L02	09/27/06	ALTO
347	BARAK, RICHARD	WAZZAN, ET AL.	11N/03E-32E01	11/29/06	BAJA
347	BARAK, RICHARD	WAZZAN, ET AL.	11N/03E-32E02	11/29/06	BAJA
349	EIRICH FAMILY TRUST	NEWBERRY CORPORATION	10N/03E-16Q04	11/29/06	BAJA
351	NELSON, MILDRED L.	P G & E	10N/03W-26M04	11/29/06	CENTRO
351	NELSON, MILDRED L.	P G & E	10N/03W-26N02	11/29/06	CENTRO
351	NELSON, MILDRED L.	P G & E	10N/03W-26N04	11/29/06	CENTRO
351	NELSON, MILDRED L.	P G & E	10N/03W-26N05	11/29/06	CENTRO
351	NELSON, MILDRED L.	P G & E	10N/03W-26N06	11/29/06	CENTRO
351	NELSON, MILDRED L.	P G & E	10N/03W-26N07	11/29/06	CENTRO
351	NELSON, MILDRED L.	P G & E	10N/03W-26N08	11/29/06	CENTRO
359	CALLAHAN, BERNERD J.	PORTER, TIMOTHY M.	09N/03E-08P02	03/28/07	BAJA
359	CALLAHAN, BERNERD J.	PORTER, TIMOTHY M.	09N/03E-08P03	03/28/07	BAJA
362	SAWYERS MOTOR SPORTS GROUP	TEISAN, JERRY	09N/04E-20D02	03/28/07	BAJA
363	BARSTOW CALICO K O A	OLD GROVE PROPERTIES, LLC	09N/01E-05H03	05/23/07	BAJA

**TABLE 9
MOJAVE BASIN AREA
FACILITY TRANSFERS REPORTED TO WATERMASTER
OCTOBER 1, 1993 THROUGH SEPTEMBER 30, 2023**

TRANSFER NUMBER	TRANSFEROR	TRANSFeree	STATE WELL NUMBER	DATE OF CHANGE	SUBAREA
365	PETTIGREW, DAN	PETTIGREW, JAMES AND CHERLYN	05N/01E-31A04	05/23/07	ESTE
365	PETTIGREW, DAN	PETTIGREW, JAMES AND CHERLYN	05N/01E-31A05	05/23/07	ESTE
366	SAN BERNARDINO COUNTY SERVICE AREA 70C	HELENDALE COMMUNITY SERVICES DISTRICT	07N/04W-06E04	05/23/07	ALTO
366	SAN BERNARDINO COUNTY SERVICE AREA 70C	HELENDALE COMMUNITY SERVICES DISTRICT	07N/04W-06E06	05/23/07	ALTO
366	SAN BERNARDINO COUNTY SERVICE AREA 70C	HELENDALE COMMUNITY SERVICES DISTRICT	07N/04W-06M06	05/23/07	ALTO
366	SAN BERNARDINO COUNTY SERVICE AREA 70C	HELENDALE COMMUNITY SERVICES DISTRICT	07N/04W-06M07	05/23/07	ALTO
366	SAN BERNARDINO COUNTY SERVICE AREA 70C	HELENDALE COMMUNITY SERVICES DISTRICT	08N/04W-29D03	05/23/07	ALTO
366	SAN BERNARDINO COUNTY SERVICE AREA 70C	HELENDALE COMMUNITY SERVICES DISTRICT	08N/04W-31A01	05/23/07	ALTO
366	SAN BERNARDINO COUNTY SERVICE AREA 70C	HELENDALE COMMUNITY SERVICES DISTRICT	08N/04W-31G01	05/23/07	ALTO
366	SAN BERNARDINO COUNTY SERVICE AREA 70C	HELENDALE COMMUNITY SERVICES DISTRICT	08N/04W-31G02	05/23/07	ALTO
366	SAN BERNARDINO COUNTY SERVICE AREA 70C	HELENDALE COMMUNITY SERVICES DISTRICT	08N/04W-31P02	05/23/07	ALTO
369	HARPER LAKE, LLC	SOLUCAR, INC.	11N/04W-29J01	07/25/07	CENTRO
369	HARPER LAKE, LLC	SOLUCAR, INC.	11N/04W-29P01	07/25/07	CENTRO
369	HARPER LAKE, LLC	SOLUCAR, INC.	11N/04W-30B01	07/25/07	CENTRO
369	HARPER LAKE, LLC	SOLUCAR, INC.	11N/04W-30D01	07/25/07	CENTRO
369	HARPER LAKE, LLC	SOLUCAR, INC.	11N/04W-30E01	07/25/07	CENTRO
369	HARPER LAKE, LLC	SOLUCAR, INC.	11N/04W-30M01	07/25/07	CENTRO
369	HARPER LAKE, LLC	SOLUCAR, INC.	11N/04W-30N06	07/25/07	CENTRO
369	HARPER LAKE, LLC	SOLUCAR, INC.	11N/04W-30N07	07/25/07	CENTRO
369	HARPER LAKE, LLC	SOLUCAR, INC.	11N/04W-30P02	07/25/07	CENTRO
369	HARPER LAKE, LLC	SOLUCAR, INC.	11N/04W-30Q03	07/25/07	CENTRO
369	HARPER LAKE, LLC	SOLUCAR, INC.	11N/04W-33B02	07/25/07	CENTRO
369	HARPER LAKE, LLC	SOLUCAR, INC.	11N/04W-33C02	07/25/07	CENTRO
369	HARPER LAKE, LLC	SOLUCAR, INC.	11N/04W-33G04	07/25/07	CENTRO
369	HARPER LAKE, LLC	SOLUCAR, INC.	11N/04W-33J01	07/25/07	CENTRO
370	REES, MICHAEL J. & SUE A	KENWOOD MANAGEMENT, LLC	08N/04W-10G01	07/25/07	CENTRO

**TABLE 9
MOJAVE BASIN AREA
FACILITY TRANSFERS REPORTED TO WATERMASTER
OCTOBER 1, 1993 THROUGH SEPTEMBER 30, 2023**

TRANSFER NUMBER	TRANSFEROR	TRANSFeree	STATE WELL NUMBER	DATE OF CHANGE	SUBAREA
370	REES, MICHAEL J. & SUE A	KENWOOD MANAGEMENT, LLC	08N/04W-10G02	07/25/07	CENTRO
372	BALDY MESA WATER DISTRICT	VICTORVILLE WATER DISTRICT, ID#2	04N/05W-01A01	09/26/07	ALTO
372	BALDY MESA WATER DISTRICT	VICTORVILLE WATER DISTRICT, ID#2	04N/05W-01C03	09/26/07	ALTO
372	BALDY MESA WATER DISTRICT	VICTORVILLE WATER DISTRICT, ID#2	04N/05W-01D01	09/26/07	ALTO
372	BALDY MESA WATER DISTRICT	VICTORVILLE WATER DISTRICT, ID#2	04N/05W-01E01	09/26/07	ALTO
372	BALDY MESA WATER DISTRICT	VICTORVILLE WATER DISTRICT, ID#2	04N/05W-01G01	09/26/07	ALTO
372	BALDY MESA WATER DISTRICT	VICTORVILLE WATER DISTRICT, ID#2	04N/05W-09R01	09/26/07	ALTO
372	BALDY MESA WATER DISTRICT	VICTORVILLE WATER DISTRICT, ID#2	04N/05W-09R01	09/26/07	ALTO
372	BALDY MESA WATER DISTRICT	VICTORVILLE WATER DISTRICT, ID#2	04N/05W-09R01	09/26/07	ALTO
372	BALDY MESA WATER DISTRICT	VICTORVILLE WATER DISTRICT, ID#2	04N/05W-09R01	09/26/07	ALTO
372	BALDY MESA WATER DISTRICT	VICTORVILLE WATER DISTRICT, ID#2	04N/05W-09R01	09/26/07	ALTO
372	BALDY MESA WATER DISTRICT	VICTORVILLE WATER DISTRICT, ID#2	04N/05W-09R01	09/26/07	ALTO
372	BALDY MESA WATER DISTRICT	VICTORVILLE WATER DISTRICT, ID#2	04N/05W-09R01	09/26/07	ALTO
372	BALDY MESA WATER DISTRICT	VICTORVILLE WATER DISTRICT, ID#2	04N/05W-09R01	09/26/07	ALTO
372	BALDY MESA WATER DISTRICT	VICTORVILLE WATER DISTRICT, ID#2	04N/05W-09R01	09/26/07	ALTO
372	BALDY MESA WATER DISTRICT	VICTORVILLE WATER DISTRICT, ID#2	04N/05W-09R01	09/26/07	ALTO
372	BALDY MESA WATER DISTRICT	VICTORVILLE WATER DISTRICT, ID#2	04N/05W-09R01	09/26/07	ALTO
372	BALDY MESA WATER DISTRICT	VICTORVILLE WATER DISTRICT, ID#2	05N/05W-35C03	09/26/07	ALTO
372	BALDY MESA WATER DISTRICT	VICTORVILLE WATER DISTRICT, ID#2	05N/05W-35G01	09/26/07	ALTO
372	BALDY MESA WATER DISTRICT	VICTORVILLE WATER DISTRICT, ID#2	05N/05W-35P02	09/26/07	ALTO
372	BALDY MESA WATER DISTRICT	VICTORVILLE WATER DISTRICT, ID#2	05N/06W-36R01	09/26/07	ALTO
373	CRANDALL, ESTHER	ITALMOOD INC., ET. AL.	11N/03E-29J02	09/26/07	BAJA
373	CRANDALL, ESTHER	ITALMOOD INC., ET. AL.	11N/03E-29P01	09/26/07	BAJA
373	CRANDALL, ESTHER	ITALMOOD INC., ET. AL.	11N/03E-29Q01	09/26/07	BAJA
374	VICTOR VALLEY WATER DISTRICT	VICTORVILLE WATER DISTRICT, ID#1	04N/04W-05M02	09/26/07	ALTO
374	VICTOR VALLEY WATER DISTRICT	VICTORVILLE WATER DISTRICT, ID#1	04N/05W-02H01	09/26/07	ALTO
374	VICTOR VALLEY WATER DISTRICT	VICTORVILLE WATER DISTRICT, ID#1	05N/04W-06R01	09/26/07	ALTO

**TABLE 9
MOJAVE BASIN AREA
FACILITY TRANSFERS REPORTED TO WATERMASTER
OCTOBER 1, 1993 THROUGH SEPTEMBER 30, 2023**

TRANSFER NUMBER	TRANSFEROR	TRANSFeree	STATE WELL NUMBER	DATE OF CHANGE	SUBAREA
374	VICTOR VALLEY WATER DISTRICT	VICTORVILLE WATER DISTRICT, ID#1	05N/04W-07N02	09/26/07	ALTO
374	VICTOR VALLEY WATER DISTRICT	VICTORVILLE WATER DISTRICT, ID#1	05N/04W-08B02	09/26/07	ALTO
374	VICTOR VALLEY WATER DISTRICT	VICTORVILLE WATER DISTRICT, ID#1	05N/04W-08N01	09/26/07	ALTO
374	VICTOR VALLEY WATER DISTRICT	VICTORVILLE WATER DISTRICT, ID#1	05N/04W-08Q01	09/26/07	ALTO
374	VICTOR VALLEY WATER DISTRICT	VICTORVILLE WATER DISTRICT, ID#1	05N/04W-09G03	09/26/07	ALTO
374	VICTOR VALLEY WATER DISTRICT	VICTORVILLE WATER DISTRICT, ID#1	05N/04W-09G04	09/26/07	ALTO
374	VICTOR VALLEY WATER DISTRICT	VICTORVILLE WATER DISTRICT, ID#1	05N/04W-09K01	09/26/07	ALTO
374	VICTOR VALLEY WATER DISTRICT	VICTORVILLE WATER DISTRICT, ID#1	05N/04W-09N01	09/26/07	ALTO
374	VICTOR VALLEY WATER DISTRICT	VICTORVILLE WATER DISTRICT, ID#1	05N/04W-09N02	09/26/07	ALTO
374	VICTOR VALLEY WATER DISTRICT	VICTORVILLE WATER DISTRICT, ID#1	05N/04W-09R01	09/26/07	ALTO
374	VICTOR VALLEY WATER DISTRICT	VICTORVILLE WATER DISTRICT, ID#1	05N/04W-10N01	09/26/07	ALTO
374	VICTOR VALLEY WATER DISTRICT	VICTORVILLE WATER DISTRICT, ID#1	05N/04W-10N04	09/26/07	ALTO
374	VICTOR VALLEY WATER DISTRICT	VICTORVILLE WATER DISTRICT, ID#1	05N/04W-16M01	09/26/07	ALTO
374	VICTOR VALLEY WATER DISTRICT	VICTORVILLE WATER DISTRICT, ID#1	05N/04W-16M03	09/26/07	ALTO
374	VICTOR VALLEY WATER DISTRICT	VICTORVILLE WATER DISTRICT, ID#1	05N/04W-19J01	09/26/07	ALTO
374	VICTOR VALLEY WATER DISTRICT	VICTORVILLE WATER DISTRICT, ID#1	05N/04W-20B01	09/26/07	ALTO
374	VICTOR VALLEY WATER DISTRICT	VICTORVILLE WATER DISTRICT, ID#1	05N/04W-20J02	09/26/07	ALTO
374	VICTOR VALLEY WATER DISTRICT	VICTORVILLE WATER DISTRICT, ID#1	05N/04W-27D08	09/26/07	ALTO
374	VICTOR VALLEY WATER DISTRICT	VICTORVILLE WATER DISTRICT, ID#1	05N/04W-27K01	09/26/07	ALTO
374	VICTOR VALLEY WATER DISTRICT	VICTORVILLE WATER DISTRICT, ID#1	05N/04W-30A01	09/26/07	ALTO
374	VICTOR VALLEY WATER DISTRICT	VICTORVILLE WATER DISTRICT, ID#1	05N/04W-30K02	09/26/07	ALTO
374	VICTOR VALLEY WATER DISTRICT	VICTORVILLE WATER DISTRICT, ID#1	05N/04W-30M01	09/26/07	ALTO
374	VICTOR VALLEY WATER DISTRICT	VICTORVILLE WATER DISTRICT, ID#1	05N/04W-30M02	09/26/07	ALTO
374	VICTOR VALLEY WATER DISTRICT	VICTORVILLE WATER DISTRICT, ID#1	05N/04W-31A02	09/26/07	ALTO
374	VICTOR VALLEY WATER DISTRICT	VICTORVILLE WATER DISTRICT, ID#1	05N/04W-33H02	09/26/07	ALTO
374	VICTOR VALLEY WATER DISTRICT	VICTORVILLE WATER DISTRICT, ID#1	05N/04W-34N01	09/26/07	ALTO
374	VICTOR VALLEY WATER DISTRICT	VICTORVILLE WATER DISTRICT, ID#1	05N/05W-13E01	09/26/07	ALTO

**TABLE 9
MOJAVE BASIN AREA
FACILITY TRANSFERS REPORTED TO WATERMASTER
OCTOBER 1, 1993 THROUGH SEPTEMBER 30, 2023**

TRANSFER NUMBER	TRANSFEROR	TRANSFeree	STATE WELL NUMBER	DATE OF CHANGE	SUBAREA
374	VICTOR VALLEY WATER DISTRICT	VICTORVILLE WATER DISTRICT, ID#1	05N/05W-13H02	09/26/07	ALTO
374	VICTOR VALLEY WATER DISTRICT	VICTORVILLE WATER DISTRICT, ID#1	05N/05W-13R02	09/26/07	ALTO
374	VICTOR VALLEY WATER DISTRICT	VICTORVILLE WATER DISTRICT, ID#1	05N/05W-23K01	09/26/07	ALTO
374	VICTOR VALLEY WATER DISTRICT	VICTORVILLE WATER DISTRICT, ID#1	05N/05W-24R01	09/26/07	ALTO
374	VICTOR VALLEY WATER DISTRICT	VICTORVILLE WATER DISTRICT, ID#1	05N/05W-24R02	09/26/07	ALTO
374	VICTOR VALLEY WATER DISTRICT	VICTORVILLE WATER DISTRICT, ID#1	05N/05W-25D01	09/26/07	ALTO
374	VICTOR VALLEY WATER DISTRICT	VICTORVILLE WATER DISTRICT, ID#1	05N/05W-25K02	09/26/07	ALTO
374	VICTOR VALLEY WATER DISTRICT	VICTORVILLE WATER DISTRICT, ID#1	06N/04W-34M10	09/26/07	ALTO
374	VICTOR VALLEY WATER DISTRICT	VICTORVILLE WATER DISTRICT, ID#1	06N/04W-34M12	09/26/07	ALTO
376	VICTORVILLE, CITY OF	VICTORVILLE WATER DISTRICT, ID#1	05N/04W-20H02	09/26/07	ALTO
376	VICTORVILLE, CITY OF	VICTORVILLE WATER DISTRICT, ID#1	05N/04W-20P01	09/26/07	ALTO
376	VICTORVILLE, CITY OF	VICTORVILLE WATER DISTRICT, ID#1	05N/04W-21M03	09/26/07	ALTO
376	VICTORVILLE, CITY OF	VICTORVILLE WATER DISTRICT, ID#1	06N/04W-34M08	09/26/07	ALTO
378	GAINES, JACK & MARY	DRIFFIN, TRAVIS AND LINDA	10N/01W-33P07	10/24/07	CENTRO
379	HARALIK, BESS & ROBERT	TURMAN, VICKIE S.	09N/03E-22R02	10/24/07	BAJA
379	HARALIK, BESS & ROBERT	TURMAN, VICKIE S.	09N/03E-22R03	10/24/07	BAJA
385	HAMILTON TRUST, DON & RUTH M.	HAMILTON FAMILY TRUST	04N/03W-19G01	02/28/08	ALTO
385	HAMILTON TRUST, DON & RUTH M.	HAMILTON FAMILY TRUST	04N/03W-19G07	02/28/08	ALTO
386	HAMILTON, ET AL.	HAMILTON FAMILY TRUST	04N/03W-19H03	02/28/08	ALTO
386	HAMILTON, ET AL.	HAMILTON FAMILY TRUST	04N/03W-19H03	02/28/08	ALTO
386	HAMILTON, ET AL.	HAMILTON FAMILY TRUST	04N/03W-19H05	02/28/08	ALTO
388	GRAVES, CHESTER B.	ELMER, JOHN AND DONNA L.	09N/03E-24B01	03/24/08	BAJA
388	GRAVES, CHESTER B.	ELMER, JOHN AND DONNA L.	09N/03E-24G03	03/24/08	BAJA
391	CHO BROTHERS RANCH	KASNER FAMILY LIMITED PARTNERSHIP	09N/03E-10K01	05/28/08	BAJA
391	CHO BROTHERS RANCH	KASNER FAMILY LIMITED PARTNERSHIP	09N/03E-10Q01	05/28/08	BAJA
391	CHO BROTHERS RANCH	KASNER FAMILY LIMITED PARTNERSHIP	09N/03E-10R01	05/28/08	BAJA

**TABLE 9
MOJAVE BASIN AREA
FACILITY TRANSFERS REPORTED TO WATERMASTER
OCTOBER 1, 1993 THROUGH SEPTEMBER 30, 2023**

TRANSFER NUMBER	TRANSFEROR	TRANSFEEE	STATE WELL NUMBER	DATE OF CHANGE	SUBAREA
392	BOWMAN, EDWIN L.	FEJFAR, MONICA KAY	09N/03E-12L01	07/23/08	BAJA
393	MEYERS, LONNIE	WELLS, DANIEL W. AND CARMEN	09N/03W-02M02	07/23/08	CENTRO
401	PEREZ, EVA	PEREZ, TRINIDAD	05N/01E-31P01	09/24/08	ESTE
402	PEREZ, TRINIDAD	PAK, KAE SOO AND MYONG HUI KANG	05N/01E-31P01	09/24/08	ESTE
403	SAN BERNARDINO COUNTY SERVICE AREA 70L	PHELAN PIÑON HILLS CSD	04N/07W-33J02	09/24/08	OESTE
403	SAN BERNARDINO COUNTY SERVICE AREA 70L	PHELAN PIÑON HILLS CSD	04N/07W-33J04	09/24/08	OESTE
403	SAN BERNARDINO COUNTY SERVICE AREA 70L	PHELAN PIÑON HILLS CSD	05N/07W-23A01	09/24/08	OESTE
403	SAN BERNARDINO COUNTY SERVICE AREA 70L	PHELAN PIÑON HILLS CSD	05N/07W-24D02	09/24/08	OESTE
403	SAN BERNARDINO COUNTY SERVICE AREA 70L	PHELAN PIÑON HILLS CSD	05N/07W-24D03	09/24/08	OESTE
403	SAN BERNARDINO COUNTY SERVICE AREA 70L	PHELAN PIÑON HILLS CSD	05N/07W-24D04	09/24/08	OESTE
403	SAN BERNARDINO COUNTY SERVICE AREA 70L	PHELAN PIÑON HILLS CSD	05N/07W-24D07	09/24/08	OESTE
403	SAN BERNARDINO COUNTY SERVICE AREA 70L	PHELAN PIÑON HILLS CSD	05N/07W-30D01	09/24/08	OESTE
403	SAN BERNARDINO COUNTY SERVICE AREA 70L	PHELAN PIÑON HILLS CSD	05N/07W-30D02	09/24/08	OESTE
403	SAN BERNARDINO COUNTY SERVICE AREA 70L	PHELAN PIÑON HILLS CSD	05N/07W-30D03	09/24/08	OESTE
403	SAN BERNARDINO COUNTY SERVICE AREA 70L	PHELAN PIÑON HILLS CSD	05N/07W-31J03	09/24/08	OESTE
403	SAN BERNARDINO COUNTY SERVICE AREA 70L	PHELAN PIÑON HILLS CSD	05N/07W-31J04	09/24/08	OESTE
403	SAN BERNARDINO COUNTY SERVICE AREA 70L	PHELAN PIÑON HILLS CSD	05N/07W-36E01	09/24/08	OESTE
404	SAN BERNARDINO COUNTY SERVICE AREA 70L	PHELAN PIÑON HILLS CSD	04N/06W-04D01	09/24/08	ALTO
404	SAN BERNARDINO COUNTY SERVICE AREA 70L	PHELAN PIÑON HILLS CSD	04N/06W-04D02	09/24/08	ALTO
404	SAN BERNARDINO COUNTY SERVICE AREA 70L	PHELAN PIÑON HILLS CSD	04N/06W-04D04	09/24/08	ALTO
406	WACKEEN, CAESAR	HELENDALE COMMUNITY SERVICES DISTRICT	08N/04W-20N02	09/24/08	ALTO
406	WACKEEN, CAESAR	HELENDALE COMMUNITY SERVICES DISTRICT	08N/04W-20N03	09/24/08	ALTO
411	HIETT, HARRY J. AND CLARICE M.	HIETT, HARRY L.	09N/01E-22B03	10/29/08	BAJA
411	HIETT, HARRY J. AND CLARICE M.	HIETT, HARRY L.	09N/01E-22B04	10/29/08	BAJA
411	HIETT, HARRY J. AND CLARICE M.	HIETT, HARRY L.	09N/01E-22B07	10/29/08	BAJA

**TABLE 9
MOJAVE BASIN AREA
FACILITY TRANSFERS REPORTED TO WATERMASTER
OCTOBER 1, 1993 THROUGH SEPTEMBER 30, 2023**

TRANSFER NUMBER	TRANSFEROR	TRANSFeree	STATE WELL NUMBER	DATE OF CHANGE	SUBAREA
417	MOST, MILTON AND JENNIE	JENNIE, MOST	11N/04W-32D03	01/28/09	CENTRO
418	JENNIE, MOST	MOST FAMILY TRUST	11N/04W-32D03	01/28/09	CENTRO
419	MOST FAMILY TRUST	ABENGOA SOLAR, INC.	11N/04W-32D03	01/28/09	CENTRO
425	RUBSCH FAMILY TRUST, G. A. AND M. A.	CAMPBELL, REGINALD F. AND JANET S.	09N/04E-31J01	02/25/09	BAJA
425	RUBSCH FAMILY TRUST, G. A. AND M. A.	CAMPBELL, REGINALD F. AND JANET S.	09N/04E-31J02	02/25/09	BAJA
----	AQUA CAPITAL MANAGEMENT, LP-AGRICULTURE	WOOD, MICHAEL AND DENISE	07N/05W-25Q01	04/23/09	ALTO
----	AQUA CAPITAL MANAGEMENT, LP-AGRICULTURE	WOOD, MICHAEL AND DENISE	07N/05W-25Q02	04/23/09	ALTO
----	AQUA CAPITAL MANAGEMENT, LP-AGRICULTURE	WOOD, MICHAEL AND DENISE	07N/05W-25R03	04/23/09	ALTO
----	AQUA CAPITAL MANAGEMENT, LP-AGRICULTURE	WOOD, MICHAEL AND DENISE	07N/05W-25R04	04/23/09	ALTO
438	RUDMAN, ROBERT T. AND SHIRLEY P. TRUSTS	AQUA CAPITAL MANAGEMENT, LP-AGRICULTURE	04N/03W-06G01	09/23/09	ALTO
438	RUDMAN, ROBERT T. AND SHIRLEY P. TRUSTS	AQUA CAPITAL MANAGEMENT, LP-AGRICULTURE	04N/03W-06G02	09/23/09	ALTO
438	RUDMAN, ROBERT T. AND SHIRLEY P. TRUSTS	AQUA CAPITAL MANAGEMENT, LP-AGRICULTURE	04N/03W-06G03	09/23/09	ALTO
439	STEIMLE FAMILY TRUST, A.B. AND Y.O.	KOERING, RICHARD AND KOERING, DONNA	11N/03E-32R01	09/23/09	BAJA
440	TRAHAN, ET AL.	TRAHAN, ELAINE	05N/03W-11E02	09/23/09	ALTO
440	TRAHAN, ET AL.	TRAHAN, ELAINE	05N/03W-11E04	09/23/09	ALTO
440	TRAHAN, ET AL.	TRAHAN, ELAINE	05N/03W-11E05	09/23/09	ALTO
441	TRAHAN, ELAINE	AQUA CAPITAL MANAGEMENT, LP-AGRICULTURE	05N/03W-11E02	09/23/09	ALTO
441	TRAHAN, ELAINE	AQUA CAPITAL MANAGEMENT, LP-AGRICULTURE	05N/03W-11E04	09/23/09	ALTO
441	TRAHAN, ELAINE	AQUA CAPITAL MANAGEMENT, LP-AGRICULTURE	05N/03W-11E05	09/23/09	ALTO
446	LEVINE, LESLIE	GABRYCH, EUGENE	08N/04E-07N01	10/28/09	BAJA
446	LEVINE, LESLIE	GABRYCH, EUGENE	09N/03E-13K01	10/28/09	BAJA
446	LEVINE, LESLIE	GABRYCH, EUGENE	09N/03E-13Q02	10/28/09	BAJA
446	LEVINE, LESLIE	GABRYCH, EUGENE	09N/03E-13Q04	10/28/09	BAJA
447	WAZZAN, ET AL.	ITALMOOD INC., ET. AL.	11N/03E-32E01	10/28/09	BAJA
447	WAZZAN, ET AL.	ITALMOOD INC., ET. AL.	11N/03E-32E02	10/28/09	BAJA

**TABLE 9
MOJAVE BASIN AREA
FACILITY TRANSFERS REPORTED TO WATERMASTER
OCTOBER 1, 1993 THROUGH SEPTEMBER 30, 2023**

TRANSFER NUMBER	TRANSFEROR	TRANSFeree	STATE WELL NUMBER	DATE OF CHANGE	SUBAREA
----	AQUA CAPITAL MANAGEMENT, LP-AGRICULTURE	NUÑEZ, LUIS SEGUNDO	05N/03W-11E02	01/06/10	ALTO
----	AQUA CAPITAL MANAGEMENT, LP-AGRICULTURE	NUÑEZ, LUIS SEGUNDO	05N/03W-11E04	01/06/10	ALTO
----	AQUA CAPITAL MANAGEMENT, LP-AGRICULTURE	NUÑEZ, LUIS SEGUNDO	05N/03W-11E05	01/06/10	ALTO
448	BRUINS, NICHOLAS	SZYNKOWSKI, RUTH J.	10N/03E-35P01	01/27/10	BAJA
448	BRUINS, NICHOLAS	SZYNKOWSKI, RUTH J.	10N/03E-35P02	01/27/10	BAJA
448	BRUINS, NICHOLAS	SZYNKOWSKI, RUTH J.	10N/03E-35P03	01/27/10	BAJA
448	BRUINS, NICHOLAS	SZYNKOWSKI, RUTH J.	10N/03E-35P04	01/27/10	BAJA
449	EVKHANIAN, JAMES H. AND PHYLLIS	BUSH, KEVIN	09N/04E-06L01	02/24/10	BAJA
449	EVKHANIAN, JAMES H. AND PHYLLIS	BUSH, KEVIN	09N/04E-06L02	02/24/10	BAJA
449	EVKHANIAN, JAMES H. AND PHYLLIS	BUSH, KEVIN	09N/04E-06L03	02/24/10	BAJA
450	CAMPBELL, BRYAN M.	CHAFa, LARRY R. AND DELINDA C.	10N/01W-31J01	03/24/10	CENTRO
450	CAMPBELL, BRYAN M.	CHAFa, LARRY R. AND DELINDA C.	10N/01W-31J02	03/24/10	CENTRO
451	LEVINE, DAVID AND MARGARET	DAGGETT RANCH, LLC	09N/01E-15N01	03/24/10	BAJA
451	LEVINE, DAVID AND MARGARET	DAGGETT RANCH, LLC	09N/01E-15N02	03/24/10	BAJA
451	LEVINE, DAVID AND MARGARET	DAGGETT RANCH, LLC	09N/01E-15N06	03/24/10	BAJA
451	LEVINE, DAVID AND MARGARET	DAGGETT RANCH, LLC	09N/01E-15N07	03/24/10	BAJA
451	LEVINE, DAVID AND MARGARET	DAGGETT RANCH, LLC	09N/01E-15P01	03/24/10	BAJA
452	ARTZ, RICHARD AND GLORIA	LAM, PHILLIP	08N/03E-03G01	05/26/10	BAJA
452	ARTZ, RICHARD AND GLORIA	LAM, PHILLIP	08N/03E-03G04	05/26/10	BAJA
453	CHANG, TIMOTHY AND JANE	MILLER LIVING TRUST	09N/03E-24C03	05/26/10	BAJA
454	DESERT VIEW DAIRY	ABENGOA SOLAR, INC.	11N/04W-32A02	05/26/10	CENTRO
455	WELLS, DANIEL W. AND CARMEN	HENSLEY, MARK P.	09N/03W-02M02	05/26/10	CENTRO
458	HESPERIA GOLF AND COUNTRY CLUB	HESPERIA, CITY OF	04N/04W-26C01	07/28/10	ALTO
----	DELANO ENTERPRISES, INC.	BARSTOW COMMUNITY DEVELOPERS, LLC	09N/02W-19G01	09/15/10	CENTRO
----	DELANO ENTERPRISES, INC.	BARSTOW COMMUNITY DEVELOPERS, LLC	09N/02W-19P01	09/15/10	CENTRO

**TABLE 9
MOJAVE BASIN AREA
FACILITY TRANSFERS REPORTED TO WATERMASTER
OCTOBER 1, 1993 THROUGH SEPTEMBER 30, 2023**

TRANSFER NUMBER	TRANSFEROR	TRANSFeree	STATE WELL NUMBER	DATE OF CHANGE	SUBAREA
----	DELANO ENTERPRISES, INC.	BARSTOW COMMUNITY DEVELOPERS, LLC	09N/02W-19P02	09/15/10	CENTRO
----	GORMAN, VIRGIL	PACIFIC GAS AND ELECTRIC	10N/03W-23K01	10/19/10	CENTRO
----	GORMAN, VIRGIL	PACIFIC GAS AND ELECTRIC	10N/03W-23Q01	10/19/10	CENTRO
----	GORMAN, VIRGIL	PACIFIC GAS AND ELECTRIC	10N/03W-23Q02	10/19/10	CENTRO
----	GORMAN, VIRGIL	PACIFIC GAS AND ELECTRIC	10N/03W-23Q03	10/19/10	CENTRO
----	GORMAN, VIRGIL	PACIFIC GAS AND ELECTRIC	10N/03W-23Q04	10/19/10	CENTRO
463	VAN BERG, JACK C.	VANHOOPS HOLDINGS, LP	03N/04W-28MD01	10/27/10	ALTO
463	VAN BERG, JACK C.	VANHOOPS HOLDINGS, LP	03N/04W-31A01	10/27/10	ALTO
463	VAN BERG, JACK C.	VANHOOPS HOLDINGS, LP	03N/04W-31AD01	10/27/10	ALTO
463	VAN BERG, JACK C.	VANHOOPS HOLDINGS, LP	03N/04W-32D01	10/27/10	ALTO
463	VAN BERG, JACK C.	VANHOOPS HOLDINGS, LP	03N/04W-32D02	10/27/10	ALTO
----	PALISADES RANCH	ROSS, CARL E. LIVING TRUST	07N/05W-24B01	11/02/10	ALTO
----	PALISADES RANCH	ROSS, CARL E. LIVING TRUST	07N/05W-24G01	11/02/10	ALTO
----	PALISADES RANCH	ROSS, CARL E. LIVING TRUST	07N/05W-24P05	11/02/10	ALTO
464	ADELANTO, CITY OF - GEORGE A F B	ADELANTO, CITY OF	06N/04W-30G01	12/09/10	ALTO
464	ADELANTO, CITY OF - GEORGE A F B	ADELANTO, CITY OF	06N/04W-30G02	12/09/10	ALTO
464	ADELANTO, CITY OF - GEORGE A F B	ADELANTO, CITY OF	06N/04W-30G03	12/09/10	ALTO
464	ADELANTO, CITY OF - GEORGE A F B	ADELANTO, CITY OF	06N/04W-30K03	12/09/10	ALTO
464	ADELANTO, CITY OF - GEORGE A F B	ADELANTO, CITY OF	06N/04W-30K04	12/09/10	ALTO
464	ADELANTO, CITY OF - GEORGE A F B	ADELANTO, CITY OF	06N/04W-30K05	12/09/10	ALTO
464	ADELANTO, CITY OF - GEORGE A F B	ADELANTO, CITY OF	06N/04W-30K10	12/09/10	ALTO
464	ADELANTO, CITY OF - GEORGE A F B	ADELANTO, CITY OF	06N/04W-30P05	12/09/10	ALTO
464	ADELANTO, CITY OF - GEORGE A F B	ADELANTO, CITY OF	06N/04W-30P06	12/09/10	ALTO
464	ADELANTO, CITY OF - GEORGE A F B	ADELANTO, CITY OF	06N/04W-30Q06	12/09/10	ALTO
470	DRIFFIN, TRAVIS AND LINDA	GAINES FAMILY TRUST, JACK AND MARY	10N/01W-33P07	01/26/11	CENTRO
473	PEARL, ALICE	AQUA CAPITAL MANAGEMENT, LP-AGRICULTURE	07N/04W-06J02	01/26/11	ALTO

**TABLE 9
MOJAVE BASIN AREA
FACILITY TRANSFERS REPORTED TO WATERMASTER
OCTOBER 1, 1993 THROUGH SEPTEMBER 30, 2023**

TRANSFER NUMBER	TRANSFEROR	TRANSFeree	STATE WELL NUMBER	DATE OF CHANGE	SUBAREA
----	DICK VAN DAM DAIRY	VAN DAM REVOCABLE FAMILY TRUST, DONALD DICK AND FRANCES L.	09N/02E-18F03	03/23/11	BAJA
----	DICK VAN DAM DAIRY	VAN DAM REVOCABLE FAMILY TRUST, DONALD DICK AND FRANCES L.	09N/02E-18H02	03/23/11	BAJA
----	DICK VAN DAM DAIRY	VAN DAM REVOCABLE FAMILY TRUST, DONALD DICK AND FRANCES L.	09N/02E-18H04	03/23/11	BAJA
----	DICK VAN DAM DAIRY	VAN DAM REVOCABLE FAMILY TRUST, DONALD DICK AND FRANCES L.	09N/02E-19E01	03/23/11	BAJA
----	DICK VAN DAM DAIRY	VAN DAM REVOCABLE FAMILY TRUST, DONALD DICK AND FRANCES L.	09N/02E-19L01	03/23/11	BAJA
----	DICK VAN DAM DAIRY	VAN DAM REVOCABLE FAMILY TRUST, DONALD DICK AND FRANCES L.	09N/02E-19L01	03/23/11	BAJA
474	BAGLEY, ROY	VACA, ANDY AND TERESITA S.	09N/03E-19E03	03/23/11	BAJA
476	HICKMAN, ALEX AND DEBE	TURNER, TERRY	10N/04E-31Q02	03/23/11	BAJA
476	HICKMAN, ALEX AND DEBE	TURNER, TERRY	10N/04E-31Q03	03/23/11	BAJA
476	HICKMAN, ALEX AND DEBE	TURNER, TERRY	10N/04E-31Q04	03/23/11	BAJA
477	HODGE, STANLEY W.	US BANK NATIONAL ASSOCIATION	05N/04W-14C01	03/23/11	ALTO
478	US BANK NATIONAL ASSOCIATION	AQUA CAPITAL MANAGEMENT, LP-AGRICULTURE	05N/04W-14C01	03/23/11	ALTO
----	AQUA CAPITAL MANAGEMENT, LP-AGRICULTURE	KANESAKA, KENJI AND YUKARI	05N/04W-14C01	05/18/11	ALTO
480	ABENGOA SOLAR, INC.	MOJAVE SOLAR, LLC	11N/04W-29J01	07/27/11	CENTRO
480	ABENGOA SOLAR, INC.	MOJAVE SOLAR, LLC	11N/04W-29P01	07/27/11	CENTRO
480	ABENGOA SOLAR, INC.	MOJAVE SOLAR, LLC	11N/04W-30B01	07/27/11	CENTRO
480	ABENGOA SOLAR, INC.	MOJAVE SOLAR, LLC	11N/04W-30D01	07/27/11	CENTRO
480	ABENGOA SOLAR, INC.	MOJAVE SOLAR, LLC	11N/04W-30E01	07/27/11	CENTRO
480	ABENGOA SOLAR, INC.	MOJAVE SOLAR, LLC	11N/04W-30M01	07/27/11	CENTRO
480	ABENGOA SOLAR, INC.	MOJAVE SOLAR, LLC	11N/04W-30N06	07/27/11	CENTRO
480	ABENGOA SOLAR, INC.	MOJAVE SOLAR, LLC	11N/04W-30N07	07/27/11	CENTRO

**TABLE 9
MOJAVE BASIN AREA
FACILITY TRANSFERS REPORTED TO WATERMASTER
OCTOBER 1, 1993 THROUGH SEPTEMBER 30, 2023**

TRANSFER NUMBER	TRANSFEROR	TRANSFeree	STATE WELL NUMBER	DATE OF CHANGE	SUBAREA
480	ABENGOA SOLAR, INC.	MOJAVE SOLAR, LLC	11N/04W-30P02	07/27/11	CENTRO
480	ABENGOA SOLAR, INC.	MOJAVE SOLAR, LLC	11N/04W-30Q03	07/27/11	CENTRO
480	ABENGOA SOLAR, INC.	MOJAVE SOLAR, LLC	11N/04W-32A02	07/27/11	CENTRO
480	ABENGOA SOLAR, INC.	MOJAVE SOLAR, LLC	11N/04W-32D03	07/27/11	CENTRO
480	ABENGOA SOLAR, INC.	MOJAVE SOLAR, LLC	11N/04W-33B02	07/27/11	CENTRO
480	ABENGOA SOLAR, INC.	MOJAVE SOLAR, LLC	11N/04W-33C02	07/27/11	CENTRO
480	ABENGOA SOLAR, INC.	MOJAVE SOLAR, LLC	11N/04W-33G04	07/27/11	CENTRO
480	ABENGOA SOLAR, INC.	MOJAVE SOLAR, LLC	11N/04W-33J01	07/27/11	CENTRO
481	GRIEDER, RAYMOND H. AND DORISANNE	FEDERAL NATIONAL MORTGAGE ASSOCIATION - FANNIE MAE	11N/04W-31J03	07/27/11	CENTRO
482	APPLE VALLEY COUNTRY CLUB	APPLE VALLEY, TOWN OF	05N/03W-18R03	09/28/11	ALTO
485	PATHFINDER INVESTORS	TSUI, RICHARD	09N/03E-14B01	09/28/11	BAJA
485	PATHFINDER INVESTORS	TSUI, RICHARD	09N/03E-14G01	09/28/11	BAJA
485	PATHFINDER INVESTORS	TSUI, RICHARD	09N/03E-14H01	09/28/11	BAJA
486	SIMMONS, JACK H. AND ETHUN, CLAUDIA	ORO GRANDE SCHOOL DISTRICT	06N/04W-19K02	09/28/11	ALTO
487	YKEMA TRUST	HUERTA, HECTOR	10N/02W-32P01	09/28/11	CENTRO
----	HANDLEY, DON R. AND MARY ANN	NORRIS TRUST, MARY ANN	05N/01W-31J01	01/12/12	ESTE
----	HANDLEY, DON R. AND MARY ANN	NORRIS TRUST, MARY ANN	05N/01W-31J02	01/12/12	ESTE
----	HANDLEY, DON R. AND MARY ANN	NORRIS TRUST, MARY ANN	05N/01W-32M01	01/12/12	ESTE
----	HANDLEY, DON R. AND MARY ANN	NORRIS TRUST, MARY ANN	05N/01W-32M02	01/12/12	ESTE
491	SANTUCCI, ANTONIO AND WILSA	SANTUCCI, ET AL.	08N/03E-01A03	01/25/12	BAJA
----	ROCK FOUNDATION, LLC	KASNER, ROBERT	09N/03E-28J02	05/23/12	BAJA
----	ROCK FOUNDATION, LLC	KASNER, ROBERT	09N/03E-28R02	05/23/12	BAJA
----	ROCK FOUNDATION, LLC	KASNER, ROBERT	09N/03E-28R03	05/23/12	BAJA
493	CAMPBELL, REGINALD F. AND JANET S.	SINGH, ET AL.	09N/04E-31J01	05/23/12	BAJA

**TABLE 9
MOJAVE BASIN AREA
FACILITY TRANSFERS REPORTED TO WATERMASTER
OCTOBER 1, 1993 THROUGH SEPTEMBER 30, 2023**

TRANSFER NUMBER	TRANSFEROR	TRANSFeree	STATE WELL NUMBER	DATE OF CHANGE	SUBAREA
493	CAMPBELL, REGINALD F. AND JANET S.	SINGH, ET AL.	09N/04E-31J02	05/23/12	BAJA
494	GOLD, HAROLD	DE JONG FAMILY TRUST	09N/03E-27R01	05/23/12	BAJA
496	SUDMEIER, TOD R AND TABITHA A	SCRAY, MICHELLE A.	03N/04W-33H05	05/23/12	ALTO
496	SUDMEIER, TOD R AND TABITHA A	SCRAY, MICHELLE A.	03N/04W-33H06	05/23/12	ALTO
496	SUDMEIER, TOD R AND TABITHA A	SCRAY, MICHELLE A.	03N/04W-33HS04	05/23/12	ALTO
497	VISOSKY, ESTATE OF JOSEPH F., SR.	SABA, SABA A. AND SHIRLEY L.	04N/01W-01E02	05/23/12	ESTE
497	VISOSKY, ESTATE OF JOSEPH F., SR.	SABA, SABA A. AND SHIRLEY L.	04N/01W-01F01	05/23/12	ESTE
----	KIEWIT PACIFIC COMPANY	SECURITY PAVING COMPANY, INC.	08N/03E-13C01	07/02/12	BAJA
499	DOCIMO, DONALD P.	STARKE, GEORGE A. AND JAYNE E.	09N/02E-14N06	07/25/12	BAJA
500	ROWLAND WATKINS 1996 TRUST, HELEN	WITHEY, CONNIE	09N/01W-10R02	07/25/12	CENTRO
500	ROWLAND WATKINS 1996 TRUST, HELEN	WITHEY, CONNIE	09N/01W-10R03	07/25/12	CENTRO
502	YANG FAMILY TRUST	PACIFIC GAS AND ELECTRIC	10N/03W-26G01	07/25/12	CENTRO
502	YANG FAMILY TRUST	PACIFIC GAS AND ELECTRIC	10N/03W-26G02	07/25/12	CENTRO
502	YANG FAMILY TRUST	PACIFIC GAS AND ELECTRIC	10N/03W-26G03	07/25/12	CENTRO
502	YANG FAMILY TRUST	PACIFIC GAS AND ELECTRIC	10N/03W-26K02	07/25/12	CENTRO
503	FARLEY, GREGGORY J.	WELLS FARGO BANK, NA	10N/04E-31M01	09/26/12	BAJA
503	FARLEY, GREGGORY J.	WELLS FARGO BANK, NA	10N/04E-31M02	09/26/12	BAJA
504	WELLS FARGO BANK, NA	RIZVI, S.R ALI	10N/04E-31M01	09/26/12	BAJA
504	WELLS FARGO BANK, NA	RIZVI, S.R ALI	10N/04E-31M02	09/26/12	BAJA
505	WALA AND WALA COMPANY, LLC	FERNANDEZ, ARTURO	09N/03E-01M01	09/26/12	BAJA
505	WALA AND WALA COMPANY, LLC	FERNANDEZ, ARTURO	09N/03E-01N01	09/26/12	BAJA
----	R.E. LOANS, LLC	HESPERIA VENTURE I, LLC	02N/04W-05ED01	11/28/12	ALTO
----	R.E. LOANS, LLC	HESPERIA VENTURE I, LLC	03N/04W-20P01	11/28/12	ALTO
----	R.E. LOANS, LLC	HESPERIA VENTURE I, LLC	03N/04W-21N01	11/28/12	ALTO
----	R.E. LOANS, LLC	HESPERIA VENTURE I, LLC	03N/04W-22K01	11/28/12	ALTO

**TABLE 9
MOJAVE BASIN AREA
FACILITY TRANSFERS REPORTED TO WATERMASTER
OCTOBER 1, 1993 THROUGH SEPTEMBER 30, 2023**

TRANSFER NUMBER	TRANSFEROR	TRANSFeree	STATE WELL NUMBER	DATE OF CHANGE	SUBAREA
----	R.E. LOANS, LLC	HESPERIA VENTURE I, LLC	03N/04W-26B01	11/28/12	ALTO
----	R.E. LOANS, LLC	HESPERIA VENTURE I, LLC	03N/04W-26B02	11/28/12	ALTO
----	R.E. LOANS, LLC	HESPERIA VENTURE I, LLC	03N/04W-26JS01	11/28/12	ALTO
----	R.E. LOANS, LLC	HESPERIA VENTURE I, LLC	03N/04W-26JS02	11/28/12	ALTO
----	R.E. LOANS, LLC	HESPERIA VENTURE I, LLC	03N/04W-26KD01	11/28/12	ALTO
----	R.E. LOANS, LLC	HESPERIA VENTURE I, LLC	03N/04W-26QD01	11/28/12	ALTO
----	R.E. LOANS, LLC	HESPERIA VENTURE I, LLC	03N/04W-27C01	11/28/12	ALTO
----	R.E. LOANS, LLC	HESPERIA VENTURE I, LLC	03N/04W-27G01	11/28/12	ALTO
----	R.E. LOANS, LLC	HESPERIA VENTURE I, LLC	03N/04W-28C01	11/28/12	ALTO
----	R.E. LOANS, LLC	HESPERIA VENTURE I, LLC	03N/04W-28G01	11/28/12	ALTO
----	R.E. LOANS, LLC	HESPERIA VENTURE I, LLC	03N/04W-28J01	11/28/12	ALTO
----	R.E. LOANS, LLC	HESPERIA VENTURE I, LLC	03N/04W-28P01	11/28/12	ALTO
----	R.E. LOANS, LLC	HESPERIA VENTURE I, LLC	03N/04W-28P02	11/28/12	ALTO
----	R.E. LOANS, LLC	HESPERIA VENTURE I, LLC	03N/04W-29L01	11/28/12	ALTO
----	R.E. LOANS, LLC	HESPERIA VENTURE I, LLC	03N/04W-29M01	11/28/12	ALTO
----	R.E. LOANS, LLC	HESPERIA VENTURE I, LLC	03N/04W-30D01	11/28/12	ALTO
----	R.E. LOANS, LLC	HESPERIA VENTURE I, LLC	03N/04W-30E01	11/28/12	ALTO
----	R.E. LOANS, LLC	HESPERIA VENTURE I, LLC	03N/04W-31A02	11/28/12	ALTO
----	R.E. LOANS, LLC	HESPERIA VENTURE I, LLC	03N/04W-31A03	11/28/12	ALTO
----	R.E. LOANS, LLC	HESPERIA VENTURE I, LLC	03N/04W-31B02	11/28/12	ALTO
----	R.E. LOANS, LLC	HESPERIA VENTURE I, LLC	03N/04W-31B03	11/28/12	ALTO
----	R.E. LOANS, LLC	HESPERIA VENTURE I, LLC	03N/04W-32AD01	11/28/12	ALTO
----	R.E. LOANS, LLC	HESPERIA VENTURE I, LLC	03N/04W-32C01	11/28/12	ALTO
----	R.E. LOANS, LLC	HESPERIA VENTURE I, LLC	03N/04W-33FS01	11/28/12	ALTO
----	R.E. LOANS, LLC	HESPERIA VENTURE I, LLC	03N/05W-25J01	11/28/12	ALTO
509	HOWSER, HUELL B.	CHAPMAN UNIVERSITY	09N/04E-21R01	11/28/12	BAJA

**TABLE 9
MOJAVE BASIN AREA
FACILITY TRANSFERS REPORTED TO WATERMASTER
OCTOBER 1, 1993 THROUGH SEPTEMBER 30, 2023**

TRANSFER NUMBER	TRANSFEROR	TRANSFeree	STATE WELL NUMBER	DATE OF CHANGE	SUBAREA
509	HOWSER, HUELL B.	CHAPMAN UNIVERSITY	09N/04E-21R02	11/28/12	BAJA
510	RIGGS, JOHN H. AND MILLICENT L.	IM, NICHOLAS NAK-KYUN	09N/04E-31H01	11/28/12	BAJA
510	RIGGS, JOHN H. AND MILLICENT L.	IM, NICHOLAS NAK-KYUN	09N/04E-32D01	11/28/12	BAJA
510	RIGGS, JOHN H. AND MILLICENT L.	IM, NICHOLAS NAK-KYUN	09N/04E-32D02	11/28/12	BAJA
510	RIGGS, JOHN H. AND MILLICENT L.	IM, NICHOLAS NAK-KYUN	09N/04E-32E01	11/28/12	BAJA
511	SL INVESTMENT GROUP, LLC	UNITED CENTRAL BANK	10N/03E-20C02	11/28/12	BAJA
511	SL INVESTMENT GROUP, LLC	UNITED CENTRAL BANK	10N/03E-20D01	11/28/12	BAJA
511	SL INVESTMENT GROUP, LLC	UNITED CENTRAL BANK	10N/03E-20E01	11/28/12	BAJA
512	MEADOWBROOK DAIRY	PHELAN PIÑON HILLS COMMUNITY SERVICES DISTRICT	06N/07W-14K01	11/28/12	OESTE
512	MEADOWBROOK DAIRY	PHELAN PIÑON HILLS COMMUNITY SERVICES DISTRICT	06N/07W-14K02	11/28/12	OESTE
512	MEADOWBROOK DAIRY	PHELAN PIÑON HILLS COMMUNITY SERVICES DISTRICT	06N/07W-14Q02	11/28/12	OESTE
512	MEADOWBROOK DAIRY	PHELAN PIÑON HILLS COMMUNITY SERVICES DISTRICT	06N/07W-23F01	11/28/12	OESTE
512	MEADOWBROOK DAIRY	PHELAN PIÑON HILLS COMMUNITY SERVICES DISTRICT	06N/07W-26J01	11/28/12	OESTE
512	MEADOWBROOK DAIRY	PHELAN PIÑON HILLS COMMUNITY SERVICES DISTRICT	06N/07W-26J02	11/28/12	OESTE
512	MEADOWBROOK DAIRY	PHELAN PIÑON HILLS COMMUNITY SERVICES DISTRICT	06N/07W-26K03	11/28/12	OESTE
513	RANCHO LAS FLORES, LLC	R.E. LOANS, LLC	02N/04W-05ED01	11/28/12	ALTO
513	RANCHO LAS FLORES, LLC	R.E. LOANS, LLC	03N/04W-20P01	11/28/12	ALTO
513	RANCHO LAS FLORES, LLC	R.E. LOANS, LLC	03N/04W-21N01	11/28/12	ALTO
513	RANCHO LAS FLORES, LLC	R.E. LOANS, LLC	03N/04W-22K01	11/28/12	ALTO
513	RANCHO LAS FLORES, LLC	R.E. LOANS, LLC	03N/04W-26B01	11/28/12	ALTO

**TABLE 9
MOJAVE BASIN AREA
FACILITY TRANSFERS REPORTED TO WATERMASTER
OCTOBER 1, 1993 THROUGH SEPTEMBER 30, 2023**

TRANSFER NUMBER	TRANSFEROR	TRANSFeree	STATE WELL NUMBER	DATE OF CHANGE	SUBAREA
513	RANCHO LAS FLORES, LLC	R.E. LOANS, LLC	03N/04W-26B02	11/28/12	ALTO
513	RANCHO LAS FLORES, LLC	R.E. LOANS, LLC	03N/04W-26JS01	11/28/12	ALTO
513	RANCHO LAS FLORES, LLC	R.E. LOANS, LLC	03N/04W-26JS02	11/28/12	ALTO
513	RANCHO LAS FLORES, LLC	R.E. LOANS, LLC	03N/04W-26KD01	11/28/12	ALTO
513	RANCHO LAS FLORES, LLC	R.E. LOANS, LLC	03N/04W-26QD01	11/28/12	ALTO
513	RANCHO LAS FLORES, LLC	R.E. LOANS, LLC	03N/04W-27C01	11/28/12	ALTO
513	RANCHO LAS FLORES, LLC	R.E. LOANS, LLC	03N/04W-27G01	11/28/12	ALTO
513	RANCHO LAS FLORES, LLC	R.E. LOANS, LLC	03N/04W-28C01	11/28/12	ALTO
513	RANCHO LAS FLORES, LLC	R.E. LOANS, LLC	03N/04W-28G01	11/28/12	ALTO
513	RANCHO LAS FLORES, LLC	R.E. LOANS, LLC	03N/04W-28J01	11/28/12	ALTO
513	RANCHO LAS FLORES, LLC	R.E. LOANS, LLC	03N/04W-28P01	11/28/12	ALTO
513	RANCHO LAS FLORES, LLC	R.E. LOANS, LLC	03N/04W-28P02	11/28/12	ALTO
513	RANCHO LAS FLORES, LLC	R.E. LOANS, LLC	03N/04W-29L01	11/28/12	ALTO
513	RANCHO LAS FLORES, LLC	R.E. LOANS, LLC	03N/04W-29M01	11/28/12	ALTO
513	RANCHO LAS FLORES, LLC	R.E. LOANS, LLC	03N/04W-30D01	11/28/12	ALTO
513	RANCHO LAS FLORES, LLC	R.E. LOANS, LLC	03N/04W-30E01	11/28/12	ALTO
513	RANCHO LAS FLORES, LLC	R.E. LOANS, LLC	03N/04W-31A02	11/28/12	ALTO
513	RANCHO LAS FLORES, LLC	R.E. LOANS, LLC	03N/04W-31A03	11/28/12	ALTO
513	RANCHO LAS FLORES, LLC	R.E. LOANS, LLC	03N/04W-31B02	11/28/12	ALTO
513	RANCHO LAS FLORES, LLC	R.E. LOANS, LLC	03N/04W-31B03	11/28/12	ALTO
513	RANCHO LAS FLORES, LLC	R.E. LOANS, LLC	03N/04W-32AD01	11/28/12	ALTO
513	RANCHO LAS FLORES, LLC	R.E. LOANS, LLC	03N/04W-32C01	11/28/12	ALTO
513	RANCHO LAS FLORES, LLC	R.E. LOANS, LLC	03N/04W-33FS01	11/28/12	ALTO
513	RANCHO LAS FLORES, LLC	R.E. LOANS, LLC	03N/05W-25J01	11/28/12	ALTO
520	MOUNTAIN VIEW, L.L.C.	PACIFIC GAS AND ELECTRIC COMPANY	10N/03W-34A02	01/23/13	CENTRO
520	MOUNTAIN VIEW, L.L.C.	PACIFIC GAS AND ELECTRIC COMPANY	10N/03W-34A03	01/23/13	CENTRO

**TABLE 9
MOJAVE BASIN AREA
FACILITY TRANSFERS REPORTED TO WATERMASTER
OCTOBER 1, 1993 THROUGH SEPTEMBER 30, 2023**

TRANSFER NUMBER	TRANSFEROR	TRANSFeree	STATE WELL NUMBER	DATE OF CHANGE	SUBAREA
520	MOUNTAIN VIEW, L.L.C.	PACIFIC GAS AND ELECTRIC COMPANY	10N/03W-34A04	01/23/13	CENTRO
520	MOUNTAIN VIEW, L.L.C.	PACIFIC GAS AND ELECTRIC COMPANY	10N/03W-34A05	01/23/13	CENTRO
520	MOUNTAIN VIEW, L.L.C.	PACIFIC GAS AND ELECTRIC COMPANY	10N/03W-34A07	01/23/13	CENTRO
520	MOUNTAIN VIEW, L.L.C.	PACIFIC GAS AND ELECTRIC COMPANY	10N/03W-34B01	01/23/13	CENTRO
520	MOUNTAIN VIEW, L.L.C.	PACIFIC GAS AND ELECTRIC COMPANY	10N/03W-34B03	01/23/13	CENTRO
521	SHIRKEY, ALAN G. AND MARY E.	PACIFIC GAS AND ELECTRIC COMPANY	10N/03W-14D01	01/23/13	CENTRO
521	SHIRKEY, ALAN G. AND MARY E.	PACIFIC GAS AND ELECTRIC COMPANY	10N/03W-14E01	01/23/13	CENTRO
521	SHIRKEY, ALAN G. AND MARY E.	PACIFIC GAS AND ELECTRIC COMPANY	10N/03W-14E02	01/23/13	CENTRO
521	SHIRKEY, ALAN G. AND MARY E.	PACIFIC GAS AND ELECTRIC COMPANY	10N/03W-14E03	01/23/13	CENTRO
521	SHIRKEY, ALAN G. AND MARY E.	PACIFIC GAS AND ELECTRIC COMPANY	10N/03W-14E04	01/23/13	CENTRO
521	SHIRKEY, ALAN G. AND MARY E.	PACIFIC GAS AND ELECTRIC COMPANY	10N/03W-14E05	01/23/13	CENTRO
521	SHIRKEY, ALAN G. AND MARY E.	PACIFIC GAS AND ELECTRIC COMPANY	10N/03W-14E06	01/23/13	CENTRO
522	VOGLER, ET AL.	VOGLER, ALBERT H. AND RITA K.	04N/03W-30D03	01/23/13	ALTO
524	VANHOY, ESTATE OF LUTHER C.	PACIFIC GAS AND ELECTRIC COMPANY	10N/03W-04J01	03/27/13	CENTRO
524	VANHOY, ESTATE OF LUTHER C.	PACIFIC GAS AND ELECTRIC COMPANY	10N/03W-04J02	03/27/13	CENTRO
525	UNITED CENTRAL BANK	GARG, OM P.	10N/03E-20C02	03/27/13	BAJA
525	UNITED CENTRAL BANK	GARG, OM P.	10N/03E-20D01	03/27/13	BAJA
525	UNITED CENTRAL BANK	GARG, OM P.	10N/03E-20E01	03/27/13	BAJA
526	HARE TRUST	PACIFIC GAS AND ELECTRIC COMPANY	09N/02W-06E07	05/22/13	CENTRO
526	HARE TRUST	PACIFIC GAS AND ELECTRIC COMPANY	09N/02W-06E12	05/22/13	CENTRO
527	RYKEN, PAUL, ET AL.	PACIFIC GAS AND ELECTRIC COMPANY	10N/03W-27M01	05/22/13	CENTRO
527	RYKEN, PAUL, ET AL.	PACIFIC GAS AND ELECTRIC COMPANY	10N/03W-27M02	05/22/13	CENTRO
527	RYKEN, PAUL, ET AL.	PACIFIC GAS AND ELECTRIC COMPANY	10N/03W-27M03	05/22/13	CENTRO
529	REEVES, RICHARD	IM, NICHOLAS NAK-KYUN	09N/04E-32M01	07/24/13	BAJA
529	REEVES, RICHARD	IM, NICHOLAS NAK-KYUN	09N/04E-32M02	07/24/13	BAJA
529	REEVES, RICHARD	IM, NICHOLAS NAK-KYUN	09N/04E-32M03	07/24/13	BAJA

**TABLE 9
MOJAVE BASIN AREA
FACILITY TRANSFERS REPORTED TO WATERMASTER
OCTOBER 1, 1993 THROUGH SEPTEMBER 30, 2023**

TRANSFER NUMBER	TRANSFEROR	TRANSFeree	STATE WELL NUMBER	DATE OF CHANGE	SUBAREA
532	JO, MYUNG HYUN	AHN REVOCABLE TRUST	04N/02E-17J02	09/25/13	ESTE
535	SANTUCCI, ET AL.	SAMRA, JAGTAR S.	08N/03E-01A03	12/12/13	BAJA
537	PAK, EDWIN H.	PARK, STEWART C.	09N/03E-14E01	12/12/13	BAJA
537	PAK, EDWIN H.	PARK, STEWART C.	09N/03E-14E02	12/12/13	BAJA
----	VAN DAM RFT, DONALD DICK AND FRANCES L.	VAN DAM FAMILY TRUST, GLEN AND JENNIFER	09N/02E-18F03	01/31/14	BAJA
----	VAN DAM RFT, DONALD DICK AND FRANCES L.	VAN DAM FAMILY TRUST, GLEN AND JENNIFER	09N/02E-18H02	01/31/14	BAJA
----	VAN DAM RFT, DONALD DICK AND FRANCES L.	VAN DAM FAMILY TRUST, GLEN AND JENNIFER	09N/02E-18H04	01/31/14	BAJA
----	VAN DAM RFT, DONALD DICK AND FRANCES L.	VAN DAM FAMILY TRUST, GLEN AND JENNIFER	09N/02E-19E01	01/31/14	BAJA
----	VAN DAM RFT, DONALD DICK AND FRANCES L.	VAN DAM FAMILY TRUST, GLEN AND JENNIFER	09N/02E-19L01	01/31/14	BAJA
539	ELMER, JOHN AND DONNA L.	BUDGET FINANCE COMPANY	09N/03E-24B01	02/26/14	BAJA
539	ELMER, JOHN AND DONNA L.	BUDGET FINANCE COMPANY	09N/03E-24G03	02/26/14	BAJA
540	HERMANAS MISIONERAS SERVIDORAS DE LA PALABRA	PACIFIC GAS AND ELECTRIC COMPANY	09N/03W-01F01	02/26/14	CENTRO
541	YKEMA TRUST	HARMSSEN FAMILY TRUST	10N/03W-36J03	02/26/14	CENTRO
541	YKEMA TRUST	HARMSSEN FAMILY TRUST	10N/03W-36J04	02/26/14	CENTRO
541	YKEMA TRUST	HARMSSEN FAMILY TRUST	10N/03W-36K02	02/26/14	CENTRO
541	YKEMA TRUST	HARMSSEN FAMILY TRUST	10N/03W-36R03	02/26/14	CENTRO
541	YKEMA TRUST	HARMSSEN FAMILY TRUST	10N/03W-36R06	02/26/14	CENTRO
544	HARMSSEN FAMILY TRUST	PACIFIC GAS AND ELECTRIC COMPANY	10N/03W-36R03	03/26/14	CENTRO
544	HARMSSEN FAMILY TRUST	PACIFIC GAS AND ELECTRIC COMPANY	10N/03W-36R06	03/26/14	CENTRO
545	NEWBERRY CORPORATION	WAZZAN, BOURHAN A. K.	10N/03E-16Q04	03/26/14	BAJA
----	AQUA CAPITAL MANAGEMENT, LP-AGRICULTURE	PHAM, ET AL.	04N/03W-06G01	04/07/14	ALTO
----	AQUA CAPITAL MANAGEMENT, LP-AGRICULTURE	PHAM, ET AL.	04N/03W-06G02	04/07/14	ALTO
----	AQUA CAPITAL MANAGEMENT, LP-AGRICULTURE	PHAM, ET AL.	04N/03W-06G03	04/07/14	ALTO
547	SHINTAKU, RICHARD AND CHERYL	LAVANH, ET AL.	09N/02E-14N07	05/28/14	BAJA

**TABLE 9
MOJAVE BASIN AREA
FACILITY TRANSFERS REPORTED TO WATERMASTER
OCTOBER 1, 1993 THROUGH SEPTEMBER 30, 2023**

TRANSFER NUMBER	TRANSFEROR	TRANSFeree	STATE WELL NUMBER	DATE OF CHANGE	SUBAREA
548	WAZZAN, BOURHAN A. K.	LO, ET AL.	10N/03E-16Q04	05/28/14	BAJA
----	AQUA CAPITAL MANAGEMENT, LP-AGRICULTURE	CROCKER, BRIAN J.	07N/04W-06J02	07/03/14	ALTO
549	HOWARD REVOCABLE TRUST	HOWARD, ET AL.	10N/02W-36P06	07/23/14	CENTRO
554	PARK, STEWART C.	AHN, CHUN SOO AND WHA JA	09N/03E-14E01	09/24/14	BAJA
554	PARK, STEWART C.	AHN, CHUN SOO AND WHA JA	09N/03E-14E02	09/24/14	BAJA
571	ABBOTT FAMILY TRUST	ABBOTT, CARRON	07N/05W-36H01	09/23/15	ALTO
571	ABBOTT FAMILY TRUST	ABBOTT, CARRON	07N/05W-36H02	09/23/15	ALTO
575	BEDINGFIELD, LYNDELL AND CHARLENE	MCDONNELL, JEFFREY P. AND MICHAEL F.	09N/03E-30D03	09/23/15	BAJA
575	BEDINGFIELD, LYNDELL AND CHARLENE	MCDONNELL, JEFFREY P. AND MICHAEL F.	09N/03E-30D05	09/23/15	BAJA
576	MCDONNELL, JEFFREY P. AND MICHAEL F.	O. F. D. L., INC.	09N/03E-30D03	09/23/15	BAJA
576	MCDONNELL, JEFFREY P. AND MICHAEL F.	O. F. D. L., INC.	09N/03E-30D05	09/23/15	BAJA
577	YERMO WATER COMPANY	APPLE VALLEY RANCHOS WATER COMPANY	09N/01E-01A01	09/23/15	BAJA
577	YERMO WATER COMPANY	APPLE VALLEY RANCHOS WATER COMPANY	09N/01E-01C01	09/23/15	BAJA
577	YERMO WATER COMPANY	APPLE VALLEY RANCHOS WATER COMPANY	09N/01E-01C02	09/23/15	BAJA
577	YERMO WATER COMPANY	APPLE VALLEY RANCHOS WATER COMPANY	09N/01E-02B01	09/23/15	BAJA
577	YERMO WATER COMPANY	APPLE VALLEY RANCHOS WATER COMPANY	09N/01E-02B05	09/23/15	BAJA
577	YERMO WATER COMPANY	APPLE VALLEY RANCHOS WATER COMPANY	09N/01E-02B08	09/23/15	BAJA
577	YERMO WATER COMPANY	APPLE VALLEY RANCHOS WATER COMPANY	09N/02E-06C01	09/23/15	BAJA
577	YERMO WATER COMPANY	APPLE VALLEY RANCHOS WATER COMPANY	09N/02E-06D01	09/23/15	BAJA
577	YERMO WATER COMPANY	APPLE VALLEY RANCHOS WATER COMPANY	10N/02E-31N05	09/23/15	BAJA
580	FAWCETT, EDWARD C.	JACKS, JAMES F.	09N/02E-12P03	10/28/15	BAJA
583	RIVERSIDE CEMENT COMPANY - AGRICULTURE	CALPORTLAND COMPANY - AGRICULTURE	06N/04W-18N01	10/28/15	ALTO
583	RIVERSIDE CEMENT COMPANY - AGRICULTURE	CALPORTLAND COMPANY - AGRICULTURE	06N/04W-19E01	10/28/15	ALTO
584	RIVERSIDE CEMENT COMPANY - ORO GRANDE PLANT	CALPORTLAND COMPANY - ORO GRANDE PLANT	06N/04W-18F05	10/28/15	ALTO

**TABLE 9
MOJAVE BASIN AREA
FACILITY TRANSFERS REPORTED TO WATERMASTER
OCTOBER 1, 1993 THROUGH SEPTEMBER 30, 2023**

TRANSFER NUMBER	TRANSFEROR	TRANSFeree	STATE WELL NUMBER	DATE OF CHANGE	SUBAREA
584	RIVERSIDE CEMENT COMPANY - ORO GRANDE PLANT	CALPORTLAND COMPANY - ORO GRANDE PLANT	06N/04W-18L03	10/28/15	ALTO
584	RIVERSIDE CEMENT COMPANY - ORO GRANDE PLANT	CALPORTLAND COMPANY - ORO GRANDE PLANT	06N/04W-19C09	10/28/15	ALTO
584	RIVERSIDE CEMENT COMPANY - ORO GRANDE PLANT	CALPORTLAND COMPANY - ORO GRANDE PLANT	06N/04W-19C10	10/28/15	ALTO
584	RIVERSIDE CEMENT COMPANY - ORO GRANDE PLANT	CALPORTLAND COMPANY - ORO GRANDE PLANT	06N/04W-19C13	10/28/15	ALTO
584	RIVERSIDE CEMENT COMPANY - ORO GRANDE PLANT	CALPORTLAND COMPANY - ORO GRANDE PLANT	06N/04W-19D01	10/28/15	ALTO
584	RIVERSIDE CEMENT COMPANY - ORO GRANDE PLANT	CALPORTLAND COMPANY - ORO GRANDE PLANT	06N/04W-30J01	10/28/15	ALTO
584	RIVERSIDE CEMENT COMPANY - ORO GRANDE PLANT	CALPORTLAND COMPANY - ORO GRANDE PLANT	06N/04W-30J02	10/28/15	ALTO
584	RIVERSIDE CEMENT COMPANY - ORO GRANDE PLANT	CALPORTLAND COMPANY - ORO GRANDE PLANT	06N/04W-30J03	10/28/15	ALTO
584	RIVERSIDE CEMENT COMPANY - ORO GRANDE PLANT	CALPORTLAND COMPANY - ORO GRANDE PLANT	06N/04W-30J04	10/28/15	ALTO
585	VIROSTECK, STEVE AND JULIE	DACOSTA, DEAN EDWARD	04N/01W-23C10	10/28/15	ESTE
585	VIROSTECK, STEVE AND JULIE	DACOSTA, DEAN EDWARD	04N/01W-23C11	10/28/15	ESTE
586	HARVEY, LISA M.	AHN, CHUN SOO AND DAVID	05N/01E-29R01	01/27/16	ESTE
586	HARVEY, LISA M.	AHN, CHUN SOO AND DAVID	05N/01E-29R02	01/27/16	ESTE
590	ROSS, CARL E. LIVING TRUST	WESTERN RIVERS CONSERVANCY	07N/05W-24B01	02/24/16	ALTO
590	ROSS, CARL E. LIVING TRUST	WESTERN RIVERS CONSERVANCY	07N/05W-24B02	02/24/16	ALTO
590	ROSS, CARL E. LIVING TRUST	WESTERN RIVERS CONSERVANCY	07N/05W-24G01	02/24/16	ALTO
590	ROSS, CARL E. LIVING TRUST	WESTERN RIVERS CONSERVANCY	07N/05W-24P04	02/24/16	ALTO
590	ROSS, CARL E. LIVING TRUST	WESTERN RIVERS CONSERVANCY	07N/05W-24P05	02/24/16	ALTO

**TABLE 9
MOJAVE BASIN AREA
FACILITY TRANSFERS REPORTED TO WATERMASTER
OCTOBER 1, 1993 THROUGH SEPTEMBER 30, 2023**

TRANSFER NUMBER	TRANSFEROR	TRANSFeree	STATE WELL NUMBER	DATE OF CHANGE	SUBAREA
591	SMITH, ROBERT A.	PACIFIC GAS AND ELECTRIC COMPANY	09N/02W-06B06	02/29/16	CENTRO
592	CAMPBELL FAMILY TRUST	S AND E 786 ENTERPRISES, LLC	04N/01E-05G02	03/23/16	ESTE
592	CAMPBELL FAMILY TRUST	S AND E 786 ENTERPRISES, LLC	05N/01E-32Q02	03/23/16	ESTE
593	CHAPMAN UNIVERSITY	EVERT FAMILY TRUST	09N/04E-21R01	03/23/16	BAJA
593	CHAPMAN UNIVERSITY	EVERT FAMILY TRUST	09N/04E-21R02	03/23/16	BAJA
----	DAILY, DAVID O. AND ELIZABETH	EAST DESERT LAND COMPANY, LLC	07N/04W-06A02	06/17/16	ALTO
----	DAILY, DAVID O. AND ELIZABETH	EAST DESERT LAND COMPANY, LLC	07N/04W-07B03	06/17/16	ALTO
----	DAILY, DAVID O. AND ELIZABETH	EAST DESERT LAND COMPANY, LLC	07N/04W-07B05	06/17/16	ALTO
----	DAILY, DAVID O. AND ELIZABETH	EAST DESERT LAND COMPANY, LLC	07N/04W-07C06	06/17/16	ALTO
----	DAILY, DAVID O. AND ELIZABETH	EAST DESERT LAND COMPANY, LLC	07N/04W-07C07	06/17/16	ALTO
----	DAILY, DAVID O. AND ELIZABETH	EAST DESERT LAND COMPANY, LLC	07N/04W-07C08	06/17/16	ALTO
----	DAILY, DAVID O. AND ELIZABETH	EAST DESERT LAND COMPANY, LLC	07N/04W-07C10	06/17/16	ALTO
603	KENWOOD MANAGEMENT, LLC	CHONG, JOAN	08N/04W-10G01	07/27/16	CENTRO
603	KENWOOD MANAGEMENT, LLC	CHONG, JOAN	08N/04W-10G02	07/27/16	CENTRO
604	OLD GROVE PROPERTIES, LLC	35250 YERMO, LLC	09N/01E-05H03	07/27/16	BAJA
605	KIEL, MARY	SAGABEAN-BARKER, KANOELOKELANI L.	09N/02E-11Q01	09/28/16	BAJA
605	KIEL, MARY	SAGABEAN-BARKER, KANOELOKELANI L.	09N/02E-11Q06	09/28/16	BAJA
605	KIEL, MARY	SAGABEAN-BARKER, KANOELOKELANI L.	09N/02E-11Q07	09/28/16	BAJA
608	D'SILVA, MELANIE	POZZATO PARTNERS, LIMITED	10N/01E-35P02	02/22/17	BAJA
608	D'SILVA, MELANIE	POZZATO PARTNERS, LIMITED	10N/01E-35P12	02/22/17	BAJA
----	LEYERLY, RICHARD	RUISCH, ET AL.	10N/02W-31P01	02/28/17	CENTRO
----	SECURITY PAVING COMPANY, INC.	CALMAT COMPANY	08N/03E-13C01	05/05/17	BAJA
625	SUNRAY ENERGY, INC.	SUNRAY LAND COMPANY, LLC	09N/01E-13K01	09/27/17	BAJA
625	SUNRAY ENERGY, INC.	SUNRAY LAND COMPANY, LLC	09N/01E-13Q09	09/27/17	BAJA
625	SUNRAY ENERGY, INC.	SUNRAY LAND COMPANY, LLC	09N/01E-24A02	09/27/17	BAJA

**TABLE 9
MOJAVE BASIN AREA
FACILITY TRANSFERS REPORTED TO WATERMASTER
OCTOBER 1, 1993 THROUGH SEPTEMBER 30, 2023**

TRANSFER NUMBER	TRANSFEROR	TRANSFeree	STATE WELL NUMBER	DATE OF CHANGE	SUBAREA
625	SUNRAY ENERGY, INC.	SUNRAY LAND COMPANY, LLC	09N/01E-24G01	09/27/17	BAJA
625	SUNRAY ENERGY, INC.	SUNRAY LAND COMPANY, LLC	09N/01E-24G02	09/27/17	BAJA
629	PEARSON, DERYL B.	BOX, GEARY S. AND LAURA	04N/03W-31A01	03/28/18	ALTO
629	PEARSON, DERYL B.	BOX, GEARY S. AND LAURA	04N/03W-31A02	03/28/18	ALTO
630	WESTERN HERITAGE, INC.	HAWKINS, JAMES B.	09N/02E-05B01	03/28/18	BAJA
----	NURSERY PRODUCTS LLC	SYNAGROW-WWT, INC. (DBA NURSURY PRODUCTS, LLC)	10N/05W-36J01	04/23/18	CENTRO
----	NURSERY PRODUCTS LLC	SYNAGROW-WWT, INC. (DBA NURSURY PRODUCTS, LLC)	10N/05W-36J02	04/23/18	CENTRO
631	TSUI, RICHARD	NEWBERRY SPRINGS RECREATIONAL LAKES ASSOCIATION	09N/03E-14B01	05/23/18	BAJA
631	TSUI, RICHARD	NEWBERRY SPRINGS RECREATIONAL LAKES ASSOCIATION	09N/03E-14G01	05/23/18	BAJA
631	TSUI, RICHARD	NEWBERRY SPRINGS RECREATIONAL LAKES ASSOCIATION	09N/03E-14H01	05/25/18	BAJA
639	SHORT, CHARLES H. REVOCABLE TRUST	BUBIER, DIANE GAIL	09N/03E-10B01	07/25/18	BAJA
641	SMITH, WILLIAM E. AND PATRICIA A.	QUAKENBUSH, SAMUEL R.	09N/04E-18R01	09/26/18	BAJA
641	SMITH, WILLIAM E. AND PATRICIA A.	QUAKENBUSH, SAMUEL R.	09N/04E-18R02	09/26/18	BAJA
648	POZZATO PARTNERS, LIMITED	FOOTHILL ESTATES MHP, LLC	10N/01E-35P02	01/23/19	BAJA
648	POZZATO PARTNERS, LIMITED	FOOTHILL ESTATES MHP, LLC	10N/01E-35P12	01/23/19	BAJA
649	WESTERN RIVERS CONSERVANCY	MOJAVE DESERT LAND TRUST	07N/05W-24B01	01/23/19	ALTO
649	WESTERN RIVERS CONSERVANCY	MOJAVE DESERT LAND TRUST	07N/05W-24B02	01/23/19	ALTO
649	WESTERN RIVERS CONSERVANCY	MOJAVE DESERT LAND TRUST	07N/05W-24G01	01/23/19	ALTO
649	WESTERN RIVERS CONSERVANCY	MOJAVE DESERT LAND TRUST	07N/05W-24P04	01/23/19	ALTO
649	WESTERN RIVERS CONSERVANCY	MOJAVE DESERT LAND TRUST	07N/05W-24P05	01/23/19	ALTO
650	HAL-DOR LTD.	DJC CORPORATION	04N/01E-09N01	02/27/19	ESTE

**TABLE 9
MOJAVE BASIN AREA
FACILITY TRANSFERS REPORTED TO WATERMASTER
OCTOBER 1, 1993 THROUGH SEPTEMBER 30, 2023**

TRANSFER NUMBER	TRANSFEROR	TRANSFeree	STATE WELL NUMBER	DATE OF CHANGE	SUBAREA
651	DJC CORPORATION	JONES TRUST DATED MARCH 16, 2002	03N/01W-12H05	02/27/19	ESTE
651	DJC CORPORATION	JONES TRUST DATED MARCH 16, 2002	03N/01W-12L01	02/27/19	ESTE
651	DJC CORPORATION	JONES TRUST DATED MARCH 16, 2002	04N/01E-09N01	02/27/19	ESTE
658	SHAW, ROBERT M. AND LORI A. SLATER-SHAW	SAMPLES, BERNARD D. AND JANICE E.	09N/03E-13M02	05/22/19	BAJA
----	OSTERKAMP, GEROLD	DE VRIES REVOCABLE TRUST 12-10-2015	08N/04W-15C01	07/10/19	CENTRO
----	OSTERKAMP, GEROLD	DE VRIES REVOCABLE TRUST 12-10-2015	08N/04W-15F03	07/10/19	CENTRO
----	OSTERKAMP, GEROLD	DE VRIES REVOCABLE TRUST 12-10-2015	08N/04W-15F04	07/10/19	CENTRO
----	LEYERLY, GENEVA	LEYERLY, RICHARD	10N/03W-27P03	07/10/19	CENTRO
----	LEYERLY, GENEVA	LEYERLY, RICHARD	10N/03W-27P04	07/10/19	CENTRO
660	CF PROPERTIES, LLC	PRECISION INVESTMENTS SERVICES, LLC	09N/03E-22L01	07/24/19	BAJA
662	DOCIMO LIVING TRUST, ALLEN LEE	NSSLC, INC.	09N/04E-19C01	07/24/19	BAJA
664	BROWN, RONALD A.	NEWBERRY SPRINGS RECREATIONAL LAKES ASSOCIATION	09N/03E-14J01	09/25/19	BAJA
664	BROWN, RONALD A.	NEWBERRY SPRINGS RECREATIONAL LAKES ASSOCIATION	09N/03E-14Q01	09/25/19	BAJA
665	MCINNIS, WILLIAM S.	FINCH, JENIFER	04N/03W-30A03	09/25/19	ALTO
665	MCINNIS, WILLIAM S.	FINCH, JENIFER	04N/03W-30A09	09/25/19	ALTO
----	NEWBERRY SPRINGS RECREATIONAL LAKES ASSOCIATION	CLARK, GARY AND BETH A.	09N/03E-14J01	11/14/19	BAJA
----	NEWBERRY SPRINGS RECREATIONAL LAKES ASSOCIATION	CLARK, GARY AND BETH A.	09N/03E-14Q01	11/14/19	BAJA
676	BORGOGNO REVOCABLE LIVING TRUST	VAN DAM FAMILY TRUST, GLEN AND JENNIFER	09N/02E-17H01	12/12/19	BAJA
676	BORGOGNO REVOCABLE LIVING TRUST	VAN DAM FAMILY TRUST, GLEN AND JENNIFER	09N/02E-17J01	12/12/19	BAJA
676	BORGOGNO REVOCABLE LIVING TRUST	VAN DAM FAMILY TRUST, GLEN AND JENNIFER	09N/02E-17Q01	12/12/19	BAJA
677	JOHNSON, JAMES R. AND ELLEN	IM, NICHOLAS NAK-KYUN	09N/03E-25R04	12/12/19	BAJA
677	JOHNSON, JAMES R. AND ELLEN	IM, NICHOLAS NAK-KYUN	09N/03E-25R05	12/12/19	BAJA

**TABLE 9
MOJAVE BASIN AREA
FACILITY TRANSFERS REPORTED TO WATERMASTER
OCTOBER 1, 1993 THROUGH SEPTEMBER 30, 2023**

TRANSFER NUMBER	TRANSFEROR	TRANSFeree	STATE WELL NUMBER	DATE OF CHANGE	SUBAREA
677	JOHNSON, JAMES R. AND ELLEN	IM, NICHOLAS NAK-KYUN	09N/04E-30P01	12/12/19	BAJA
677	JOHNSON, JAMES R. AND ELLEN	IM, NICHOLAS NAK-KYUN	09N/04E-30P02	12/12/19	BAJA
678	WEISER, ET AL.	CROWN CAMBRIA, LLC	05N/01E-33B02	01/22/20	ESTE
678	WEISER, ET AL.	CROWN CAMBRIA, LLC	05N/01E-33G03	01/22/20	ESTE
678	WEISER, ET AL.	CROWN CAMBRIA, LLC	05N/01E-33G04	01/22/20	ESTE
678	WEISER, ET AL.	CROWN CAMBRIA, LLC	05N/01E-33G05	01/22/20	ESTE
678	WEISER, ET AL.	CROWN CAMBRIA, LLC	05N/01E-33G06	01/22/20	ESTE
680	KOROGHLIAN, TED AND NAJWA	MUSIC, ZAJO	09N/03E-19Q03	02/26/20	BAJA
680	KOROGHLIAN, TED AND NAJWA	MUSIC, ZAJO	09N/03E-19Q05	02/26/20	BAJA
681	BEEBE, DOROTHEY K.	HOLY HEAVENLY LAKE, LLC	04N/04W-13K03	04/22/20	ALTO
682	BEINSCHROTH FAMILY TRUST	BEINSCHROTH FAMILY TRUST	04N/03W-08P01	04/22/20	ALTO
682	BEINSCHROTH FAMILY TRUST	BEINSCHROTH FAMILY TRUST	04N/03W-08P02	04/22/20	ALTO
682	BEINSCHROTH FAMILY TRUST	BEINSCHROTH FAMILY TRUST	05N/04W-24F02	04/22/20	ALTO
682	BEINSCHROTH FAMILY TRUST	BEINSCHROTH FAMILY TRUST	05N/04W-24F03	04/22/20	ALTO
686	PETTIGREW, JAMES AND CHERLYN	AMERICA UNITED DEVELOPMENT, LLC	05N/01E-31A04	05/27/20	ESTE
686	PETTIGREW, JAMES AND CHERLYN	AMERICA UNITED DEVELOPMENT, LLC	05N/01E-31A05	05/27/20	ESTE
685	ARGUELLES REVOCABLE TRUST, ALFREDO A. AND ANA. M.	LAKE WAINANI OWNERS ASSOCIATION	09N/03E-24A01	06/01/20	BAJA
685	ARGUELLES REVOCABLE TRUST, ALFREDO A. AND ANA. M.	LAKE WAINANI OWNERS ASSOCIATION	09N/03E-24A02	06/01/20	BAJA
685	ARGUELLES REVOCABLE TRUST, ALFREDO A. AND ANA. M.	LAKE WAINANI OWNERS ASSOCIATION	09N/03E-24H01	06/01/20	BAJA
----	VAN DAM FAMILY TRUST, GLEN AND JENNIFER	DAGGETT LAND HOLDINGS LLC	09N/02E-17H01	12/14/20	BAJA
----	VAN DAM FAMILY TRUST, GLEN AND JENNIFER	DAGGETT LAND HOLDINGS LLC	09N/02E-17J01	12/14/20	BAJA
----	VAN DAM FAMILY TRUST, GLEN AND JENNIFER	DAGGETT LAND HOLDINGS LLC	09N/02E-17Q01	12/14/20	BAJA
----	VAN DAM FAMILY TRUST, GLEN AND JENNIFER	DAGGETT LAND HOLDINGS LLC	09N/02E-18F03	12/14/20	BAJA

**TABLE 9
MOJAVE BASIN AREA
FACILITY TRANSFERS REPORTED TO WATERMASTER
OCTOBER 1, 1993 THROUGH SEPTEMBER 30, 2023**

TRANSFER NUMBER	TRANSFEROR	TRANSFeree	STATE WELL NUMBER	DATE OF CHANGE	SUBAREA
----	VAN DAM FAMILY TRUST, GLEN AND JENNIFER	DAGGETT LAND HOLDINGS LLC	09N/02E-18H02	12/14/20	BAJA
----	VAN DAM FAMILY TRUST, GLEN AND JENNIFER	DAGGETT LAND HOLDINGS LLC	09N/02E-18H02	12/14/20	BAJA
----	VAN DAM FAMILY TRUST, GLEN AND JENNIFER	DAGGETT LAND HOLDINGS LLC	09N/02E-18H04	12/14/20	BAJA
----	VAN DAM FAMILY TRUST, GLEN AND JENNIFER	DAGGETT LAND HOLDINGS LLC	09N/02E-19E01	12/14/20	BAJA
----	HARTER, JOE AND SUE	DAGGETT LAND HOLDINGS LLC	09N/02E-07Q01	12/15/20	BAJA
----	HARTER, JOE AND SUE	DAGGETT LAND HOLDINGS LLC	09N/02E-07Q02	12/15/20	BAJA
----	HARTER, JOE AND SUE	DAGGETT LAND HOLDINGS LLC	09N/02E-07Q03	12/15/20	BAJA
----	HARTER, JOE AND SUE	DAGGETT LAND HOLDINGS LLC	09N/02E-21H01	12/15/20	BAJA
----	HARTER, JOE AND SUE	DAGGETT LAND HOLDINGS LLC	09N/02E-21H02	12/15/20	BAJA
----	HARTER, JOE AND SUE	DAGGETT LAND HOLDINGS LLC	09N/02E-21H03	12/15/20	BAJA
----	HARTER, JOE AND SUE	DAGGETT LAND HOLDINGS LLC	09N/02E-21J01	12/15/20	BAJA
----	HARTER, JOE AND SUE	DAGGETT LAND HOLDINGS LLC	09N/02E-21J02	12/15/20	BAJA
----	KASNER, ROBERT	DAGGETT LAND HOLDINGS LLC	09N/02E-08N02	12/17/20	BAJA
700	HAWKINS, JAMES B.	VAN DAM FAMILY TRUST, GLEN AND JENNIFER	09N/02E-05B01	02/24/21	BAJA
701	JONES TRUST DATED MARCH 16, 2002	DESERT GIRLZ LLC	04N/01E-09N01	03/24/21	ESTE
703	BRACHT, WILLIAM F. AND ALEXANDER, ALICIA M.	DOUGLAS, TINA	04N/01W-14F03	05/26/21	ESTE
----	HARTER, JOE AND SUE	DAGGETT LAND HOLDINGS LLC	09N/02E-15Q01	06/04/21	BAJA
----	HARTER, JOE AND SUE	DAGGETT LAND HOLDINGS LLC	09N/02E-15R03	06/04/21	BAJA
----	HARTER, JOE AND SUE	DAGGETT LAND HOLDINGS LLC	09N/02E-15P01	06/24/21	BAJA
----	HARTER, JOE AND SUE	DAGGETT LAND HOLDINGS LLC	09N/02E-09R02	07/28/21	BAJA
708	THE CUSHENBURY TRUST, C/O SPECIALTY MINERALS, INC.	SPECIALTY MINERALS, INC.	03N/01E-07RS02	07/28/21	ESTE
----	VANDER DUSSEN TRUST, AGNES AND EDWARD	DAGGETT LAND HOLDINGS LLC	09N/02E-16N01	07/29/21	BAJA
----	VANDER DUSSEN TRUST, AGNES AND EDWARD	DAGGETT LAND HOLDINGS LLC	09N/02E-16R01	07/29/21	BAJA
----	KASNER, ROBERT	DAGGETT LAND HOLDINGS LLC	09N/02E-17L01	07/29/21	BAJA

**TABLE 9
MOJAVE BASIN AREA
FACILITY TRANSFERS REPORTED TO WATERMASTER
OCTOBER 1, 1993 THROUGH SEPTEMBER 30, 2023**

TRANSFER NUMBER	TRANSFEROR	TRANSFeree	STATE WELL NUMBER	DATE OF CHANGE	SUBAREA
----	KASNER, ROBERT	DAGGETT LAND HOLDINGS LLC	09N/02E-23C01	10/29/21	BAJA
----	KASNER, ROBERT	DAGGETT LAND HOLDINGS LLC	09N/02E-23L01	10/29/21	BAJA
----	KASNER, ROBERT	DAGGETT LAND HOLDINGS LLC	09N/02E-15B01	11/02/21	BAJA
711	HARPER LAKE COMPANY VIII	LUZ SOLAR PARTNERS LTD. IX	11N/04W-19E01	01/26/22	CENTRO
711	HARPER LAKE COMPANY VIII	LUZ SOLAR PARTNERS LTD. IX	11N/04W-19E02	01/26/22	CENTRO
711	HARPER LAKE COMPANY VIII	LUZ SOLAR PARTNERS LTD. IX	11N/04W-19J01	01/26/22	CENTRO
711	HARPER LAKE COMPANY VIII	LUZ SOLAR PARTNERS LTD. IX	11N/04W-19Q02	01/26/22	CENTRO
711	HARPER LAKE COMPANY VIII	LUZ SOLAR PARTNERS LTD. IX	11N/04W-28R01	01/26/22	CENTRO
711	HARPER LAKE COMPANY VIII	LUZ SOLAR PARTNERS LTD. IX	11N/04W-28R02	01/26/22	CENTRO
711	HARPER LAKE COMPANY VIII	LUZ SOLAR PARTNERS LTD. IX	11N/05W-24L01	01/26/22	CENTRO
711	HARPER LAKE COMPANY VIII	LUZ SOLAR PARTNERS LTD. IX	11N/05W-24P02	01/26/22	CENTRO
711	HARPER LAKE COMPANY VIII	LUZ SOLAR PARTNERS LTD. IX	11N/05W-24Q02	01/26/22	CENTRO
712	HERT, SCOTT	DESERT GIRLZ LLC	05N/01E-32L01	01/26/22	ESTE
712	HERT, SCOTT	DESERT GIRLZ LLC	05N/01E-32L02	01/26/22	ESTE
713	SAMPLES, BERNARD D. AND JANICE E.	HU, MINSHENG	09N/03E-13M02	02/23/22	BAJA
714	LUZ SOLAR PARTNERS LTD. IX	LOCKHART LAND HOLDING, LLC	11N/04W-19E01	05/25/22	CENTRO
714	LUZ SOLAR PARTNERS LTD. IX	LOCKHART LAND HOLDING, LLC	11N/04W-19E02	05/25/22	CENTRO
714	LUZ SOLAR PARTNERS LTD. IX	LOCKHART LAND HOLDING, LLC	11N/04W-19J01	05/25/22	CENTRO
714	LUZ SOLAR PARTNERS LTD. IX	LOCKHART LAND HOLDING, LLC	11N/04W-19Q02	05/25/22	CENTRO
714	LUZ SOLAR PARTNERS LTD. IX	LOCKHART LAND HOLDING, LLC	11N/04W-28R01	05/25/22	CENTRO
714	LUZ SOLAR PARTNERS LTD. IX	LOCKHART LAND HOLDING, LLC	11N/04W-28R02	05/25/22	CENTRO
714	LUZ SOLAR PARTNERS LTD. IX	LOCKHART LAND HOLDING, LLC	11N/05W-24L01	05/25/22	CENTRO
714	LUZ SOLAR PARTNERS LTD. IX	LOCKHART LAND HOLDING, LLC	11N/05W-24P02	05/25/22	CENTRO
714	LUZ SOLAR PARTNERS LTD. IX	LOCKHART LAND HOLDING, LLC	11N/05W-24Q02	05/25/22	CENTRO
719	VAN DAM REVOCABLE TRUST, E AND S	OOSTDAM FAMILY TRUST, JOHN P. AND MARGIE K.	09N/02W-03D03	06/22/22	CENTRO
719	VAN DAM REVOCABLE TRUST, E AND S	OOSTDAM FAMILY TRUST, JOHN P. AND MARGIE K.	09N/02W-03D05	06/22/22	CENTRO

**TABLE 9
MOJAVE BASIN AREA
FACILITY TRANSFERS REPORTED TO WATERMASTER
OCTOBER 1, 1993 THROUGH SEPTEMBER 30, 2023**

TRANSFER NUMBER	TRANSFEROR	TRANSFEE	STATE WELL NUMBER	DATE OF CHANGE	SUBAREA
719	VAN DAM REVOCABLE TRUST, E AND S	OOSTDAM FAMILY TRUST, JOHN P. AND MARGIE K.	09N/02W-03D06	06/22/22	CENTRO
----	CONTRATTO, ERSULA	BNSF RAILWAY COMPANY	09N/03W-27E07	10/01/22	CENTRO
----	CONTRATTO, ERSULA	BNSF RAILWAY COMPANY	09N/03W-27E09	10/01/22	CENTRO
----	CONTRATTO, ERSULA	BNSF RAILWAY COMPANY	09N/03W-27M02	10/01/22	CENTRO
----	CONTRATTO, ERSULA	BNSF RAILWAY COMPANY	09N/03W-27M05	10/01/22	CENTRO
----	CONTRATTO, ERSULA	BNSF RAILWAY COMPANY	09N/03W-27M11	10/01/22	CENTRO
722	ITALMOOD INC., ET AL.	UPPAL, GAGAN	11N/03E-29J02	10/26/22	BAJA
722	ITALMOOD INC., ET AL.	UPPAL, GAGAN	11N/03E-29P01	10/26/22	BAJA
722	ITALMOOD INC., ET AL.	UPPAL, GAGAN	11N/03E-29Q01	10/26/22	BAJA
722	ITALMOOD INC., ET AL.	UPPAL, GAGAN	11N/03E-32E01	10/26/22	BAJA
722	ITALMOOD INC., ET AL.	UPPAL, GAGAN	11N/03E-32E02	10/26/22	BAJA
726	ATCHISON TOPEKA AND SANTA FE RAIL WAY COMPANY	BNSF RAILWAY COMPANY	09N/03E-33E01	05/09/23	BAJA
726	ATCHISON TOPEKA AND SANTA FE RAIL WAY COMPANY	BNSF RAILWAY COMPANY	09N/03E-33E05	05/09/23	BAJA
727	ATCHISON TOPEKA AND SANTA FE RAIL WAY COMPANY	BNSF RAILWAY COMPANY	09N/02W-02M01	05/09/23	CENTRO
----	SERVICE ROCK PRODUCTS CORPORATION	ROBERTSON'S READY MIX	12N/02E-17A01	05/24/23	BAJA
728	KOSHAREK, NANCY	VAAGE, GAGE V.	09N/03E-23H02	05/24/23	BAJA
729	SERVICE ROCK PRODUCTS CORPORATION	ROBERTSON'S READY MIX	06N/04W-33N03	05/24/23	ALTO
729	SERVICE ROCK PRODUCTS CORPORATION	ROBERTSON'S READY MIX	06N/04W-33N06	05/24/23	ALTO
730	SERVICE ROCK PRODUCTS CORPORATION	ROBERTSON'S READY MIX	09N/01W-10P01	05/24/23	CENTRO
730	SERVICE ROCK PRODUCTS CORPORATION	ROBERTSON'S READY MIX	09N/01W-10P03	05/24/23	CENTRO
730	SERVICE ROCK PRODUCTS CORPORATION	ROBERTSON'S READY MIX	09N/01W-10P04	05/24/23	CENTRO
730	SERVICE ROCK PRODUCTS CORPORATION	ROBERTSON'S READY MIX	09N/01W-15A01	05/24/23	CENTRO
730	SERVICE ROCK PRODUCTS CORPORATION	ROBERTSON'S READY MIX	09N/01W-15B01	05/24/23	CENTRO

**TABLE 9
MOJAVE BASIN AREA
FACILITY TRANSFERS REPORTED TO WATERMASTER
OCTOBER 1, 1993 THROUGH SEPTEMBER 30, 2023**

TRANSFER NUMBER	TRANSFEROR	TRANSFeree	STATE WELL NUMBER	DATE OF CHANGE	SUBAREA
730	SERVICE ROCK PRODUCTS CORPORATION	ROBERTSON'S READY MIX	09N/01W-15C01	05/24/23	CENTRO
734	VAN LEEUWEN TRUST, JOHN A. AND IETIE	BNSF RAILWAY COMPANY	09N/03W-22J02	07/26/23	CENTRO
734	VAN LEEUWEN TRUST, JOHN A. AND IETIE	BNSF RAILWAY COMPANY	09N/03W-22J03	07/26/23	CENTRO
734	VAN LEEUWEN TRUST, JOHN A. AND IETIE	BNSF RAILWAY COMPANY	09N/03W-22J04	07/26/23	CENTRO
734	VAN LEEUWEN TRUST, JOHN A. AND IETIE	BNSF RAILWAY COMPANY	09N/03W-22Q01	07/26/23	CENTRO
734	VAN LEEUWEN TRUST, JOHN A. AND IETIE	BNSF RAILWAY COMPANY	09N/03W-22R02	07/26/23	CENTRO
734	VAN LEEUWEN TRUST, JOHN A. AND IETIE	BNSF RAILWAY COMPANY	09N/03W-22R03	07/26/23	CENTRO
734	VAN LEEUWEN TRUST, JOHN A. AND IETIE	BNSF RAILWAY COMPANY	09N/03W-22R04	07/26/23	CENTRO
734	VAN LEEUWEN TRUST, JOHN A. AND IETIE	BNSF RAILWAY COMPANY	09N/03W-22R06	07/26/23	CENTRO
734	VAN LEEUWEN TRUST, JOHN A. AND IETIE	BNSF RAILWAY COMPANY	09N/03W-23N02	07/26/23	CENTRO
734	VAN LEEUWEN TRUST, JOHN A. AND IETIE	BNSF RAILWAY COMPANY	09N/03W-27A01	07/26/23	CENTRO
----	CLARK, GARY AND BETH A.	GREEN HAY PACKERS LLC	09N/03E-14J01	08/04/23	BAJA
----	CLARK, GARY AND BETH A.	GREEN HAY PACKERS LLC	09N/03E-14Q01	08/04/23	BAJA
735	EYGNOR, ROBERT E.	REIDO FARMS, LLC	08N/04W-15R03	09/27/23	CENTRO
736	LANGLEY REVOCABLE TRUST AND SHARON LANGLEY	HANG, PHU QUANG	11N/03E-20L01	09/27/23	BAJA

EXHIBIT 7



Article

Estimation of Seasonal Evapotranspiration for Crops in Arid Regions Using Multisource Remote Sensing Images

Mingxing Cha, Mengmeng Li and Xiaoqin Wang

Special Issue

Remote Sensing of Evapotranspiration (ET) II


Edited by

Dr. Nishan Bhattarai and Dr. Pradeep Wagle



Article

Estimation of Seasonal Evapotranspiration for Crops in Arid Regions Using Multisource Remote Sensing Images

Mingxing Cha, Mengmeng Li *  and Xiaoqin Wang

Key Laboratory of Spatial Data Mining and Information Sharing of Ministry of Education, National & Local Joint Engineering Research Centre of Satellite Geospatial Information Technology, Academy of Digital China (Fujian), Fuzhou University, Fuzhou 350108, China; N185527001@fzu.edu.cn (M.C.); wangxq@fzu.edu.cn (X.W.)

* Correspondence: mli@fzu.edu.cn

Received: 19 June 2020; Accepted: 21 July 2020; Published: 26 July 2020



Abstract: An accurate estimation of evapotranspiration (ET) from crops is crucial in irrigation management, crop yield assessment, and optimal allocation of water resources, particularly in arid regions. This study explores the estimation of seasonal evapotranspiration for crops using multisource remote sensing images. The proposed estimation framework starts with estimating daily evapotranspiration (ET_d) values, which are then used to calculate ET estimates during the crop growing season (ET_s). We incorporated Landsat images into the surface energy balance algorithm over land (SEBAL) model, and we used the trapezoidal and sinusoidal methods to estimate the seasonal ET. The trapezoidal method used multitemporal ET_d images, while the sinusoidal method employs time-series Moderate Resolution Imaging Spectroradiometer (MODIS) images and multitemporal ET_d images. Experiments were implemented in the agricultural lands of the Kai-Kong River Basin, Xinjiang, China. The experimental results show that the obtained ET_d estimates using the SEBAL model are comparable with those from the Penman–Monteith method. The ET_s obtained using the trapezoidal and sinusoidal methods both have a relatively high spatial resolution of 30 m. The sinusoidal method performs better than the trapezoidal method when using low temporal resolution Landsat images. We observed that the omission of Landsat images during the middle stage of crop growth has the greatest impact on the estimation results of ET_s using the sinusoidal method. Based on the results of the study, we conclude that the proposed sinusoidal method, with integrated multisource remote sensing images, offers a useful tool in estimating seasonal evapotranspiration for crops in arid regions.

Keywords: evapotranspiration; SEBAL; multisource remote sensing; trapezoidal method; sinusoidal method

1. Introduction

Water is an essential resource, especially for agriculture in arid and semiarid regions [1,2]. One vital component to describe the hydrological cycle in ecological systems and to estimate water balance is evapotranspiration (ET). ET is the process by which water is transported from the earth's surface to the atmosphere by the evaporation from surfaces (soils and wet vegetation) and by the transpiration from plants through the stomata present in the plant leaves [3,4]. Crop evapotranspiration is a fundamental variable in the hydrological cycle and is thus significant for the management of irrigation and water resources [5]. However, accurately assessing ET for crops is challenging because of its high spatial and temporal variability.

Many studies have been conducted to estimate ET using methods such as sap flow [6], lysimeters [7,8], the Bowen ratio [9], and eddy covariance [10,11]. These traditional methods rely on

field surveys and are limited to small areas. For larger areas, directly applying traditional approaches is often difficult due to the complexity of hydrological processes and land surface factors. An observation network is generally required to measure ET for vast regions, which is labor-intensive and costly. In recent years, numerous approaches have been developed that allow for the dynamic estimation of ET using satellite images [12]. Remote sensing has been considered as an effective means to obtain ET over various spatial and temporal scales [13–19]. In the literature, increasing attention has been given towards the estimation of ET using remote sensing technology [20–22]. Several ET products and models have been proposed (e.g., ETMonitor with a spatial resolution of 1 km and a temporal resolution of one day [23–25], Moderate Resolution Imaging Spectroradiometer (MODIS) MOD16 with 1 km/8 day [26–28], EUMETSAT Satellite Application Facility on Land Surface Analysis (LSA-SAF) MSG ET with 5 km/30 min [29], Global Land Evaporation Amsterdam Model (GLEAM) with 25 km/1 day [30–32], and FLUXCOM with 50 km/1 month [33]). References [34–36] reviewed the available methods for ET estimation based on different structural complexities, theories, and assumptions. These methods can be grouped into four categories: (1) empirical methods using statistically-derived relationships between ET and vegetation indices; (2) residual surface energy balance models, such as single and dual-source models, the Surface Energy Balance System (SEBS) [37], Surface Energy Balance Index (SEBI) [38], and the surface energy balance algorithm over land (SEBAL) [39]; (3) physically-based methods based on the Penman–Monteith (PM) [40,41] and Priestley–Taylor (PT) [42] equations; and (4) data assimilation methods with heat diffusion equation and radiometric surface temperature sequences. The spatial resolution of remote sensing images affects the accuracy of ET estimates. Since most ET products offer a coarse spatial resolution at either the national, continental, or global scales, the accuracy of their estimates is significantly constrained [27]. In order to improve the accuracy of ET estimates, new approaches would have to be developed that utilize remote sensing images with a high spatial resolution at a regional scale.

Among existing models, SEBAL is one of the most widely used models for arid and semiarid regions because of its flexibility in different vegetation types and climatic characteristics and its strong physical foundation. The applicability of the SEBAL model has been evaluated in many different regions. For example, the SEBAL model has been used to estimate ET in various studies areas in China, India, Spain, and Pakistan, and results have shown that the accuracy of estimated ET is about 85% compatible with the field measurements without calibration [39,43]. Researchers have conducted studies estimating ET with the SEBAL model by using Landsat [44–47] and MODIS satellite images [48,49]. Compared with lysimetric measurements, eddy correlation, and Penman–Monteith methods, the ET estimated by incorporating the Landsat images into the SEBAL model performed better than when incorporating the MODIS images. An existing study showed that Landsat ET can be better than MODIS ET due to its high spatial resolution [50]. Most of the SEBAL-related studies estimated ET on a daily scale; few studies have estimated ET for crops using Landsat remote sensing images during the growing season. Linear and spline interpolation are the most popular methods to estimate seasonal ET (ET_s) in existing studies [51–53]. The ET, however, does not change linearly with time during the crop growing season. A possible practice to improve the estimation of ET_s is to combine the change curve of ET with time. In addition, an alternative is to derive monthly ET based on the monthly average crop coefficient, for which the ET_s can be obtained using the monthly ET [54,55], but this strategy is data-intensive. The estimation of evapotranspiration for crops during the growing season is essential for scientific irrigation. Therefore, it is necessary to explore more effective methods to estimate the ET_s for crops.

This study aims to develop more efficient methods to estimate seasonal evapotranspiration for crops with a relatively high spatial resolution and only based upon multisource remote sensing images within one year. We propose a trapezoidal method and a sinusoidal method to achieve this objective. The novelty and innovation of this study are as follows:

- (1) The SEBAL model is used to obtain ET_d for crops in arid regions from Landsat images;
- (2) A trapezoidal method is employed to extend ET_d to ET_s using multitemporal ET_d data; and,

(3) A sinusoidal method is proposed to derive ET_s from ET_d using multisource remote sensing images.

The remainder of this paper is structured as follows. Section 2 describes the study area and datasets. Section 3 discusses the proposed methodology for ET_d and ET_s estimation. Section 4 presents the experimental results, followed by the discussion and conclusions in Sections 5 and 6, respectively.

2. Study Area and Data

2.1. Study Area

The agricultural land of the Kai-Kong River Basin in Xinjiang, China, was selected as the study area (Figure 1). Located in Northwestern China, Xinjiang is characterized as having an extreme arid climate [56] and is considered as an important region for crop production. The agricultural lands of the Kai-Kong River Basin are important planting regions for crops in Xinjiang. The Kai-Kong River Basin is located at $40^{\circ}48'–43^{\circ}20'N$ and $82^{\circ}56'–88^{\circ}12'E$, covering an area of around 5.7×10^4 km². It includes the Kaidu River Basin in the upstream and the Kongque River Basin in the downstream. The terrain is characterized as rugged in the northwest and flat in the southeast, and the altitude ranges from 600 to 4800 m [57]. Figure 1 shows the agricultural land of the Kai-Kong River Basin, which is delineated by a red line. The area includes 1.02×10^3 km² agricultural lands of Bosten Lake, 2.46×10^3 km² agricultural lands of the Kaidu River, and 2.79×10^3 km² agricultural lands of the Kongque River [58]. The study area is characterized by an arid continental climate with a long sunshine time, a large temperature difference between day and night, frequent climate fluctuations, sparse rainfall, and severe evaporation. The precipitation in this area is concentrated from April to July, with maximum precipitation at 20–40 mm. The agricultural land of the Kai-Kong River Basin provides a representative area for research on crop evapotranspiration in arid regions. The major crops in the study area are wheat, corn, cotton, chili, and pear, and the cropping period runs from March to October. The cropping system is one crop per annum, and the crop phenology includes the following: wheat and pear are cultivated and turn green in mid-March and mature in July and October; chili is planted in mid-April and harvested in late September; corn and cotton emerge in early May and mature in September and October.

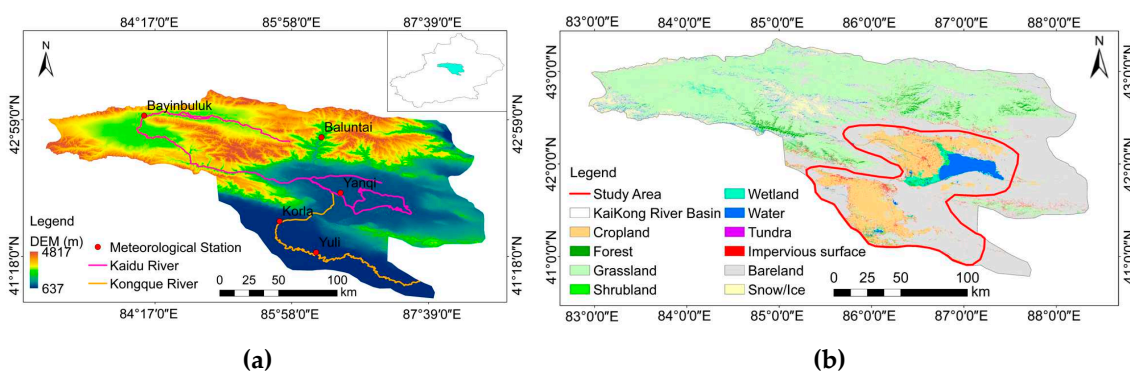


Figure 1. Overview of the study area. The location of the Kai-Kong River Basin in Xinjiang is highlighted shown in the left picture (a), and the agricultural land in the Kai-Kong River Basin is surrounded by the red boundary in the right picture (b).

2.2. Study Data

Three kinds of data were used in this study: remote sensing images, meteorological data, and ancillary data. Remote sensing data include Landsat and MODIS images acquired in 2016. The Landsat images were obtained from Landsat 7 Enhanced Thematic Mapper Plus (ETM+) and Landsat-8 Operational Land Imager and Thermal Infrared Sensor (OLI/TIRS) (Path = 143, Row = 31). In total, we collected 13 cloud-free multitemporal Landsat images during the 2016 cropping season with a level correction 1T (terrain corrected) from the USGS Earth Explorer site (<https://earthexplorer.usgs.gov/>).

The spatial resolution of visible bands is 30 m, and the spatial resolution of the thermal infrared bands of Landsat 7 ETM+ and Landsat-8 OLI/TIRS is 60 and 100 m, respectively. Details of the Landsat images are presented in Table 1. The Landsat images were preprocessed by applying radiometric calibration, atmospheric correction, and clipping. Due to the banding phenomenon caused by the failure of the satellite scan line corrector for the Landsat 7 ETM+ images acquired after 31 May 2003, stripping processing was required for Landsat 7 ETM+ images. For the MODIS data, we downloaded 46 time-series MOD16A2 images, with the spatial and temporal resolutions of 500 m over 8 days, for 2016 from the NASA Earth Data site (<http://earthdata.nasa.gov>). We preprocessed the MODIS data by applying project transformation (sinusoidal projection to UTM_Zone_45N), format conversion (HDF to TIF), band extraction (ET band), real value calculation ($\text{valid_data} \times \text{scale_factor}$), image clipping, and S-G filtering [59,60]. For the digital elevation model (DEM), we downloaded 18 ASTER Global Digital Elevation Model 2 (ASTGTM2) images with 30 m resolution from the website (<http://www.gscloud.cn/>), whose processing consisted of image mosaic and clipping operations.

For the meteorological dataset, we obtained data for wind speed, air temperature, average air pressure, precipitation, air humidity (vapor pressure or dew point temperature), solar radiation, and meteorological station characteristics (height of wind measurement and vegetation height). The daily meteorological dataset was downloaded from the China Meteorological Data Sharing Service Network (<http://data.cma.cn/>). Ancillary data, which include crop sample points, planting structure, and phenology information, were also collected for the study. A detailed description of these data can be found in our previous study [61].

Table 1. Details of the collected Landsat images.

Date	DOY	Satellite and Sensors
6 April	97	Landsat 7 ETM+
14 April	105	Landsat-8 OLI/TIRS
22 April	113	Landsat 7 ETM+
16 May	137	Landsat-8 OLI/TIRS
1 June	153	Landsat-8 OLI/TIRS
25 June	177	Landsat 7 ETM+
27 July	209	Landsat 7 ETM+
4 August	217	Landsat-8 OLI/TIRS
5 September	249	Landsat-8 OLI/TIRS
21 September	265	Landsat-8 OLI/TIRS
7 October	281	Landsat-8 OLI/TIRS
15 October	289	Landsat-8 OLI/TIRS
31 October	305	Landsat-8 OLI/TIRS

3. Methods

The proposed framework for ET_s estimation is shown in Figure 2. The SEBAL model was applied to obtain instantaneous evapotranspiration values (ET_{inst}) using multitemporal Landsat images, meteorological data, and DEM data, which were then converted into ET_d . A trapezoidal method and a sinusoidal method were then used to upscale the ET_d to the ET_s . The trapezoidal method estimates ET_s based only on the multitemporal ET_d images derived by SEBAL, while the sinusoidal method estimates ET_s using multisource remote sensing images. For the trapezoidal method, the formula for the trapezoidal area was applied to estimate ET_s for crops. For the sinusoidal method, we used time-series MOD16A2 images to obtain the change in the crops' ET between phenological dates (day of year, DOY). Multitemporal ET_d images were then used to calculate the ET_s for crops.

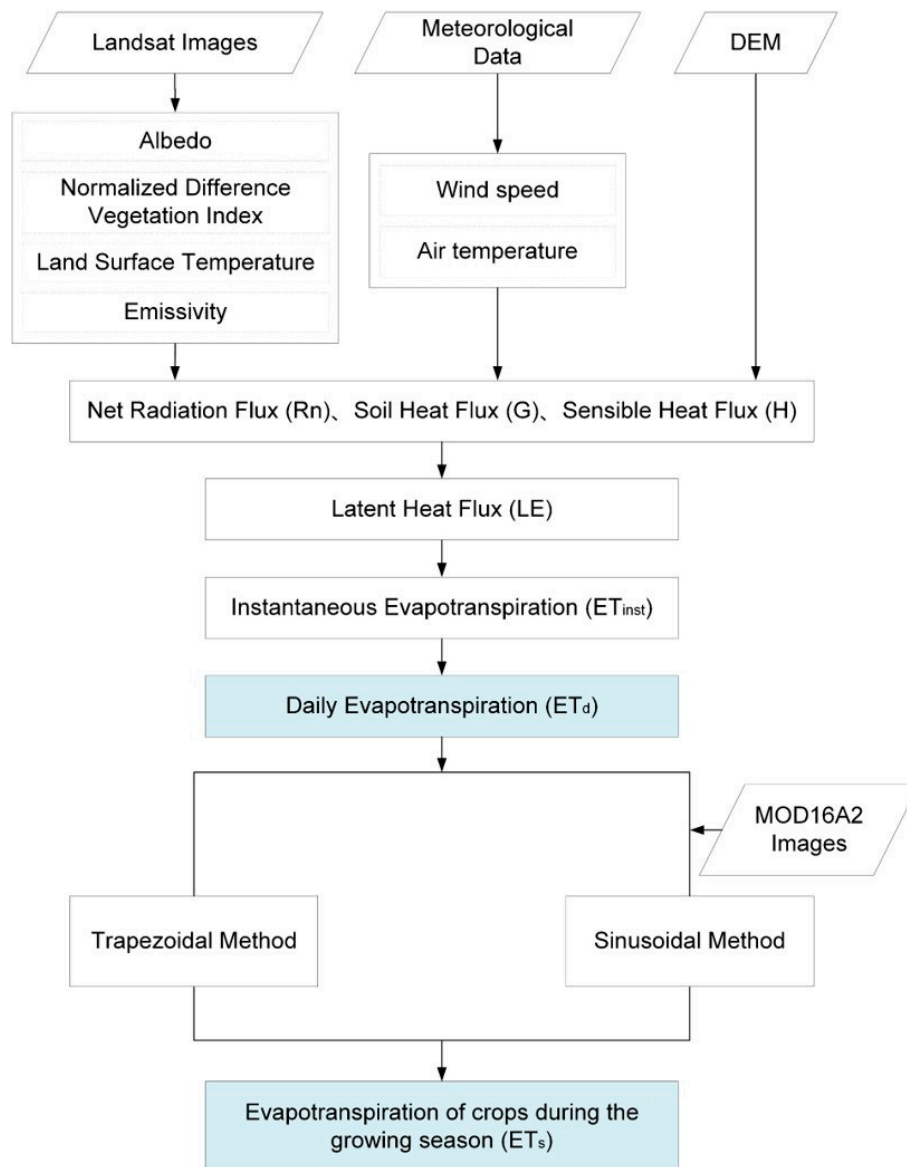


Figure 2. The proposed framework of the ET_s (seasonal evapotranspiration) estimation for crops using multisource remote sensing images.

3.1. ET_d Estimation Based on the SEBAL Model

SEBAL is a flux algorithm based on a complete radiation and energy balance, along with resistances for momentum, heat, and water vapor transport for every pixel [62,63]. It estimates ET through a simplified land surface energy balance method. When using SEBAL, the values for albedo, normalized difference vegetation index (NDVI), land surface temperature (T_s), and emissivity from Landsat images are calculated first. Together with meteorological and DEM data, these values are used to estimate key variables in the energy balance equation, including net radiation flux (Rn), soil heat flux (G), and the sensible heat flux (H). We can obtain the latent heat flux (LE) as a residual using the equation:

$$LE = R_n - G - H. \quad (1)$$

Based on the latent heat flux (LE), the instantaneous evapotranspiration (ET_{inst}) is defined as follows [64–66]:

$$ET_{inst} = 3600 \times \frac{LE}{\lambda} \quad (2)$$

$$\lambda = (2.501 - 0.002361 \times (T_s - 273.16)) \times 10^6 \quad (3)$$

where λ indicates the latent evaporation heat. Previous studies have shown the effectiveness of the sine method to convert ET_{inst} to ET_d using this expression [67,68]:

$$ET_d = \frac{ET_{inst} \times 2N}{\pi \times \sin(\pi \times t/N)} \quad (4)$$

where N is the number of daily ET hours, and t is the time interval between sunrise and data-collecting time of the Landsat satellite. This equation is inspired by the ET_{inst} change curve on a clear day, which closely conforms to a sine relation. In this paper, we use the same method to convert ET_{inst} into ET_d .

3.2. Validation of the SEBAL Algorithm Performance

We used the Penman–Monteith (PM) model proposed by the Food and Agriculture Organization (FAO) in 1998 [69] to verify the accuracy of the ET_d obtained by the SEBAL model. The actual evapotranspiration (ET_c , mm·day⁻¹) of the crops is calculated using the formula:

$$ET_c = K_c \times ET_0 \quad (5)$$

where K_c is the crop coefficient, and ET_0 is the reference evapotranspiration (mm·day⁻¹). The ET_c obtained by the PM model has generally been used to verify the accuracy of ET_d estimated by other models [3,70], which is why the PM model was selected to validate the results of this study.

3.3. ET_s Estimation Based on the Trapezoidal Method

We propose a trapezoidal method to estimate the ET of crops using multitemporal ET_d images derived by SEBAL. Suppose that multitemporal Landsat images are acquired during the crop growing season. Let D_m , $m \in \{1, \dots, n\}$, be the acquired time (DOY) of the m_{th} Landsat image, and n is the total number of the acquired images. Let ET_k be the ET_d estimated at different periods, ET_m as the ET_d of Landsat image on the m_{th} period, and Δd as the time difference between adjacent images. The ET_d change curves with the DOY of crops during the growing season are shown in Figure 3. The blue trapezoid area in Figure 3 is bounded by the ET_d curve of crop 1 between two adjacent dates D_m and D_{m+1} . The default value of ET_0 is 0, and the area of the trapezoid is then $(ET_m + ET_{m+1}) \times \Delta d_m / 2$. The calculated area is regarded as the cumulative ET for D_m to D_{m+1} . To obtain the ET_s , the areas of all trapezoids during the crop growing season were aggregated for the crops. The formula of the trapezoidal method is given in Equation (6), as follows:

$$ET_s = \sum_{m=1}^{n-1} \frac{(ET_m + ET_{m+1}) \times \Delta d_m}{2} \quad (6)$$

According to the definition, the estimation accuracy of the trapezoidal method is dependent on the intensity of the ET_d time-series. The ET_s can be derived with a high estimation accuracy when a sufficient number of Landsat images is used.

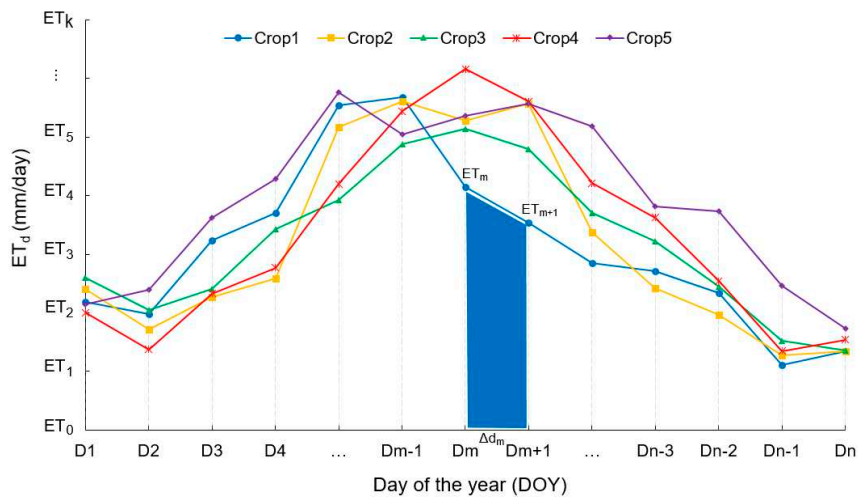


Figure 3. Daily evapotranspiration (ET_d) change curves with the DOY (day of the year) of crops during the growing season. The horizontal axis represents the acquired time (day of the year, DOY) of Landsat images and the vertical axis represents the ET_d .

3.4. ET_s Estimation Based on the Sinusoidal Method

Acquiring over 15 Landsat images with satisfactory quality for a specific area within a year is usually difficult due to low temporal resolution and meteorological factors, such as cloud and rain. To deal with this problem, we propose a new method to estimate the ET of crops during the growing season using multisource remote sensing images. MOD16A2 images have high temporal resolution, i.e., eight days, and can reflect the change of crop ET during the year and crop growing season, while Landsat images have a relatively high spatial resolution, i.e., 30 m, and can estimate ET at a finer level. The proposed method, referred to as the sinusoidal method in this paper, estimates the ET_s of crops using time-series MOD16A2 images and the ET_d images produced by SEBAL. The workflow of the sinusoidal method is shown in Figure 4.

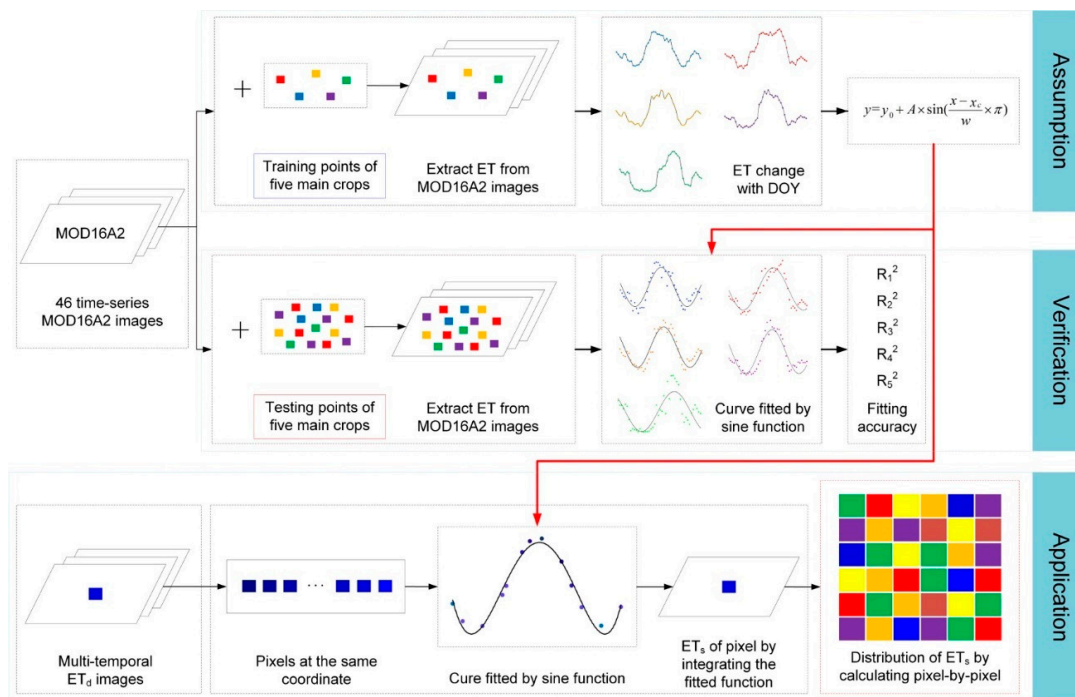


Figure 4. The workflow of the proposed sinusoidal method. Time-series MOD16A2 images used to obtain ET change with DOY and multitemporal ET_d images used to estimate ET_s for crops.

We first randomly selected ten sample points from each crop as the training points and the remaining sample points as testing points. We used the training points to extract the ET from 46 time-series MOD16A2 images and obtain the ET change curve of the five main crops, which intuitively, is similar to the shape of a trigonometric curve. Based on the conversion method (ET_{inst} to ET_d) discussed in Section 3.1, we assumed that the ET_d change meets the form of a sine function (Equation (7)) within a year and is given by the expression:

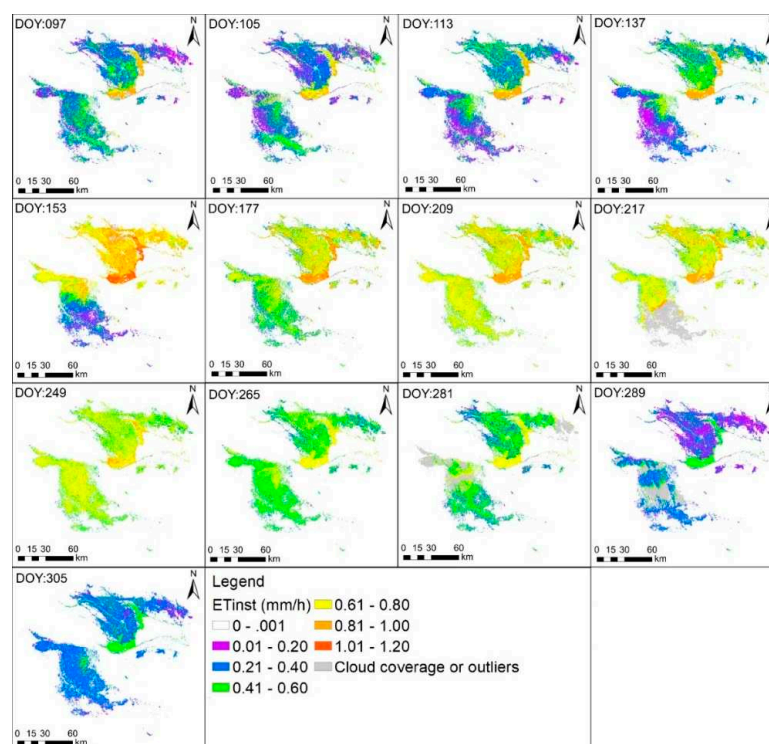
$$y = y_0 + A \times \sin\left(\frac{x - x_c}{w} \times \pi\right) \quad (7)$$

where y is the ET_d of crops, and x represents the image acquisition date (DOY). The coefficients y_0 , A , x_c , and w were then determined by the time-series ET_d for every pixel. To verify our assumption, we used the testing points to extract the ET from 46 time-series (MOD16A2) images and obtained the ET values for the five crops. We applied the sine function (Equation (7)) to the ET data and obtained the y_0 , A , x_c , w , and the coefficient of determination (R^2) for each crop. If the $R^2 \in [0.60, 1]$, we considered that the pattern of the change of the ET_d can be formulated as a sine function. We then applied the sine function form to the multitemporal ET_d images and obtained the fitted sine function for each pixel at the same coordinate. Finally, we integrated the fitted sine function to obtain ET_s for each pixel and acquired the distribution of ET_s by calculating every pixel in the multitemporal ET_d images.

4. Results

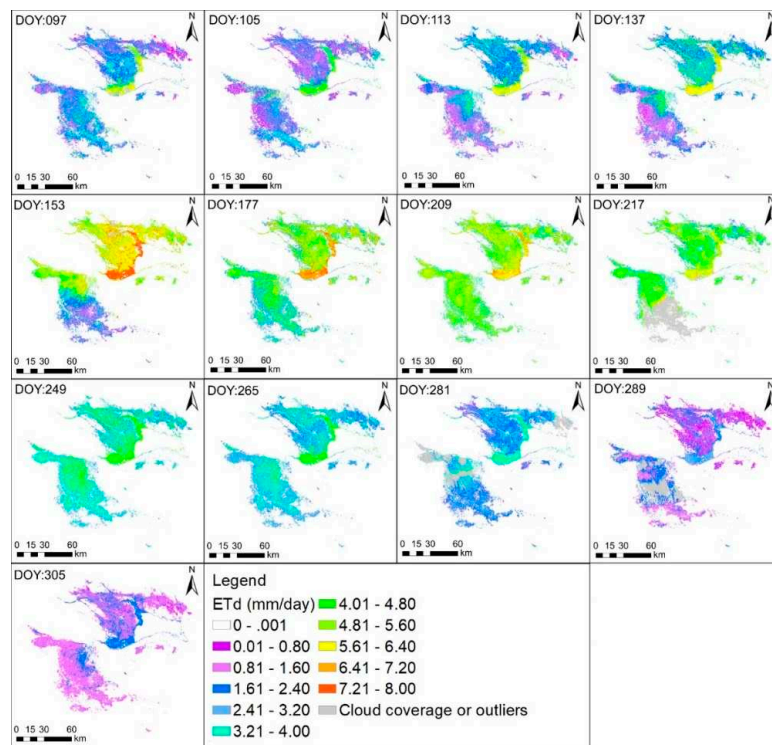
4.1. Temporal-Spatial Variation of ET_{inst} and ET_d Obtained by the SEBAL Model

We used the SEBAL model to obtain ET_{inst} and ET_d using Landsat images (Figure 5). The figure shows high consistency for both the ET_{inst} and ET_d , ranging between $0-1.20 \text{ mm}\cdot\text{h}^{-1}$ and $0-8.00 \text{ mm}\cdot\text{d}^{-1}$, respectively. We then used sample points for the five main crops to extract the ET from the ET_d images, and we obtained the change curve of ET_d , as shown in Figure 6.



(a)

Figure 5. Cont.



(b)

Figure 5. Temporal-spatial variation of (a) instantaneous ET (ET_{inst}) and (b) ET_d obtained by the surface energy balance algorithm over land (SEBAL) model.

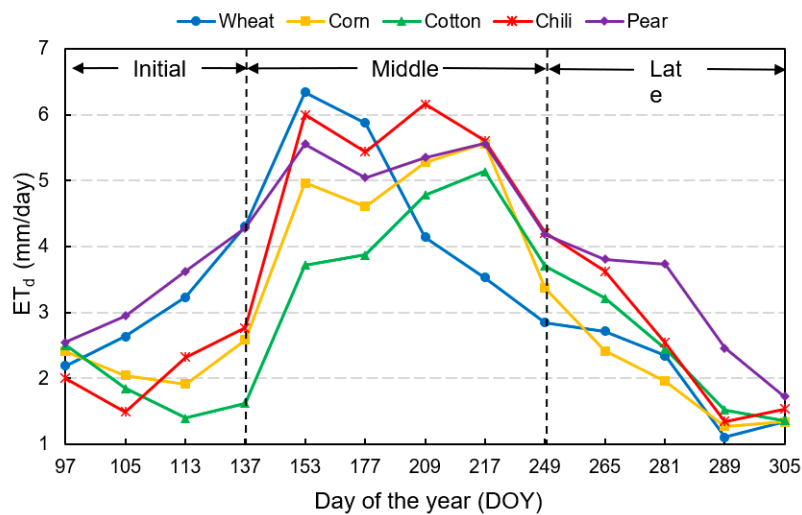


Figure 6. The change curves of ET_d at a given DOY for five main crops.

Based on the phenological information of the five main crops in the study area, we divided the DOY into three stages: the initial stage of growth from 97 to 137, the middle stage from 137 to 249, and the late stage from 249 to 305. In Figure 5, the ET_{inst} and ET_d values gradually increased with the growth of crops in the initial stage and reached their peaks in the middle stage. The range of the ET_{inst} and ET_d values are similar to that in the initial stage but gradually decreased at the late stage. Based on the crop planting structure in the study area, the high ET_{inst} and ET_d values were concentrated in the pear fields, while the low values were concentrated in the cotton fields. Wheat was the first to be planted and the earliest to mature. The ET_d associated with wheat started to increase on DOY 79 and began to decrease on DOY 177 (see Figure 6). Pear had the longest growing period, which was sown

the earliest and was the last to mature. The ET_d of pear started to increase on DOY 97 and had the slowest rate of decrease among the five main crops. Chili was sown after wheat and pear, which was then followed by corn and cotton. The ET_d of chili started to increase on DOY 105 while the ET_d of corn and cotton started to rise on DOY 113.

4.2. Accuracy Assessment of ET_d Obtained by the SEBAL Model

In this study, we referred to existing studies to obtain the crop coefficients of cotton for accuracy assessment because of the difficulty in the acquisition of field data of K_c . Cotton is the most widely planted crop in Xinjiang. Most of the related studies focused on cotton but few on the derivation of crop coefficients for other crops. It is therefore hard to obtain the validation data of other crops for the accuracy assessment. Here, we referred to the K_c of cotton from related studies and used the FAO model to verify the accuracy of ET_d derived from the SEBAL model. We estimated ET_c using meteorological data and the crop coefficient (K_c) for cotton, where the K_c of cotton was provided by [71]. The estimation accuracy of the SEBAL model is defined as $1 - (|ET_c - ET_d| / ET_c)$. Accuracy verification for cotton's ET_d was obtained using the SEBAL model, as summarized in Table 2. This table shows that the difference between the ET_d obtained using the SEBAL model and the actual evapotranspiration (ET_c) derived using the PM model was within one $mm \cdot day^{-1}$, and the accuracy of ET_d was more than 80%.

Table 2. Accuracy of ET_d estimated by the SEBAL model.

Date	ET_d (mm/day)	ET_0 (mm/day)	K_c	ET_c (mm/day)	Difference (mm/day)	Accuracy
22 April	1.28	4.38	0.26	1.14	-0.14	0.88
27 July	5.14	5.01	1.20	6.01	0.87	0.86
15 October	1.52	2.46	0.70	1.72	0.20	0.88

4.3. Validation Results of the Sinusoidal Method

We used the testing points to extract the ET from 46 time-series MOD16A2 images and obtain the ET values for the five main crops. We also used the MOD16A2 images covering the crop growing season to extract the ET values during the crop growth period based on crop phenology. We then applied the sine function (Equation (7)) to obtain the ET change curves for the entire year (Figure 7a) and the growing season (Figure 7b). The function fitting formula and the coefficient of determination (R^2) for each crop are shown in Table 3.

Table 3. Function fitting formula and the coefficient of determination.

Crop Type	During the Interannual		During Crop Growing Season	
	Fitting Formula	R^2	Fitting Formula	R^2
Wheat	$y = 7.80 + 4.87 \times \sin(\frac{x - 124.33}{116.23} \times \pi)$	0.81	$y = 8.15 + 6.56 \times \sin(\frac{x - 132.25}{105.65} \times \pi)$	0.92
Corn	$y = 7.40 + 4.63 \times \sin(\frac{x + 95.31}{115.45} \times \pi)$	0.81	$y = 4.96 + 7.98 \times \sin(\frac{x + 152.72}{140.21} \times \pi)$	0.94
Cotton	$y = 4.70 + 4.07 \times \sin(\frac{x - 175.13}{142.15} \times \pi)$	0.65	$y = 4.51 + 4.00 \times \sin(\frac{x + 30.89}{106.25} \times \pi)$	0.75
Chili	$y = 9.23 + 6.52 \times \sin(\frac{x - 136.82}{138.87} \times \pi)$	0.85	$y = 11.00 + 10.22 \times \sin(\frac{x + 40.94}{-97.65} \times \pi)$	0.86
Pear	$y = 9.47 + 7.80 \times \sin(\frac{x - 138.37}{124.36} \times \pi)$	0.82	$y = 8.09 + 7.76 \times \sin(\frac{x - 135.54}{146.59} \times \pi)$	0.84

The results show that the coefficients of determination (R^2) for the main crops during the entire year are greater than 0.80, while the R^2 values of the fitting functions during the crop growing season were over 0.85 except for cotton in both cases. The sinusoidal function of cotton had low fitting accuracy, and the shape of the fitted curve was different from other crops. This is mainly due to some missing pixels in the cotton region of the MODIS images, which resulted from the low image quality. When using the sample points of cotton to extract ET values from the time-series MOD16A2 images,

there were about 47% null values in the missing pixels. These missing pixels may affect the accuracy of function fitting for cotton.

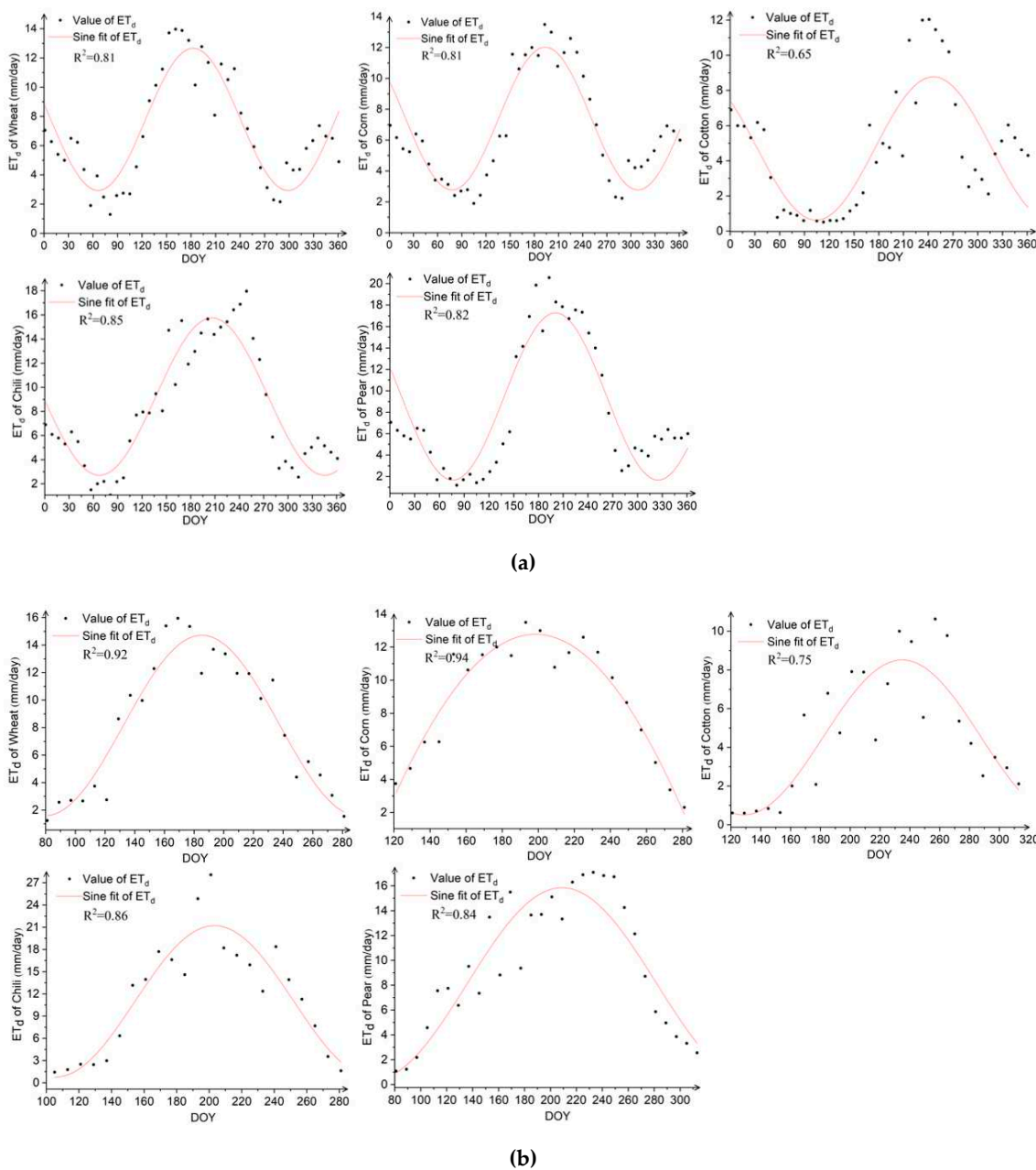


Figure 7. (a) ET change curve with DOY of crops during the whole year; (b) ET change curve with the DOY of crops during the growing season. DOY during the crop growth stage of wheat, corn, cotton, chili, and pear are 81 to 281, 121 to 281, 121 to 313, 105 to 281, and 81 to 313, respectively.

4.4. Distribution of ET during Crop Growing Season

The use of the trapezoidal method in estimating ET_s is dependent on the date of acquisition (DOY) of the Landsat images and requires that the estimation interval is discrete. In contrast, the sinusoidal method is not constrained by the image acquisition date and has the advantage of continuous estimation interval. In this study, we designed three experiments to test the estimation results using the trapezoidal and sinusoidal methods. To estimate the ET_s for five main crops, we used the ET_d images covering the growth period of each crop to estimate the ET_s based on their different phenological information. In Experiments A and B, the estimation intervals were set up using similar acquisition dates and crop

phenology to compare the ET_s results using the two methods. The discrete estimation intervals (DOY) of the trapezoidal method were set as follows: wheat (97, 105, 113, 137, 153, 177, 209, 217, 249, 265, 281), corn (113, 137, 153, 177, 209, 217, 249, 265, 281), cotton (113, 137, 153, 177, 209, 217, 249, 265, 281, 289, 305), chili (105, 113, 137, 153, 177, 209, 217, 249, 265, 281), and pear (97, 105, 113, 137, 153, 177, 209, 217, 249, 265, 281, 289, 305). The distribution of ET_s by the trapezoidal method is shown in Figure 8a. For the sinusoidal method, the continuous estimation intervals were set as follows: wheat (97,281) corn (113,281) cotton (113,305) chili (105,281) and pear (97,305) The spatial distribution of ET_s is shown in Figure 8b. In Experiment C, we changed the estimation intervals from Experiment B based on the growth period mentioned in Section 4.3. This was to evaluate the influence of the estimation interval on the ET_s estimates from the sinusoidal method. The estimation intervals were set as follows: wheat (81,281) corn (121,281), cotton (121,313) chili (105,281) and pear (81,313) The distribution of ET_s is shown in Figure 8c. The calculation process of ET_s was implemented through Interactive Data Language (IDL) programming, and the frequency distribution of ET_s is shown in Figure 9.

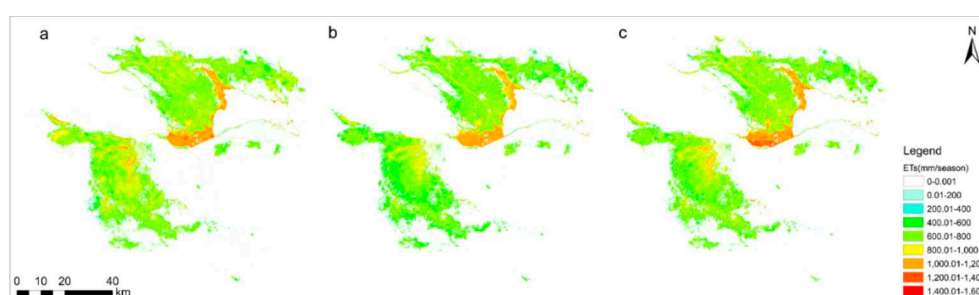


Figure 8. Distribution of ET_s during crop growing season. (a), (b), and (c) refer to the three experiments A, B, and C, respectively.

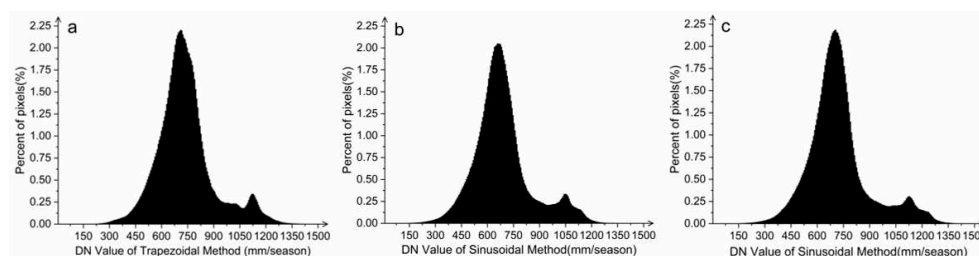


Figure 9. The frequency of ET_s . (a), (b), and (c) refer to the three experiments A, B, and C, respectively.

The distribution shape of the ET_s obtained by the trapezoidal method was consistent with that of the sinusoidal method, as shown in Figures 8 and 9. In both methods, ET_s values in pear fields were found with relatively high values, mainly because it had the longest growing period. There were some noticeable differences between the ET_s obtained from the trapezoidal and sinusoidal methods. Under the same estimation intervals, the ET_s estimates from the trapezoidal method are higher than that of the sinusoidal method, as presented in Figure 8a,b. Based on the results of Experiments B and C, the ET_s estimates change when the estimation intervals are modified. When estimation intervals are set based on the crop phenology, more accurate ET_s estimates can be obtained.

4.5. ET of Five Main Crops during the Growing Season

Figure 10 presents the box plots of ET_s values for wheat, corn, cotton, chili, and pear, while the average ET_s for the five crops are shown in Table 4. The results show pear had the highest evapotranspiration during the growing season, followed by chili. The ET_s of wheat, corn, and cotton were found to be similar. Under the same estimation interval, the ET_s estimates derived using the trapezoidal method were higher than those obtained using the sinusoidal method. Comparing the average ET_s values from Experiments B and C, the change in the estimation interval resulted in different

ET_s estimates using the sinusoidal method. For wheat, the estimation interval expanded from (97,281) in Experiment B to (81,281) in Experiment C, and its average ET_s increased from 634.57 to 660.18 mm. Similarly, the estimation interval for pear was extended from (97,305) to (81,313), and its average ET_s increased from 891 to 943.81 mm. For corn, the contraction of the estimation interval by eight days, from (113,281) to (121,281), caused a slight decrease in the average ET_s from 645.53 to 641.43 mm. For chili, the estimation interval in Experiments B and C was identical, and the average ET_s were almost the same.

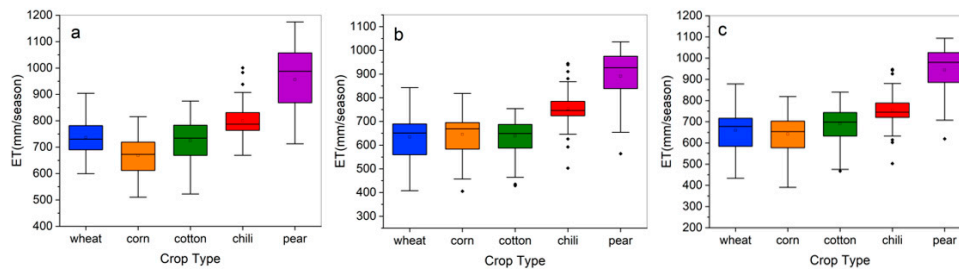


Figure 10. ET of five main crops during the growing season. (a), (b), and (c) refer to the three experiments A, B, and C, respectively.

Table 4. The average ET_s of five main crops.

Crop Type	Average ET_s (mm)					
	a	b	c	a-b	a-c	c-b
Wheat	736.63	634.57	660.18	102.06	76.45	25.61
Corn	668.18	645.53	641.43	22.65	26.75	-4.10
Cotton	725.18	638.52	690.61	86.66	34.57	52.09
Chili	800.33	753.29	755.08	47.04	45.25	1.79
Pear	956.37	891.00	943.81	65.37	12.56	52.81

4.6. Performance of the Proposed Methods for Different Acquisition Frequency of Landsat Images

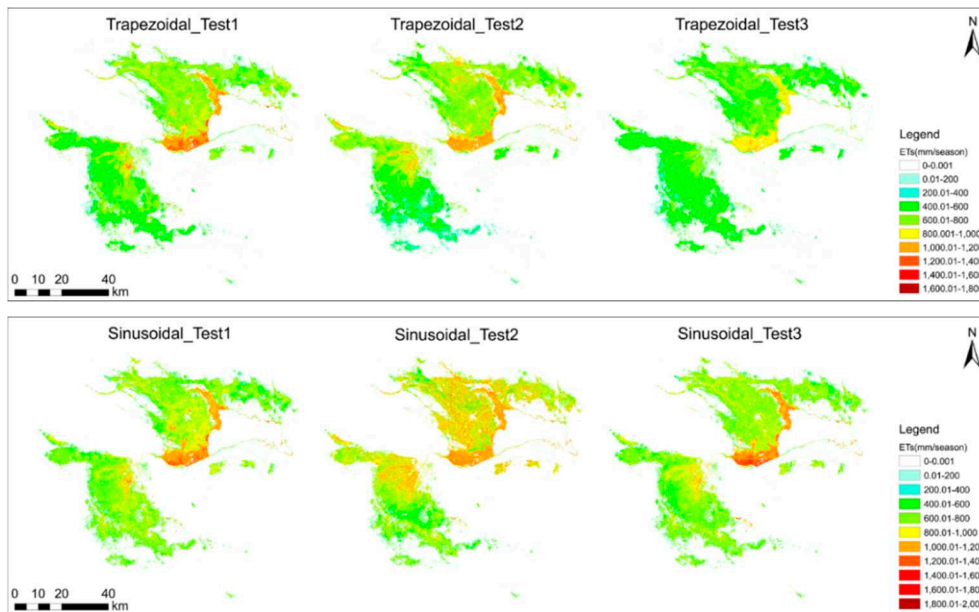
Obtaining time-intensive Landsat images is often challenging for areas with high precipitation and frequent cloud cover. To explore the impact of missing images at various stages of growth on the accuracy of ET_s estimates, the trapezoidal and sinusoidal methods proposed in this paper were used to estimate ET_s using different combinations of multitemporal Landsat images. The experimental design is shown in Table 5.

Three sets of experiments were implemented: (1) the early stage of crop growth was excluded (DOY: 97, 105, 113, 137); (2) the middle stage of crop growth was excluded (DOY: 153, 177, 209, 217); and (3) the final stage of growth was excluded (DOY: 249, 265, 281, 289). We set the intersection of the estimation interval in Section 4.4 Experiment A and the involved images in each test as the estimation interval for each crop because the estimation interval is discrete for the trapezoidal method. Taking the wheat in Test 1 as an example, the discrete estimation interval (DOY) of wheat in Section 4.4 Experiment A is (97, 105, 113, 137, 153, 177, 209, 217, 249, 265, 281), images involved in Test 1 are (DOY: 153, 177, 209, 217, 249, 265, 281), and the intersection of the two datasets is (DOY: 153, 177, 209, 217, 249, 265, 281). Then, we set the estimation interval of wheat as (DOY: 153, 177, 209, 217, 249, 265, 281). We used a similar method to set estimation intervals for other crops in the three experiments. The estimation interval is continuous for the sinusoidal method, and the setting of the integration interval was the same as that in Section 4.4 Experiment C. Figure 11a shows the distributions of ET_s for the three experiments, while the frequency distributions are presented in Figure 11b.

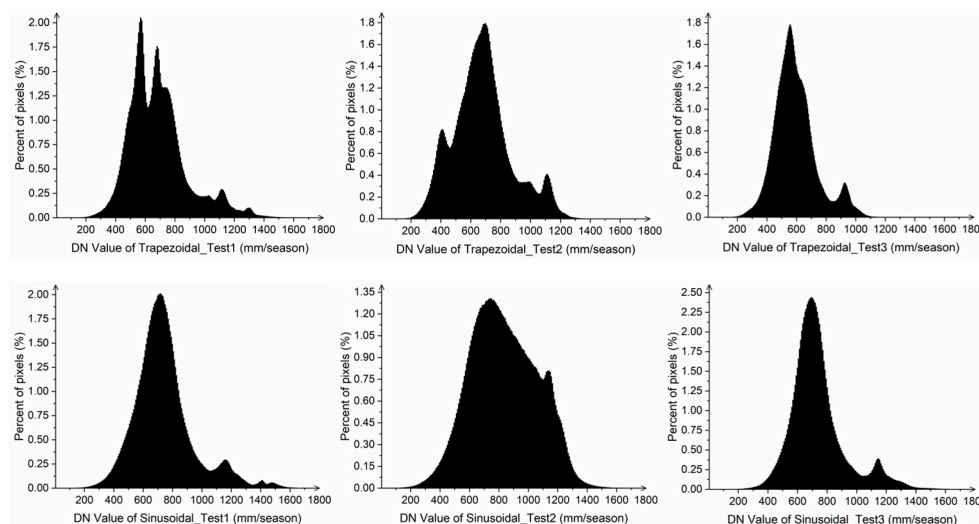
Table 5. The design table of three comparative experiments.

Test	Acquisition Date of Landsat Images (DOY)												
	97	105	113	137	153	177	209	217	249	265	281	289	305
1					✓	✓	✓	✓	✓	✓	✓	✓	✓
2	✓	✓	✓	✓					✓	✓	✓	✓	✓
3	✓	✓	✓	✓	✓	✓	✓	✓					✓

Note: ✓ refers to images that need to be involved in the estimation.



(a)



(b)

Figure 11. (a) The distribution of ET during the growing season and (b) the frequency of ETs.

The tests with excluded images showed lower ET_s results compared with the estimates using all 13 Landsat images (see Figure 8a) using the trapezoidal method, whereas higher ET_s results were found using the sinusoidal method compared with the estimates using all 13 Landsat images (see Figure 8c). Results showed that the frequency of ET_s estimated using 9 Landsat images had a significant difference

from the frequency using 13 Landsat images (Figure 9) for the trapezoidal method. The frequency of estimated ET_s , however, was similar for the sinusoidal method when using either 13 or 9 Landsat images covering the early stage (Test 1) and final stage (Test 3) of crop growth period. This indicates that the sinusoidal method performed better than the trapezoidal method when using Landsat images with low temporal resolution. Moreover, in Test 2 using the sinusoidal method, the ET_s of wheat, corn, and chili were higher, as indicated by vast areas of land shown in orange and red (Figure 11a). This suggests that the effect of missing images at the middle stage of crop growth on ET_s estimation is more significant than that of missing images at the early or final stages.

5. Discussion

In this study, we investigated the estimation of seasonal evapotranspiration for crops in the arid region using multisource remote sensing images. We applied the SEBAL model to estimate the ET_d and proposed a trapezoidal method and a sinusoidal method to estimate evapotranspiration of crops during the growing season. We found that the estimation results from the SEBAL model using Landsat images can reasonably reflect the ET_d of cotton in the study area. We also learned that the sinusoidal method performed better than the trapezoidal method when using Landsat images with low temporal resolution. When we tried excluding images in the analysis, we found that the omission of images during the middle stage of crop growth has the greatest impact on the estimation results of ET_s using the sinusoidal method. Based on these results, we found that the sinusoidal method integrated with multisource remote sensing images offers a useful tool to estimate ET_s with a spatial resolution of 30 m.

The change of ET_d is related to the stages of growth and phenology of the crops (see Figure 6). In the initial stage of growth, while the crops grow fast, the ET_d steadily increases. In the middle stage, when the crops reach their maximum growth, the ET_d reaches its peak. In the late stage, the crops mature and are harvested, resulting in the decrease of ET_d values. Estimated ET values of cotton derived from the SEBAL model were close to the actual ET values obtained using the Penman–Monteith model (see Table 2). This means that the results derived from the SEBAL model were able to properly estimate the ET_d of cotton in the agricultural lands of the Kai-Kong River Basin. However, this study validated the accuracy of the ET_d that is only based on one crop due to the lack of K_c data for other crops. Future research can be conducted to further assess the estimation accuracy of the SEBAL model by using the crops coefficients for other crops. In addition, we used the Gapfill extension tool implemented in the ENVI software to deal with the stripping errors of Landsat 7 ETM+ images. Nevertheless, some error pixels still exist in the strips. Since these pixels only account for a small portion (i.e., less than 10%) of the total image pixels, the estimated ET_d and ET_s might be influenced only slightly by stripping errors.

The actual ET_d is generally difficult to measure due to the high spatial and temporal variability. During the crop growing season, obtaining field measurements of evapotranspiration is often highly problematic. In the absence of actual measurements, previous studies validated their ET_d estimates by comparing them with the data provided in the literature [72]. Similarly, we also used the results from related studies to verify the accuracy of our ET_s estimates, due to the lack of actual field data. Previous studies showed that the average annual water requirement for cotton was 679.00 mm in the Tarim River Basin in Xinjiang from 1989 to 2010, and the average annual effective rainfall was 63.00 mm [73]. Thus, the average annual evapotranspiration for cotton is about 743.00 mm in the Tarim River Basin, which is composed of nine river systems, including the Kai-Kong River Basin. The average annual water requirement for cotton in the Kai-Kong River Basin ranges from 555.70 to 810.20 mm from 1963 to 2012 in another research [74], where the average annual evapotranspiration was about 618.70–873.20 mm. The estimated ET_s of cotton were 725.18, 638.52, and 690.61 mm all within the range, indicating that the estimated results are reasonable. Future work can be conducted to further evaluate the accuracy of the proposed methods using actual measurements from lysimeters.

In this paper, we used 13 Landsat images to estimate ET_s , and we achieved good results via both the trapezoidal and sinusoidal methods. To evaluate the performance of the proposed methods for the

different acquisition frequencies of the Landsat images, we designed three sets of experiments that excluded images in the early stage, the middle stage, and the final stage of crop growth. The results indicate that the trapezoidal method is suitable when using Landsat images with high temporal resolution, while the sinusoidal method is suitable when using Landsat images with low temporal resolution. Furthermore, the middle stage of crop growth is an important integral component of ET estimation for the sinusoidal method. When obtaining time-intensive Landsat images is difficult, the sinusoidal method can still be used to estimate ET_s even with the absence of some images in the early or final stages of the crop growing season. The sinusoidal method, integrated with multisource remote sensing images, offers a useful tool to estimate ET_s with a spatial resolution of 30 m for crops in the study area. Moreover, we used the sine function to fit the time-series ET data, extracted from MOD16A2 images, mainly inspired by the method of extending ET_{inst} to ET_d estimates in this paper. In future endeavors, we will apply the polynomial function and other functional forms to the time-series ET data, and we will compare the fitting accuracy of the sine function.

Compared with other methods for estimating ET_s , the main advantage of the proposed sinusoidal method is that it estimates ET_s for crops using remote sensing images only covering the crop growth period within one year. In this paper, we applied the sinusoidal method to estimate the ET_s in the arid region of the agricultural land of the Kai-Kong River Basin in Xinjiang. This method also has the potential to be applied in semiarid or temperate regions. The ET_d derived from the SEBAL serves as an input for the estimation of ET_s by the sinusoidal method. Since the SEBAL has been widely used in arid and semiarid regions, as well as temperate regions [75], we believe that the sinusoidal model can also be used to estimate ET_s in semiarid and temperate regions based on the multitemporal ET_d images derived from the SEBAL model and time-series of MOD16A2 images. Nonetheless, future research can be conducted to further test the applicability of the sinusoidal method in these regions. In addition, the spatial resolution of the ET_s obtained for crops depends on the resolution of the input of multitemporal ET_d images, i.e., 30 m resolution in this paper. Theoretically, the proposed method can also be used to obtain ET_s with different resolutions when using ET_d images with different resolutions, leading to our future work.

6. Conclusions

This study investigated the estimation of seasonal evapotranspiration for crops in an arid region using multisource remote sensing images. We applied the SEBAL model to estimate the ET_d in the agricultural lands of the Kai-Kong River Basin, Xinjiang, China. We proposed a trapezoidal and a sinusoidal method to upscale ET_d values to ET_s . Based on the results of the study, we conclude the following:

- (1) The SEBAL model is effective in estimating the ET_d of cotton using Landsat images in the agricultural lands of the Kai-Kong River Basin, Xinjiang, China.
- (2) Compared with the trapezoidal method, the sinusoidal method can obtain more accurate ET_s when using Landsat images with low temporal resolution.
- (3) The sinusoidal method integrated with multisource remote sensing images offers a useful tool to estimate ET_s with a spatial resolution of 30 m for crops in the arid area.

Author Contributions: M.C. and X.W. conceived and designed the experiments; M.C. and M.L. performed the experiments; M.C., M.L., and X.W. analyzed the results; M.C. and M.L. wrote the paper; M.C., M.L., and X.W. revised the paper. All authors have read and agreed to the published version of the manuscript.

Funding: This research was funded by National Key Research and Development Project (2017YFB0504203) and the Central Guide Local Science and Technology Development Project (2017L3012).

Acknowledgments: The authors thank Yali Li, Wuhan University, for her support in the collection and preprocessing of Landsat satellite images, and thank the funding for financial support.

Conflicts of Interest: The authors declare no conflict of interest.

References

- Duarte, R.; Yang, H. Input–Output and Water: Introduction to the Special Issue. *Econ. Syst. Res.* **2011**, *23*, 341–351. [[CrossRef](#)]
- Yu, O.; Raichle, B.; Sink, S. Impact of biochar on the water holding capacity of loamy sand soil. *Int. J. Energy Environ. Eng.* **2013**, *4*. [[CrossRef](#)]
- Rawat, K.S.; Singh, S.K.; Bala, A.; Szabó, S. Estimation of crop evapotranspiration through spatial distributed crop coefficient in a semi-arid environment. *Agric. Water Manag.* **2019**, *213*, 922–933. [[CrossRef](#)]
- Allen, R.G.; Pereira, L.S.; Raes, D.; Smith, M. *Crop Evapotranspiration-Guidelines for Computing Crop Water Requirements-FAO Irrigation and Drainage Paper 56*; FAO: Rome, Italy, 1998; Volume 300, p. D05109.
- Guo, E.W.; Zhang, L.J. Estimating Evapotranspiration Using SEBAL Model and Landsat-8 RS Data. *J. Irrig. Drain.* **2019**, *38*, 83–89.
- Wilson, K.B.; Hanson, P.J.; Mulholland, P.J.; Baldocchi, D.D.; Wullschleger, S.D. A comparison of methods for determining forest evapotranspiration and its components: Sap-flow, soil water budget, eddy covariance and catchment water balance. *Agric. For. Meteorol.* **2001**, *106*, 153–168. [[CrossRef](#)]
- Tyagi, N.; Sharma, D.; Luthra, S. Determination of evapotranspiration and crop coefficients of rice and sunflower with lysimeter. *Agric. Water Manag.* **2000**, *45*, 41–54. [[CrossRef](#)]
- Young, M.H.; Wierenga, P.J.; Mancino, C.F. LARGE WEIGHING LYSIMETERS FOR WATER USE AND DEEP PERCOLATION STUDIES. *Soil Sci.* **1996**, *161*, 491–501. [[CrossRef](#)]
- Dugas, W.; Fritschen, L.; Gay, L.; Held, A.; Matthias, A.; Reicosky, D.; Steduto, P.; Steiner, J. Bowen ratio, eddy correlation, and portable chamber measurements of sensible and latent heat flux over irrigated spring wheat. *Agric. For. Meteorol.* **1991**, *56*, 1–20. [[CrossRef](#)]
- Massman, W.J. A simple method for estimating frequency response corrections for eddy covariance systems. *Agric. For. Meteorol.* **2000**, *104*, 185–198. [[CrossRef](#)]
- Wagle, P.; Gowda, P.H.; Neel, J.P.; Northup, B.K.; Zhou, Y. Integrating eddy fluxes and remote sensing products in a rotational grazing native tallgrass prairie pasture. *Sci. Total. Environ.* **2020**, *712*. [[CrossRef](#)] [[PubMed](#)]
- Yinglan, A.; Wang, G.; Liu, T.; Xue, B.; Kuczera, G. Spatial variation of correlations between vertical soil water and evapotranspiration and their controlling factors in a semi-arid region. *J. Hydrol.* **2019**, *574*, 53–63. [[CrossRef](#)]
- Su, Z.; Yacob, A.; Wen, J.; Roerink, G.; He, Y.; Gao, B.; Boogaard, H.; Van Diepen, C. Assessing relative soil moisture with remote sensing data: Theory, experimental validation, and application to drought monitoring over the North China Plain. *Phys. Chem. Earth, Parts A/B/C* **2003**, *28*, 89–101. [[CrossRef](#)]
- Kang, S.Z.; Wang, P.X.; Ling, T. Comparative Analysis of Regional Evapotranspiration Estimation Models Using Remotely Sensed Data. *Trans. Chin. Soc. Agric. Eng.* **2006**, *7*, 6–13.
- Zhang, X.D.; Yang, X.G.; Li, H.Y. Model to Compute the Actual Evapo-Transpiration in the Field of Rainfed Wheat. *Agric. Res. Arid Areas* **2005**, *1*, 34–38.
- Wang, J.; Li, H.P.; Li, H.Y. Review of Regional Evapotranspiration Estimation Models Basing on the Remote Sensing. *Water Sav. Irrig.* **2016**, *8*, 195–199.
- Xu, X.; Zhang, L.; Chen, L.; Liu, C. The Role of Soil N₂O Emissions in Agricultural Green Total Factor Productivity: An Empirical Study from China around 2006 when Agricultural Tax Was Abolished. *Agriculture* **2020**, *10*, 150. [[CrossRef](#)]
- Xu, X.; Chen, L. Projection of Long-Term Care Costs in China, 2020–2050, Based on the Bayesian Quantile Regression Method. *Sustainability* **2019**, *11*, 3530. [[CrossRef](#)]
- Xu, X.; Xu, Z.; Chen, L.; Li, C. How Does Industrial Waste Gas Emission Affect Health Care Expenditure in Different Regions of China: An Application of Bayesian Quantile Regression. *Int. J. Environ. Res. Public Heal.* **2019**, *16*, 2748. [[CrossRef](#)]
- Jahangir, M.H.; Arast, M. Remote Sensing Products for Predicting Actual Evapotranspiration and Water Stress Footprints under Different Land Cover. *J. Clean. Prod.* **2020**, *266*. [[CrossRef](#)]
- Xue, J.Y.; Bali, K.M.; Light, S. Evaluation of Remote Sensing-Based Evapotranspiration Models Against Surface Renewal in Almonds, Tomatoes and Maize. *Agric. Water Manag.* **2020**, *238*. [[CrossRef](#)]
- Jin, X.; Zhu, X.; Xue, Y. Satellite-based analysis of regional evapotranspiration trends in a semi-arid area. *Int. J. Remote. Sens.* **2019**, *40*, 3267–3288. [[CrossRef](#)]

23. Zheng, C.; Jia, L.; Hu, G.; Lu, J. Earth Observations-Based Evapotranspiration in Northeastern Thailand. *Remote Sens.* **2019**, *11*, 138. [[CrossRef](#)]
24. Hu, G.; Jia, L. Monitoring of Evapotranspiration in a Semi-Arid Inland River Basin by Combining Microwave and Optical Remote Sensing Observations. *Remote Sens.* **2015**, *7*, 3056–3087. [[CrossRef](#)]
25. Zheng, C.; Jia, L.; Hu, G.; Menenti, M.; Lu, J.; Zhou, J.; Wang, K.; Li, Z. Assessment of Water Use in Pan-Eurasian and African Continents by ETMonitor with Multi-Source Satellite Data. In Proceedings of the International Symposium on Earth Observation for One Belt and One Road (EOBAR), Beijing, China, 16–17 May 2016; Volume 57. [[CrossRef](#)]
26. Zhang, Y.; Hao, X.M.; Ding, H. A Simplified Method and Its Application for Estimating Potential Evapotranspiration. *Arid Zone Res.* **2019**, *6*, 1431–1439.
27. Hu, G.; Jia, L.; Menenti, M. Comparison of MOD16 and LSA-SAF MSG evapotranspiration products over Europe for 2011. *Remote Sens. Environ.* **2015**, *156*, 510–526. [[CrossRef](#)]
28. Song, J.; Xu, C.C.; Yang, Y.Y. Temporal and Spatial Variation Characteristics of Evapotranspiration and Dry-Wet Climate in Xinjiang Based on MODIS16. *Res. Soil Water Conserv.* **2019**, *5*, 210–214.
29. Ghilain, N.; De Roo, F.; Gellens-Meulenberghs, F. Evapotranspiration monitoring with Meteosat Second Generation satellites: Improvement opportunities from moderate spatial resolution satellites for vegetation. *Int. J. Remote Sens.* **2014**, *35*, 2654–2670. [[CrossRef](#)]
30. Ren, L.L.; Wei, L.Y.; Hu, J.S. Drought Monitoring Utility Assessment of CHIRPS and GLEAM Satellite Products in China. *Trans. Chin. Soc. Agric. Eng.* **2019**, *15*, 146–154.
31. Yang, X.Q.; Wang, G.J.; Pan, X. Spatio-Temporal Variability of Terrestrial Evapotranspiration in China from 1980 to 2011 Based on GLEAM Data. *Trans. Chin. Soc. Agric. Eng.* **2015**, *21*, 132–141.
32. Martens, B.; De Jeu, R.; Verhoest, N.E.C.; Schuurmans, H.; Kleijer, J.; Miralles, D.G. Towards Estimating Land Evaporation at Field Scales Using GLEAM. *Remote Sens.* **2018**, *10*, 1720. [[CrossRef](#)]
33. Martin, J.; Sujan, K.; Ulrich, W. The Fluxcom Ensemble of Global Land-Atmosphere Energy Fluxes. *Scientific Data* **2019**, *6*, 74–88.
34. Courault, D.; Séguin, B.; Olliso, A. Review on estimation of evapotranspiration from remote sensing data: From empirical to numerical modeling approaches. *Irrig. Drain. Syst.* **2005**, *19*, 223–249. [[CrossRef](#)]
35. Song, Y.; Wang, J.; Yang, K.; Ma, M.; Li, X.; Zhang, Z.; Wang, X. A revised surface resistance parameterisation for estimating latent heat flux from remotely sensed data. *Int. J. Appl. Earth Obs. Geoinformation* **2012**, *17*, 76–84. [[CrossRef](#)]
36. Kool, D.; Agam, N.; Lazarovitch, N.; Heitman, J.; Sauer, T.; Ben-Gal, A. A review of approaches for evapotranspiration partitioning. *Agric. For. Meteorol.* **2014**, *184*, 56–70. [[CrossRef](#)]
37. Su, Z. The Surface Energy Balance System (SEBS) for estimation of turbulent heat fluxes. *Hydrol. Earth Syst. Sci.* **2002**, *6*, 85–100. [[CrossRef](#)]
38. Maniruzzaman, M.; Boateng, J.S.; Chowdhry, B.Z.; Snowden, M.; Douroumis, D. A review on the taste masking of bitter APIs: Hot-melt extrusion (HME) evaluation. *Drug Dev. Ind. Pharm.* **2013**, *40*, 145–156. [[CrossRef](#)]
39. Bastiaanssen, W.G.M.; Menenti, M.; Feddes, R.A.; Holtslag, A.A.M. A Remote Sensing Surface Energy Balance Algorithm for Land (SEBAL) 1. Formulation. *J. Hydrol.* **1998**, *212–213*, 198–212. [[CrossRef](#)]
40. Penman, H.L. Natural evaporation from open water, bare soil and grass. *Proc. R. Soc. London. Ser. A Math. Phys. Sci.* **1948**, *193*, 120–145. [[CrossRef](#)]
41. Monteith, J.L. Evaporation and environment. *Symp. Soc. Exp. Boil.* **1965**, *19*, 205–234.
42. Priestley, C.H.B.; Taylor, R.J. On the Assessment of Surface Heat Flux and Evaporation Using Large-Scale Parameters. *Mon. Weather Rev.* **1972**, *100*, 81–92. [[CrossRef](#)]
43. Bastiaanssen, W.; Pelgrum, H.; Wang, J.; Ma, Y.; Moreno, J.; Roerink, G.; Van Der Wal, T. A remote sensing surface energy balance algorithm for land (SEBAL). *J. Hydrol.* **1998**, *212*, 213–229. [[CrossRef](#)]
44. Rawat, K.S.; Bala, A.; Singh, S.K.; Pal, R.K. Quantification of wheat crop evapotranspiration and mapping: A case study from Bhiwani District of Haryana, India. *Agric. Water Manag.* **2017**, *187*, 200–209. [[CrossRef](#)]
45. Bala, A.; Rawat, K.S.; Misra, A.K.; Srivastava, A. Assessment and Validation of Evapotranspiration using SEBAL algorithm and Lysimeter data of IARI Agricultural Farm, India. *Geocarto Int.* **2015**, *31*, 1–29. [[CrossRef](#)]
46. Rahimzadegan, M.; Janani, A. Estimating evapotranspiration of pistachio crop based on SEBAL algorithm using Landsat 8 satellite imagery. *Agric. Water Manag.* **2019**, *217*, 383–390. [[CrossRef](#)]

47. Bhattarai, N.; Quackenbush, L.; Im, J.; Shaw, S.B. A new optimized algorithm for automating endmember pixel selection in the SEBAL and METRIC models. *Remote Sens. Environ.* **2017**, *196*, 178–192. [[CrossRef](#)]
48. Ruhoff, A.L.; Paz, A.R.; Collischonn, W.; Aragão, L.E.; Rocha, H.R.; Malhi, Y. A MODIS-Based Energy Balance to Estimate Evapotranspiration for Clear-Sky Days in Brazilian Tropical Savannas. *Remote Sens.* **2012**, *4*, 703–725. [[CrossRef](#)]
49. Du, J.; Song, K.; Wang, Z.; Zhang, B.; Liu, D. Evapotranspiration estimation based on MODIS products and surface energy balance algorithms for land (SEBAL) model in Sanjiang Plain, Northeast China. *Chin. Geogr. Sci.* **2013**, *23*, 73–91. [[CrossRef](#)]
50. Simaie, E.; Homae, M.; Norouzi, A.A. Evaluating SEBAL Model to Estimate Evapotranspiration Using MODIS and TM Sensors Data. *J. Soil Water Resour. Conserv.* **2013**, *2*, 29–40.
51. Singh, R.K.; Liu, S.; Tieszen, L.L.; Suyker, A.E.; Verma, S.B. Estimating seasonal evapotranspiration from temporal satellite images. *Irrig. Sci.* **2011**, *30*, 303–313. [[CrossRef](#)]
52. Bhattarai, N.; Quackenbush, L.J.; Dougherty, M.; Marzen, L.J. A simple Landsat–MODIS fusion approach for monitoring seasonal evapotranspiration at 30 m spatial resolution. *Int. J. Remote Sens.* **2014**, *36*, 115–143. [[CrossRef](#)]
53. Wagle, P.; Bhattarai, N.; Gowda, P.H.; Zhou, Y. Performance of five surface energy balance models for estimating daily evapotranspiration in high biomass sorghum. *ISPRS J. Photogramm. Remote Sens.* **2017**, *128*, 192–203. [[CrossRef](#)]
54. Allen, R.G.; Tasumi, M.; Morse, A.; Trezza, R.; Wright, J.L.; Bastiaanssen, W.; Kramber, W.J.; Lorite, I.J.; Robison, C.W. Satellite-Based Energy Balance for Mapping Evapotranspiration with Internalized Calibration (METRIC)—Applications. *J. Irrig. Drain. Eng.* **2007**, *133*, 395–406. [[CrossRef](#)]
55. Elnmer, A.; Khadr, M.; Kanae, S.; Tawfik, A. Mapping daily and seasonally evapotranspiration using remote sensing techniques over the Nile delta. *Agric. Water Manag.* **2019**, *213*, 682–692. [[CrossRef](#)]
56. Zhang, P.; Long, A.H.; Hai, Y. The Spatiotemporal Variations and the Driving Forces of Agricultural Water Consumption in Xinjiang (1988–2015): Based on the Statistical Analysis of Crop Water Footprint. *J. Glaciol. Geocryol.* **2019**. Available online: <http://kns.cnki.net/kcms/detail/62.1072.P.20190918.1456.002.Html> (accessed on 18 September 2019).
57. Wang, W.H.; Huang, Y.; Liu, T. Optimized Redistribution of Water Resources in the Kaidu-Kongque River Basin. *Arid Zone Res.* **2018**, *5*, 1030–1039.
58. Chen, Z.S.; Li, B.F.; Fu, A.H. Analysis of Water Demand and Stability for Oasis in Kaidu-Kongque River Basin, Southern Xinjiang. *J. Glaciol. Geocryol.* **2012**, *6*, 1470–1477.
59. Krishnan, S.R.; Seelamantula, C.S. On the Selection of Optimum Savitzky-Golay Filters. *IEEE Trans. Signal. Process.* **2013**, *61*, 380–391. [[CrossRef](#)]
60. Wang, X.-J. Participatory geographic information system review. *Chin. J. Eco-Agric.* **2010**, *18*, 1138–1144. [[CrossRef](#)]
61. Cha, M.X.; Wang, X.Q.; Li, Y.L. Crop Planting Structure Extraction Based on Remote Sensing Data in Kai-Kong River Basin, Xinjiang. *Arid Zone Res.* **2020**, *37*, 532–540. [[CrossRef](#)]
62. Yang, X.; Ren, L.; Jiao, D.; Yong, B.; Jiang, S.; Song, S. Estimation of Daily Actual Evapotranspiration from ETM+ and MODIS Data of the Headwaters of the West Liaohe Basin in the Semiarid Regions of China. *J. Hydrol. Eng.* **2013**, *18*, 1530–1538. [[CrossRef](#)]
63. Allen, R.G.; Irmak, A.; Trezza, R.; Hendrickx, J.M.H.; Bastiaanssen, W.; Kjaersgaard, J. Satellite-based ET estimation in agriculture using SEBAL and METRIC. *Hydrol. Process.* **2011**, *25*, 4011–4027. [[CrossRef](#)]
64. Gao, X.; Sun, M.; Luan, Q.; Zhao, X.; Wang, J.; He, G.; Zhao, Y.; Miao, S. The spatial and temporal evolution of the actual evapotranspiration based on the remote sensing method in the Loess Plateau. *Sci. Total. Environ.* **2020**, *708*. [[CrossRef](#)] [[PubMed](#)]
65. Senkondo, W.; Munishi, S.E.; Tumbo, M.; Nobert, J.; Lyon, S.W. Comparing Remotely-Sensed Surface Energy Balance Evapotranspiration Estimates in Heterogeneous and Data-Limited Regions: A Case Study of Tanzania’s Kilombero Valley. *Remote Sens.* **2019**, *11*, 1289. [[CrossRef](#)]
66. Sun, H.; Yang, Y.; Wu, R.; Gui, D.; Xue, J.; Liu, Y.; Yan, D. Improving Estimation of Cropland Evapotranspiration by the Bayesian Model Averaging Method with Surface Energy Balance Models. *Atmosphere* **2019**, *10*, 188. [[CrossRef](#)]
67. Jackson, R.; Hatfield, J.; Reginato, R.; Idso, S.; Pinter, P. Estimation of daily evapotranspiration from one time-of-day measurements. *Agric. Water Manag.* **1983**, *7*, 351–362. [[CrossRef](#)]

68. Xie, X.Q. Estimation of Daily Evapo-Transpiration (ET) From One Time-of-Daily Remotely Sensed Canopy Temperature. *J. Remote Sens.* **1991**, *4*, 253–260.
69. Vörösmarty, C.; Federer, C.; Schloss, A. Potential evaporation functions compared on US watersheds: Possible implications for global-scale water balance and terrestrial ecosystem modeling. *J. Hydrol.* **1998**, *207*, 147–169. [[CrossRef](#)]
70. Grosso, C.; Manoli, G.; Martello, M.; Chemin, Y.; Pons, D.; Teatini, P.; Piccoli, I.; Morari, F. Mapping Maize Evapotranspiration at Field Scale Using SEBAL: A Comparison with the FAO Method and Soil-Plant Model Simulations. *Remote Sens.* **2018**, *10*, 1452. [[CrossRef](#)]
71. Lv, N.N.; Bai, J.; Chang, C. Spatial-Temporal Changes in Evapotranspiration Based on Planting Patterns of Major Crops in the Xinjiang Oasis During 1960–2010. *Geograph. Res.* **2017**, *8*, 1443–1454.
72. Kamali, M.I.; Nazari, R. Determination of maize water requirement using remote sensing data and SEBAL algorithm. *Agric. Water Manag.* **2018**, *209*, 197–205. [[CrossRef](#)]
73. Shen, Y.J.; Li, S.; Chen, Y.; Qi, Y.; Zhang, S. Estimation of regional irrigation water requirement and water supply risk in the arid region of Northwestern China 1989–2010. *Agric. Water Manag.* **2013**, *128*, 55–64. [[CrossRef](#)]
74. Wang, M.; Yang, Q.; Zheng, J.H.; Liu, Z.H. Spatial and Temporal Distribution of Water Requirement of Cotton in Xinjiang from 1963 to 2012. *Acta Ecologica Sinica* **2016**, *36*, 4122–4130. [[CrossRef](#)]
75. Jin, K.L.; Hao, L. Evapotranspiration Estimation in the Jiangsu-Zhejiang-Shanghai Area Based on Remote Sensing Data and SEBAL Model. *Remote Sens. Land. Res.* **2020**, *32*, 204–212.



© 2020 by the authors. Licensee MDPI, Basel, Switzerland. This article is an open access article distributed under the terms and conditions of the Creative Commons Attribution (CC BY) license (<http://creativecommons.org/licenses/by/4.0/>).

EXHIBIT 8

Review

Remote Sensing of River Discharge: A Review and a Framing for the Discipline

Colin J Gleason ^{1,*} and Michael T Durand ²

¹ Department of Civil and Environmental Engineering, University of Massachusetts Amherst, Amherst, MA 01002, USA

² School of the Environment, The Ohio State University; Columbus, OH 43210, USA; durand.8@osu.edu

* Correspondence: cgleason@umass.edu

Received: 13 February 2020; Accepted: 25 March 2020; Published: 31 March 2020



Abstract: Remote sensing of river discharge (RSQ) is a burgeoning field rife with innovation. This innovation has resulted in a highly non-cohesive subfield of hydrology advancing at a rapid pace, and as a result misconceptions, mis-citations, and confusion are apparent among authors, readers, editors, and reviewers. While the intellectually diverse subfield of RSQ practitioners can parse this confusion, the broader hydrology community views RSQ as a monolith and such confusion can be damaging. RSQ has not been comprehensively summarized over the past decade, and we believe that a summary of the recent literature has a potential to provide clarity to practitioners and general hydrologists alike. Therefore, we here summarize a broad swath of the literature, and find after our reading that the most appropriate way to summarize this literature is first by application area (into methods appropriate for gauged, semi-gauged, regionally gauged, politically ungauged, and totally ungauged basins) and next by methodology. We do not find categorizing by sensor useful, and everything from un-crewed aerial vehicles (UAVs) to satellites are considered here. Perhaps the most cogent theme to emerge from our reading is the need for context. All RSQ is employed in the service of furthering hydrologic understanding, and we argue that nearly all RSQ is useful in this pursuit provided it is properly contextualized. We argue that if authors place each new work into the correct application context, much confusion can be avoided, and we suggest a framework for such context here. Specifically, we define which RSQ techniques are and are not appropriate for ungauged basins, and further define what it means to be ‘ungauged’ in the context of RSQ. We also include political and economic realities of RSQ, as the objective of the field is sometimes to provide data purposefully cloistered by specific political decisions. This framing can enable RSQ to respond to hydrology at large with confidence and cohesion even in the face of methodological and application diversity evident within the literature. Finally, we embrace the intellectual diversity of RSQ and suggest the field is best served by a continuation of methodological proliferation rather than by a move toward orthodoxy and standardization.

Keywords: remote sensing; rivers; discharge; hydrology; modelling; geomorphology; ungauged basins

1. Introduction

Remote sensing (RS) provides value to the earth science community as a source of primary data (electromagnetic radiation recorded directly by the satellite/aircraft) obtained from a unique frame of reference. Although raw electromagnetic radiation received by sensors needs to be carefully calibrated to transform these observations into useable science signals, remote sensing platforms provide high quality primary data at a variety of spatial, temporal, and spectral scales. Hydrology in particular has been traditionally open to the use of RS (e.g., ([1–4]); Calmant et al., 2008; Lettenmaier et al. 2015;

Doell et al. 2016; Lettenmaier et al., 2006), in part because this physically integrative discipline is quite often subject to political data restrictions or difficulties in field data collection.

RS can contribute to both basic and applied hydrology equally from its unique vantage point. Take for example recent work by Allen et al. ([5]; 2018), which provides a new and interesting insight into stream dynamics and organization at the global scale only possible via combining detailed field observations with global remote sensing of rivers. Likewise, Smith et al. ([6]; 2017) used fixed-wing un-crewed aerial vehicles (UAVs) to reveal previously unknown perennial stream networks atop the Greenland Ice Sheet, which suggested a complete revamp of understanding in how ice sheet meltwater is routed to the global ocean. At broader spatial scales, Lehner and Doll ([7]; 2004) offered an early global mapping of lakes and reservoirs, Prigent et al. ([8]; 2001) similarly mapped wetland dynamics, Allen and Pavelsky ([9]; 2015) and Yamazaki et al. ([10]; 2019) provided new maps of global rivers, and Pekel et al. ([11]; 2016) mapped all global hydromorphic features as seen by the Landsat family of satellites over the past 32 years. These important interventions in our understanding of the observed, rather than modelled, positions of the planet's water features represent insight into the earth system only possible with remote sensing. We argue that remote sensing hydrology is therefore poised to respond to the charge laid by McDonnell et al. ([12]; 2007) to use primary data and hypothesis driven science to push the discipline forward.

Remote sensing is also well positioned to respond to the charge of Wood et al. ([13]; 2011) to focus on hydrologic model improvement in pursuit of advancing knowledge of water resources. Lin et al. ([14]; 2019) recently published new simulations of global hydrology that pull from tens of thousands of river gauges and numerous remote sensing products to bring remote sensing to bear in the fullest expression of global hydrologic modelling to date. Such efforts will continue to play important roles in both climate reanalysis and prediction. Remote sensing has also been noted for its ability to observe human impacts on hydrology (e.g., [4,15,16]; Lettenmaier and Famiglietti, 2006; Martin et al., 2016; Yoon and Beighley, 2015), and the impact of hydrology on humans in the form of floods and flood forecasting (e.g., [17–21]; Barton and Bathols, 1989; Biancamaria et al., 2011; Grimaldi et al., 2016, Li et al., 2016; Schumann et al., 2016). These approaches reflect the role hydrology plays in society: water is fundamental to all civilizations and any advance in our predictive capability is welcomed. Ultimately, the unique vantage point of remotely sensed platforms (especially spaceborne sensors) feed hydrology's need for primary data to drive both fundamental discovery and practical application.

River discharge is one of the most important and frequent targets for remote sensing in hydrology. Discharge is the product of river flow area and velocity, or the volume of water passing a specified point at any instant in time. The only method truly capable of *measuring* discharge is a bucket and a stopwatch: literally quantifying a volume of collected water for some given time period. This is obviously impractical for all but the smallest streams, and as such the most respected discharge *estimates* come from an Acoustic doppler current profiler (ADCP) or weir equations. These techniques are commonly referred to as measurements, but they are in fact approximations of discharge (albeit accurate approximations), and are themselves subject to error, especially at very high and very low flows. Stream gauges are discharge estimates as well that transform automated measurements of river stage to discharge via an empirically calibrated rating curve. The data points to calibrate such curves are normally driven by ADCP estimates of discharge. These gauge discharge estimates form the backbone of human water management decisions and hydrologic science.

Remote sensing of river discharge (RSQ) is thus not surprisingly a vibrant field of study in the scholarly literature, but this vibrancy has led to some confusion. There are varying degrees of processing involved in turning primary remotely sensed information into discharge. Remote sensors record electromagnetic radiation, which is then converted to a signal of interest to the hydrologist. These raw signals include recorded reflectances, range and interferometric phase observations, and emittances. Usually, these signals are radiometrically calibrated to conditions at the top of the atmosphere and then georeferenced to a regular grid on the earth's surface to provide the most basic form of primary data in

RSQ. At the other end of the spectrum, gravity recovery and climate experiment (GRACE) observations of relative satellite positions are first turned into a model of the geoid and then processed into mass anomalies via the application of a hydrologic model: the remote sensing signal has indeed driven the data, but many other sources of information and model physics have been invoked to produce the desired output. Thus, many users are confused about remotely sensed data products, and it can be difficult for the non-specialist to determine which products rely on ancillary data and which do not. In the case of RSQ, all methodologies must transform observations to discharge, as we cannot instantaneously and simultaneously measure river depth, cross sectional area, and depth-averaged velocity from space. Accordingly, hundreds of manuscripts have been written on this subject, all fundamentally seeking to use remotely sensed data to estimate river discharge.

We believe that a review of the RSQ literature is timely and necessary. A recent explosion of the literature (and journals willing to publish that literature, including this one) requires careful summarization to understand advances of the past decade. Along with this recent proliferation, many common misconceptions about RSQ have emerged, with authors sometimes incorrectly citing other work and sometimes missing wide swaths of the relevant RSQ literature when introducing new studies. We argue that a fruitful examination of the literature is not based on differentiation via sensor or sensor class as in past sketches of the field (e.g., active vs passive, microwave vs. optical), but based on application area and methodological approach, what is the purpose for the manuscript, and how does a remotely sensed signal turn into discharge? We will thus be sensor agnostic in this regard, and everything from UAVs to satellites are considered here. Such a lens affords us a broad swath of the literature to review, and we are able to bring numerous and seemingly disparate subfields of RSQ together under unifying themes. Ultimately, we hope this paper can serve as a guide to hydrologists in choosing what methods and data might work for them.

The goals of this paper are as follows. (1) We review the literature (mostly since 2010) without downloading and reading every single paper available: we were not uncritically exhaustive. It is inevitable that we have not canvassed some of the relevant literature or very recent literature, but we do believe we have captured a snapshot of important work of the past decade and beyond. Our goal is a broad survey rather than deep discussion in any specific area of the RSQ literature. (2) We introduce terminology and a context for RSQ to differentiate different meanings of the term 'ungauged,' and argue this is necessary for a comprehensive understanding of the RSQ literature. (3) Further, we categorize the literature on two axes: a "gauged" axis and a methodological axis, and find that these distinctions place the literature into the most useful context. (4) Finally, we attempt to debunk common misconceptions about RSQ and discuss its ethics and politics. We believe that what emerges is a holistic picture of the literature as it stands now and where it might fruitfully go next.

Overview and Organization

Sections 2.1 and 2.2 divide the literature into those techniques that are appropriate for politically and totally ungauged basins (Section 2.2) and those that are not (Section 2.1). These terms are introduced in Figure 1. Section 2.1 contains almost twice the number of papers as Section 2.2, reflecting the priorities of many authors. We believe that this high level separation is an important axis of differentiation that should be used to clearly categorize RSQ work in the past and future, and the discussion in Section 3 interrogates our use of this classifying scheme. Following this broad division, we have lumped the almost 170 manuscripts reviewed here into further broad categories within the gauged/ungauged divide as appropriate from our reading (Figure 2). For gauged, semi-gauged, and regionally gauged basins, these categories include calibration/assimilation into hydrologic models that use ancillary in situ data (Section 2.1.1), calibration of hydraulic models (Section 2.1.2), and the largest subsection in the entire RSQ literature: calibration of local channel hydraulics (Section 2.1.3). For politically and totally ungauged basins our subsections include calibration/assimilation into hydrologic (Section 2.2.1) and hydraulic (Section 2.2.2) models as well as geomorphic inverse problems (Section 2.2.3). We have

made these categorizations after careful scrutiny of the literature, and the length of each subsection loosely reflects the volume of the literature in that subfield.

Basin Type	Description	Role of RSQ
Gauged	A watershed with gauges at the outlet and numerous other channels. Well understood hydrologically.	Extend gauge record in space and time
Semi-Gauged	A watershed with a few gauges relative to the entire network. Some reaches well understood.	Extend gauge record in space and time, and provide calibrated input at ungauged reaches
Regionally Gauged	An ungauged watershed nearby other well gauged watersheds. Hydrologically similar to gauged watersheds.	Provide discharge informed by nearby basins
Politically Ungauged	A watershed that may be well gauged, but for which gauge data are not shared publicly.	Improve on existing knowledge
Totally Ungauged	A watershed with no gauges, either due to remoteness, harshness of the environment, or resource deficiency.	Improve on existing knowledge



Figure 1. RSQ adds value to hydrology in different ways based on what we already know about the basin, from improving on that knowledge in the most basic sense (ungauged) to finely augmenting existing data in space and time for specific purposes (gauged). We note rivers in the same basin may change category depending on the specific study reach or sub-watershed of interest: a sub-watershed may be gauged while the basin as a whole is semi-gauged.

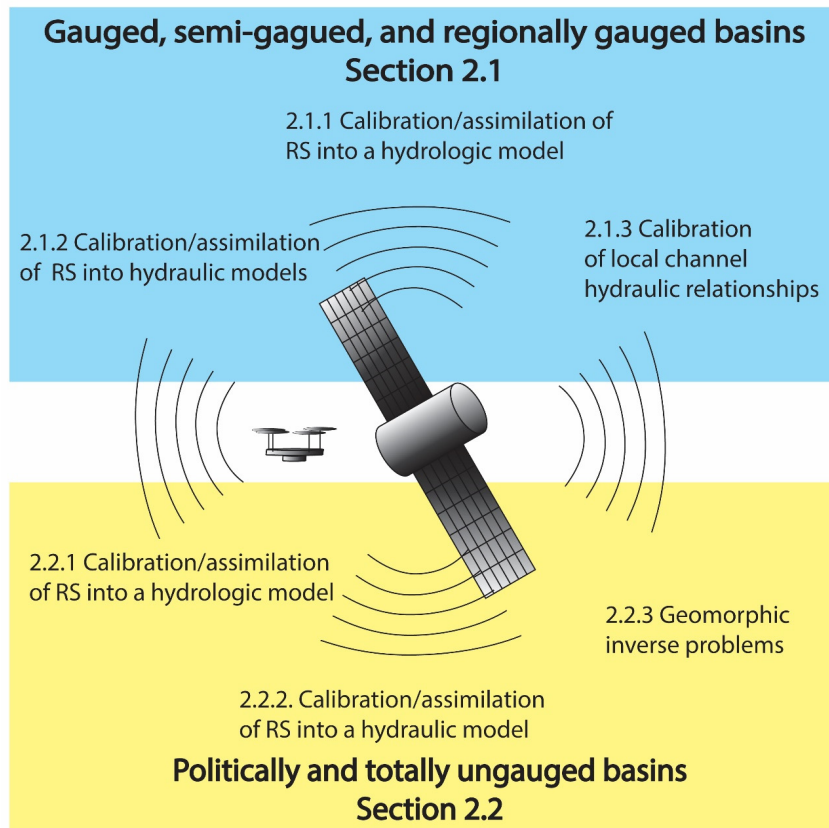


Figure 2. Our classification of the remote sensing of the discharge literature after our reading of the manuscripts cited here. We have purposely brought hydrologic modelling and channel remote sensing together, as we believe they are united by the common goal of discharge prediction.

We note that our reading is broader than previous reviews, and is especially different from an early and influential view of RSQ offered by Alsdorf et al. ([22]; 2007). They noted the rise of then-nascent satellite hydrology and theorized that measurements of water surface elevation and surface slope made from an active sensor would be the best and perhaps only way to provide needed data to address data gaps in hydrology. This perspective on the river channel and its hydraulics as the object of sensing has had a strong influence on the field, and even today our inclusion of Sections 2.1.1 and 2.2.1 bridging between remote sensing and modeling will be surprising to some readers. As recently as 2016, for example, Sichangi et al. [23] begin their introduction to a new RSQ method with their view on the field, which offers a succinct synthesis of many methods boiled down to four bullet points. These authors summarized RSQ into four basic approaches: use of altimetry data to calibrate rating curves, inference of discharge from corrolatory indices based on inundation area, remote sensing of hydraulic components of discharge directly, and the at-many-stations hydraulic geometry (AMHG) approach of Gleason and Smith ([24]; 2014), later to become known as an example of a mass conserved flow law inversion (McFLI, [25]; Gleason et al., 2017). Sichangi et al. thus offer a classification scheme that is effective and focused but excludes much of the relevant literature, particularly on hydrologic modelling. Our reading has indicated that the global hydrologic modelling community relies heavily on remote sensing and has many similar outcomes and goals to the traditionally channel-focused RSQ community, and thus we wish to use this manuscript as an opportunity to view the problem of discharge estimation in as holistic a paradigm as possible.

2. Summary of Remote Sensing of River Discharge

Our organization of the literature relies first on the application area of RSQ: in either a gauged or an ungauged basin. Rather than view an ungauged basin as a binary condition, we believe ungauged status to be a continuum after our reading: ranging from a true lack of data at any relevant spatial or temporal proximity (totally ungauged) to rivers well-monitored by continuous gauge data (gauged, Figure 1). Between these extremes, we consider other examples of ungauged status: some watersheds have sparse gauges through a watershed but not in a channel of interest (semi-gauged), others have gauges in nearby climatologically and geologically similar watersheds (regionally ungauged), while still others are well monitored by gauge data that are not publicly shared (politically ungauged). These tags represent distinct hydrologic realities that all manifest as ‘ungauged’ or ‘gauged’ in much of the literature. We argue that the RSQ goals and appropriate methodologies for these cases are distinct from one another, and that this organizational context is essential for understanding RSQ as a whole.

2.1. Gauged, Semi-Gauged, and Regionally Ungauged Basins

In all of the approaches in Section 2.1, the goal of RSQ is to provide as-accurate-as-possible discharge estimates. These approaches leverage whatever data they can find in order to make the best estimates of discharge possible, and in doing so gain accuracy and precision but become more beholden to the ancillary data/assumptions needed to make each approach successful. Thus, RSQ in this section could be driven almost entirely by a hydrologic model or an in situ gauging station, with RS data used to extend this knowledge in space and time. For example, RSQ could be used to extend gauges to ungauged headwater streams or rivers in a neighboring basin, particularly useful in important but sparsely gauged locations (e.g., the Tibetan Plateau, Siberia). This is in contrast to Section 2.2, where RSQ methods assume very little is known about the watershed according to the context given in Section 3.1.

2.1.1. Calibration/Assimilation of RS into a Hydrologic Model

Hydrologic models seek to parse the components of the hydrologic cycle (precipitation (P), evapotranspiration (ET), terrestrial storage) to calculate water excess (i.e., runoff), which is then routed through a channel network to become river discharge. Often, these models rely on a land-surface module that explicitly parameterizes water and energy fluxes across schema of varying

complexity, and the hydrologic literature has shown itself to be open to bold conclusions made at global scales by models integrating remotely sensed data (e.g., [4,26]; Lettenmaier and Famiglietti, 2006; Rodell et al., 2009). Models frequently require calibration to function well, and remote sensing was seen as an early source of independent calibration/validation data for such models ([27,28]; Gupta et al., 1998; Sivapalan et al., 2003). In fact, Gelati et al. ([29]; 2018) refer to RS data as “ideal benchmarks for spatially distributed evaluations of land surface models.” As a consequence, we believe that no review of RSQ is complete without inclusion of the literature coupling hydrologic modelling and remote sensing to produce discharge. There are hundreds if not thousands of modelling studies using RS information as targets for calibration and assimilation with a goal of producing discharge. We have here distilled the literature into a non-exhaustive survey that we believe captures the spirit of that scholarship. This paradigm for RSQ is not channel based: remote sensing is not asked to provide data on river channels themselves, but rather on the interconnected whole of land surface hydrology in a quest to provide accurate local, regional, or global discharge estimates. Previous characterizations of RSQ (e.g., [22,23,30]; Alsdorf et al., 2007; Sichangi et al., 2016; Tarpanelli et al., 2019) do not include this paradigm in their sketches of the field.

We are aware of the differences between calibration and assimilation. Chief among these is a distinction between tuning parameters that produce a model state variable (calibration), updating this model state directly (assimilation), or updating states and parameters simultaneously (also assimilation: [31]; Reichle, 2008). However, for the purposes of RSQ, we argue that these non-trivial differences are in service of the same goal—to use RS to improve a model of discharge. We thus lump them together here. Also, as Jodar et al. ([32]; 2018) note, a classic approach in hydrologic modelling is to turn to regionalization, where in situ information in one basin is mapped onto another ungauged basin. This regionalization is, for our purposes, another form of calibration. Finally, both Reichle et al., ([33]; 2014) and Maxwell et al., ([34]; 2018) urge caution in assimilation work, as the likelihood function ‘under the hood’ of data assimilation is complex and requires care and consideration in its formulation rather than off the shelf deployment.

Chen et al. ([35]; 1998) were among the first to show how models may be combined with RS to produce discharge, using Topex/Poseidon data to track changes in sea levels and understand anomalies in sea surface heights. They argued that if the ocean is the ultimate reservoir for all terrestrial water, then tracking ocean anomalies is a way to understand necessary changes in the global hydrologic cycle that produced those anomalies. At smaller scales, Dziubanski and Franz [36] 2016) assimilated RS into a snow model to improve estimates of snow water equivalent, but in turn improve estimates of discharge, and Fortin et al. [37] explored the concept of this coupling as early as 2001. Similarly, watershed storage change can be addressed through RS using GRACE satellite observations. GRACE geoid observations can resolve mass fluxes at relevant hydrologic timescales ([38]; Rowlands et al., 2005), and these large-area fluxes of water are used for assimilation and calibration in many hydrology models with a goal of producing river discharge ([39–46]; Syed et al., 2005; 2007; 2009; 2010; Schmidt et al., 2008; Werth et al., 2009; Frappart et al., 2011; Eom et al., 2017). We note that GRACE mass anomalies are themselves often a product of hydrologic modelling ([47]; Wiese et al., 2016), and thus by using GRACE as an RS signal, a hydrologist has perhaps already invoked a calibrated model whether they had intended to or not.

Ultimately, many successful attempts at hydrologic calibration/assimilation invoke more than one RS signal (e.g., [48–51]; Siquera et al., 2018; Chandanpurker et al., 2017; Zhang et al., 2016; Silvestro et al., 2015). The most recent of these efforts ([14]; Lin et al., 2019) delivers on the promise of a previous decade of work. In their study, Lin et al. use large quantities of both ground and RS data (mainly for precipitation and ET) in conjunction with the latest in RS hydrography to produce a coherent global reanalysis of daily river discharge at almost three million river reaches. This level of temporal and spatial precision had not previously been demonstrated, and illustrates the power of RS for global hydrologic modelling. Lin et al. used a calibration approach that considers uncertainty: calibrating with gauges where available, calibrating with RS products where gauges are unavailable,

and calibrating with reanalysis data where RS and gauges are available. This allows optimal use of both in situ and RS data to produce discharge that would be impossible without the use of remote sensing. We note that the approach taken by Lin et al. ([14]; 2019) need not be global; in fact, previous work has taken the same tack toward addressing water resources challenges in the Congo, Himalayas, and Tibetan Plateau ([52–54]; Lee et al., 2011; Wang et al., 2015; Wulf et al., 2016). All of these studies used RS data where gauges were not available to calibrate their model, but all rely on in situ data to provide the bulk of model skill.

We have barely scratched the surface of this literature, but have included these brief examples to make our assertion that the regional and global hydrologic modelling community are as much a part of RSQ as traditional channel-based RSQ. In fact, hydrologic modelling can overcome the spatial and temporal limitations of RS data (which themselves augment the spatial limitations of gauges), and clever assimilation and calibration can account for uncertainties in both RS and in situ parameters and thus lead to a final product greater than the sum of its parts. Rivers are but one part of a hydrologic whole, and authors in this section move forward with this in mind.

2.1.2. Calibration/Assimilation RS into Hydraulic Models

More traditionally, RSQ is grounded in the fields of fluid mechanics, hydraulics, and fluvial geomorphology. These large fields of study have long been interested in how river channels respond to channel form, sediment transport, and landscape evolution and have yielded numerous empirical and first principles equations that govern precisely how water in a river channel responds to different environmental conditions. The famous Manning's equation is one such example that seeks to balance friction losses with gravity-driven flow in a river channel, despite its simplified insistence on a fixed velocity-depth exponent and a stage-constant roughness. Similarly, hydraulic geometry predicts responses in width, depth, and velocity given changes in discharge (e.g [55,56]; Ferguson, 1986; Gleason, 2015), and many additional empirical fluvial geomorphic phenomena relating satellite-observable quantities with discharge have been observed beyond these traditional ground-based parameters. These hydraulic phenomena thus form hydraulic models of river behavior, which can be as simple as the Manning's equation or as complex as a full 3D conservation of mass and momentum in a finite element model. These hydraulics can be coupled with information from the hydrologic cycle, as the shape of hydrographs themselves has information about watershed processes that may inform RSQ ([57]; Fleischmann et al., 2016). The studies in Sections 2.1.2 and 2.1.3 invoke these hydraulic relations as the basis for RSQ in conjunction with data and assumptions only available for gauged, semi-gauged, and regionally gauged basins. An earlier review germane to this topic and specific to the Amazon is given by Hall et al. ([58]; 2011).

Among the most interesting and innovative hydraulically based approaches was pioneered by hydrologist Dave Bjerklie. Bjerklie and his collaborators were writing principally in the early 2000s, and if their approach had been devised today, we would likely label it as a 'big data' approach. Bjerklie et al. ([59]; 2003) noted that discharge can be reduced to a function of width, depth, slope, and Manning's n assuming the restrictive and limiting assumption of a parabolic channel shape. Using thousands of field observations, Bjerklie et al. built statistical relationships between these parameters, and argued on the strength of their training data that mean values of these parameters are reliably estimated globally by this purely empirical approach and RS observations. Bjerklie et al. ([60]; 2005) built on this to fit a calibration between maximum channel width and slope as a power function using multiple regression on a ~1000 river dataset of hydraulic observations, and Bjerklie ([61]; 2007) derived an equation for bankfull velocity from channel slope and lengths of meander bends. Thus, Bjerklie et al. have simplified the underconstrained RSQ hydraulic problem by using big-data empirical geomorphic relationships that theoretically represent all global rivers, creating new generalized hydraulic models ripe for remote sensing in the process. Further work has explicitly compared this Bjerklie approach to space-based rating curves ([62] Kebede et al., 2020). This raises an interesting question about whether or not this approach is best placed in Section 2.1 or Section 2.2. This approach would not be

possible without mining thousands of in situ observations (hence Section 2.1), but once these empirical relations are defined, they are globally applicable without further calibration (Section 2.2). However, any statistical learning is subject to the representativeness of the training data, which in the case of Bjerklie et al.'s work comes entirely from the US. Frasson et al. ([63]; 2019) have recently updated this framework with additional observations, this time built at the truly global scale, which places their work better in the context of Section 2.2. We therefore argue that the works of Bjerklie are only truly applicable within their training samples, and this work is more continental than global, while the work of Frasson et al. is a better example of how this paradigm might apply in ungauged basins. Further, we argue that Bjerklie's work is closer to regionalization than to global modelling as in Section 2.1, and this distinction will become important as we seek context for the field of RSQ in Section 3.

Neal et al. ([64]; 2009) offer a different tack for calibrating hydraulic models. In their and the rest of the papers in this section, the goal is to remotely sense the components of discharge separately (e.g., depth, velocity, width, flow resistance) before passing these to a model. In these cases, the hydraulic model in question is a finite element or finite difference model capable of prediction in space and time, rather than the generalized models of Bjerklie. Neal et al. ([64]; 2009) used SAR to estimate discharge using a Kalman Filter and assumptions of a given initial flow, the river as linear reservoir, stress and flow thresholds, a lidar DEM, ground surveys, an assumed Manning's n , and a soil moisture deficit. Given all of these assumptions, their method worked well. However, the authors acknowledge the amount of 'expert judgement' required for a good result, and this approach is useful only in situations in which a good deal of information is already known about the channel. Similarly, Temimi et al. ([65]; 2011) assimilated different RS signals into a model coupled to assumptions of hydraulic geometry to assess flood discharge. They too were successful, but like Neal et al. required in situ data to correctly parameterize the channel. King et al. ([66]; 2018) improved on this approach to eliminate many of these assumptions using UAV stereo photogrammetry to drive the US Army Corps' Hydraulic Engineering Center's River Analysis System (HEC RAS) hydraulic model. Given an input flow from an upstream gauge and a rating curve, they adjusted the water levels in the hydraulic model until they matched area changes observed by the UAV, relying on the fine-scale DEM created photogrammetrically. This labor intensive RSQ algorithm is effective, but only at the scales for which it can be replicated. Harada and Li ([67]; 2018) combined numerous field inputs with multispectral imagery to calibrate sediment grain size distributions and shear stresses along with discharge, and Try et al. ([68]; 2018) used an empirical width-depth formula in their model to estimate discharge from river width. In all of these cases, authors start from a few known and a few unknown hydraulic parameters of a particular hydraulic model, and use RS for the unknowns. The success of such an approach is, not surprisingly, a function of how well the problem can be posed, with the caveat that the better posed the problem, the more data are required.

2.1.3. Calibration of Local Channel Hydraulic Relationships

Remotely Sensed Rating Curves

Perhaps the most logical transition from traditional hydrology to RSQ is the realization that empirical relationships might be built from RS signals and calibrated directly to observed discharge for a specific channel. In its simplest form, this paradigm takes shape as a space-based rating curve. Among the earliest examples of the space rating curve uses altimetry estimates of river stage directly in a rating curve together with in situ measured flows ([69]; Koblinsky et al., 1993). This is an analog to the gauging station, and forms a powerful discharge monitoring approach provided sufficient in situ data are available to populate the rating curve. Other early work included SAR studies of floodplains, rivers, and lakes interested in deriving levels and/or widths in service of these rating goals ([70–75]; Smith et al., 1996; Alsdorf, 2003; Alsdorf et al., 2001; 2001; Frappart et al., 2005; LeFavour and Alsdorf, 2005), and Smith ([76]; 1997) reviewed work to date at the time of writing. Kouraev et al. ([77]; 2004) and similar studies continued to expand and refine the capabilities of traditional radar altimetry to

compute discharge at locations where in situ data are available, and this work continues through today (e.g., [78–84]; Pavelsky, 2014; Pavelsky and Smith, 2009; Schneider et al., 2017; Young et al., 2015; Paris et al., 2016; Nathanson et al., 2012; Feng et al., 2019). The field has matured to the point where detailed considerations of RS signal quality are becoming important (e.g., [85]; Normandin et al., 2018), rather than repeated proof of concept of the viability of space-based rating. We note also that altimetry signals often used in space based rating curves are generally only applicable over large rivers; most altimeters have been designed for ocean applications and reprocessing these signals over smaller rivers is often challenging. Width measurements can also drive rating curves. These are straightforward to derive for RSQ purposes on rivers as narrow as 12 m with the advent of CubeSats, but these signals are often of less radiometric quality than those available from conventional satellites ([84]; Feng et al., 2019). Research in this area also goes beyond the use of satellites. Ashmore and Sauks ([86]; 2006), Gleason et al. ([87]; 2015), and Young et al. ([81]; 2016) all used time lapse cameras to provide an RS signal for river effective width extraction for remote Arctic rivers coupled with in situ discharge measurements. Huang et al. ([88]; 2018) used UAVs in conjunction with satellite data and a gauge on the information-sparse Tibetan plateau, similar to King et al. ([66]; 2018). These small-area applications highlight how not all RSQ work is driven by either global or ungauged basin interests, and provide innovative solutions to practical fieldwork issues via RSQ. In sum, this section represents the most straightforward and non-controversial application of RSQ reviewed here, as RS has simply replaced a ground measurement in a traditional discharge estimation paradigm.

Correlations between RS Observations and Discharge

Whatever the RS signal, the idea that RS observations correlate with discharge is powerful. This can move the idea of a rating curve beyond measuring channel stage and/or width toward measuring other targets that can reliably drive RSQ. The work pioneered by Brakenridge et al. ([89]; 2007) illustrates this concept excellently. In this 2007 paper, building off their previous work, Brakenridge et al. identify a simple and powerful phenomenon. They observed that the response of passive microwave satellite observations of river channels relative to a nearby ‘dry’ land area (what they call the ratio between a calibration area C and measurement area M) is strongly correlated with river discharge. The logic behind the Brakenridge ratio is that rivers get wider as discharge increases (the same as the width-based rating curves noted above), but it is not necessary to precisely quantify this top width change (see Figure 3). Rivers do indeed get wider with discharge, but soil moisture near the river also increases and there are numerous spatial changes to the river surface not captured by cross sectional top width changes. A ‘wet’ pixel thus reflects quantities changing with discharge, even if it does not track changes in width directly, while the nearby ‘dry’ pixel is relatively insensitive to these changes. Using a ratio between wet and dry allows a finer response to hydrologic forcing than tracking uncalibrated changes to the ‘wet’ area alone. Further, this approach has the advantage of spatial resolution—coarser ground areas may be considered rather than precise measurements of river width, thus overcoming errors in discharge that propagate from width measurement errors. With this ratio in hand, Brakenridge et al. made rating curves from in situ discharges using higher order polynomial regression.

Since this 2007 publication, this ratio approach has grown into a successful subfield of RSQ that was born from the unique hydrologic vantage point of RS, unlike space based rating curves, which are extensions of ground hydrology. The McFLI approaches covered in Section 2.2.2 are similarly fundamentally tied to a RS vantage point, and both of these ‘schools’ of RSQ are conceived with RS data in mind from the onset. In 2012, Brakenridge et al. [90] pushed their approach to thousands of global stations, using a previously in-situ calibrated hydrology model to provide the training data for discharge predictions. In this case the model provides ‘truth’ to guide the remote sensing, so applicability of this method is dependent on faith in the model output, and in this we see a strong parallel with the studies of Section 2.1.1. Tarpanelli et al. [91]; 2013) proved the same ratio concept is viable from visible and near-infrared observations, and Van Dijk et al. ([92]; 2016) investigated the global potential for the ratio approach while explicitly considering tradeoffs between passive and active

sensors. Tarpanelli et al. have led efforts to refine this approach, with papers in 2017 [93] and 2018 [94] that consider fusion between optical imagery and altimetry while also investigating machine learning (rather than regression) for training algorithms. This work also branches toward the spatial extension of training data through hydrologic modelling, which moves this application squarely beyond well- and semi-gauged basins and into regionally gauged basins.

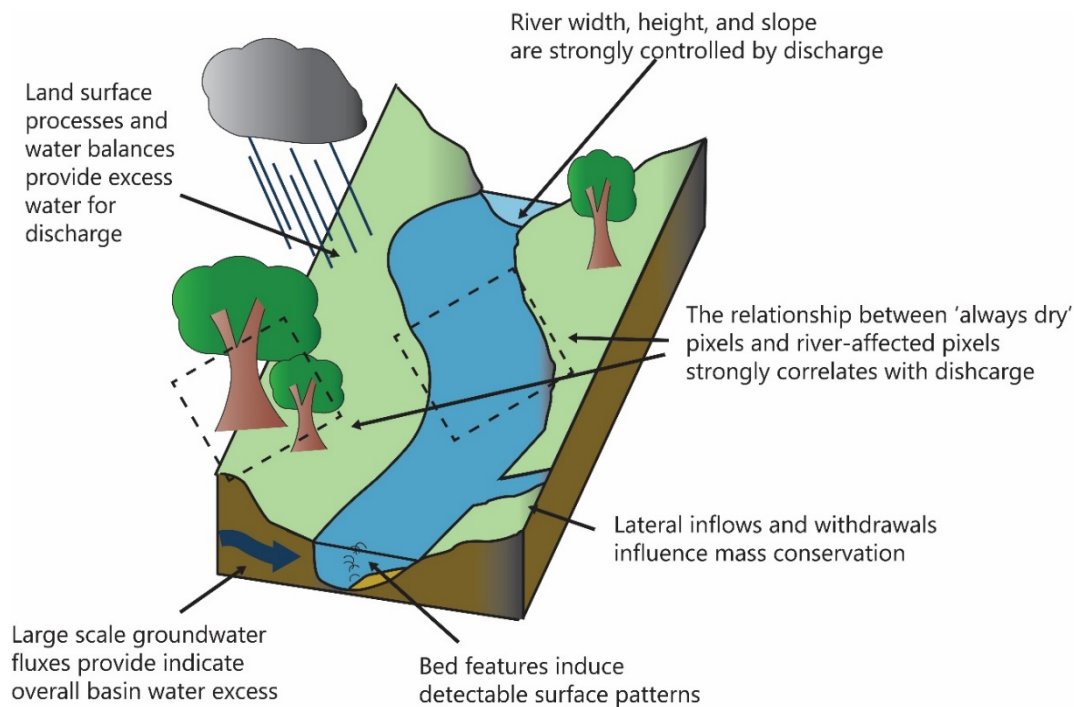


Figure 3. This graphical representation of a river channel encompasses nearly all of the different RS signals considered by authors reviewed here. By presenting them in one image, we hope to highlight the similarities across different techniques.

In Pursuit of Local Channel Hydraulic Parameters

A final channel hydraulic calibration was recognized by scientists as early as the 1970s, when Lynzenga ([95]; 1978) calibrated the reflectance of the bottom of a water column to field measurements to yield a remotely sensed estimate of depth. The principle behind remote sensing of depth is driven by attenuation of light in a water column (Beer's Law). Lee et al. ([96,97]; 1998; 1999) describe this process for vertically homogenous, optically shallow waters (i.e., water columns in which light is able to reflect from the channel bottom and back through the water surface). They separated observed upwelling radiance into three parts—bottom reflectance, surface reflectance, and air column radiance, while controlling for water column attenuation. Lee et al. noted that slight changes in turbidity affect the performance of depth retrieval, so the model must be parameterized according to the properties of the water in both space and time, making this approach impractical in a global sense. Contemporary work continued in this vein (e.g., [98]; Gould et al., 1999), until Fonstad and Marcus ([99]; 2005) and Marcus and Fonstad ([100]; 2008) were among the first to translate this approach to rivers. Remote sensing scientist Carl Legleiter has built on this heritage with a calibrated approach termed optical band ratio analysis (OBRA), first published in 2009 [101]. This approach is built on the same principles of reflection and attenuation as earlier work, and requires calibration or assumption of optical properties to back out river depth. This OBRA approach has been successfully demonstrated in numerous contexts ([102–104]; Legleiter, 2015; Legleiter et al., 2017; Smith et al., 2015). Alternatively, Johnson and Cowen ([105]; 2016) used highly controlled flume experiments to provide estimates of bathymetry based on observed turbulence structures. For example, riffles or hydraulic jumps on a water surface

are indications of changes in channel structure. In all cases, these observations need be calibrated with some in situ information to yield discharge.

If calibrated optical attenuation and other approaches can be used to provide depth estimates, then only channel velocity is needed for a discharge estimate. Costa et al. ([106]; 2000) provide an early remote sensing of velocity method, but this approach requires sophisticated equipment, highly trained personnel, and a bridge: it is not a practical approach for numerous rivers. Further, surface velocity is not the same as the depth-averaged velocity needed to estimate discharge, and more reductive assumptions are needed to transform one to the other. However, Costa et al. provide a proof of concept for remote sensing of channel velocity. More recent work has focused on two basic techniques: Particle Image Velocimetry (tracking particles on water surfaces using image processing techniques) and leveraging turbulence structures. Legleiter et al. ([103]; 2017), for instance, used the OBRA technique for river depth and bridge-based thermal imagery to track surface velocity. A number of recent papers flesh this out, in the context of applying entropy theory to the cross-sectional velocity profile ([107–110]; Chiu, 1991; Fulton and Ostrowski, 2008; Moramarco et al., 2017; 2019). All of these investigations are aided by better geomorphic knowledge of channels, and RS can be useful here too, often through lidar mapping of topography and sometimes bathymetry (e.g., [111]; Hilldale and Raff, 2008). These and the other papers in Section 2.1 show that highly accurate discharge can be estimated from RS, and there seems to be a tradeoff in discharge accuracy vs. the amount of prior data we have on a river, making the most accurate RSQ estimates in the best-understood basins.

2.2. Politically and Totally Ungauged Basins

Fundamentally, RSQ in ungauged basins is an ill posed problem. We cannot measure enough hydraulics from RS to solve for discharge directly, as bathymetry, friction, and discharge will always be unknown in a channel without calibration. The approaches in Section 2.1 might use reasonable values for friction based on knowledge of the basin/channels, or pull bathymetry from a regional regression, or use a hydrologic model, or bypass the hydraulics and calibrate discharge directly to a RS signal to circumvent this problem. The approaches in Section 2.2, however, seek to overcome the problem solely from outer space, limiting themselves to assumptions about rivers that may be made only from RS data or other global data that are independent of specific calibration. The accuracy of these approaches tends to be much lower than the approaches in Section 2.1, yet as we note in Figure 1 the goal of these authors is to improve on what we know in ungauged basins. Given that in many ungauged basins we know very little, even approaches with high errors in discharge can be useful. This literature is much smaller than the scholarly output for Section 2.1, and as such we cover this literature in slightly more depth.

2.2.1. Calibration/Assimilation of an RS Signal into a Hydrologic Model

We first consider RSQ as seen again from a hydrologic perspective, yet this time we focus on RS as the *sole* source of calibration data, as opposed to use of RS data in conjunction with an in situ calibrated model as in Section 2.1. The balance of these fluxes is water excess, and so a valid RSQ approach is to emulate a hydrologic model solely from outer space. Various authors have investigated RS of each of these specific components in an effort to better constrain each one. Parr et al. ([112]; 2015) used RS ET and leaf area index products in conjunction with the VIC model, while Lopez-Lopez et al. ([113]; 2018) explored downscaling and in 2017 calibrated the PCR GLOBWB model for a basin in Morocco with RS ET and soil moisture, and both concluded that their approach is viable and improves discharge accuracy [114]. However, Mendiguren et al. ([115]; 2017) and Bowman et al. ([116]; 2016) explicitly compared RS ET energy balance models against traditionally calibrated hydrological models and found low correlation between the two products. These authors further argued that the spatial component of errors in ET are important and well-suited to remote sensing. Remote sensing of precipitation is a huge field given the importance of precipitation to flood forecasting, and thus this literature is not covered here despite providing important grounding and uncertainty analysis to RSQ; see Lettenmaier et al. ([2];

2015) for a recent review. While this precipitation literature is certainly germane, any satisfactory review would render this manuscript overlong. The GRACE signals covered in Section 2.1.1 can provide the final storage term, and thus a simple water balance may be made at very large spatial footprints for totally and politically ungauged basins from RS estimates of precipitation, ET, and storage.

Moving beyond a simple water balance, Sun et al. ([117]; 2015) provide a basin-scale approach that seeks to use no in situ data to calibrate their hydrologic model, instead using river width observations as a calibration target. This decision required a reconfiguration of traditional model physics to represent width as the state variable (i.e., rearranging the discharge equation so width is on the left hand side). Sun et al. then attempt to force their hydrology model with only globally available data, using the dynamic river width signal to calibrate. Emery et al. ([118]; 2018) follow Brakenridge et al. ([90]; 2012) in using a hydrologic model ‘off the shelf’ to provide calibration data, where their calibrating model was itself previously calibrated using altimetry to track water levels ([82]; Paris et al. 2016). Emery et al. then use this RS-driven model and new, independent altimetry estimates of river stage as inputs to a second hydrologic model, tuning the model based on the Paris et al. ([82]; 2016) discharges. In this approach we see the coupling of the work in Sections 2.1.1 and 2.1.3: using RS signals for both hydraulic and hydrologic components. We have placed this work in the ‘ungauged’ category. On the one hand, Sun et al. and Emery et al. needed no in situ data in their specific approaches and can rightly claim their techniques work in ungauged basins. However, their forcing data, while uniformly available, relied on in situ calibration data from either precipitation gauges or stream gauges in the US and Europe (Sun et al.), or from a specific region (Emery et al.). This idea can be taken further in the context of the Lin et al. ([14]; 2019) paper discussed earlier: that study used over 10,000 in situ gauges to produce the best possible global discharge estimates at almost 3 million river reaches. These Lin et al. data are globally available and consistent, and offer a starting point for any model assimilation/calibration study, be it hydrologic, hydraulic, or both. However, using these outputs necessarily invokes the gauges used to produce them: even discharge information in gauge-sparse locations like Siberia implicitly relies on gauge knowledge via coupling with well-gauged basins. Thus, we expect future work to struggle with what it means for a basin to be ungauged when all global basins have been modelled in a fully coupled land surface framework. We leave further discussion for Section 3.

2.2.2. Assimilation/Calibration of an RS Signal into a Hydraulic Model

RS signals can also be incorporated into models that explicitly represent some aspect of channel hydraulics without in situ data, just as in Section 2.1.2. These representations of hydraulics could range from a full computational fluid dynamics finite element model solving for full four dimensional conservation of energy, mass, and momentum in time, to simple box-channel routing models capable of reproducing channel stage but not width, to Manning’s equation. This channel-based paradigm is perhaps more familiar to readers, as two of the river variables with the longest remote sensing heritage, width and stage, are often employed in these approaches. Bates et al. ([119]; 1997) summarized early work on RS and flood hydraulic modelling, noting the sharp change in fluvial behavior once a river enters its floodplain. Bates et al. noted that computationally efficient one-dimensional flow modelling is acceptable within bank, but not in overbank situations, but also argued that RS signals are ideally poised to capture actual flood events (also noted by [120]; Brakenridge et al., 1998). Thus, RS is well suited to locations where traditional one-dimensional hydraulic models poorly represent hydraulics. Bates et al. conclude by noting that floodplains in particular are excellently suited to RS, as when they are dry, they may be mapped and their elevations recorded for future flood models (furthered in nuance by [121–123]; Horritt and Bates, 2001, Poole et al., 2002, and Horritt, 2006). Then, RS can capture actual floodwater occupation of the floodplain area and transform this into floodplain water depth in order to calibrate the model. Following these early works, many examples of calibration of hydraulic models with RS information have since focused on a flooding context (e.g., [63,124–131], Gumley and King, 1995; Mason et al., 2007; Schumann et al., 2007; 2008; 2009; Coe et al., 2008, Di Baldassarre et al., 2009;

Khan et al., 2011; Frasson et al., 2019). Some of these studies assume upstream flow is known and then use RS to improve downstream flow, but it is possible to iteratively force a model with different flows and an explicit hydraulic model until model output matches RS observations in the floodplain, as Sun et al. did with width in Section 2.2.1. Thus, here we see calibration of a model to RS data, rather than calibrating RS data to a gauge or a model as in Section 2.1.

More recently, advances in global mapping, computational power, and the lengthening of the satellite data record has made a quantum leap in the amount of RS signals available for calibration of hydraulic models. Consider the Pekel et al. ([11]; 2016) product, which classified every single Landsat image in the archive into areas of water and non-water, allowing researchers to track global changes in inundation dynamics and river surface areas (i.e., width) directly for a 32 year period. Using the logic of Bates et al. ([119,132]; 1997; 2003), these changes in surface area can reveal flood stage extents and even heights when mapped onto newly available DEMs built for hydrology (e.g., MERIT DEM, [10] Yamazaki 2019). These inundation signals can also be obtained from non-optical satellites (e.g., [133]; Du et al., 2018), or even from non-satellites (e.g., UAVs, [134]; Niedzielski et al., 2016). As the satellite archive grows, and especially if new commercial CubeSats continue to improve their radiometric calibration and geolocation errors, we predict that approaches built on assimilating/calibrating these signals will proliferate.

Some of this proliferation is underway and is potentially overcoming reliance on gauges we see in the work of the late 2000s. Sichangi et al. ([23]; 2016) offer an interesting approach coupling altimetry, MODIS, and a DEM for eight very large rivers globally. They assume a wide channel with a constant width (greatly simplifying hydraulics), which allows a set of hydraulic equations to be driven by altimetry, which they calibrated with the nearest available altimetry gauge station. This rightly places this paper in Section 2.1.3, but this example shows that the field is moving toward consciously focusing on attempting to eliminate the need for in situ data, presumably to better understand ungauged basins in future.

Andreadis et al. ([135]; 2007) and Durand et al. ([136]; 2008) laid groundwork for RSQ from hydraulic models without any in situ data or global model inputs via detailed experiments to understand how well data assimilation was able to reproduce unknown channel parameters (e.g., friction, bathymetry, flow) from synthetic RS measurements of channel width, slope, and height within a simple hydraulic model. Biancamaria et al. [137]; 2011) and Yoon et al. ([138]; 2012) performed the next generation of this work, which lead to '4D' variational data assimilation (VDA) within an uncalibrated hydraulic model ([139–142]; Gejadze and Malaterre, 2017; Oubanas et al. 2018a; b; Larnier et al., 2020), and these recent efforts offer the most sophisticated take on this problem. This computationally expensive approach is able to consider model states both forward and backward in time and consider uncertainties of both initial model expectations and RS data. 4D VDA considers that initial flow is a static hydrograph, thus removing a dependency on external hydrologic modelling. These authors have shown that accurate discharges can be estimated using this approach, and that these approaches are viable indeed in politically and totally ungauged basins, but sensitivity to the initial hydrograph and computational burden are challenges for large-area application.

2.2.3. Geomorphic Inverse Problems

Finally, we consider approaches to RSQ that again independently consider hydraulic components of discharge (as in Section 2.1.3), but here explicitly rely on geomorphology, RS, and global databases. These approaches are driven by many of the same geomorphic hydraulic models of Section 2.1.2. A special case of geomorphically driven inverse problems is the mass conserved flow law inversion (McFLI) approach. Gleason et al. ([25]; 2017) coined the term as a response to a growing body of the RSQ literature that made the same basic assumptions about how to approach RSQ. Many of these approaches were motivated by the upcoming surface water and ocean topography (SWOT) mission as authors thought about how to best to use SWOT's novel and simultaneous measurements of river width, height, and slope, but McFLI approaches are fundamentally independent from SWOT. Durand et al. ([143];

2010) laid the groundwork for McFLI with a mathematical approach that required known friction coefficients a priori, but the first true examples of McFLI capable of working in totally ungauged basins without this restrictive assumption were all published in 2014 or 2015. In a McFLI approach, authors first assume that a set of cross sections in a reach, or alternatively a set of short connected reaches, are mass conserved. What remains is to solve for unknown parameters in a flow law (e.g., Manning's, hydraulic geometry) given RS observations, meaning the problem remains ill-posed but is now more constrained and solutions may be approximated *exclusively* from remotely sensed data. Like the ratio approach pioneered by Brakenridge et al. ([89]; 2007), McFLI approaches are fundamentally a product of a remotely sensed paradigm. To a McFLI, a remotely sensed snapshot of a river is just that—a moment frozen in time capturing data over a large spatial area. Traditional geomorphology tends to consider evolution of rivers at a single point over long time periods or considers geologically synoptic spatial patterns. McFLI considers the temporal co-evolution of interconnected fluvial entities, which matches RS observations perfectly.

Both Garambois and Monnier ([144]; 2015) and Durand et al. ([145]; 2014) published McFLI algorithms based on Manning's equation assuming known (vis RS) river surface elevation, width, and slope. Unknown parameters are thus Manning's n , some unobserved area below the lowest water surface elevation observation, and discharge. We must note that these data are currently not available from RS without painstaking fusion of optical and altimetry datasets confounded by cloud issues and orbit geometry. Bjerklie et al. ([146]; 2018) were able to produce such signals for one river in Alaska, but most Manning's based McFLI approaches use model data to simulate RS measurements. Durand et al. used these simulated data to solve this problem in a Bayesian context by using likelihood functions in a Markov chain to allow estimates of these unobserved parameters to converge toward a likely posterior distribution. Tuozzolo et al. ([147]; 2019) have explored the impact of reach vs cross section based formulations of Manning's equation for this purpose. Garambois and Monnier used an optimization algorithm to define the pareto parameters that best minimized errors given a set of constraints (including mass conservation) for the same simulated data. Moving toward real data, Altenau et al. ([148]; 2017) showed that SWOT's Ka-Band observations should function as intended, using an airborne Ka-band radar to produce the same observations as SWOT, and Tuozzolo et al. ([149]; 2019) were able to use these airborne observations to successfully give first demonstration of a Manning based McFLI from wide swath altimetry.

Manning's equation is not the only Flow Law invoked in McFLI. Gleason et al. ([24,150]; 2014a;b) proposed a McFLI based on hydraulic geometry (both at a station and at many stations), which requires only river width as an observable input. Unknown parameters in this McFLI are the width exponent of the hydraulic geometry power law and two at many stations' hydraulic geometry constants specific to each river. This width-based McFLI has been successfully demonstrated for Landsat, Sentinel, and Planet optical imagery ([24,84,151]; Gleason and Smith, 2014; Gleason et al., 2014; Gleason and Hamdan, 2015; Feng et al., 2019), first using a genetic algorithm to solve for discharge and later using a Bayesian formulation capable of width-only or width, height, and slope discharge inversion ([152]; Hagemann et al., 2016). Currently, this width-based McFLI is the only known technique capable of leveraging existing satellite data to run a McFLI at all totally ungauged basins at the global scale given our definitions here.

Both Bonnema et al. ([153]; 2016) and Durand et al. ([154]; 2016) have intercompared McFLI approaches using a variety of hydraulic model data to stand in for remotely sensed observations. Durand et al. in particular provided the first ever exhaustive comparison of multiple McFLI approaches on model output representing almost 20 rivers. This controlled experiment allowed Durand et al. to more deeply understand controls on error and accuracy in McFLI approaches. They concluded that approaches that use multiple inputs (i.e., width, height, and slope) generally outperform approaches that use only a single input (i.e., width alone), as expected. They also concluded that all McFLI approaches provide good estimates of discharge dynamics, but all frequently have large biases. These biases are difficult to overcome without better prior estimates of unknown parameters because of the

equifinal nature of McFLI. Finally, Durand et al. found that methods are sensitive to prior expectations of unknown parameters (either the ‘first guess’ in an optimization problem or the Bayesian ‘prior distribution’), but that all methods improve upon these priors. That is, McFLI methods estimate discharge on rivers more accurately than our initial estimate of discharge without in situ or calibration data of any kind, but the more we know about a river to start with, the better the final estimate of discharge will be. This point becomes a critical determinant in choosing an RSQ method in the context of Figures 1 and 4.

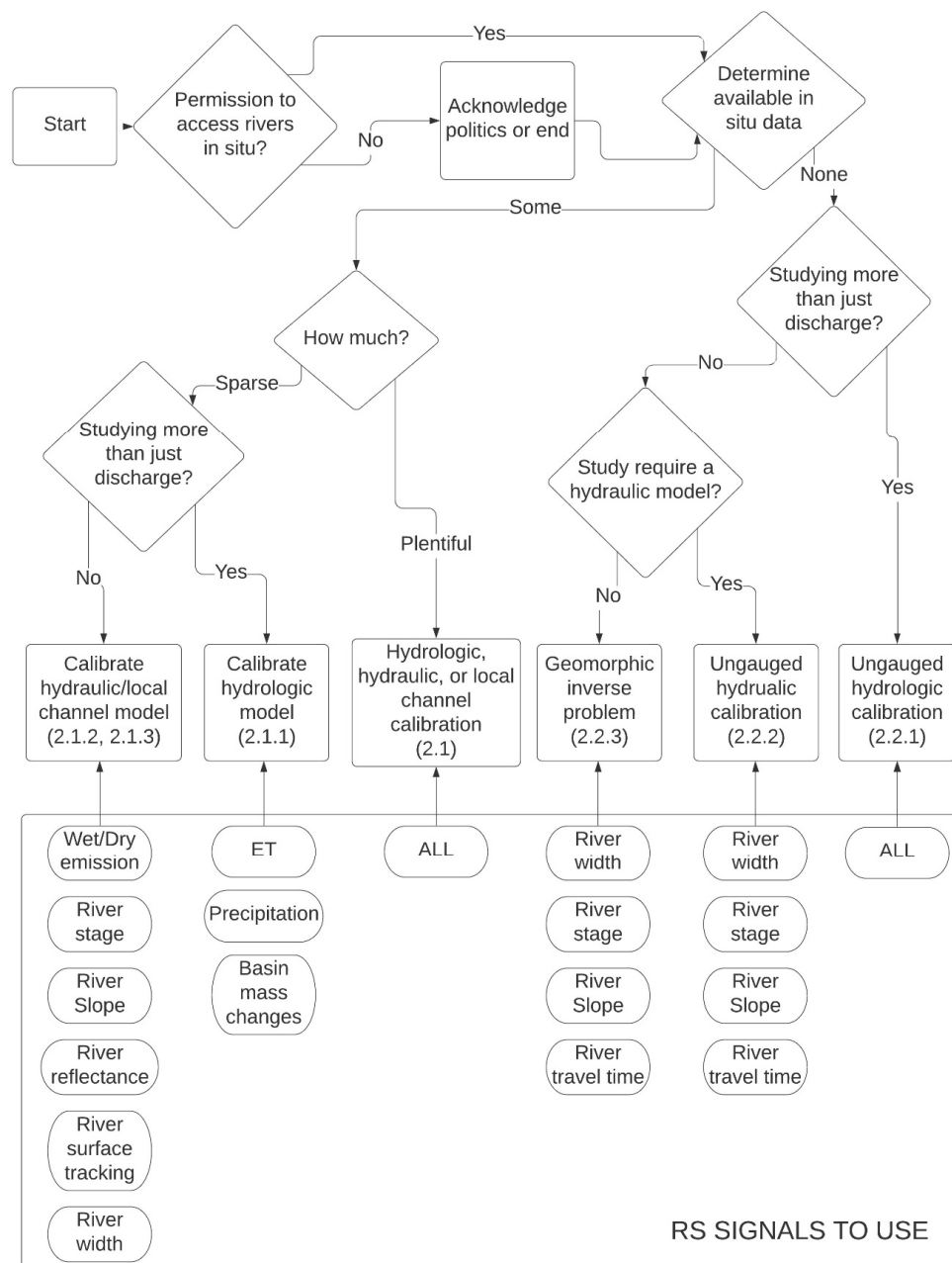


Figure 4. We suggest that this decision chart could be useful in organizing this paper and as a guide for future studies in helping new practitioners decide which approach to use. This organization also reflects our conclusion that the most important determinant between RSQ methods is their need for in situ data. At the bottom of the chart, the RS signals from Figure 3 label each method based on our reading here.

Sichangi et al., ([155]; 2018) offer a different take on underconstrained geomorphic inversion. They used MODIS to back out the travel time of a flood wave by looking at the peak of a width signal at multiple stations in a MODIS river width-time plot. That is, they assumed that maximum widths at any cross section correspond to maximum discharge (a safe assumption per hydraulic geometry) and that the peaks in both stations correspond to the same hydrologic event. Thus, two stations 500 km apart yielded a bulk channel velocity (travel time) by tracking the time delay between width peaks at the two stations. This is an innovative and clever approach to sensing channel velocity from space, but did require Sichangi et al. to assume a Manning's n from look up tables of values ([156]; Chow, 1964) to back out channel depth, and relies on a conversion from celerity to velocity. This rather exciting idea is only useful on large rivers where bulk velocity is stable over long distances and where the assumption of a travelling maximum width is valid. This again also highlights how not all ungauged approaches are applicable globally, and how some assumptions are considered restrictive and others are not. If, for instance, an author can study imagery of a river and a global DEM to determine probable Rosgen ([157]; 1994) classes, then assumptions about friction and width/depth ratios, for example, are well founded and did not invoke in situ data.

3. Discussion

Our broad sketch of the literature has hopefully revealed the numerous ways hydrologists have approached RSQ. We have deliberately included as wide a swath of the literature as possible to fully contextualize the field for practitioners and other interested parties alike. We have raised several discussion points above without bringing them to conclusion, saving them instead for this present section. Specifically, we wish to further probe several ideas that render even our nuanced classification of what it means to be 'gauged' or 'ungauged' problematic vis a vis RSQ; we wish to address common misconceptions about RSQ; and finally we wish to consider human political and economic realities of RSQ.

3.1. A Framework for Understanding RSQ, Ungauged Basins, and Hydrologic Knowledge

Although we did not keep a tally, a majority of the literature surveyed mentioned ungauged basins in their introduction as a justification for the work. We have thus used our gauge continuum to explicitly parse the literature at this highest level, placing each study into our understanding of the appropriate context. However, we have repeatedly raised the question of what it means to be ungauged in an era of global hydrologic modelling. Traditionally, RSQ authors have argued only those studies invoking absolutely no in situ data whatsoever qualify as appropriate for ungauged. RSQ via regionalization (parameter transfer) thus fails this test, and so too does parameterization from a global or regional model as there are almost no global hydrology datasets available that do not invoke in situ calibration data. Even the most basic RS water balance relies on precipitation gauges to calibrate the precipitation signal—without it, these estimates would likely be so wildly wrong as to be not useable. While we maintain an explicit difference between regionalization/ regional calibration vs. coupled modelling, we recognize that global hydrology has advanced tremendously in the RSQ era and thus believe that any RSQ investigation in an ungauged basin will (and should) likely start from an off the shelf global hydrology model to provide a first guess or Bayesian prior. Therefore, following our survey of the literature, we propose the following four conditions for when an RSQ approach is truly capable of tackling totally or politically ungauged basins.

In order to be applicable in totally and politically ungauged basins:

1. The study uses only globally available hydrologic (e.g., P, ET, runoff) forcing
2. If a global model is used, the study must not calibrate an RS signal explicitly to it
3. The study does not transfer parameters or calibrate to regionally available gauges
4. Specific assumptions about channel hydraulics must be obtained exclusively from remotely sensed platforms

These tests should be applied to each new ungauged study to ensure that the primary RS data is indeed driving the discharge result, rather than in situ data available elsewhere. We argue that this independence is essential for politically and totally ungauged basins, as otherwise reviewers and the public will rightly question whether or not discharges in these basins are simply a regurgitation of what we knew before. Hence, we believe that if basins are truly ungauged, models can only guide or bound RSQ, not drive it. Applying these restrictions could limit the accuracy of the resulting discharges ([144,154]; Garambois and Monnier, 2014; Durand et al., 2016), but we argue that these less accurate but independent discharges represent the largest furthering of hydrologic knowledge in these cases and allow hydrologists to make declarative statements about the water cycle.

This is not to say that studies that do not meet these criteria are not RSQ: on the contrary, the vast majority of the literature surveyed here is uninterested entirely with meeting these criteria. Rather, we introduce these tests as a useful filter for future reviewers and authors to help decide what technique is best for a particular application. Thus, RSQ methods need not change if these tests are failed, rather, their introduction should highlight the context of regionally or locally available information and place the study into the appropriate category. Our emphasis on avoiding transferability is grounded in field hydrology, as we, like McDonnell et al. ([12]; 2007), are wary of assuming hydrologic process in unknown and unstudied watersheds. For example, using gauges from one watershed to calibrate a fully coupled earth system model at the continental scale is, to us, fundamentally different than assuming the parameters calibrated for that one watershed should apply to all basins across the continent. The lines between 'regionally gauged' and 'totally ungauged' are becoming blurred as coupled earth system models produce fluxes with greater accuracy and precision. Even so, we maintain a fundamental difference between using a global hydrology product as a starting point for an RSQ method vs. calibrating an RS signal to that model to produce discharge. In the latter, the resulting discharges are fundamentally a product of the original model: at best, RSQ would give you the model discharge back again. In this case, RS would be better used in conjunction with other data to produce the global product in a hydrologic model as in Section 2.1.1, rather than exist as a derived product. Finally, we assert that while in situ data are important to improve the accuracy of RSQ, they are not indispensable. The breadth of the literature covered here makes this abundantly clear, and we see value in pursuing RSQ research across the entire gauge spectrum.

We believe that review of the myriad of techniques for RSQ herein is secondary to definition of the paradigm in which they are employed. While methodological innovation is essential, the literature has revealed that the more data an author has in hand to begin an RSQ study, the more accurate their final discharges. While we have very purposefully avoided the tedium of reporting individual discharge retrieval accuracies across the literature given the impossibility of direct comparison following specific sets of assumptions, RS data, and ancillary data used in each case, we can assert in general that the literature in Section 2.1 is more accurate than the literature in Section 2.2. This is of course intuitive—studies in Section 2.1 all used local or regional gauge data or tailored assumptions of hydraulics specifically to study channels given prior knowledge. However, the methods of Section 2.2 can perform as accurately as those of Section 2.1 given the same calibration data ((141,144); Garambois and Monnier, 2015; Oubanas et al., 2018). Thus, we have chosen to organize the literature by application area first and methodology second, as differences in accuracy are driven largely by prior data and not methodology. Nowhere have we split the literature via sensor, as we find papers arguing for or against specific sensing platforms at the cost of others unhelpful. We do recognize the advantages of passive/active sensors at varying resolutions for specific tasks, but argue that ultimately what matters is whether or not the study has achieved its goal. Figure 3 exists in service of this goal, highlighting all the usable RS signals we have reviewed here in a single figure.

At its core, RSQ seeks to advance hydrologic understanding. In basins that are gauged, semi-gauged, or regionally gauged, hydrologists start with some of this understanding in hand, and RSQ should improve our ability to parse the hydrologic cycle in space and time. For water resource managers, even a well-gauged basin can have insufficient understanding when attempting

to balance hydropower, environmental flows, drought/flood protection, and recreational use ([158]; Brown et al., 2015). RSQ can thus provide real advances in hydrologic understanding that improve human decision making, even in gauged basins. In politically and totally ungauged basins, we suggest that methods that produce hydrographs in error by even a factor of two or more (although we must rely on their performance in gauged basins to characterize this error) might still be an improvement on our existing knowledge. Therefore, we assert that nearly all RSQ is useful to the hydrology community provided authors place their study in the proper context. This context, given here and in Figure 1, is essential for practitioners, authors, reviewers, and editors. Without it, non RS hydrologists can be confused as to whether or not a given technique will work for their application, and editors and reviewers may accept otherwise excellent RSQ work that makes claims of being “ungauged” that it cannot support.

3.2. “The Goal of Remote Sensing of Discharge is to Entirely Replace Gauges”: A Common Misconception

RSQ is designed to produce river discharge and the advantages of air and spaceborne platforms over grueling fieldwork are clear and much touted by RSQ authors. This might lead some to believe that a goal of RSQ is to replace expensive and politically sensitive gauge data. Thus, this section title represents a pernicious misconception about RSQ. The majority of the work cited above requires gauges to produce successful discharge estimates, and even those methods in Section 2.2 that do not require gauge data improve dramatically when informed by gauge data. There will never be any hydrologic substitute for gauge data—these data are carefully monitored by dedicated staff of numerous agencies worldwide, and many agencies go to great lengths to ensure that only the highest quality data are presented as the gauge record. This can have political consequences, as many gauge data receive the ‘seal of approval’ of officially sanctioned government agencies, and a hydrologic world without sanctioned discharges would place much of climate science and water treaties in jeopardy. With that stated, there has been a precipitous decline in available gauge data globally ([159]; Hannah, 2011), and public gauge records are practically nonexistent in places where water politics are thorny ([151]; Gleason and Hamdan, 2015). Gauges that are here today may be gone tomorrow at the whims of economics and politics.

Thus, we believe that RSQ is a natural *complement* to river gauges and other in situ discharge monitoring. In this we agree with Fekete et al. ([160]; 2012), even if we have drawn this conclusion via very different means. The benefits of in situ data to RSQ are clear and have been discussed extensively above. Here, we discuss the benefits of RS signals to in situ monitoring. Consider a well-gauged river network, with a gauge at the outlet and across a large proportion of ungauged upstream reaches. RSQ may actually be at its most beneficial in this case, as high quality gauge calibration data allow RS signals to extend point gauge measurements in space and time. As networks move along the continuum from completely gauged to ungauged, RSQ provides more novel primary information, but RSQ retrievals reduce in accuracy. Alsdorf et al. ([22]; 2007) also highlight that RSQ can document water resources in diverse channel forms and in flood contexts: situations where gauges struggle. Discontinued gauges are another area where RSQ can shine, as gauges that overlap the RS record in the past can be calibrated and then used to parameterize models as they move into the future (e.g., [161,162]; Birkinshaw et al., 2010; Gleason et al., 2018).

In sum, we argue that no RSQ practitioner can or should cogently argue that RSQ is a complete replacement for gauges. Both forms of discharge monitoring have strengths and it is only by merging the two that hydrology can move forward toward more complete understanding of the global hydrologic cycle. The Arctic and much of Asia are almost complete hydrologic black boxes, despite the almost certain existence of un-shared high quality gauge data in these places. Lin et al. ([14]; 2019) highlight the benefits of even sparse global gauging by considering a coupled land-atmosphere system, primary data with low uncertainty might be used to reduce uncertainty in poorly monitored areas, and in this case RS data provide a welcome and irreplaceable source of primary data. We believe that hydrology,

like many geophysical disciplines, should rest on primary data, and loss of either gauge or remotely sensed data is a detriment to the field.

3.3. Ethics and Politics

Finally, we wish to make a brief note on the ethics and politics of RSQ. Gleason and Hamdan ([151]; 2016) and Alvarez-Leon and Gleason ([163]; 2017) have recently explored this topic and have concluded that RSQ is an inherently political act. They reached this conclusion following two different logical tacks. First, since states (the preferred term for ‘country’ in the geographical literature) own their water resources, they are allowed to express their national sovereignty by withholding hydrometric data (i.e., politically ungauged basins). There is no international legal mechanism to force states to release water data, and even bi- or multi-lateral treaties have proven ineffective at forcing water data transparency, despite assertions that such transparency is essential for good governance ([164–168]; Sneddon and Fox, 2006; 2011; 2012; Dore and Lebel, 2010; Ho, 2014). Circumventing these data restrictions via the use of satellites is thus in fact a direct violation of national sovereignty and an inherently political act, regardless of the intent of the scientist ([151] Gleason and Hamdan, 2016). This is not to say that practitioners should not engage in RSQ—on the contrary, there are humanitarian and climate reasons why scientists should perform this very political act. However, scientists have no recourse to state that they are ‘simply observing the earth’ are thus somehow immune to politics. This is a naïve view that has long been debunked in social sciences and the humanities, but is slow to catch on in the non-social sciences, especially in remote sensing. Second, access to satellite data themselves is a result of political decisions ([163] Alvarez-Leon and Gleason, 2017). The United States government has launched a fleet of earth observing satellites, and made it their policy that all of these data are available to anyone with access to the internet. Despite this, the United States government could change its mind at any point and restrict access to these data, thus blanketing access to these crucial primary data in an instant. We do not suggest this is a likely scenario, but it is possible. Consider the numerous other commercial and state-satellites that exist but for whom data are not free or simply not available outside of the home state. Public access to high quality earth system data is ultimately subject to the whims of the owners of the satellites themselves, and this access has profound impacts on hydrologists’ ability to perform RSQ. Taken together, these two arguments suggest that practitioners should take care and make thoughtful choices when applying RSQ in contexts where it would be politically impossible to gather the same data in the field. This forms a good test, and ‘Would I have permission to do this RS work as fieldwork?’ should be a question practitioners ask themselves when beginning a study. If the answer is ‘no,’ practitioners should proceed if believe it is appropriate, but they should be aware of the implications of the study.

4. Conclusions

The existing RSQ literature has frequently justified itself based on whether it is highly accurate or whether it is applicable in ungauged basins. Each new manuscript generally begins with an explicit statement on the utility of RSQ and why this new work belongs in the pantheon of that particular application, yet much work claiming to function in ungauged basins often cannot, by our definitions, truly work in ungauged basins. This leads to evident division in citations within RSQ studies—authors typically only cite work within the categories (i.e., sections and subsections) presented here, and papers frequently do not incorporate information from different ‘families’ of RSQ. What we have shown, however, is that many of these seemingly disparate methods are in fact slight variations on the same paradigm, and that the entirety of the literature has more in common than individual papers would suggest. Our inclusion of ‘non channel’ RSQ here is perhaps controversial to some along this vein, as many RSQ practitioners might suggest that using RS signals within a hydrologic model is somehow not RSQ. It is our hope that this review serves as a reminder that in all cases reviewed here, remotely sensed data were used to estimate discharge in service of furthering discharge understanding. There are nuances in how this was achieved, but all ~170 papers here have the same goal. Finally, we suggest

that our newly defined framing for application of RSQ (e.g., Figure 1 and Section 3.1, Figure 4) might offer much clarity to readers, authors, editors, reviewers, and importantly users of RSQ.

Our review has also implicitly outlined some future directions for the field, which we make explicit here. Data mining/big data approaches seem particularly understudied despite the success of Bjerklie in the early 2000s, and the availability of powerful computer science techniques available to hydrologists today makes this area ripe for potential powerful interventions in RSQ. Satellites dedicated to surface water and sponsored by large state entities (like SWOT), and commercial fleets of CubeSats alike also stand to transform the field. While SWOT has received much attention in the literature from many schools of RSQ, CubeSats are relatively underused. Diverse signals can only improve what we know about the hydrologic system. Finally, we repeat our call for a broadening of perspective of RSQ practitioners. We have shown here that the field is robust, rapidly growing, and rich with an extraordinary diversity of ideas. The field would suffer, we believe, from a descent into orthodoxy, which might stifle creativity. Instead, we hope that new works can use this review as a basis to situate their work in broader context.

Author Contributions: C.J.G. drafted the manuscript and figures. C.J.G. and M.T.D. shared in every aspect of producing this manuscript. All authors have read and agreed to the published version of the manuscript.

Funding: Research was funded by NASA New Investigator Grant 80NSSC18K0741 and NSF CAREER Grant 1748653 to CJ Gleason, and NASA SWOT Science Team grant number NNX16AH82G to MT Durand and CJ Gleason.

Acknowledgments: We apologize to authors of those relevant works we have not cited. Our survey is necessarily broad, and while we have cited more than 160 published works, we have of course missed some relevant literature. The authors disagree strongly on whether or not the letter ‘u’ should appear in the word ‘gauge.’ The first author’s preference has been adopted. We thank also two anonymous reviewers for their prompt comments. This review deviates from journal style to include both numbered citation format and author-date citation information for ease of cross reference by readers.

Conflicts of Interest: The authors declare no conflict of interest.

References

1. Calmant, S.; Seyler, F.; Cretaux, J.F. Monitoring Continental Surface Waters by Satellite Altimetry. *Surv. Geophys.* **2008**, *29*, 247–269. [[CrossRef](#)]
2. Lettenmaier, D.P.; Alsdorf, D.; Dozier, J.; Huffman, G.J.; Pan, M.; Wood, E.F. Inroads of remote sensing into hydrologic science during the WRR era. *Water Resour. Res.* **2015**, *51*, 7309–7342. [[CrossRef](#)]
3. Doell, P.; Douville, H.; Guentner, A.; Mueller Schmied, H.; Wada, Y. Modelling Freshwater Resources at the Global Scale: Challenges and Prospects. *Surv. Geophys.* **2016**, *37*, 195–221. [[CrossRef](#)]
4. Lettenmaier, D.P.; Famiglietti, J.S. Hydrology—Water from on high. *Nature* **2006**, *444*, 562–563. [[CrossRef](#)]
5. Allen, G.H.; Pavelsky, T.M.; Barefoot, E.A.; Lamb, M.P.; Butman, D.; Tashie, A.; Gleason, C.J. Similarity of stream width distributions across headwater systems. *Nat. Commun.* **2018**, *9*, 610. [[CrossRef](#)]
6. Smith, L.C.; Yang, K.; Pitcher, L.H.; Overstreet, B.T.; Chu, V.W.; Rennermalm, Å.K.; Ryan, J.C.; Cooper, M.G.; Gleason, C.J.; Tedesco, M.; et al. Direct measurements of meltwater runoff on the Greenland ice sheet surface. *Proc. Natl. Acad. Sci. USA* **2017**, *114*, E10622–E10631. [[CrossRef](#)]
7. Lehner, B.; Döll, P. Development and validation of a global database of lakes, reservoirs and wetlands. *J. Hydrol.* **2004**, *296*, 1–22. [[CrossRef](#)]
8. Prigent, C.; Matthews, E.; Aires, F.; Rossow, W.B. Remote sensing of global wetland dynamics with multiple satellite data sets. *Geophys. Res. Lett.* **2001**, *28*, 4631–4634. [[CrossRef](#)]
9. Allen, G.H.; Pavelsky, T.M. Patterns of river width and surface area revealed by the satellite-derived North American River Width data set. *Geophys. Res. Lett.* **2015**, *42*, 395–402. [[CrossRef](#)]
10. Yamazaki, D.; Ikeshima, D.; Sosa, J.; Bates, P.D.; Allen, G.H.; Pavelsky, T.M. MERIT Hydro: A High-Resolution Global Hydrography Map Based on Latest Topography Dataset. *Water Resour. Res.* **2019**, *55*, 5053–5073. [[CrossRef](#)]
11. Pekel, J.-F.; Cottam, A.; Gorelick, N.; Belward, A.S. High-resolution mapping of global surface water and its long-term changes. *Nature* **2016**, *540*, 418–422. [[CrossRef](#)] [[PubMed](#)]

12. McDonnell, J.J.; Sivapalan, M.; Vaché, K.; Dunn, S.; Grant, G.; Haggerty, R.; Hinz, C.; Hooper, R.; Kirchner, J.; Roderick, M.L.; et al. Moving beyond heterogeneity and process complexity: A new vision for watershed hydrology. *Water Resour. Res.* **2007**, *43*. [[CrossRef](#)]
13. Wood, E.F.; Roundy, J.K.; Troy, T.J.; van Beek, L.P.H.; Bierkens, M.F.P.; Blyth, E.; de Roo, A.; Döll, P.; Ek, M.; Famiglietti, J.; et al. Hyperresolution global land surface modeling: Meeting a grand challenge for monitoring Earth's terrestrial water. *Water Resour. Res.* **2011**, *47*. [[CrossRef](#)]
14. Lin, P.; Pan, M.; Beck, H.E.; Yang, Y.; Yamazaki, D.; Frasson, R.; David, C.H.; Durand, M.; Pavelsky, T.M.; Allen, G.H.; et al. Global Reconstruction of Naturalized River Flows at 2.94 Million Reaches. *Water Resour. Res.* **2019**, *55*, 6499–6516. [[CrossRef](#)] [[PubMed](#)]
15. Martin, E.; Gascoin, S.; Grusson, Y.; Murgue, C.; Bardeau, M.; Anctil, F.; Ferrant, S.; Lardy, R.; Le Moigne, P.; Leenhardt, D.; et al. On the Use of Hydrological Models and Satellite Data to Study the Water Budget of River Basins Affected by Human Activities: Examples from the Garonne Basin of France. *Surv. Geophys.* **2016**, *37*, 223–247. [[CrossRef](#)]
16. Yoon, Y.; Beighley, E. Simulating streamflow on regulated rivers using characteristic reservoir storage patterns derived from synthetic remote sensing data. *Hydrol. Process.* **2015**, *29*, 2014–2026. [[CrossRef](#)]
17. Barton, I.J.; Bathols, J.M. Monitoring floods with AVHRR. *Remote Sens. Environ.* **1989**, *30*, 89–94. [[CrossRef](#)]
18. Biancamaria, S.; Hossain, F.; Lettenmaier, D.P. Forecasting transboundary river water elevations from space. *Geophys. Res. Lett.* **2011**, *38*, L11401. [[CrossRef](#)]
19. Grimaldi, S.; Li, Y.; Pauwels, V.R.N.; Walker, J.P. Remote Sensing-Derived Water Extent and Level to Constrain Hydraulic Flood Forecasting Models: Opportunities and Challenges. *Surv. Geophys.* **2016**, *37*, 977–1034. [[CrossRef](#)]
20. Li, Y.; Grimaldi, S.; Walker, J.P.; Pauwels, V.R.N. Application of Remote Sensing Data to Constrain Operational Rainfall-Driven Flood Forecasting: A Review. *Remote Sens.* **2016**, *8*, 456. [[CrossRef](#)]
21. Schumann, G.J.-P.; Stampoulis, D.; Smith, A.M.; Sampson, C.C.; Andreadis, K.M.; Neal, J.C.; Bates, P.D. Rethinking flood hazard at the global scale. *Geophys. Res. Lett.* **2016**, *43*, 10249–10256. [[CrossRef](#)]
22. Alsdorf, D.E.; Rodriguez, E.; Lettenmaier, D.P. Measuring surface water from space. *Rev. Geophys.* **2007**, *45*. [[CrossRef](#)]
23. Sichangi, A.W.; Wang, L.; Yang, K.; Chen, D.; Wang, Z.; Li, X.; Zhou, J.; Liu, W.; Kuria, D. Estimating continental river basin discharges using multiple remote sensing data sets. *Remote Sens. Environ.* **2016**, *179*, 36–53. [[CrossRef](#)]
24. Gleason, C.J.; Smith, L.C. Toward global mapping of river discharge using satellite images and at-many-stations hydraulic geometry. *Proc. Natl. Acad. Sci. USA* **2014**, *111*, 4788–4791. [[CrossRef](#)] [[PubMed](#)]
25. Gleason, C.J.; Garambois, P.A.; Durand, M. Tracking River Flows from Space. Available online: <https://eos.org/science-updates/tracking-river-flows-from-space> (accessed on 25 March 2020).
26. Rodell, M.; Velicogna, I.; Famiglietti, J.S. Satellite-based estimates of groundwater depletion in India. *Nature* **2009**, *460*, 999–1002. [[CrossRef](#)] [[PubMed](#)]
27. Gupta, H.V.; Sorooshian, S.; Yapo, P.O. Toward improved calibration of hydrologic models: Multiple and noncommensurable measures of information. *Water Resour. Res.* **1998**, *34*, 751–763. [[CrossRef](#)]
28. Sivapalan, M.; Takeuchi, K.; Franks, S.W.; Gupta, V.K.; Karambiri, H.; Lakshmi, V.; Liang, X.; McDonnell, J.J.; Mendiondo, E.M.; O'Connell, P.E.; et al. IAHS decade on Predictions in Ungauged Basins (PUB), 2003–2012: Shaping an exciting future for the hydrological sciences. *Hydrol. Sci. J. Des.* **2003**, *48*, 857–880. [[CrossRef](#)]
29. Gelati, E.; Decharme, B.; Calvet, J.-C.; Minvielle, M.; Polcher, J.; Fairbairn, D.; Weedon, G.P. Hydrological assessment of atmospheric forcing uncertainty in the Euro-Mediterranean area using a land surface model. *Hydrol. Earth Syst. Sci.* **2018**, *22*, 2091–2115. [[CrossRef](#)]
30. Tarpanelli, A.; Camici, S.; Nielsen, K.; Brocca, L.; Moramarco, T.; Benveniste, J. Potentials and limitations of Sentinel-3 for river discharge assessment. *Adv. Space Res.* **2019**, in press. [[CrossRef](#)]
31. Reichle, R.H. Data assimilation methods in the Earth sciences. *Adv. Water Resour.* **2008**, *31*, 1411–1418. [[CrossRef](#)]
32. Jodar, J.; Carpintero, E.; Martos-Rosillo, S.; Ruiz-Constan, A.; Marin-Lechado, C.; Cabrera-Arrabal, J.A.; Navarrete-Mazariegos, E.; Gonzalez-Ramon, A.; Lamban, L.J.; Herrera, C.; et al. Combination of lumped hydrological and remote-sensing models to evaluate water resources in a semi-arid high altitude ungauged watershed of Sierra Nevada (Southern Spain). *Sci. Total Environ.* **2018**, *625*, 285–300. [[CrossRef](#)] [[PubMed](#)]

33. Reichle, R.H.; De Lannoy, G.J.M.; Forman, B.A.; Draper, C.S.; Liu, Q. Connecting Satellite Observations with Water Cycle Variables Through Land Data Assimilation: Examples Using the NASA GEOS-5 LDAS. *Surv. Geophys.* **2014**, *35*, 577–606. [[CrossRef](#)]
34. Maxwell, D.H.; Jackson, B.M.; McGregor, J. Constraining the ensemble Kalman filter for improved streamflow forecasting. *J. Hydrol.* **2018**, *560*, 127–140. [[CrossRef](#)]
35. Chen, J.L.; Wilson, C.R.; Chambers, D.P.; Nerem, R.S.; Tapley, B.D. Seasonal global water mass budget and mean sea level variations. *Geophys. Res. Lett.* **1998**, *25*, 3555–3558. [[CrossRef](#)]
36. Dziubanski, D.J.; Franz, K.J. Assimilation of AMSR-E snow water equivalent data in a spatially-lumped snow model. *J. Hydrol.* **2016**, *540*, 26–39. [[CrossRef](#)]
37. Fortin, J.; Turcotte, R.; Massicotte, S.; Moussa, R.; Fitzback, J.; Villeneuve, J. Distributed Watershed Model Compatible with Remote Sensing and GIS Data. I: Description of Model. *J. Hydrol. Eng.* **2001**, *6*, 91–99. [[CrossRef](#)]
38. Rowlands, D.D.; Luthcke, S.B.; Klosko, S.M.; Lemoine, F.G.R.; Chinn, D.S.; McCarthy, J.J.; Cox, C.M.; Anderson, O.B. Resolving mass flux at high spatial and temporal resolution using GRACE intersatellite measurements. *Geophys. Res. Lett.* **2005**, *32*. [[CrossRef](#)]
39. Syed, T.H.; Famiglietti, J.S.; Zlotnicki, V.; Rodell, M. Contemporary estimates of Pan-Arctic freshwater discharge from GRACE and reanalysis. *Geophys. Res. Lett.* **2007**, *34*. [[CrossRef](#)]
40. Syed, T.H.; Famiglietti, J.S.; Chen, J.; Rodell, M.; Seneviratne, S.I.; Viterbo, P.; Wilson, C.R. Total basin discharge for the Amazon and Mississippi River basins from GRACE and a land-atmosphere water balance. *Geophys. Res. Lett.* **2005**, *32*. [[CrossRef](#)]
41. Syed, T.H.; Famiglietti, J.S.; Chambers, D.P. GRACE-Based Estimates of Terrestrial Freshwater Discharge from Basin to Continental Scales. *J. Hydrometeorol.* **2009**, *10*, 22–40. [[CrossRef](#)]
42. Syed, T.H.; Famiglietti, J.S.; Chambers, D.P.; Willis, J.K.; Hilburn, K. Satellite-based global-ocean mass balance estimates of interannual variability and emerging trends in continental freshwater discharge. *Proc. Natl. Acad. Sci. USA* **2010**, *107*, 17916–17921. [[CrossRef](#)] [[PubMed](#)]
43. Schmidt, R.; Petrovic, S.; Guentner, A.; Barthelmes, F.; Wuensch, J.; Kusche, J. Periodic components of water storage changes from GRACE and global hydrology models. *J. Geophys. Res. Solid Earth* **2008**, *113*. [[CrossRef](#)]
44. Werth, S.; Güntner, A.; Petrovic, S.; Schmidt, R. Integration of GRACE mass variations into a global hydrological model. *Earth Planet. Sci. Lett.* **2009**, *277*, 166–173. [[CrossRef](#)]
45. Frappart, F.; Papa, F.; Güntner, A.; Werth, S.; Santos da Silva, J.; Tomasella, J.; Seyler, F.; Prigent, C.; Rossow, W.B.; Calmant, S.; et al. Satellite-based estimates of groundwater storage variations in large drainage basins with extensive floodplains. *Remote Sens. Environ.* **2011**, *115*, 1588–1594. [[CrossRef](#)]
46. Eom, J.; Seo, K.-W.; Ryu, D. Estimation of Amazon River discharge based on EOF analysis of GRACE gravity data. *Remote Sens. Environ.* **2017**, *191*, 55–66. [[CrossRef](#)]
47. Wiese, D.N.; Landerer, F.W.; Watkins, M.M. Quantifying and reducing leakage errors in the JPL RL05M GRACE mascon solution. *Water Resour. Res.* **2016**, *52*, 7490–7502. [[CrossRef](#)]
48. Siqueira, V.A.; Paiva, R.C.D.; Fleischmann, A.S.; Fan, F.M.; Ruhoff, A.L.; Pontes, P.R.M.; Paris, A.; Calmant, S.; Collischonn, W. Toward continental hydrologic-hydrodynamic modeling in South America. *Hydrol. Earth Syst. Sci.* **2018**, *22*, 4815–4842. [[CrossRef](#)]
49. Chandanpurkar, H.A.; Reager, J.T.; Famiglietti, J.S.; Syed, T.H. Satellite- and Reanalysis-Based Mass Balance Estimates of Global Continental Discharge (1993–2015). *J. Clim.* **2017**, *30*, 8481–8495. [[CrossRef](#)]
50. Zhang, Y.; Pan, M.; Wood, E.F. On Creating Global Gridded Terrestrial Water Budget Estimates from Satellite Remote Sensing. *Surv. Geophys.* **2016**, *37*, 249–268. [[CrossRef](#)]
51. Silvestro, F.; Gabellani, S.; Rudari, R.; Delogu, F.; Laiolo, P.; Boni, G. Uncertainty reduction and parameter estimation of a distributed hydrological model with ground and remote-sensing data. *Hydrol. Earth Syst. Sci.* **2015**, *19*, 1727–1751. [[CrossRef](#)]
52. Lee, H.; Beighley, R.E.; Alsdorf, D.; Jung, H.C.; Shum, C.K.; Duan, J.; Guo, J.; Yamazaki, D.; Andreadis, K. Characterization of terrestrial water dynamics in the Congo Basin using GRACE and satellite radar altimetry. *Remote Sens. Environ.* **2011**, *115*, 3530–3538. [[CrossRef](#)]
53. Wang, S.; Liu, S.; Mo, X.; Peng, B.; Qiu, J.; Li, M.; Liu, C.; Wang, Z.; Bauer-Gottwein, P. Evaluation of Remotely Sensed Precipitation and Its Performance for Streamflow Simulations in Basins of the Southeast Tibetan Plateau. *J. Hydrometeorol.* **2015**, *16*, 2577–2594. [[CrossRef](#)]

54. Wulf, H.; Bookhagen, B.; Scherler, D. Differentiating between rain, snow, and glacier contributions to river discharge in the western Himalaya using remote-sensing data and distributed hydrological modeling. *Adv. Water Resour.* **2016**, *88*, 152–169. [[CrossRef](#)]
55. Ferguson, R.I. Hydraulics and hydraulic geometry. *Prog. Phys. Geogr.* **1986**, *10*, 1–31. [[CrossRef](#)]
56. Gleason, C.J. Hydraulic geometry of natural rivers a review and future directions. *Prog. Phys. Geogr.* **2015**, *39*, 337–360. [[CrossRef](#)]
57. Fleischmann, A.S.; Paiva, R.C.D.; Collischonn, W.; Sorribas, M.V.; Pontes, P.R.M. On river-floodplain interaction and hydrograph skewness. *Water Resour. Res.* **2016**, *52*, 7615–7630. [[CrossRef](#)]
58. Hall, A.C.; Schumann, G.J.-P.; Bamber, J.L.; Bates, P.D. Tracking water level changes of the Amazon Basin with space-borne remote sensing and integration with large scale hydrodynamic modelling: A review. *Phys. Chem. Earth Parts A/B/C* **2011**, *36*, 223–231. [[CrossRef](#)]
59. Bjerklie, D.M.; Lawrence Dingman, S.; Vorosmarty, C.J.; Bolster, C.H.; Congalton, R.G. Evaluating the potential for measuring river discharge from space. *J. Hydrol.* **2003**, *278*, 17–38. [[CrossRef](#)]
60. Bjerklie, D.M.; Moller, D.; Smith, L.C.; Dingman, S.L. Estimating discharge in rivers using remotely sensed hydraulic information. *J. Hydrol.* **2005**, *309*, 191–209. [[CrossRef](#)]
61. Bjerklie, D.M. Estimating the bankfull velocity and discharge for rivers using remotely sensed river morphology information. *J. Hydrol.* **2007**, *341*, 144–155. [[CrossRef](#)]
62. Kebede, M.G.; Wang, L.; Li, X.; Hu, Z. Remote sensing-based river discharge estimation for a small river flowing over the high mountain regions of the Tibetan Plateau. *Int. J. Remote Sens.* **2020**, *41*, 3322–3345. [[CrossRef](#)]
63. De Frasson, R.P.M.; Pavelsky, T.M.; Fonstad, M.A.; Durand, M.T.; Allen, G.H.; Schumann, G.; Lion, C.; Beighley, R.E.; Yang, X. Global Relationships Between River Width, Slope, Catchment Area, Meander Wavelength, Sinuosity, and Discharge. *Geophys. Res. Lett.* **2019**, *46*, 3252–3262. [[CrossRef](#)]
64. Neal, J.; Schumann, G.; Bates, P.; Buytaert, W.; Matgen, P.; Pappenberger, F. A data assimilation approach to discharge estimation from space. *Hydrol. Process.* **2009**, *23*, 3641–3649. [[CrossRef](#)]
65. Temimi, M.; Lacava, T.; Lakhankar, T.; Tramutoli, V.; Ghedira, H.; Ata, R.; Khanbilvardi, R. A multi-temporal analysis of AMSR-E data for flood and discharge monitoring during the 2008 flood in Iowa. *Hydrol. Process.* **2011**, *25*, 2623–2634. [[CrossRef](#)]
66. King, T.V.; Neilson, B.T.; Rasmussen, M.T. Estimating Discharge in Low-Order Rivers with High-Resolution Aerial Imagery. *Water Resour. Res.* **2018**, *54*, 863–878. [[CrossRef](#)]
67. Harada, S.; Li, S.S. Combining remote sensing with physical flow laws to estimate river channel geometry. *River Res. Appl.* **2018**, *34*, 697–708. [[CrossRef](#)]
68. Try, S.; Lee, G.; Yu, W.; Oeurng, C.; Jang, C. Large-Scale Flood-Inundation Modeling in the Mekong River Basin. *J. Hydrol. Eng.* **2018**, *23*, 05018011. [[CrossRef](#)]
69. Koblinsky, C.J.; Clarke, R.T.; Brenner, A.C.; Frey, H. Measurement of river level variations with satellite altimetry. *Water Resour. Res.* **1993**, *29*, 1839–1848. [[CrossRef](#)]
70. Smith, L.C.; Isacks, B.L.; Bloom, A.L.; Murray, A.B. Estimation of discharge from three braided rivers using synthetic aperture radar satellite imagery: Potential application to ungaged basins. *Water Resour. Res.* **1996**, *32*, 2021–2034. [[CrossRef](#)]
71. Alsdorf, D.E. Water Storage of the Central Amazon Floodplain Measured with GIS and Remote Sensing Imagery. *Ann. Assoc. Am. Geogr.* **2003**, *93*, 55–66. [[CrossRef](#)]
72. Alsdorf, D.E.; Smith, L.C.; Melack, J.M. Amazon floodplain water level changes measured with interferometric SIR-C radar. *IEEE Trans. Geosci. Remote Sens.* **2001**, *39*, 423–431. [[CrossRef](#)]
73. Alsdorf, D.; Birkett, C.; Dunne, T.; Melack, J.; Hess, L. Water level changes in a large Amazon lake measured with spaceborne radar interferometry and altimetry. *Geophys. Res. Lett.* **2001**, *28*, 2671–2674. [[CrossRef](#)]
74. Frappart, F.; Seyler, F.; Martinez, J.-M.; León, J.G.; Cazenave, A. Floodplain water storage in the Negro River basin estimated from microwave remote sensing of inundation area and water levels. *Remote Sens. Environ.* **2005**, *99*, 387–399. [[CrossRef](#)]
75. LeFavour, G.; Alsdorf, D. Water slope and discharge in the Amazon River estimated using the shuttle radar topography mission digital elevation model. *Geophys. Res. Lett.* **2005**, *32*. [[CrossRef](#)]
76. Smith, L.C. Satellite remote sensing of river inundation area, stage, and discharge: A review. *Hydrol. Process.* **1997**, *11*, 1427–1439. [[CrossRef](#)]

77. Kouraev, A.V.; Zakharova, E.A.; Samain, O.; Mognard, N.M.; Cazenave, A. Ob' river discharge from TOPEX/Poseidon satellite altimetry (1992–2002). *Remote Sens. Environ.* **2004**, *93*, 238–245. [[CrossRef](#)]
78. Pavelsky, T.M.; Durand, M.T.; Andreadis, K.M.; Beighley, R.E.; Paiva, R.C.D.; Allen, G.H.; Miller, Z.F. Assessing the potential global extent of SWOT river discharge observations. *J. Hydrol.* **2014**, *519*, 1516–1525. [[CrossRef](#)]
79. Pavelsky, T.M.; Smith, L.C. Remote sensing of suspended sediment concentration, flow velocity, and lake recharge in the Peace-Athabasca Delta, Canada. *Water Resour. Res.* **2009**, *45*. [[CrossRef](#)]
80. Schneider, R.; Godiksen, P.N.; Villadsen, H.; Madsen, H.; Bauer-Gottwein, P. Application of CryoSat-2 altimetry data for river analysis and modelling. *Hydrol. Earth Syst. Sci.* **2017**, *21*, 651–664. [[CrossRef](#)]
81. Young, D.S.; Hart, J.K.; Martinez, K. Image analysis techniques to estimate river discharge using time-lapse cameras in remote locations. *Comput. Geosci.* **2015**, *76*, 1–10. [[CrossRef](#)]
82. Paris, A.; de Paiva, R.D.; da Silva, J.S.; Moreira, D.M.; Calmant, S.; Garambois, P.-A.; Collischonn, W.; Bonnet, M.-P.; Seyler, F. Stage-discharge rating curves based on satellite altimetry and modeled discharge in the Amazon basin. *Water Resour. Res.* **2016**, *52*, 3787–3814. [[CrossRef](#)]
83. Nathanson, M.; Kean, J.W.; Grabs, T.J.; Seibert, J.; Laudon, H.; Lyon, S.W. Modelling rating curves using remotely sensed LiDAR data. *Hydrol. Process.* **2012**, *26*, 1427–1434. [[CrossRef](#)]
84. Feng, D.; Gleason, C.J.; Yang, X.; Pavelsky, T.M. Comparing Discharge Estimates Made via the BAM Algorithm in High-Order Arctic Rivers Derived Solely From Optical CubeSat, Landsat, and Sentinel-2 Data. *Water Resour. Res.* **2019**, *55*, 7753–7771. [[CrossRef](#)]
85. Normandin, C.; Frappart, F.; Diepkile, A.T.; Mariieu, V.; Mougin, E.; Blarel, F.; Lubac, B.; Braquet, N.; Ba, A. Evolution of the Performances of Radar Altimetry Missions from ERS-2 to Sentinel-3A over the Inner Niger Delta. *Remote Sens.* **2018**, *10*, 833. [[CrossRef](#)]
86. Ashmore, P.; Sauks, E. Prediction of discharge from water surface width in a braided river with implications for at-a-station hydraulic geometry. *Water Resour. Res.* **2006**, *42*. [[CrossRef](#)]
87. Gleason, C.J.; Smith, L.C.; Finnegan, D.C.; LeWinter, A.L.; Pitcher, L.H.; Chu, V.W. Technical Note: Semi-automated effective width extraction from time-lapse RGB imagery of a remote, braided Greenlandic river. *Hydrol. Earth Syst. Sci.* **2015**, *19*, 2963–2969. [[CrossRef](#)]
88. Huang, Q.; Long, D.; Du, M.; Zeng, C.; Qiao, G.; Li, X.; Hou, A.; Hong, Y. Discharge estimation in high-mountain regions with improved methods using multisource remote sensing: A case study of the Upper Brahmaputra River. *Remote Sens. Environ.* **2018**, *219*, 115–134. [[CrossRef](#)]
89. Brakenridge, G.R.; Nghiem, S.V.; Anderson, E.; Mic, R. Orbital microwave measurement of river discharge and ice status. *Water Resour. Res.* **2007**, *43*. [[CrossRef](#)]
90. Brakenridge, G.; Cohen, S.; Kettner, A.J.; De Groeve, T.; Nghiem, S.V.; Syvitski, J.P.M.; Fekete, B.M. Calibration of satellite measurements of river discharge using a global hydrology model. *J. Hydrol.* **2012**, *475*, 123–136. [[CrossRef](#)]
91. Tarpanelli, A.; Brocca, L.; Lacava, T.; Melone, F.; Moramarco, T.; Faruolo, M.; Pergola, N.; Tramutoli, V. Toward the estimation of river discharge variations using MODIS data in ungauged basins. *Remote Sens. Environ.* **2013**, *136*, 47–55. [[CrossRef](#)]
92. Van Dijk, A.I.J.M.; Brakenridge, G.R.; Kettner, A.J.; Beck, H.E.; De Groeve, T.; Schellekens, J. River gauging at global scale using optical and passive microwave remote sensing. *Water Resour. Res.* **2016**, *52*, 6404–6418. [[CrossRef](#)]
93. Tarpanelli, A.; Amarnath, G.; Brocca, L.; Massari, C.; Moramarco, T. Discharge estimation and forecasting by MODIS and altimetry data in Niger-Benue River. *Remote Sens. Environ.* **2017**, *195*, 96–106. [[CrossRef](#)]
94. Tarpanelli, A.; Santi, E.; Tourian, M.J.; Filippucci, P.; Amarnath, G.; Brocca, L. Daily River Discharge Estimates by Merging Satellite Optical Sensors and Radar Altimetry Through Artificial Neural Network. *IEEE Trans. Geosci. Remote Sens.* **2018**, *57*, 329–341. [[CrossRef](#)]
95. Lyzenga, D.R. Passive remote sensing techniques for mapping water depth and bottom features. *Appl. Opt.* **1978**, *17*, 379. [[CrossRef](#)]
96. Lee, Z.; Carder, K.L.; Mobley, C.D.; Steward, R.G.; Patch, J.S. Hyperspectral Remote Sensing for Shallow Waters. I. A Semianalytical Model. *Appl. Opt.* **1998**, *37*, 6329. [[CrossRef](#)]
97. Lee, Z.; Carder, K.L.; Mobley, C.D.; Steward, R.G.; Patch, J.S. Hyperspectral Remote Sensing for Shallow Waters. 2. Deriving Bottom Depths and Water Properties by Optimization. *Appl. Opt.* **1999**, *38*, 3831. [[CrossRef](#)]

98. Gould, R.W., Jr.; Arnone, R.A.; Martinolich, P.M. Spectral Dependence of the Scattering Coefficient in Case 1 and Case 2 Waters. *Appl. Opt.* **1999**, *38*, 2377. [[CrossRef](#)]
99. Fonstad, M.A.; Marcus, W.A. Remote sensing of stream depths with hydraulically assisted bathymetry (HAB) models. *Geomorphology* **2005**, *72*, 320–339. [[CrossRef](#)]
100. Marcus, W.A.; Fonstad, M.A. Optical remote mapping of rivers at sub-meter resolutions and watershed extents. *Earth Surf. Process. Landf.* **2008**, *33*, 4–24. [[CrossRef](#)]
101. Legleiter, C.J.; Roberts, D.A.; Lawrence, R.L. Spectrally based remote sensing of river bathymetry. *Earth Surf. Process. Landf.* **2009**, *34*, 1039–1059. [[CrossRef](#)]
102. Legleiter, C.J. Calibrating remotely sensed river bathymetry in the absence of field measurements: Flow REsistance Equation-Based Imaging of River Depths (FREEBIRD). *Water Resour. Res.* **2015**, *51*, 2865–2884. [[CrossRef](#)]
103. Legleiter, C.J.; Kinzel, P.J.; Nelson, J.M. Remote measurement of river discharge using thermal particle image velocimetry (PIV) and various sources of bathymetric information. *J. Hydrol.* **2017**, *554*, 490–506. [[CrossRef](#)]
104. Smith, L.C.; Chu, V.W.; Yang, K.; Gleason, C.J.; Pitcher, L.H.; Rennermalm, A.K.; Legleiter, C.J.; Behar, A.E.; Overstreet, B.T.; Moustafa, S.E.; et al. Efficient meltwater drainage through supraglacial streams and rivers on the southwest Greenland ice sheet. *Proc. Natl. Acad. Sci. USA* **2015**, *112*, 1001–1006. [[CrossRef](#)] [[PubMed](#)]
105. Johnson, E.D.; Cowen, E.A. Remote monitoring of volumetric discharge employing bathymetry determined from surface turbulence metrics. *Water Resour. Res.* **2016**, *52*, 2178–2193. [[CrossRef](#)]
106. Costa, J.E.; Spicer, K.R.; Cheng, R.T.; Haeni, F.P.; Melcher, N.B.; Thurman, E.M.; Plant, W.J.; Keller, W.C. measuring stream discharge by non-contact methods: A Proof-of-Concept Experiment. *Geophys. Res. Lett.* **2000**, *27*, 553–556. [[CrossRef](#)]
107. Chiu, C.-L. Application of Entropy Concept in Open-Channel Flow Study. *J. Hydraul. Eng.* **1991**, *117*, 615–628. [[CrossRef](#)]
108. Fulton, J.; Ostrowski, J. Measuring real-time streamflow using emerging technologies: Radar, hydroacoustics, and the probability concept. *J. Hydrol.* **2008**, *357*, 1–10. [[CrossRef](#)]
109. Moramarco, T.; Barbeta, S.; Tarpanelli, A. From Surface Flow Velocity Measurements to Discharge Assessment by the Entropy Theory. *Water* **2017**, *9*, 120. [[CrossRef](#)]
110. Moramarco, T.; Barbeta, S.; Bjerklie, D.M.; Fulton, J.W.; Tarpanelli, A. River Bathymetry Estimate and Discharge Assessment from Remote Sensing. *Water Resour. Res.* **2019**, *55*, 6692–6711. [[CrossRef](#)]
111. Hildale, R.C.; Raff, D. Assessing the ability of airborne LiDAR to map river bathymetry. *Earth Surf. Process. Landf.* **2008**, *33*, 773–783. [[CrossRef](#)]
112. Parr, D.; Wang, G.; Bjerklie, D. Integrating Remote Sensing Data on Evapotranspiration and Leaf Area Index with Hydrological Modeling: Impacts on Model Performance and Future Predictions. *J. Hydrometeorol.* **2015**, *16*, 2086–2100. [[CrossRef](#)]
113. Lopez, P.L.; Immerzeel, W.W.; Sandoval, E.A.R.; Sterk, G.; Schellekens, J. Spatial Downscaling of Satellite-Based Precipitation and Its Impact on Discharge Simulations in the Magdalena River Basin in Colombia. *Front. Earth Sci.* **2018**, *6*, 68. [[CrossRef](#)]
114. Lopez, P.L.; Sutanudjaja, E.H.; Schellekens, J.; Sterk, G.; Bierkens, M.F.P. Calibration of a large-scale hydrological model using satellite-based soil moisture and evapotranspiration products. *Hydrol. Earth Syst. Sci.* **2017**, *21*, 3125–3144. [[CrossRef](#)]
115. Mendiguren, G.; Koch, J.; Stisen, S. Spatial pattern evaluation of a calibrated national hydrological model—A remote-sensing-based diagnostic approach. *Hydrol. Earth Syst. Sci.* **2017**, *21*, 5987–6005. [[CrossRef](#)]
116. Bowman, A.L.; Franz, K.J.; Hogue, T.S.; Kinoshita, A.M. MODIS-Based Potential Evapotranspiration Demand Curves for the Sacramento Soil Moisture Accounting Model. *J. Hydrol. Eng.* **2016**, *21*, 04015055. [[CrossRef](#)]
117. Sun, W.; Ishidaira, H.; Bastola, S.; Yu, J. Estimating daily time series of streamflow using hydrological model calibrated based on satellite observations of river water surface width: Toward real world applications. *Environ. Res.* **2015**, *139*, 36–45. [[CrossRef](#)]
118. Emery, C.M.; Paris, A.; Biancamaria, S.; Boone, A.; Calmant, S.; Garambois, P.-A.; Santos da Silva, J. Large-scale hydrological model river storage and discharge correction using a satellite altimetry-based discharge product. *Hydrol. Earth Syst. Sci.* **2018**, *22*, 2135–2162. [[CrossRef](#)]
119. Bates, P.D.; Horritt, M.S.; Smith, C.N.; Mason, D. Integrating remote sensing observations of flood hydrology and hydraulic modelling. *Hydrol. Process.* **1997**, *11*, 1777–1795. [[CrossRef](#)]

120. Brakenridge, G.R.; Tracy, B.T.; Knox, J.C. Orbital SAR remote sensing of a river flood wave. *Int. J. Remote Sens.* **1998**, *19*, 1439–1445. [[CrossRef](#)]
121. Horritt, M.S.; Bates, P.D. Predicting floodplain inundation: Raster-based modelling versus the finite-element approach. *Hydrol. Process.* **2001**, *15*, 825–842. [[CrossRef](#)]
122. Poole, G.C.; Stanford, J.A.; Frissell, C.A.; Running, S.W. Three-dimensional mapping of geomorphic controls on flood-plain hydrology and connectivity from aerial photos. *Geomorphology* **2002**, *48*, 329–347. [[CrossRef](#)]
123. Horritt, M.S. A methodology for the validation of uncertain flood inundation models. *J. Hydrol.* **2006**, *326*, 153–165. [[CrossRef](#)]
124. Gumley, L.E.; King, M.D. Remote Sensing of Flooding in the U.S. Upper Midwest during the Summer of 1993. *Bull. Am. Meteorol. Soc.* **1995**, *76*, 933–943. [[CrossRef](#)]
125. Mason, D.C.; Horritt, M.S.; Dall’Amico, J.T.; Scott, T.R.; Bates, P.D. Improving River Flood Extent Delineation From Synthetic Aperture Radar Using Airborne Laser Altimetry. *IEEE Trans. Geosci. Remote Sens.* **2007**, *45*, 3932–3943. [[CrossRef](#)]
126. Schumann, G.; Matgen, P.; Hoffmann, L.; Hostache, R.; Pappenberger, F.; Pfister, L. Deriving distributed roughness values from satellite radar data for flood inundation modelling. *J. Hydrol.* **2007**, *344*, 96–111. [[CrossRef](#)]
127. Schumann, G.; Matgen, P.; Cutler, M.E.J.; Black, A.; Hoffmann, L.; Pfister, L. Comparison of remotely sensed water stages from LiDAR, topographic contours and SRTM. *ISPRS J. Photogramm. Remote Sens.* **2008**, *63*, 283–296. [[CrossRef](#)]
128. Schumann, G.; Baldassarre, G.D.; Bates, P.D. The Utility of Spaceborne Radar to Render Flood Inundation Maps Based on Multialgorithm Ensembles. *IEEE Trans. Geosci. Remote Sens.* **2009**, *47*, 2801–2807. [[CrossRef](#)]
129. Coe, M.T.; Costa, M.H.; Howard, E.A. Simulating the surface waters of the Amazon River basin: Impacts of new river geomorphic and flow parameterizations. *Hydrol. Process.* **2008**, *22*, 2542–2553. [[CrossRef](#)]
130. Di Baldassarre, G.; Schumann, G.; Bates, P.D. A technique for the calibration of hydraulic models using uncertain satellite observations of flood extent. *J. Hydrol.* **2009**, *367*, 276–282. [[CrossRef](#)]
131. Khan, S.I.; Hong, Y.; Wang, J.H.; Yilmaz, K.K.; Gourley, J.J.; Adler, R.F.; Brakenridge, G.R.; Policelli, F.; Habib, S.; Irwin, D. Satellite Remote Sensing and Hydrologic Modeling for Flood Inundation Mapping in Lake Victoria Basin: Implications for Hydrologic Prediction in Ungauged Basins. *IEEE Trans. Geosci. Remote Sens.* **2011**, *49*, 85–95. [[CrossRef](#)]
132. Bates, P.D.; Marks, K.J.; Horritt, M.S. Optimal use of high-resolution topographic data in flood inundation models. *Hydrol. Process.* **2003**, *17*, 537–557. [[CrossRef](#)]
133. Du, J.; Kimball, J.S.; Galantowicz, J.; Kim, S.-B.; Chan, S.K.; Reichle, R.; Jones, L.A.; Watts, J.D. Assessing global surface water inundation dynamics using combined satellite information from SMAP, AMSR2 and Landsat. *Remote Sens. Environ.* **2018**, *213*, 1–17. [[CrossRef](#)] [[PubMed](#)]
134. Niedzielski, T.; Witek, M.; Spallek, W. Observing river stages using unmanned aerial vehicles. *Hydrol. Earth Syst. Sci.* **2016**, *20*, 3193–3205. [[CrossRef](#)]
135. Andreadis, K.M.; Clark, E.A.; Lettenmaier, D.P.; Alsdorf, D.E. Prospects for river discharge and depth estimation through assimilation of swath-altimetry into a raster-based hydrodynamics model. *Geophys. Res. Lett.* **2007**, *34*. [[CrossRef](#)]
136. Durand, M.; Andreadis, K.M.; Alsdorf, D.E.; Lettenmaier, D.P.; Moller, D.; Wilson, M. Estimation of bathymetric depth and slope from data assimilation of swath altimetry into a hydrodynamic model. *Geophys. Res. Lett.* **2008**, *35*. [[CrossRef](#)]
137. Biancamaria, S.; Durand, M.; Andreadis, K.M.; Bates, P.D.; Boone, A.; Mognard, N.M.; Rodríguez, E.; Alsdorf, D.E.; Lettenmaier, D.P.; Clark, E.A. Assimilation of virtual wide swath altimetry to improve Arctic river modeling. *Remote Sens. Environ.* **2011**, *115*, 373–381. [[CrossRef](#)]
138. Yoon, Y.; Durand, M.; Merry, C.J.; Clark, E.A.; Andreadis, K.M.; Alsdorf, D.E. Estimating river bathymetry from data assimilation of synthetic SWOT measurements. *J. Hydrol.* **2012**, *464–465*, 363–375. [[CrossRef](#)]
139. Gejadze, I.; Malaterre, P.-O. Discharge estimation under uncertainty using variational methods with application to the full Saint-Venant hydraulic network model. *Int. J. Numer. Methods Fluids* **2017**, *83*, 405–430. [[CrossRef](#)]
140. Oubanas, H.; Gejadze, I.; Malaterre, P.-O.; Mercier, F. River discharge estimation from synthetic SWOT-type observations using variational data assimilation and the full Saint-Venant hydraulic model. *J. Hydrol.* **2018**, *559*, 638–647. [[CrossRef](#)]

141. Oubanas, H.; Gejadze, I.; Malaterre, P.-O.; Durand, M.; Wei, R.; Frasson, R.P.M.; Domeneghetti, A. Discharge Estimation in Ungauged Basins Through Variational Data Assimilation: The Potential of the SWOT Mission. *Water Resour. Res.* **2018**, *54*, 2405–2423. [[CrossRef](#)]
142. Larnier, K.; Monnier, J.; Garambois, P.-A.; Verley, J. River Discharge and Bathymetry Estimations from SWOT Altimetry Measurements. 2019. Available online: <https://hal.archives-ouvertes.fr/hal-01811683v2> (accessed on 1 February 2020).
143. Durand, M.; Fu, L.-L.; Lettenmaier, D.P.; Als, D.E.; Rodriguez, E.; Esteban-Fernandez, D. The Surface Water and Ocean Topography Mission: Observing Terrestrial Surface Water and Oceanic Submesoscale Eddies. *Proc. IEEE* **2010**, *98*, 766–779. [[CrossRef](#)]
144. Garambois, P.-A.; Monnier, J. Inference of effective river properties from remotely sensed observations of water surface. *Adv. Water Resour.* **2015**, *79*, 103–120. [[CrossRef](#)]
145. Durand, M.; Neal, J.; Rodríguez, E.; Andreadis, K.M.; Smith, L.C.; Yoon, Y. Estimating reach-averaged discharge for the River Severn from measurements of river water surface elevation and slope. *J. Hydrol.* **2014**, *511*, 92–104. [[CrossRef](#)]
146. Bjerklie, D.M.; Birkett, C.M.; Jones, J.W.; Carabajal, C.; Rover, J.A.; Fulton, J.W.; Garambois, P.-A. Satellite remote sensing estimation of river discharge: Application to the Yukon River Alaska. *J. Hydrol.* **2018**, *561*, 1000–1018. [[CrossRef](#)]
147. Tuozzolo, S.; Langhorst, T.; de Moraes Frasson, R.P.; Pavelsky, T.; Durand, M. The impact of reach averaging Manning’s equation for an in-situ dataset of water surface elevation, width, and slope. *J. Hydrol.* **2019**, *578*, 123866. [[CrossRef](#)]
148. Altenau, E.H.; Pavelsky, T.M.; Moller, D.; Lion, C.; Pitcher, L.H.; Allen, G.H.; Bates, P.D.; Calmant, S.; Durand, M.; Smith, L.C. AirSWOT measurements of river water surface elevation and slope: Tanana River, AK. *Geophys. Res. Lett.* **2017**, *44*, 181–189. [[CrossRef](#)]
149. Tuozzolo, S.; Lind, G.; Overstreet, B.; Mangano, J.; Fonstad, M.; Hagemann, M.; Frasson, R.P.M.; Larnier, K.; Garambois, P.-A.; Monnier, J.; et al. Estimating River Discharge With Swath Altimetry: A Proof of Concept Using AirSWOT Observations. *Geophys. Res. Lett.* **2019**, *46*, 1459–1466. [[CrossRef](#)]
150. Gleason, C.J.; Smith, L.C.; Lee, J. Retrieval of river discharge solely from satellite imagery and at-many-stations hydraulic geometry: Sensitivity to river form and optimization parameters. *Water Resour. Res.* **2014**, *50*, 9604–9619. [[CrossRef](#)]
151. Gleason, C.J.; Hamdan, A.N. Crossing the (Watershed) Divide: Satellite Data and the Changing Politics of International River Basins. *Geogr. J.* **2017**, *183*, 2–15. [[CrossRef](#)]
152. Hagemann, M.W.; Gleason, C.J.; Durand, M.T. BAM: Bayesian AMHG-Manning Inference of Discharge Using Remotely Sensed Stream Width, Slope, and Height. *Water Resour. Res.* **2017**, *53*, 9692–9707. [[CrossRef](#)]
153. Bonnema, M.G.; Sikder, S.; Hossain, F.; Durand, M.; Gleason, C.J.; Bjerklie, D.M. Benchmarking wide swath altimetry-based river discharge estimation algorithms for the Ganges river system. *Water Resour. Res.* **2016**, *52*, 2439–2461. [[CrossRef](#)]
154. Durand, M.; Gleason, C.J.; Garambois, P.A.; Bjerklie, D.; Smith, L.C.; Roux, H.; Rodriguez, E.; Bates, P.D.; Pavelsky, T.M.; Monnier, J.; et al. An intercomparison of remote sensing river discharge estimation algorithms from measurements of river height, width, and slope. *Water Resour. Res.* **2016**, *52*, 4527–4549. [[CrossRef](#)]
155. Sichangi, A.W.; Wang, L.; Hu, Z. Estimation of River Discharge Solely from Remote-Sensing Derived Data: An Initial Study over the Yangtze River. *Remote Sens.* **2018**, *10*, 1385. [[CrossRef](#)]
156. Chow, V.T. *Handbook of Applied Hydrology*; McGraw-Hill: New York, NY, USA, 1964.
157. Rosgen, D.L. A classification of natural rivers. *Catena* **1994**, *22*, 169–199. [[CrossRef](#)]
158. Brown, C.M.; Lund, J.R.; Cai, X.; Reed, P.M.; Zagona, E.A.; Ostfeld, A.; Hall, J.; Characklis, G.W.; Yu, W.; Brekke, L. The future of water resources systems analysis: Toward a scientific framework for sustainable water management. *Water Resour. Res.* **2015**, *51*, 6110–6124. [[CrossRef](#)]
159. Hannah, D.M.; Demuth, S.; van Lanen, H.A.J.; Looser, U.; Prudhomme, C.; Rees, G.; Stahl, K.; Tallaksen, L.M. Large-scale river flow archives: Importance, current status and future needs. *Hydrol. Process.* **2011**, *25*, 1191–1200. [[CrossRef](#)]
160. Fekete, B.M.; Looser, U.; Pietroniro, A.; Robarts, R.D. Rationale for Monitoring Discharge on the Ground. *J. Hydrometeorol.* **2012**, *13*, 1977–1986. [[CrossRef](#)]

161. Birkinshaw, S.J.; O'Donnell, G.M.; Moore, P.; Kilsby, C.G.; Fowler, H.J.; Berry, P.A.M. Using satellite altimetry data to augment flow estimation techniques on the Mekong River. *Hydrol. Process.* **2010**, *24*, 3811–3825. [[CrossRef](#)]
162. Gleason, C.J.; Wada, Y.; Wang, J. A Hybrid of Optical Remote Sensing and Hydrological Modeling Improves Water Balance Estimation. *J. Adv. Model. Earth Syst.* **2018**, *10*, 2–17. [[CrossRef](#)]
163. León, L.F.A.; Gleason, C.J. Production, Property, and the Construction of Remotely Sensed Data. *Ann. Am. Assoc. Geogr.* **2017**, *107*, 1075–1089.
164. Sneddon, C.; Fox, C. Water, Geopolitics, and Economic Development in the Conceptualization of a Region. *Eurasian Geogr. Econ.* **2012**, *53*, 143–160. [[CrossRef](#)]
165. Sneddon, C.; Fox, C. Rethinking transboundary waters: A critical hydrogeopolitics of the Mekong basin. *Polit. Geogr.* **2006**, *25*, 181–202. [[CrossRef](#)]
166. Sneddon, C.; Fox, C. The Cold War, the US Bureau of Reclamation, and the technopolitics of river basin development, 1950–1970. *Polit. Geogr.* **2011**, *30*, 450–460. [[CrossRef](#)]
167. Dore, J.; Lebel, L. Deliberation and Scale in Mekong Region Water Governance. *Environ. Manag.* **2010**, *46*, 60–80. [[CrossRef](#)] [[PubMed](#)]
168. Ho, S. River Politics: China's policies in the Mekong and the Brahmaputra in comparative perspective. *J. Contemp. China* **2014**, *23*, 1–20. [[CrossRef](#)]



© 2020 by the authors. Licensee MDPI, Basel, Switzerland. This article is an open access article distributed under the terms and conditions of the Creative Commons Attribution (CC BY) license (<http://creativecommons.org/licenses/by/4.0/>).

EXHIBIT 9

Geophysical Research Letters[®]



RESEARCH LETTER

10.1029/2023GL105839

Satellite Video Remote Sensing for Estimation of River Discharge

Christopher Masafu¹ , Richard Williams¹ , and Martin D. Hurst¹ 

¹School of Geographical and Earth Sciences, University of Glasgow, Glasgow, UK

Key Points:

- Satellite video acquired along 12.6 km of the River Darling, Australia, at 5 Hz for 28 s during a 1-in-5-year storm event
- Satellite video-based velocities coupled with high resolution topography estimate riverine discharges to within 15% of in situ gauge data
- Parametrization of non-contact velocimetry and choice of a depth-averaging coefficient (α) influence the accuracy of discharge estimates

Supporting Information:

Supporting Information may be found in the online version of this article.

Correspondence to:

C. Masafu,
christopher.masafu@glasgow.ac.uk;
masafu@gmail.com

Citation:

Masafu, C., Williams, R., & Hurst, M. D. (2023). Satellite video remote sensing for estimation of river discharge. *Geophysical Research Letters*, 50, e2023GL105839. <https://doi.org/10.1029/2023GL105839>

Received 10 AUG 2023

Accepted 18 NOV 2023

Author Contributions:

Conceptualization: Christopher Masafu, Richard Williams

Data curation: Christopher Masafu, Richard Williams

Formal analysis: Christopher Masafu

Investigation: Christopher Masafu

Methodology: Christopher Masafu, Richard Williams

Supervision: Richard Williams, Martin D. Hurst

Visualization: Christopher Masafu

Writing – original draft: Christopher Masafu

Abstract We demonstrate that river discharge can be estimated by deriving water surface velocity estimates from satellite-derived video imagery when combined with high-resolution topography of channel geometry. Large Scale Particle Image Velocimetry (LSPIV) was used to map surface velocity from 28 s of 5 Hz satellite video acquired at a 1.2 m nominal ground spacing over the Darling River, Tilpa, Australia, during a 1-in-5-year flood. We stabilized and assessed the uncertainty of the residual motion induced by the satellite platform, enhancing our sub-pixel motion analysis, and quantified the sensitivity of image extraction rates on computed velocities. In the absence of in situ observations, LSPIV velocity estimates were validated against predictions from a calibrated 2D hydrodynamic model. Despite the confounding influence of selecting a surface velocity depth-averaging coefficient, inference of discharge was within 0.3%–15% compared with gauging station measurements. These results provide a valuable foundation for refining satellite video LSPIV techniques.

Plain Language Summary Estimates of river flow are needed to manage water resources and flood risk. However, many of the world's rivers are not gauged, limiting hydrological understanding of river response to changing environmental conditions and storm events. We demonstrate that satellite video can be used to map velocity by tracking surface water features from one video frame to the next, and scaled to compute discharge where river geometry is known. Using a video of a flood on the River Tilpa, Australia, our results agree with ground-based measurements to within 0.3%–15%. The ability to deploy satellites to acquire video anywhere globally could contribute to measuring discharge on ungauged rivers.

1. Introduction

Globally, 29% of the world's population is exposed to flood risk and insecure water supplies, yet knowledge of the river discharges upon which flood and water resource management depends remains inadequate (Rentschler & Salhab, 2020). Global monitoring networks for quantifying river discharge are in decline, gauging remains logistically difficult and there are political influences on data sharing (King et al., 2018; Lins, 2008; Zakharova et al., 2020). However, satellite-based remote sensing approaches to monitoring discharge are helping to alleviate these issues (e.g., Sichangi et al., 2016).

Approaches to satellite-based river discharge monitoring typically rely upon statistical and hydraulic approximations to make indirect estimates of river discharge. Widely applied satellite radar altimetry measures water elevations at virtual river cross-sections (Revel et al., 2023; Tarpanelli et al., 2013; Zakharova et al., 2020) and near-simultaneous optical imagery can be used to infer water surface flow velocity from space (Kääb et al., 2019). Other satellite approaches have relied on remote sensing of discharge (RSQ) algorithms, which retrieve hydraulic variables from remotely sensed data and then relate these quantities to river discharge (Q) (e.g., Gleason & Durand, 2020; Riggs et al., 2022). These techniques are limited by relatively coarse spatial resolution and the requirement for near-simultaneous satellite swath overlaps, constraining global coverage.

High resolution commercial satellite video sensors can record the dynamics of river flow and floods. Optical flow measurement algorithms can estimate velocity by tracking the movement of visible features between frames (e.g., Eltner et al., 2020; Perks et al., 2020). Currently, optical satellite video acquired by low earth orbiting sensors offer spatial resolutions (pixel sizes) ranging from 0.9–1.2 m at frame rates up to 30 Hz [for example, SkySat (Bhushan et al., 2021) and Jilin-1 (European Space Agency, 2022) constellations]. Inference of flow velocities using satellite video has previously been demonstrated by Legleiter and Kinzel (2021a), who used 17 frames of cloud-free satellite video acquired by Planet Labs SkySat constellation of the Tanana River in central Alaska. Surface flow velocities were estimated to within 8.65% of radar gauging measurements and were further assessed using asynchronously acquired acoustic Doppler current profiler (aDcp) velocity data.

© 2023. The Authors.

This is an open access article under the terms of the [Creative Commons Attribution License](https://creativecommons.org/licenses/by/4.0/), which permits use, distribution and reproduction in any medium, provided the original work is properly cited.

Writing – review & editing: Christopher Masafu, Richard Williams, Martin D. Hurst

We apply and test the use of satellite video-based velocities for estimating discharge. We couple freely available, high-resolution topographic data with velocity estimates derived from satellite video Large-Scale Image Velocimetry (LSPIV) (Lewis et al., 2018; Muste et al., 2008) and some critical assumptions regarding channel hydraulics to estimate flood discharge following monsoonal rainfall in Darling River at Tilpa, Australia. The accuracy of satellite video-derived velocity estimates was assessed via comparison to hydraulic model simulations; and discharge estimates were compared with in situ gauging station observations.

2. Study Area

The River Darling at Tilpa (Figure 1) is located within the 502,500 km² Murray-Darling basin (Matheson & Thoms, 2018; Murray-Darling Basin Authority, 2010). The basin has a strongly episodic climate, with large floods followed by lengthy dry spells due to the influence of the El Niño Southern Oscillation (Grimaldi et al., 2019). Extensive and prolonged rainfall from late February to early April 2022 led to a flood with a 5-year return period ($Q = 722 \text{ m}^3 \text{ s}^{-1}$). This location is ideally suited to testing our ability to measure discharge using non-contact, image-based velocity calculation techniques due to the availability of: (a) cloud-free satellite video; (b) a high-resolution LiDAR digital elevation model (DEM) acquired during dry river bed conditions; and (c) gauged in situ discharge observations at Tilpa (Water NSW, 2023).

3. Data and Methods

3.1. Satellite Video

Satellite video was acquired over our study area on 5 February 2022 at 23:12 UTC by a Jilin-1 GF-03 sensor, part of the constellation by the Chang Guang Satellite Technology Company. Video had a 1.22 m spatial resolution and native frame rate of 5 Hz for 28 s. To counter sensor platform movement and scene “morphing” due to the changing view angle of the satellite overpass, we stabilized the video using FIJI's TrakEM2 plugin (Cardona et al., 2012; FIJI-ImageJ, 2020; Schindelin et al., 2012). FIJI is an open-source image processing toolkit. TrakEM2 relies on a Scale Invariant Feature Transform (SIFT) algorithm to align image stacks based on common features. To avoid geometric distortions, and because all video frames had a similar resolution, we utilized an affine transform to register our image stacks.

Temporal displacement errors related to image stabilization can significantly influence the accuracy of LSPIV velocities. We quantified the temporal distribution of frame-by-frame residual motion, by evaluating the cumulative frame-by-frame displacement (d) of six manually selected ground control points (GCPs; Figure 1) in every frame of the stabilized frame sequence. The movement of these GCPs post-stabilization provided a clear picture of the residual motion. To analyze this residual motion, we employed the differential Root Mean Square Difference metric ($d(\text{RMSD})$) (Ljubičić et al., 2021). The $d(\text{RMSD})$ metric quantified the magnitude of the residual displacement of static features, based on a pixel intensity RMSD. This RMSD metric operates by directly comparing several subregions within subsequent images. In each subregion, it calculates the differences in pixel intensities at corresponding locations between two images. These differences are then squared, summed over all pixels in the subregions, and averaged. The square root of this average provides the $d(\text{RMSD})$ value. This value quantified residual motion magnitude and aided in understanding the temporal distribution of residual displacements in the video.

3.2. Large-Scale Particle Image Velocimetry

LSPIV, based on Eulerian principles of motion (Euler, 2008), was originally introduced by Fujita et al. (1998), enabling the estimation of instantaneous flow velocities from a series of consecutive images. Here, LSPIV velocities were computed using PIVlab (Thielicke & Sonntag, 2021; Thielicke & Stamhuis, 2014).

Computation of surface flow velocities in PIVlab is attained by cross-correlation algorithms applied to orthorectified images recorded at a known time interval. We evaluate the accuracy of both Fast Fourier Transform window deformation (direct FFT correlation with multiple passes and deforming windows) and Ensemble correlation (Figure 2). Interrogation areas (IA), which are small windows of defined size (in pixels), are used to track the displacement of image patterns within a chosen larger search area (SA) in subsequent images. The multi-pass FFT window deformation approach allows for the spatial resolution of velocity measurements to be improved through multiple reductions in the size of the interrogation areas over which correlations are calculated. Ensemble correlation is better suited for sparsely seeded images as it relies on averaging correlation matrices followed

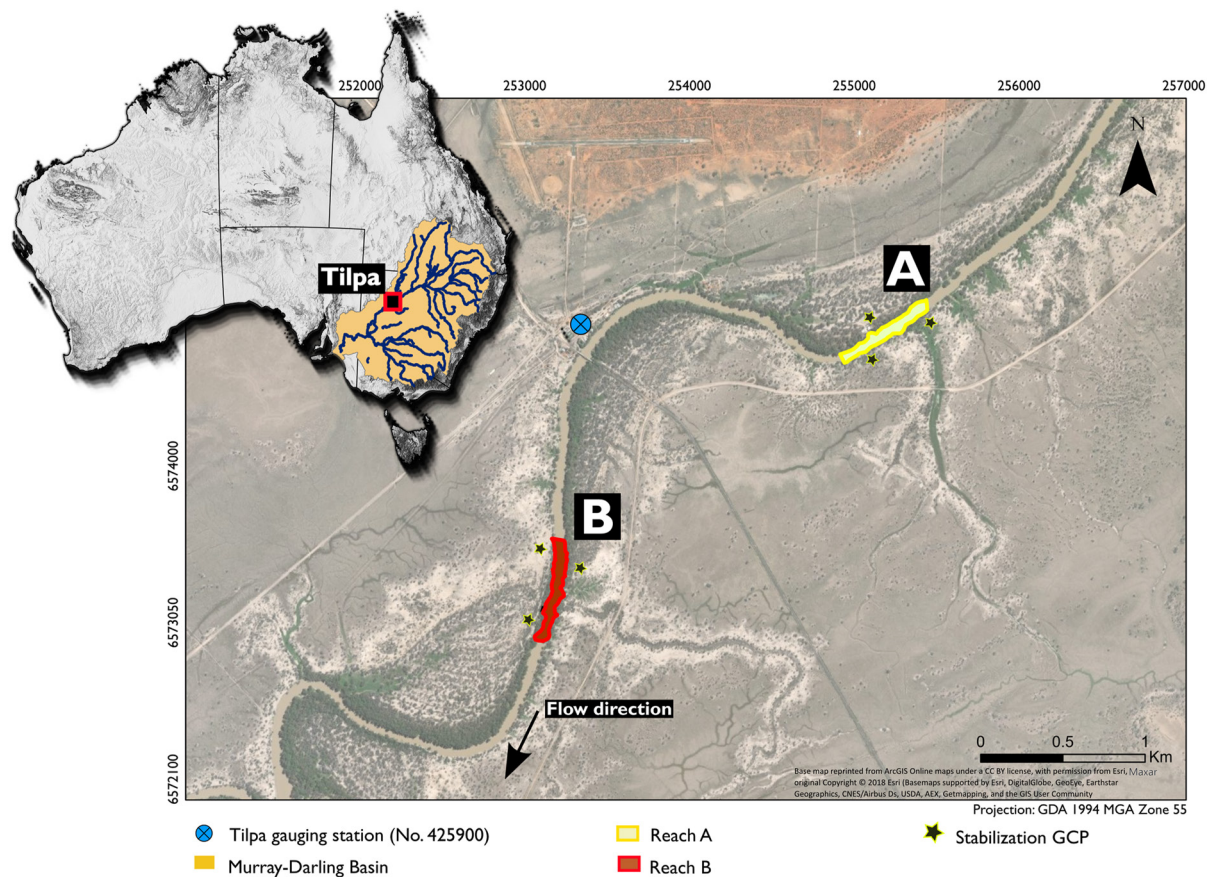


Figure 1. Study area indicating investigated reaches A and B.

by detecting a correlation peak with the resultant benefit of lower bias and displacement errors (Thielicke & Sonntag, 2021). Given the relatively coarse spatial resolution of satellite video frames for PIV, where inter-frame movement of features are small, often less than the width of a single pixel (e.g., Legleiter & Kinzel, 2021a), PIVlab's sub-pixel motion estimation functions allow for more accurate and reliable sub-pixel peak determination. PIVlab implements both 2.3-point and 9-point Gaussian functions to resolve sub-pixel displacements (see Thielicke, 2014 for detail) making sub-pixel motion estimation possible.

We focused on two cloud-free and straight river reaches A and B (Figure 1) to reduce computational cost. Image pre-processing was performed to amplify the visibility of surface tracers with respect to the background (river-banks/static ground), applying a Contrast-limited adaptive histogram equalization (CLAHE) filter (with a window size of 8 pixels, matching our smallest IA size, see Section 3.2.1) to enhance image contrast (Li & Yan, 2022; Masafu et al., 2022). Pre-processing of images for LSPIV has a significant impact on the quality of flow velocity estimates. Although image enhancement techniques such as high pass filters and intensity capping (amongst a multitude of others) exist, CLAHE offered a balanced approach to image enhancement due to its ability to enhance local contrast and visibility of tracer particles without excessively amplifying noise.

Distinct features on the water surface were difficult to discern in the raw images, which would be expected in natural rivers observed from the height of the optical sensor. However, CLAHE contrast enhancement enabled the tracking of seeding surrogates in the image sequences, which occur when specular reflection formed by incident light interacts with free-surface deformations on the river. Image intensity variations associated with these surface deformations were visible in post-processed images.

3.2.1. Sensitivity to Image Frame Rate and PIV Algorithm

The primary free parameters in LSPIV are the sampling frequency (frame extraction rate), interrogation (IA) and search (SA) areas; optimal configurations vary significantly (Kim et al., 2008; Legleiter & Kinzel, 2020; Sharif, 2022). IA should be small enough to eliminate spurious velocities whilst being large enough to

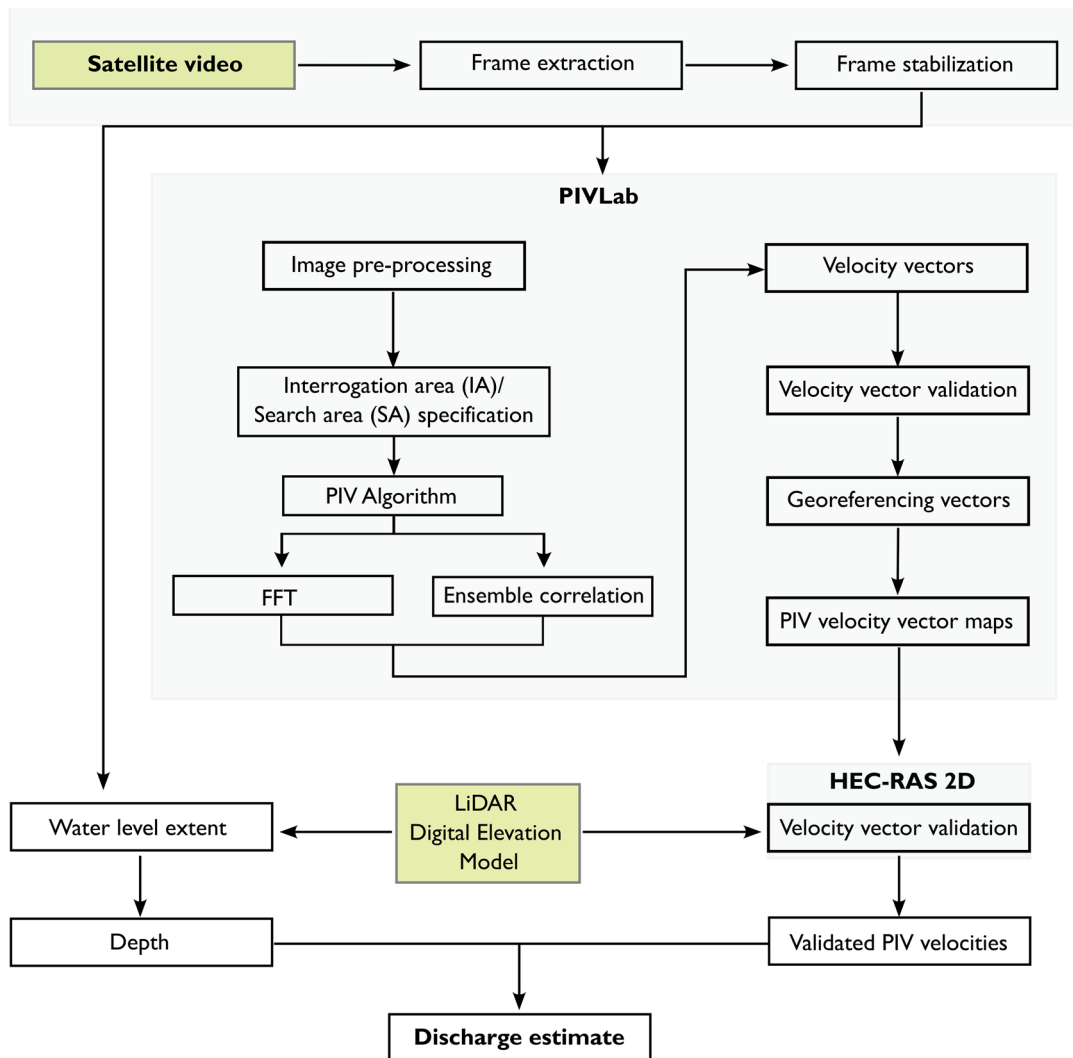


Figure 2. Discharge estimation and validation workflow. Green shaded boxes show the required input data.

accommodate an adequate window for surface pattern tracking (Tauro et al., 2018; Zhu & Lipeme Kouyi, 2019). Sampling frequency (frame extraction rate) and the IA are closely coupled and must be considered in tandem, with frame-to-frame displacement influencing the accuracy of pattern/particle detection on images.

FFT window deformation and Ensemble correlation algorithms were utilized with the maximum allowable number of PIV algorithm passes within PIVlab (four) for our sensitivity analysis (see Zhu & Lipeme Kouyi, 2019). We processed images using an IA of 64×64 pixels, with successive passes of 32×32 , 16×16 , and 8×8 pixels, all with 50% overlaps, corresponding to a minimum spatial distance of 9.8 m. SA sizes for our analyses were 128, 64, 32, and 16 pixels. For the ~ 70 m wide river, this was sufficient to allow the detection of displaced surface features. Whilst smaller IAs would allow for higher-resolution vector maps, this would also significantly increase noise and thus the number of erroneous correlations.

We processed two configurations based on FFT window deformation and ensemble correlation algorithms at three sampling rates (1, 0.5, and 0.25 Hz), resulting in 6 different LSPIV runs for each scenario. These sampling frequencies resulted in image sequences consisting of 28, 14, and 7 frames which enabled us to experiment with varied frame extraction rates for image-based velocity analysis. Subsampling our original 5 Hz video to lower frame rates (similar to the approach taken by Legleiter & Kinzel, 2021a) was beneficial for detecting velocities, especially for slower-moving phenomena. At a lower frame rate, features in our video had more time to move between frames, resulting in larger displacements that are easier to detect and measure, particularly when dealing with a nominal ground resolution of 1.2 m.

Following LSPIV cross-correlation, we post-processed the resultant velocity fields to filter out spurious velocities. Specifically, we utilized filters that removed velocity vectors that differed by $8 \times$ (PIVLab's default threshold) the standard deviation from the mean velocity, and further applied a local median filter threshold of 3×3 pixels to remove outliers. Velocity vectors were georeferenced within PIVlab from an image coordinate system back into a projected coordinate reference system (GDA 1994 MGA Zone 55). We used GCP coordinates to assess the accuracy of our georeferencing against actual locations, using 1 m Maxar satellite imagery.

3.2.2. Validation of PIV Velocity Vectors

Validation of LSPIV velocities with 2D hydrodynamic models offers an alternative where the deployment of velocity sensors (e.g., aDeps) is complex, time-consuming, or hazardous. We used velocity predictions from a calibrated 2D HEC-RAS (Brunner et al., 2020) hydraulic model (see Supporting Information S1), which solved the full-momentum Saint-Venant equations. A discharge hydrograph from the Tilpa gauging station (Figure 1) was used as the upstream boundary condition.

3.3. Discharge Estimation Using LSPIV Velocities

The standard velocity-area method was used to calculate discharge (Q) (Turnipseed & Sauer, 2010) (see Text S2 in Supporting Information S1, for detail). Water depths were estimated by intersecting the flood extent limits in the satellite imagery with a DEM. Depths at each vertical are computed by subtracting the local bed elevation from the maximum water elevation along a cross-section from a 1 m resolution LiDAR DEM with a vertical and horizontal accuracy of 0.3 and 0.8 m respectively (Geoscience Australia, 2022). The DEM was acquired when the river channel was dry, thus incorporating bathymetry. Discrete PIVLab velocity measurements were interpolated by inverse distance weighting to obtain continuous velocity maps. LSPIV-derived surface velocities were converted to depth-averaged using a specified coefficient α . Hauet et al. (2018) and Le Coz et al. (2010) constrain α between 0.8–1 for deep natural channels experiencing flood discharges.

4. Results

4.1. LSPIV Velocity Accuracy

Stabilization and georectification of frames used in PIV are subject to errors that propagated uncertainty to computed velocity estimates. Maximum, minimum, and mean displacement errors associated with stabilization of extracted frame sequences were 0.420, 0.055, 0.237 and 0.442, 0.15, 0.261 pixels for reach A and B respectively, all less than a single pixel width. Total georectification root mean square error (RMSE) was 0.50 and 0.77 m at reach A and B, respectively. Since our smallest search area was 8 pixels, equivalent to a distance of 9.8 m, our residual georeferencing errors were 5.1% and 7.9% of the spacing between our PIV velocity vectors.

Results of the frame-by-frame analysis of residual motion showed that our GCP locations had a high R^2 of the $d(\text{RMSD})$ metric at both reach A and B (Figures 3a and 3b). The displacement of our GCPs in the stabilized frame sequence further confirmed that all our residual motion at both reaches was within the subpixel range, with average displacements of 0.475 and 0.462 pixels at reach A and B respectively (Figures 3c and 3d).

Figure 4 summarizes the results of the quantitative velocity accuracy assessment of LSPIV (processed using both FFT and Ensemble correlation PIV algorithms at frame rates of 0.25, 0.5, and 1 Hz) against calibrated HEC-RAS 2D model predictions. Regression analysis results in R^2 values of 0.32–0.51 ($p < 0.001$) between LSPIV estimates and HEC-RAS 2D model velocities. To contextualize these results, Legleiter and Kinzel (2021a) attained R^2 values of between 0.34–0.39 when comparing aDcp versus satellite video-based PIV velocities across their study area. Root Mean Square Error (RMSE) values at the 0.25 Hz frame rate were 0.18 m s⁻¹ for FFT and 0.22 m s⁻¹ for EC in Reach A, and 0.16 m s⁻¹ for FFT and 0.20 m s⁻¹ for EC in Reach B. Our results indicated a tendency of the FFT algorithm to underestimate flow velocities in both study reaches. Specifically, for Reach A, the Mean Error observed was -0.071 m s⁻¹ suggesting that the FFT algorithm, on average, estimated velocities lower than those predicted by the HEC-RAS model. Similarly, in Reach B, this underestimation persisted, albeit to a slightly lesser degree, with a Mean Error of -0.041 m s⁻¹.

4.2. Discharge Accuracy

The measured discharge was 582.01 m³ s⁻¹ at the Tilpa gauge at 23:12 UTC on 5/2/2022. LSPIV-based discharge estimates were computed at three cross-sections located in each reach (Figure 1) and ranged from 429.7 m³ s⁻¹

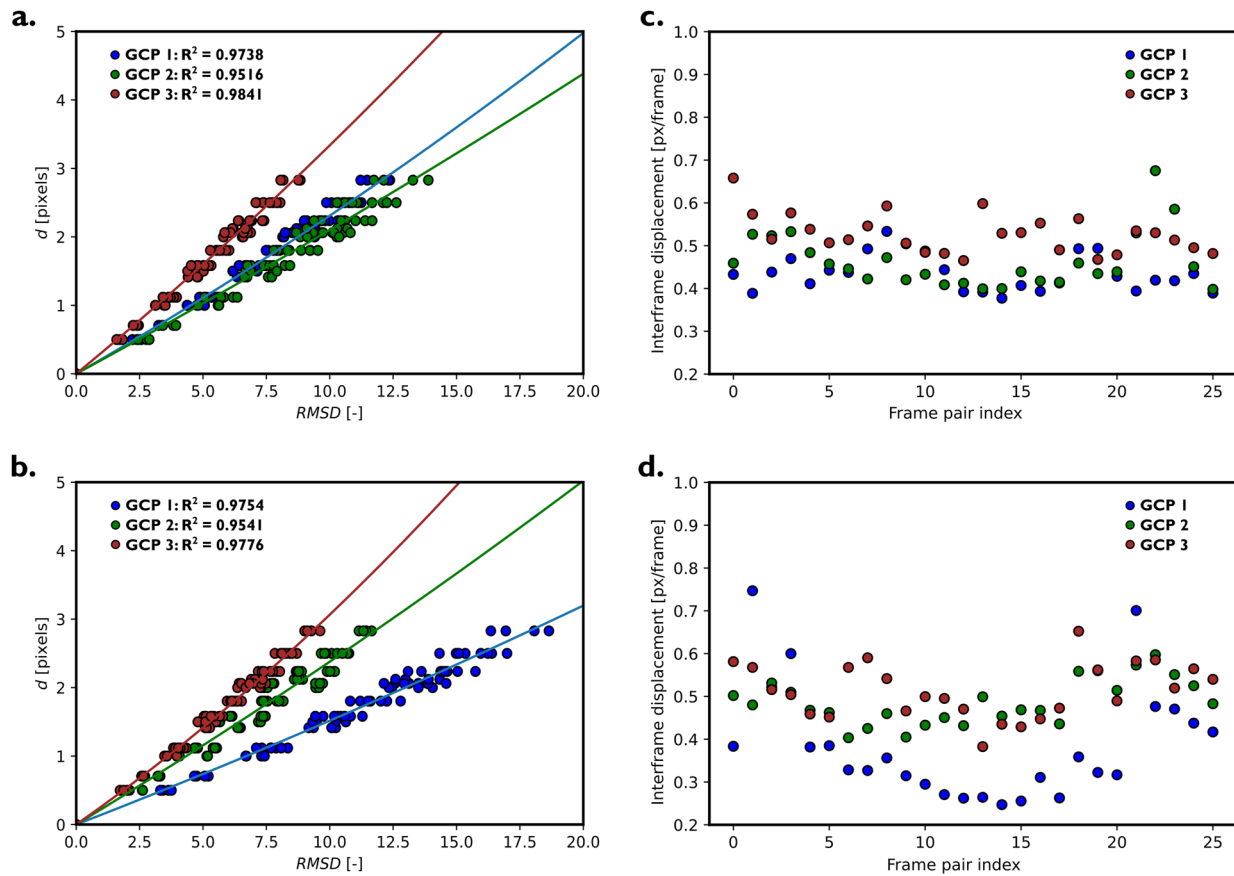


Figure 3. Displacement versus RMSD for Ground Control Points in reach A (a) and B (b). Each color-coded scatter point corresponds to a different GCP, showing how the displacement within a predefined area around each point affects the RMSD. Stabilization effectiveness across Ground Control Points (GCPs) in reach A (c) and B (d). These plots present the calculated RMSD values for each GCP across different frames, showing the stabilization performance. Each point represents the distance (distortion measure) at a GCP for a specific frame, offering insights into the temporal consistency of stabilization accuracy.

to $710.1 \text{ m}^3 \text{ s}^{-1}$, with median discharges of $536.2 \text{ m}^3 \text{ s}^{-1}$ (reach A) and $483.4 \text{ m}^3 \text{ s}^{-1}$ (reach B). Mean absolute percentage error for LSPIV-based discharge estimate was 10% (reach A) and 19.7% (reach B), with significant sensitivity to α . At both reaches, we experimented with α values between 0.7–1.0; previous studies have found that α values of between 0.8–1 are appropriate for computing depth-averaged velocities in natural rivers with a depth of greater than 2 m (Hauet et al., 2018; Vigoureux et al., 2022). At reach A, α values in the range 0.8–0.9 minimize the difference between PIV-derived discharge and gauged discharge to within 15%. At reach B a narrow band of α values in the range 0.94–0.97 minimize the error, and values in the range 0.9–1.0 result in MAE < 10%.

5. Discussion

5.1. LSPIV Velocity Estimation

We quantified video stabilization uncertainties using the $d(\text{RMSD})$ metric. Our mean values of displacement following stabilization were both within the subpixel range, with mean $d(\text{RMSD})$ being slightly higher than the mean displacement values we obtained following initial stabilization using SIFT (Section 4.1). The presence of a lower mean displacement alongside higher $d(\text{RMSD})$ values highlighted the complex nature of surface flow dynamics and the challenges in capturing these using satellite based LSPIV. It underscored the importance of considering not just the average movement but also the distribution and variability of movement across the video frames. Given our discharge analysis was conducted using velocities derived from a 0.25 Hz sampling rate (i.e., displacements > 1 pixel), stabilization errors did not significantly impact the accuracy of our computed velocities (at the 0.25 Hz sampling rate, which provided best correspondence to modeled velocities).

Our sensitivity analysis (Section 3.2.1) highlighted the significance of frame sampling frequency when computing LSPIV velocities, similar to other investigations (e.g., Legleiter & Kinzel, 2021a; Muste et al., 2008; Pearce

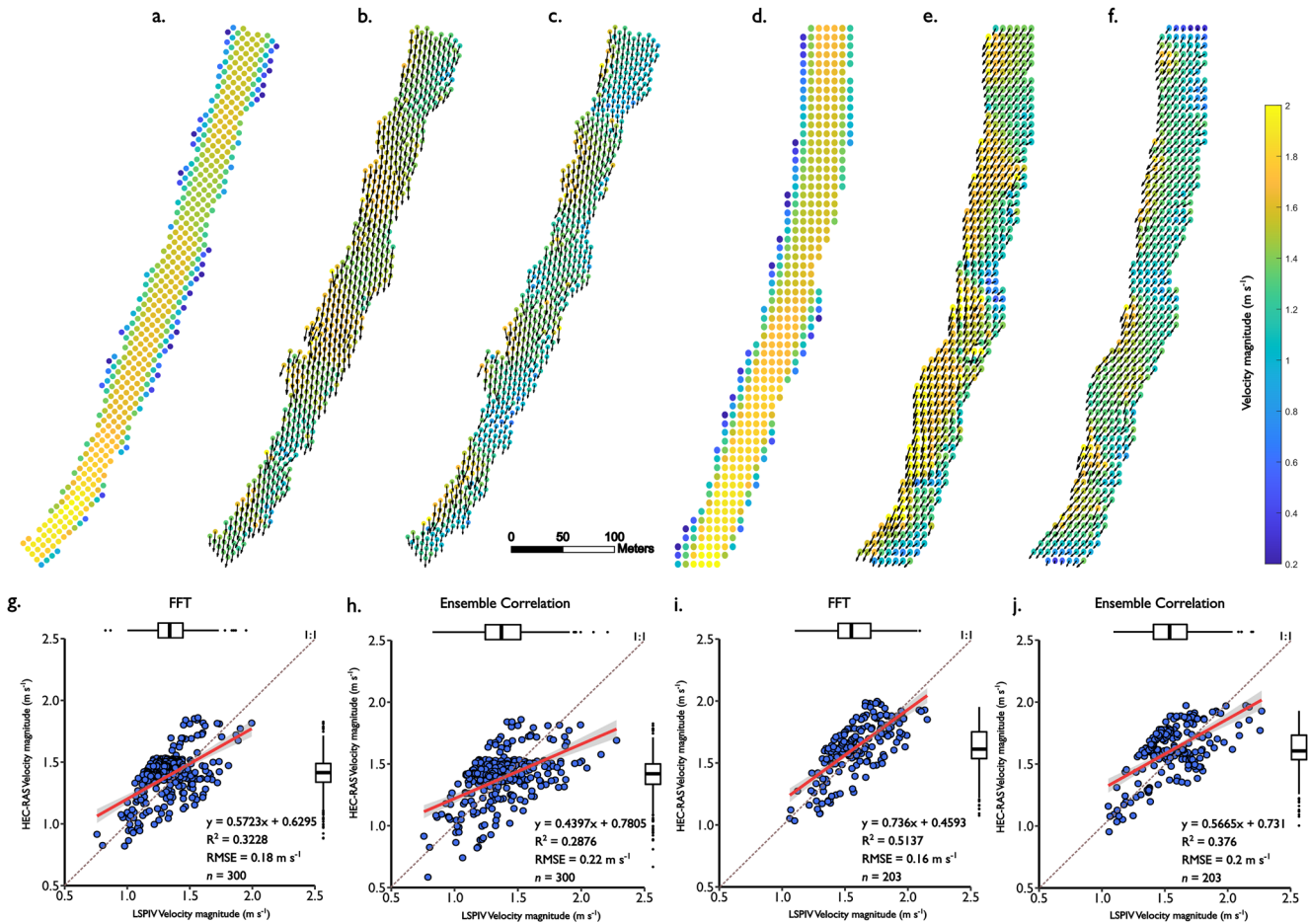


Figure 4. Comparative visualization of river flow velocities. (a, d): HEC-RAS 2D model-derived velocity fields at reaches A and B. (b, c, e, and f): Surface velocity vectors derived from satellite-based LSPIV, computed using different algorithms. The LSPIV velocity vectors are positioned to correspond precisely with the locations used in the HEC-RAS 2D model. (g–h): scatter plots showing correlations between LSPIV velocities and HEC-RAS 2D model predictions.

et al., 2020). In lieu of reference field velocity measurements, we conducted a direct comparison to 2D model velocity predictions. Statistical analysis of LSPIV velocity deviations, using our best-case scenario of 0.25 Hz processed using the FFT algorithm, showed that LSPIV tended to underestimate velocities compared to 2D model predictions. Our analysis showed variability in the performance metrics (R^2 , RMSE, ME) across different algorithms and settings, indicating the accuracy and reliability of satellite PIV can be context-dependent: R^2 values for both algorithms ranged from 0.29 to 0.51. Potential reasons for this variability include limitations due to satellite image resolution, atmospheric interference, and the inherent limitations of PIV in capturing the complex flow dynamics. Both algorithms generally performed better at Reach B than at Reach A, indicating that channel geometry and flow conditions could impact PIV accuracy. Additionally, some variability may be associated with 2D hydrodynamic model uncertainty (Bates, 2022; Dewals et al., 2023; Pasternack, 2011). Whilst calibrated 2D models are a viable means to assess PIV velocities for cases where flows exceed the safe operating ranges of conventional sensors, we recommend PIV velocity assessment with aDcp measurements.

5.2. Discharge Accuracy Assessment

LSPIV-based surface velocities, combined with preexisting, independent information on channel bathymetry, have been successfully used to obtain river discharge estimates in previous studies (e.g., Le Coz et al., 2010; Lewis et al., 2018). Using the velocity-area technique, we estimate discharge with a maximum mean absolute error of 35% which could be reduced to 0.3% and 3.78% at reaches A and B, respectively, by tuning α . The accuracy and precision of our reported discharge estimates compare favorably with Sun et al. (2010) and Lewis et al. (2018) who computed river discharges using LSPIV-based measurements to within -5 to 7% and $<20\%$

respectively. The ephemeral nature of the River Darling at Tilpa is advantageous for acquiring high accuracy bathymetric topography, here using airborne LiDAR. In other ephemeral locations, lower resolution data sets with near-global coverage could be used for large rivers. In temperate and tropical locations, direct bathymetric surveys or bathymetry derived from multispectral satellite imagery, altimetry (e.g., Liu et al., 2020; Moramarco et al., 2019) or the inference of depths from PIV-derived velocities using a flow resistance equation-based framework (Legleiter & Kinzel, 2021b) would be required. Despite these additional data demands, our results demonstrate that satellite-based optical video sensors could be deployed for near real-time estimation of riverine velocity and discharge, within tolerable uncertainties common to traditional discharge estimation techniques.

5.3. Variability of Surface Coefficient Values, α

Our satellite-video based LSPIV discharge estimation procedure yielded promising results, in terms of absolute flow magnitude, but the selection of the coefficient (α), used to convert surface to depth-averaged velocities, remains a source of uncertainty in discharge estimation. Fulton et al. (2020), Moramarco et al. (2017), and Welber et al. (2016) all observed local variability of α (0.52–0.78; 0.85–1.05, and 0.71–0.92 respectively) when estimating discharge using non-contact techniques, attributable to variations in stage (especially during higher flows due to changes in wetted channel perimeter), channel geometry, slope, and channel alignment. Significant shifts in the error of LSPIV-based discharges due to variations in α indicated that sufficient cross-section specificity in defining α is critical to our technique.

Higher α values generally led to less error in our discharge estimates, particularly in areas where LSPIV velocities differed substantially from velocities in the hydraulic model used for benchmarking. Hauet et al., 's. (2018) recommendation of α values based on a river's hydraulic radius and depth, with a noted uncertainty of $\pm 15\%$ at a 90% confidence level, are consistent with the optimal values reported here. However, without an empirically formulated, river-specific α based on in situ measurements, the appropriate values of α remains largely unclear (Legleiter et al., 2023).

When estimating flood flows in remote locations where remote sensing instruments are the sole source of depths (i.e., derived from a DEM), experimenting with values provided by Rantz (1982) ($\alpha = 0.85$ or 0.86), Turnipseed and Sauer (2010) ($\alpha = 0.84$ – 0.90), and, in extreme cases, $\alpha > 1$ due to non-standard velocity distributions (see, e.g., Moramarco et al., 2017) is a sensible approach to improve the precision of flow measurements from surface velocimetry techniques. On average, in our study the α values that led to the closest approximations of observed discharge were all less than unity, indicating our velocity-depth distributions could be well approximated using logarithmic or power laws. The variability of our best fitting, cross-section averaged α at our reaches implies that the commonly used default value of 0.85 is not always appropriate in field conditions where spatial heterogeneities in channel beds have a significant impact on velocity profiles. Although we provide a method for assessing the variability of α , calibration of site-specific α values based on traditional contact measurements remains the preferred solution for accurate discharge estimation.

6. Conclusion

Satellite-based PIV presents a promising tool for estimating river discharges during cloud-free conditions. Key to constraining uncertainty and enhancing the accuracy and reliability of LSPIV-derived velocity estimates is the stabilization of satellite video frames and the independent assessment of residual error, particularly for sub-pixel displacements. Performance metrics from the comparison of PIV velocity magnitude vectors against 2D model predictions of surface velocity exhibited reasonable correspondence. The FFT algorithm at a frame rate of 0.25 Hz, revealed best correspondence, but differences between study reaches highlight how site-specific characteristics can influence LSPIV performance. The observed R^2 values (0.3–0.5) highlight the need for careful consideration in the application of PIV techniques, particularly for low-frame-rate satellite videos. LSPIV accuracy also depends on α . Using realistic α values (0.7–1.0) from literature, our resulting errors were $-6.9 \text{ m}^3 \text{ s}^{-1}$ and $-85.6 \text{ m}^3 \text{ s}^{-1}$, and biases were -0.01 and -0.15 , at our two study reaches, respectively. Despite these uncertainties, when combined with high-resolution topographic data, the ability of satellite-based LSPIV to provide large-scale, non-intrusive river surface discharge measurements in inaccessible or dangerous areas remains a compelling advantage. The level of accuracy offers a promising foundation for enhancing LSPIV methodologies; uncertainties are comparable to traditional methods and avoid the need for extrapolation of rating curves during

high flow conditions. While acknowledging the necessity for further ground truthing to assess uncertainty, there is considerable potential for satellite video to be used to estimate discharge.

Data Availability Statement

Data used in this study are available at Masafu et al. (2023).

Acknowledgments

We extend our sincere gratitude to the editor, Valeriy Ivanov, and the insightful reviewers, Carl Legleiter and Matthew Perks for their constructive feedback and valuable suggestions that significantly enhanced the quality and clarity of this manuscript. We would also like to thank Robert Ljubičić for providing the script used in our stabilization analysis. Christopher Masafu was funded by the Lord Kelvin Adam Smith (LKAS) PhD scholarship at the University of Glasgow.

References

- Bates, P. D. (2022). Flood inundation prediction. *Annual Review of Fluid Mechanics*, 54(1), 287–315. <https://doi.org/10.1146/annurev-fluid-030121-113138>
- Bhushan, S., Shean, D., Alexandrov, O., & Henderson, S. (2021). Automated digital elevation model (DEM) generation from very-high-resolution Planet SkySat triplet stereo and video imagery. *ISPRS Journal of Photogrammetry and Remote Sensing*, 173, 151–165. <https://doi.org/10.1016/j.isprsjprs.2020.12.012>
- Brunner, G. W., United States, Army, Corps of Engineers, Institute for Water Resources (U.S.), & Hydrologic Engineering Center (U.S.) (2020). *HEC-RAS river analysis system: Hydraulic reference manual*. US Army Corps of Engineers, Institute for Water Resources, Hydrologic Engineering Center.
- Cardona, A., Saalfeld, S., Schindelin, J., Arganda-Carreras, I., Preibisch, S., Longair, M., et al. (2012). TrakEM2 software for neural circuit reconstruction. *PLoS One*, 7(6), e38011. <https://doi.org/10.1371/journal.pone.0038011>
- Dewals, B., Kitsikoudis, V., Angel Mejía-Morales, M., Archambeau, P., Mignot, E., Proust, S., et al. (2023). Can the 2D shallow water equations model flow intrusion into buildings during urban floods? *Journal of Hydrology*, 619, 129231. <https://doi.org/10.1016/j.jhydrol.2023.129231>
- Eltner, A., Sardemann, H., & Grundmann, J. (2020). Technical Note: Flow velocity and discharge measurement in rivers using terrestrial and unmanned-aerial-vehicle imagery. *Hydrology and Earth System Sciences*, 24(3), 1429–1445. <https://doi.org/10.5194/hess-24-1429-2020>
- Euler, L. (2008). Principles of the motion of fluids. *Physica D: Nonlinear Phenomena*, 237(14–17), 1840–1854. <https://doi.org/10.1016/j.physd.2008.04.019>
- European Space Agency. (2022). Technical note on quality assessment for Jilin-1 SP and GF03C video missions. Retrieved from <https://earth.esa.int/eogateway/activities/edap/vhr-hr-mr-optical-missions>
- FJI-ImageJ. (2020). FJI-ImageJ. Available online at: Retrieved from <https://imagej.net/Fiji>
- Fujita, I., Muste, M., & Kruger, A. (1998). Large-scale particle image velocimetry for flow analysis in hydraulic engineering applications. *Journal of Hydraulic Research*, 36(3), 397–414. <https://doi.org/10.1080/00221689809498626>
- Fulton, J. W., Mason, C. A., Eggleston, J. R., Nicotra, M. J., Chiu, C.-L., Henneberg, M. F., et al. (2020). Near-field remote sensing of surface velocity and river discharge using radars and the probability concept at 10 U.S. Geological Survey Streamgages. *Remote Sensing*, 12(8), 1296. <https://doi.org/10.3390/rs12081296>
- Geoscience Australia. (2022). Elvis—Elevation and depth—Foundation spatial data. Retrieved from <https://www.ga.gov.au/scientific-topics/national-location-information/digital-elevation-data>
- Gleason, C. J., & Durand, M. T. (2020). Remote sensing of river discharge: A review and a framing for the discipline. *Remote Sensing*, 12(7), 1107. <https://doi.org/10.3390/rs12071107>
- Grimaldi, S., Schumann, G. J.-P., Shokri, A., Walker, J. P., & Pauwels, V. R. N. (2019). Challenges, opportunities, and pitfalls for global coupled hydrologic-hydraulic modeling of floods. *Water Resources Research*, 55(7), 5277–5300. <https://doi.org/10.1029/2018WR024289>
- Hauet, A., Morlot, T., & Daubagnan, L. (2018). Velocity profile and depth-averaged to surface velocity in natural streams: A review over a large sample of rivers. In *River flow 2018—ninth international conference on fluvial hydraulics. E3S web of conferences* (Vol. 40, p. 06015). <https://doi.org/10.1051/e3sconf/20184006015>
- Kääb, A., Altena, B., & Mascaro, J. (2019). River-ice and water velocities using the Planet optical cubesat constellation. *Hydrology and Earth System Sciences*, 23(10), 4233–4247. <https://doi.org/10.5194/hess-23-4233-2019>
- Kim, Y., Muste, M., Hauet, A., Krajewski, W. F., Kruger, A., & Bradley, A. (2008). Stream discharge using mobile large-scale particle image velocimetry: A proof of concept. *Water Resources Research*, 44(9). <https://doi.org/10.1029/2006WR005441>
- King, T. V., Neilson, B. T., & Rasmussen, M. T. (2018). Estimating discharge in Low-order Rivers with high-resolution aerial imagery. *Water Resources Research*, 54(2), 863–878. <https://doi.org/10.1002/2017WR021868>
- Le Coz, J., Hauet, A., Pierrefeu, G., Dramais, G., & Camenen, B. (2010). Performance of image-based velocimetry (LSPIV) applied to flash-flood discharge measurements in Mediterranean rivers. *Journal of Hydrology*, 394(1–2), 42–52. <https://doi.org/10.1016/j.jhydrol.2010.05.049>
- Legleiter, C. J., & Kinzel, P. J. (2020). Inferring surface flow velocities in sediment-laden Alaskan rivers from optical image sequences acquired from a helicopter. *Remote Sensing*, 12(8), 1282. <https://doi.org/10.3390/rs12081282>
- Legleiter, C. J., & Kinzel, P. J. (2021a). Surface flow velocities from space: Particle image velocimetry of satellite video of a large, sediment-Laden River. *Frontiers in Water*, 3, 652213. <https://doi.org/10.3389/frwa.2021.652213>
- Legleiter, C. J., & Kinzel, P. J. (2021b). Depths inferred from velocities estimated by remote sensing: A flow resistance equation-based approach to mapping multiple river attributes at the reach scale. *Remote Sensing*, 13(22), 4566. <https://doi.org/10.3390/rs13224566>
- Legleiter, C. J., Kinzel, P. J., Laker, M., & Conaway, J. S. (2023). Moving aircraft river velocimetry (MARV): Framework and proof-of-concept on the Tanana River. *Water Resources Research*, 59(2), e2022WR033822. <https://doi.org/10.1029/2022WR033822>
- Lewis, Q. W., Lindroth, E. M., & Rhoads, B. L. (2018). Integrating unmanned aerial systems and LSPIV for rapid, cost-effective stream gauging. *Journal of Hydrology*, 560, 230–246. <https://doi.org/10.1016/j.jhydrol.2018.03.008>
- Li, L., & Yan, H. (2022). A robust filtering algorithm based on the estimation of tracer visibility and stability for large scale particle image velocimetry. *Flow Measurement and Instrumentation*, 87, 102204. <https://doi.org/10.1016/j.flowmeasinst.2022.102204>
- Lins, H. F. (2008). Challenges to hydrological observations. *World Meteorological Organization Bulletin*, 57, 55–58.
- Liu, K., Song, C., Wang, J., Ke, L., Zhu, Y., Zhu, J., et al. (2020). Remote sensing-based modeling of the bathymetry and water storage for channel-type reservoirs worldwide. *Water Resources Research*, 56(11), e2020WR027147. <https://doi.org/10.1029/2020WR027147>
- Ljubičić, R., Strelnikova, D., Perks, M. T., Eltner, A., Peña-Haro, S., Pizarro, A., et al. (2021). A comparison of tools and techniques for stabilising unmanned aerial system (UAS) imagery for surface flow observations. *Hydrology and Earth System Sciences*, 25(9), 5105–5132. <https://doi.org/10.5194/hess-25-5105-2021>
- Masafu, C., Williams, R., & Hurst, M. (2023). Satellite video remote sensing for estimation of river discharge [Dataset]. University of Glasgow. <https://doi.org/10.5525/gla.researchdata.1538>

- Masafu, C., Williams, R., Shi, X., Yuan, Q., & Trigg, M. (2022). Unpiloted Aerial Vehicle (UAV) image velocimetry for validation of two-dimensional hydraulic model simulations. *Journal of Hydrology*, 612, 128217. <https://doi.org/10.1016/j.jhydrol.2022.128217>
- Matheson, A., & Thoms, M. C. (2018). The spatial pattern of large wood in a large low gradient river: The Barwon–Darling River. *International Journal of River Basin Management*, 16(1), 21–33. <https://doi.org/10.1080/15715124.2017.1387123>
- Moramarc, T., Barbetta, S., Bjerklie, D. M., Fulton, J. W., & Tarpanelli, A. (2019). River bathymetry estimate and discharge assessment from remote sensing. *Water Resources Research*, 55(8), 6692–6711. <https://doi.org/10.1029/2018WR024220>
- Moramarc, T., Barbetta, S., & Tarpanelli, A. (2017). From surface flow velocity measurements to discharge assessment by the entropy theory. *Water*, 9(2), 120. <https://doi.org/10.3390/w9020120>
- Murray-Darling Basin Authority. (2010). *Guide to the proposed basin plan: Technical background*. MDBA Publication. no. 61/10. Retrieved from <https://cdn.environment.sa.gov.au/environment/docs/guide-to-basin-plan-vol-1-gen.pdf>
- Muste, M., Fujita, I., & Hauet, A. (2008). Large-scale particle image velocimetry for measurements in riverine environments: Large-scale particle velocimetry. *Water Resources Research*, 44(4). <https://doi.org/10.1029/2008WR006950>
- Pasternack, G. B. (2011). 2D modeling and ecohydraulic analysis. Createspace.
- Pearce, S., Ljubičić, R., Peña-Haro, S., Perks, M., Tauro, F., Pizarro, A., et al. (2020). An evaluation of image velocimetry techniques under low flow conditions and high seeding densities using unmanned aerial systems. *Remote Sensing*, 12(2), 232. <https://doi.org/10.3390/rs12020232>
- Perks, M. T., Sasso, S. F. D., Hauet, A., Jamieson, E., Coz, J. L., Pearce, S., et al. (2020). Towards harmonisation of image velocimetry techniques for river surface velocity observations. *Earth System Science Data*, 12(3), 1545–1559. <https://doi.org/10.5194/essd-12-1545-2020>
- Rantz, S. E. (1982). Measurement and computation of streamflow (USGS Numbered Series No. 2175). In *Water supply paper*. United States Government Publishing Office. <https://doi.org/10.3133/wsp2175>
- Rentschler, J., & Salhab, M. (2020). People in harm's way: Flood exposure and poverty in 189 countries. In *Policy research working papers*. The World Bank. <https://doi.org/10.1596/1813-9450-9447>
- Revel, M., Zhou, X., Yamazaki, D., & Kanae, S. (2023). Assimilation of transformed water surface elevation to improve river discharge estimation in a continental-scale river. *Hydrology and Earth System Sciences*, 27(3), 647–671. <https://doi.org/10.5194/hess-27-647-2023>
- Riggs, R. M., Allen, G. H., David, C. H., Lin, P., Pan, M., Yang, X., & Gleason, C. (2022). RODEO: An algorithm and Google Earth Engine application for river discharge retrieval from Landsat. *Environmental Modelling & Software*, 148, 105254. <https://doi.org/10.1016/j.envsoft.2021.105254>
- Schindelin, J., Arganda-Carreras, I., Frise, E., Kaynig, V., Longair, M., Pietzsch, T., et al. (2012). Fiji: An open-source platform for biological-image analysis. *Nature Methods*, 9(7), 676–682. <https://doi.org/10.1038/nmeth.2019>
- Sharif, O. (2022). Measuring surface water flow velocities by a drone and large-scale particle image velocimetry (LSPIV). [WWW Document]. URL Retrieved from <http://essay.utwente.nl/93022/>
- Sichangi, A. W., Wang, L., Yang, K., Chen, D., Wang, Z., Li, X., et al. (2016). Estimating continental river basin discharges using multiple remote sensing data sets. *Remote Sensing of Environment*, 179, 36–53. <https://doi.org/10.1016/j.rse.2016.03.019>
- Sun, X., Shiono, K., Chandler, J. H., Rameshwaran, P., Sellin, R. H. J., & Fujita, I. (2010). Discharge estimation in small irregular river using LSPIV. *Proceedings of the Institution of Civil Engineers - Water Management*, 163(5), 247–254. <https://doi.org/10.1680/wama.2010.163.5.247>
- Tarpanelli, A., Barbetta, S., Brocca, L., & Moramarco, T. (2013). River discharge estimation by using altimetry data and simplified flood routing modeling. *Remote Sensing*, 5(9), 4145–4162. <https://doi.org/10.3390/rs5094145>
- Tauro, F., Petroselli, A., & Grimaldi, S. (2018). Optical sensing for stream flow observations: A review. *Journal of Agricultural Engineering*, 49(4), 199–206. <https://doi.org/10.4081/jae.2018.836>
- Thielicke, W. (2014). *The flapping flight of birds*. Diss. University of Groningen. Retrieved from https://research.rug.nl/files/14094713/Chapter_8.pdf
- Thielicke, W., & Sonntag, R. (2021). Particle image velocimetry for MATLAB: Accuracy and enhanced algorithms in PIVlab. *Journal of Open Research Software*, 9(1), 12. <https://doi.org/10.5334/jors.334>
- Thielicke, W., & Stammhuis, E. (2014). PIVlab—Towards user-friendly, affordable and accurate digital particle image velocimetry in MATLAB. *Journal of Open Research Software*, 2, e30. <https://doi.org/10.5334/jors.bl>
- Turnipseed, D. P., & Sauer, V. B. (2010). *Discharge measurements at gaging stations (USGS Numbered Series No. 3-A8), Discharge measurements at gaging stations, Techniques and Methods*. U.S. Geological Survey. <https://doi.org/10.3133/tm3A8>
- Vigoureaux, S., Liebard, L.-L., Chonoski, A., Robert, E., Torchet, L., Poveda, V., et al. (2022). Comparison of streamflow estimated by image analysis (LSPIV) and by hydrologic and hydraulic modelling on the French Riviera during November 2019 flood. In P. Gourbesville & G. Caignaert (Eds.), *Advances in hydroinformatics* (pp. 255–273). Springer Water. Springer Nature. https://doi.org/10.1007/978-981-19-1600-7_16
- Water NSW. (2023). Station number 425900. Retrieved from <https://realtime.data.watersnsw.com.au/>
- Welber, M., Le Coz, J., Laronne, J. B., Zolezzi, G., Zamler, D., Dramais, G., et al. (2016). Field assessment of noncontact stream gauging using portable surface velocity radars (SVR): Field assessment of portable surface velocity radars. *Water Resources Research*, 52(2), 1108–1126. <https://doi.org/10.1002/2015WR017906>
- Zakharova, E., Nielsen, K., Kamenev, G., & Kouraev, A. (2020). River discharge estimation from radar altimetry: Assessment of satellite performance, river scales and methods. *Journal of Hydrology*, 583, 124561. <https://doi.org/10.1016/j.jhydrol.2020.124561>
- Zhu, X., & Lipeme Kouyi, G. (2019). An analysis of LSPIV-based surface velocity measurement techniques for stormwater detention basin management. *Water Resources Research*, 55(2), 888–903. <https://doi.org/10.1029/2018WR023813>

References From the Supporting Information

- Costabile, P., Costanzo, C., Ferraro, D., Macchione, F., & Petaccia, G. (2020). Performances of the new HEC-RAS version 5 for 2-D hydrodynamic-based rainfall-runoff simulations at basin scale: Comparison with a state-of-the art model. *Water*, 12(9), 2326. <https://doi.org/10.3390/w12092326>
- Dasallas, L., Kim, Y., & An, H. (2019). Case study of HEC-RAS 1D–2D coupling simulation: 2002 Baeksan flood event in Korea. *Water*, 11(10), 2048. <https://doi.org/10.3390/w11102048>
- Iroume, J. Y.-A., Onguéné, R., Djanna Koffi, F., Colmet-Daage, A., Stieglitz, T., Essoh Sone, W., et al. (2022). The 21st August 2020 flood in Douala (Cameroon): A major urban flood investigated with 2D HEC-RAS modeling. *Water*, 14(11), 1768. <https://doi.org/10.3390/w14111768>
- Patel, D. P., Ramirez, J. A., Srivastava, P. K., Bray, M., & Han, D. (2017). Assessment of flood inundation mapping of Surat city by coupled 1D/2D hydrodynamic modeling: A case application of the new HEC-RAS 5. *Natural Hazards*, 89(1), 93–130. <https://doi.org/10.1007/s11069-017-2956-6>

- Timbadiya, P. V., Patel, P. L., & Porey, P. D. (2011). Calibration of HEC-RAS model on prediction of flood for lower Tapi River, India. *Journal of Water Resource and Protection*, 3(11), 805–811. <https://doi.org/10.4236/jwarp.2011.311090>
- Zeiger, S. J., & Hubbart, J. A. (2021). Measuring and modeling event-based environmental flows: An assessment of HEC-RAS 2D rain-on-grid simulations. *Journal of Environmental Management*, 285, 112125. <https://doi.org/10.1016/j.jenvman.2021.112125>

EXHIBIT 10

Remote Sensing of Streamflow in Alaska Rivers—New Technology to Improve Safety and Expand Coverage of USGS Streamgaging

Why Measuring River Flow in Alaska Is Important

The U.S. Geological Survey (USGS) monitors water level (water surface elevation relative to an arbitrary datum) and measures streamflow in Alaska rivers to compute and

compile river flow records for use by water resource planners, engineers, and land managers to design infrastructure, manage floodplains, and protect life, property, and aquatic resources. Alaska has over 800,000 miles of rivers including the Yukon River, the third longest river in the United States. These rivers are home to rare and important ecosystems and are used for recreation, hydropower generation, commercial fishing, and transportation. River flow measurements are essential for wise and safe development and use of Alaska rivers.

Alaska River Facts

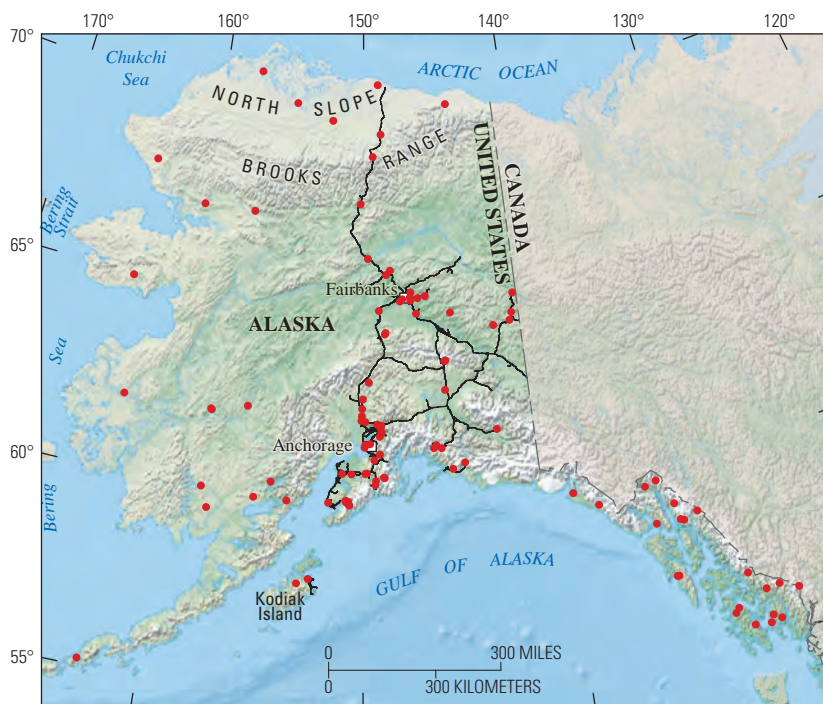
- Alaska has more than 800,000 miles of rivers and streams
- The Yukon River is the third longest river in the U.S. and second largest by flow volume
- Alaska rivers are usually frozen from December to April
- Alaska rivers drain to the Arctic Ocean, Bering Sea, and Pacific Ocean

USGS Flow Measurements in Alaska

- USGS has partnered with NASA and is using data from NASA satellites.
- Alaska has one streamgage per 6,500 mi², compared to one streamgage per 400 mi² in the lower 48 States
- Hydrologic technicians visit streamgages six to ten times annually for maintenance and data collection
- On frozen rivers, USGS hydrologic technicians drill holes through the ice to take streamflow measurements
- Streamflow measurements at remote sites can take up to 3 days, including travel time, and some locations are only accessible by airplane or helicopter because of difficult terrain

How Streamflow Is Measured Today

The USGS monitors water levels at more than 100 streamgages in Alaska (fig. 1). Converting the streamgage water-level data into flow (or discharge) data requires hydrologic technicians to travel to river



Base image copyright from Esri, 2019. Map projection: Alaska Albers Conic. Horizontal datum is North American Datum of 1983.

Figure 1. Dots show U.S. Geological Survey continuous river monitoring stations in Alaska as of 2018.

monitoring sites to collect direct flow measurements several times each year, including when rivers are flooded or covered with ice.

Hydrologic technicians regularly visit streamgages to measure river flow with handheld mechanical-impeller and hydroacoustic velocity meters with depth-sounding rods, or with an Acoustic Doppler Current Profiler (ADCP) that simultaneously measures water velocity and channel depth across the channel as it is pulled across the river surface by boat or cable (fig. 2). Many streamgage stations are remote and are only accessible by airplane or helicopter, requiring multiple days per visit. When rivers are covered with ice, typically from December through April, technicians drill holes through the ice to access the flowing water. River conditions are particularly hazardous during periods of ice breakup, when shore ice becomes unstable and ice floes move downstream.



Figure 2. U.S. Geological Survey hydrologic technicians collecting flow measurement data using in-water methods: (A) technician measuring flow depth and velocity at Evaingiknuk Creek near Noatak, Alaska; (B) technician augering ice to measure flow depth and velocity beneath the ice at Copper River near Cordova, Alaska; and (C) technician ferrying hydroacoustic equipment across Ikalukrok Creek near Kivalina, Alaska.

How Remote Sensing Can Improve Flow Measurement

Measuring river flow with remote sensing from satellites or aircraft (such as airplanes, helicopters, and unmanned aerial systems [UAS], or drones) can improve field safety and increase the total number and frequency of streamflow measurements, particularly for isolated rivers (fig. 3). Measurements can be taken during floods without exposing hydrologic technicians to dangerous river conditions. River flow measurement during ice breakup, which is difficult or impossible with traditional streamgaging techniques, becomes feasible with remote sensing. Remote sensing can help the USGS expand its monitoring network to cover more rivers, which is a major focus of the agency, particularly in Alaska (figs. 4 and 5).

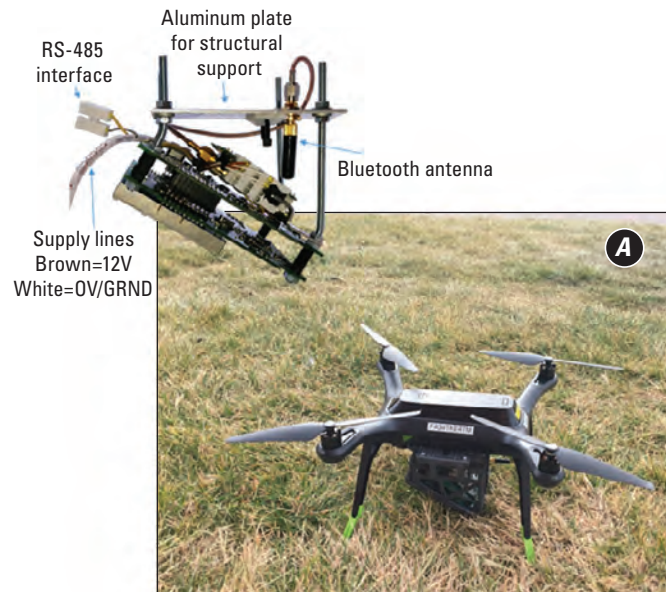


Figure 3. River surface velocities can be measured with (A) doppler radar mounted on small unmanned aerial systems as shown during field trials (B) at the Tanana River, Nenana, Alaska, July 2018.

New Remote Sensing Technology

Monitoring flow from the air or space is now possible using new technology and improvements in:

- the number of satellites;
- image processing techniques;
- unmanned aerial systems (UAS);
- advanced sensors for water-velocity and depth measurements; and,
- data storage and processing capabilities.

Analysis of remote sensing data yields estimates of river properties such as width, depth, water-surface slope, and water-surface velocity. River discharge is calculated by using hydrodynamic equations and measurements made by multiple sensors.

Surface Velocimetry

Measurement of water velocities on a river surface (surface velocimetry) is based on time-lapse images of the river surface and computer analysis of features moving on the river surface. Surface velocity data is then paired with channel bathymetry (water depth) data to calculate river discharge.

Image processing techniques such as Large-Scale Particle Image Velocimetry (LSPIV), calculate displacement of surface features such as foam or other debris, on a river surface.



Figure 4. Measurements of river flow have been tested using a helicopter-mounted thermal camera, optical camera, and lidar; all fully integrated with a global navigation satellite system (GNSS) for direct geo-referencing, Anchorage, Alaska.

Displacement distances and time between frames in the video are used to compute flow velocities at many locations on the river surface (fig. 6). A variety of velocimetry techniques and imagery can be used to compute surface velocities. For example, thermal cameras with high sensitivity to medium and long wavelengths can resolve features on the water surface caused by turbulent mixing. Thermal images are then processed to compute surface velocities based on the displacement of thermal features on the surface as they move downstream (Legleiter and others, 2017).

Doppler Radar

Doppler radar technology, commonly used to track weather conditions and to measure vehicle speeds, can also be used to measure river surface velocities. Radar signals are transmitted towards the surface of the water and the reflected signal is shifted to a different frequency because the water is moving. This Doppler shift is used to calculate the velocity of the water surface relative to the radar. Both hand-held and bridge-mounted radar Doppler velocity sensors are currently in use (Fulton and Ostrowski, 2008) and UAS mounted sensors are being tested.

Bathymetry Measurement

Knowledge of river depths (bathymetry) improves flow estimates. In clear-flowing rivers, sunlight reflected from the river bed can be measured to estimate bathymetry using spectral analysis, as demonstrated using reflectance measurements made from a bridge over the Salcha River in Alaska (Legleiter and others, 2017). In other rivers, airplane-mounted green



Figure 5. River surface height and slope of large rivers can be measured by radar altimetry from satellites, such as the Jason-2 OSTM shown here (image from NASA Jet Propulsion Laboratory, California Institute of Technology, <https://www.jpl.nasa.gov/news/news.php?feature=6890>).

lidar (light detection and ranging) systems have been used to measure river bathymetry (fig. 7; Miller-Corbett, 2018). New technologies are being tested for UAS deployment including midar (multispectral imaging, detection and active reflectance) that uses multispectral light-emitting diodes (LEDs). These techniques are limited to relatively clear and shallow streams in which sunlight, lasers, or LED light can penetrate the water and reflect from the river bed back to the surface (fig. 8).

Ground penetrating radar is another promising technology for measuring bathymetry (Costa and others, 2006) and, unlike the other methods mentioned here, can also be used in turbid or muddy streams but performs poorly in high conductance (salty) water and against channel beds comprised of low-reflectance materials.

Altimetry

Satellites are used to measure river surface altitudes or elevations of wide rivers (more than 100 m) with an accuracy of 5 cm (Zlinszki and others, 2017) and can measure changes in river elevation with accuracies of less than 1 cm. River surface altitudes measured by satellite can be converted to river flow values using hydraulic equations such as Manning’s equation (Bjerklie and others, 2018) and at-many-stations hydraulic geometry equations (Gleason and Smith, 2014).

The Future of Remote Sensing Streamgages in Alaska

In Alaska, the USGS is establishing remote sensing streamgages on river reaches that have frequent satellite overpasses and channel shapes—ideally straight and steep, more than 100 m wide, and with little turbulence or flood debris such as boulders or trees that are well suited for measurement by satellite. The first four remote sensing streamgages have been established at the Tanana River at Nenana, Tanana River at Fairbanks, Susitna River at Sunshine, and Yukon River at Stevens Village. These locations coincide with existing streamgaging stations so that the accuracy of remotely sensed flow measurements can be assessed. The goal is to expand the network of remote sensing streamgages to cover additional rivers, including some of the many rivers in Alaska that are not currently monitored. As methods for computing river flow with remote sensing become more refined from this effort in Alaska,

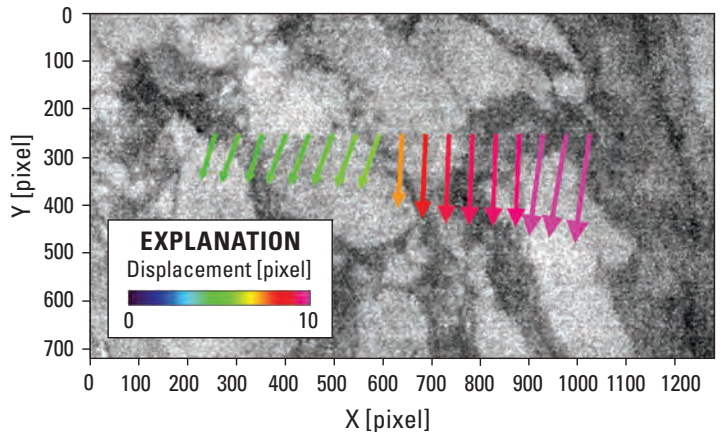


Figure 6. Infrared image overlain with flow velocity vectors derived from infrared video velocimetry analysis, Chena River, Alaska (from Kinzel and others, 2017).

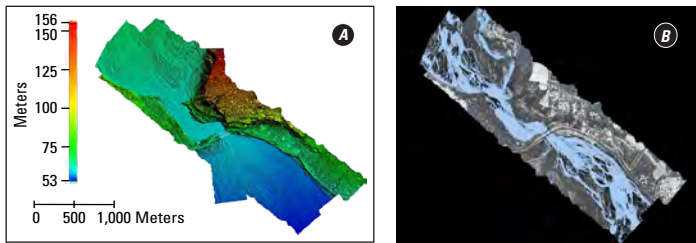


Figure 7. Images showing (A) topography and (B) laser intensity, Matanuska River near Palmer, Alaska. Water surfaces shown in blue. Data collected by helicopter-mounted Riegl VQ-580 lidar (light detection and ranging) scanning system (data from U.S. Army Corp of Engineers).

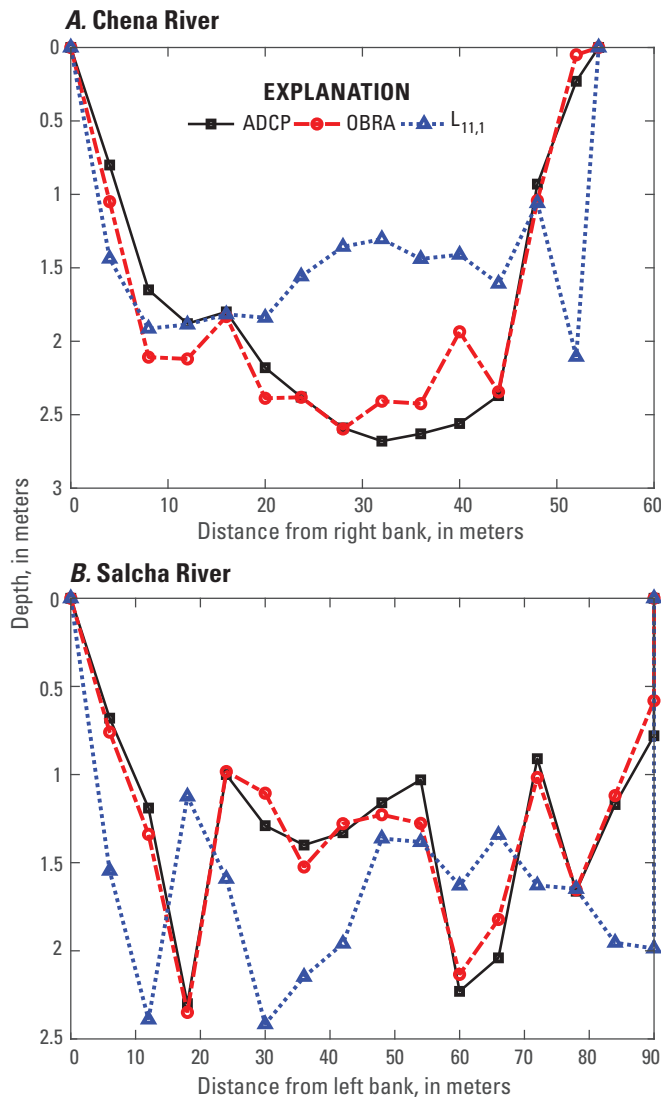


Figure 8. River bathymetry for two study sites in Alaska, the Chena and Salcha Rivers. Field-based ADCP data provided measured ground truth for evaluating depths estimated from field spectra based on Optimal Band Ratio Analysis (OBRA) and from the length scale ($L_{11,1}$) of turbulent features expressed at the river surface and captured in thermal image time series

they can be applied elsewhere in the United States and the world to provide valuable data for use in emergency response, water-supply development, hydroelectric planning and operation, transportation, and natural resource management.

References

- Bjerklie, D.J., Birkett, C.M., Jones, J.W., Carabjal, C., Rover, J., Fulton, J.W., and Pierre-André, G., 2018, Satellite remote sensing estimation of river discharge—Application to the Yukon River, Alaska: *Journal of Hydrology*, v. 561, p. 1,000–1,018, 10.1016/j.jhydrol.2018.04.005.
- Costa, J. E., Cheng, R.T., Haeni, F.P., Melcher, N., Spicer, N.R., Hayes, E., Plant, W., Hayes, K., Teague, C., and Barrick, D., 2006, Use of radars to monitor stream discharge by noncontact methods: *Water Resources Research*, v. 42, W07422, 14 p., doi:10.1029/2005WR004430.
- Fulton, J.W., and Ostrowski, J., 2008, Measuring real-time streamflow using emerging technologies—Radar, hydroacoustics, and the probability concept: *Journal of Hydrology*, v. 357, p. 1–10, 10.1016/j.jhydrol.2008.03.028.
- Gleason, C.J., and Smith, L.C., 2014, Toward global mapping of river discharge using satellite images and at-many-stations hydraulic geometry: *Proceedings of the National Academy of Sciences of the United States of America*, v. 111, n. 13, p. 4788–4791, doi:10.1073/pnas.1317606111.
- Kinzel P.J., Legleiter C., Nelson J.M., and Conaway J.S., 2017, Remote measurement of surface-water velocity using infrared videography and PIV—A proof-of-concept for Alaskan rivers: E-proceedings of the 37th IAHR World Congress, August 13–18, 2017, Kuala Lumpur, Malaysia, 9 p.
- Legleiter, C.J., Kinzel, P.J., and Nelson, J.M., 2017, Remote measurement of river discharge using thermal particle image velocimetry (PIV) and various sources of bathymetric information: *Journal of Hydrology*, v. 554 (Supplement C), p. 490–506.
- Miller-Corbett, C., 2018, A comparison of synthetic flowpaths derived from light detection and ranging topobathymetric data and National Hydrography Dataset high resolution flowlines: U.S. Geological Survey Open-File Report 2018–1058, 29 p., <https://doi.org/10.3133/ofr20181058>.
- Zlinszky A., Boergens E., Glira P., and Pfeifer N., 2017, Airborne laser scanning for calibration and validation of inshore satellite altimetry—A proof of concept: *Remote Sensing of Environment*, v. 197, August 2017, p. 35–42.

Authors: Jeff Conaway, Alaska Science Center; John Eggleston, WMA—Observing Systems Division; Carl J. Legleiter, WMA—Integrated Modeling and Prediction Division; John W. Jones, WMA—Observing Systems Division; Paul J. Kinzel, WMA—Integrated Modeling and Prediction Division; John W. Fulton, Colorado Water Science Center

Photographs: All photographs by U.S. Geological Survey

For more information: U.S. Geological Survey, 4210 University Drive, Anchorage, AK 99508

<http://alaska.usgs.gov>

Publishing support provided by the U.S. Geological Survey Science Publishing Network, Tacoma Publishing Service Center

EXHIBIT 11



Remote sensing techniques for estimating evaporation

Thomas R.H. Holmes

Hydrological Science Lab, NASA Goddard Space Flight Center, Greenbelt, MD, United States



5.1 Introduction

In most general terms, evaporation is the process by which a substance is transformed from its liquid state into vapor. To a hydrologist, evaporation (E) refers specifically to the volume of water that evaporates in a given time-period from the Earth's surface into the atmosphere. Evaporation of water completes the hydrological cycle for $\sim 60\%$ of the precipitation that falls on the land areas of the Earth (e.g., Oki and Kanae, 2006). This exchange of water vapor between surface and atmosphere is associated with a large transfer of energy in the form of *latent heat*, the conversion of thermal energy into the molecular formation of water vapor from liquid. Latent energy is the dominant source of atmospheric heating when it is liberated through *condensation*. The process of evaporation and condensation transfers more than half of the annual solar energy received by the Earth's land masses to the atmosphere. Evaporation also accompanies the exchange of carbon dioxide and oxygen between growing vegetation and the atmosphere.

Despite this central role for evaporation as a link between the energy, water, and carbon cycles it is one of the least constrained components of the hydrological cycle in land surface models (LSM). Evaporation is difficult to measure remotely because it lacks a direct electromagnetic fingerprint that can be exploited by satellite retrievals. Even if the bulk portion of available energy that is diverted to latent heat can be estimated as a residual of the surface energy balance, the attribution to its source water reservoirs often depends on physical model assumptions. In order to improve estimates of overall evaporation and gain process understanding of the coupled carbon and water cycle, it is important to accurately

estimate the partitioning of the bulk water flux into soil and vegetation source components. This is because the immediate source of liquid water that evaporates into the atmosphere determines the relative importance of meteorological, biophysiological, and hydrological controls on evaporation. The pathway of the water molecule also affects the circulation rate of the hydrological cycle, with implications for the prediction of available renewable freshwater resources (Oki and Kanae, 2006).

Passive sources of water for evaporation respond predominantly to meteorological conditions in proportion with water availability and surface texture. There is no biological control on these processes. If the immediate source is the moisture in the soil it is called *soil evaporation*. Globally this constitutes 20%–40% of the total evaporation. Similar to this is evaporation from open water bodies like lakes, rivers, but also temporary pools of rainwater, snow, and ice. A special case of a temporary source of water are pools or drops of water in the canopy that develop when rainwater is intercepted by the leaves. When this water evaporates before it reaches the soil it is referred to as *evaporation of intercepted water* (or interception for short) and can account for 10%–35% of the incident precipitation in forests (Miralles et al., 2011). Finally, some rainwater (or water from sprinkler irrigation (Cavero et al., 2009) evaporates before it reaches the ground, but this source of latent heat is typically neglected in land surface models.

In contrast to these passive sources of water for evaporation, the water contained in vegetation tissue is subject to biophysical regulation which can act to moderate the influence of evaporative demand. Plants are also connected to a larger soil reservoir through the root network which may sustain the water supply through periods of drought. When leaf-water evaporates it is called *transpiration* (T), which reflects its role as the main leaf-cooling process and can affect regional temperatures (e.g., Mueller et al., 2016). Transpiration is the dominant pathway for the total *Evapotranspiration* (ET) and is estimated to account for two-thirds of global land ET based on flux tower measurements (Jasechko et al., 2013; Schlesinger and Jasechko, 2014). While transpiration helps to keep plants cool, it is also a necessary side-effect of the plants need to breath in CO₂ for photosynthesis and sustain their growth. The biomass yield per unit of water use (crop-per-drop) is an important indicator of agricultural efficiency in water limited regions. Estimating crop water requirements and comparing it to antecedent precipitation is also a straightforward way to assess irrigation requirements (Allen et al., 1998). If the rate of water loss

cannot be matched by water uptake from the roots, the leaf water potential drops, and ultimately the leaves will wilt. Different species of plants may have different strategies for optimizing their carbon gain while limiting the associated water loss through transpiration and this complicates the modeling of ecosystem response to drought (Konings and Gentine, 2017; Konings et al., 2017). Combined with a longer-term (climatological) baseline, remote sensing estimates of ET are used for (agricultural) drought monitoring (Anderson et al., 2007; Otkin et al., 2016).

Techniques for direct measurement of evaporation include the eddy-covariance (EC) method, Bowen ratio energy balance, and measurement of water loss with lysimeters or mass-balance methods, see for example, Allen et al. (2011) for details. Gas exchange measurements through the EC flux system is now a standard component of the experimental set-up of flux towers, many of which are organized in a global network that includes over 200 towers (Fluxnet; Baldocchi et al., 2001). EC systems have also been mounted on aircraft to measure gas exchange in the boundary layer over larger areal domains (e.g., Anderson et al., 2008; Wolfe et al., 2018). These in situ measurements are invaluable for the development and validation of process descriptions due to their continuous diurnal sampling and wealth of collocated instrumentation. However, to achieve regular monitoring of areal evaporation over land these sparse tower and aircraft measurements need to be combined with sustained satellite remote sensing. This chapter gives a broad overview of the satellite data products (Section 5.2) and the types of observation-based methodologies (Section 5.3) employed in the remote estimation of terrestrial evaporation at diverse spatial domains. Two specific examples of contrasting remote-sensing strategies for estimating evaporation over land are detailed in Sections 5.3.1 and 5.3.2. A brief discussion of more recent developments is included in Section 5.4.



5.2 Satellite measurements for evaporation retrievals

There is no single frequency-band that gives a unique fingerprint of evaporation of water into the atmosphere. Remote-sensing approaches for estimating evaporation from space typically rely on an assortment of more readily measurable meteorological and biophysical variables. This makes

remote-sensing of evaporation reliant on several unique parts of the electromagnetic spectrum, from the visible, through infrared and microwave parts of the spectrum.

Many aspects of the vegetation state can be deduced from specific spectral features in the visible to shortwave infrared part of the spectrum. Such information is traditionally summarized in vegetation indices (VI) like leaf area index (LAI, see also Chapter 1.6 for further details) and normalized difference vegetation index (NDVI), and used for land classification. Simple relationships have been developed to estimate areal vegetation fraction from LAI (Carlson and Ripley, 1997). VI in combination with precipitation and air temperature has some explanatory information on monthly ET measurements. This was utilized by Jung et al. (2010) who trained a machine learning method on global flux tower observations of ET (Fluxnet) to predict global (monthly) land evaporation for 1982–2008 from satellite records of NDVI. Meteorological information like cloud properties and the resulting shortwave and longwave radiative budget of the land surface are dependent on measurements in the visible to infrared parts of the spectrum (e.g., CERES). Several authors have demonstrated the ability to retrieve more detailed plant functional traits and biophysical parameters from the spectral reflectance (e.g., Serbin et al., 2014; Frankenberg et al., 2011), but these have not yet been incorporated in global ET measurement approaches.

The microwave part of the spectrum has wavelengths of 1 mm to 1 m. These longer waves can penetrate soil, vegetation, and clouds to varying degrees depending on exact wavelength. Microwaves convey information on water content and temperature from the intervening soil, vegetation, and atmospheric layers. Since 1979, space-based passive-microwave (PMW) radiometers measure the emitted radiative energy at frequencies chosen for a variety of remote sensing applications. Their low spatial resolution (10–40 km) is appropriate for continental or global approaches. Radars are used to measure the microwave reflectance at somewhat higher resolution and are important for precipitation measurement (Smith et al., 2007; Skofronick-Jackson et al., 2017), and surface humidity (Jackson et al., 2009; Tomita et al., 2018). PMW land surface measurements with particular relevance to ET estimation are long-term soil moisture records (e.g., Dorigo et al., 2017). PMW observations also convey information on vegetation optical depth (Owe et al., 2008) which can be used to estimate vegetation water content or biomass

(Liu et al., 2013; Momen et al., 2017), and land surface temperature (LST) (Prigent et al., 2016; Holmes et al., 2016).

The most important part of the spectrum for the remote measurement of ET is the thermal infrared (TIR) region from 1 to 16 μm . Because the phase change of water from liquid to gas represents such a large sink in the surface energy balance, the thermal fingerprint is the most direct diagnostic of latent heat available to remote sensing. This is exploited by surface energy balance approaches (see below) that can leverage the high spatial resolution of TIR-based land surface temperature (LST). Satellites provide thermal radiance with spatial resolutions down to 30 m from low Earth orbit (e.g., Landsat-8 with a bi-weekly revisit time). More moderate spatial resolution but almost daily sampling is afforded by large-swath imagers like VIIRS (375 m) and MODIS (1 km). Multiband thermal infrared radiometers are also available from satellites in geostationary orbit, resulting in diurnal sampling at lower spatial resolution, e.g., 5-minute temporal and 4-km spatial sampling for the GOES Advanced Baseline Imager (ABI), and MSG-SEVIRI (3 km, 15 minutes). The accuracy of the LST retrieval depends on the ability to simultaneously estimate spectral emissivity, which depends on the number of thermal bands. Clouds are almost completely opaque to TIR emission which prevents the retrieval of TIR-based LST from cloud-covered surfaces. It can also impact the analysis of surrounding clear-sky surfaces if clouds are not adequately screened. The efficacy of the cloud screening is an important factor in the precision of LST product and is aided by additional thermal channels.



5.3 Evaporation retrieval approaches

ET retrieval approaches combine observable drivers within statistical or process-based methodologies. These process descriptions make use of the concept of *potential evaporation* (E_p), which is the rate of evaporation that a large area with growing vegetation would sustain if there is no limit on water availability. It is used in models to represent the atmospheric demand for water, and depends on meteorological conditions like surface humidity, net radiation, wind speed, and near-surface temperature gradients. Only in humid areas does the *actual evaporation* approach (or surpass) the potential for a large part of the year. The challenge is in estimating

the actual evaporation from space, because it also depends on the surface hydrology and biophysical state of the surface.

There are two main categories of satellite-based methodologies to estimate the actual evaporation of water from the land surface. The first category includes methods that combine top-down E_p estimates with a bottom-up estimate of *evaporative stress*, or reduction from evaporative demand, that is, based on statistical parameterizations and observation-informed surface states. The second category of methodologies takes an entirely top-down approach and solves for actual evaporation as a residual of the surface energy-balance (EB). Although E_p is used to give context to the estimated E , it is not a driving dataset in energy-balance solutions.

There are several approaches to parameterize E_p and evaporative stress that have been adapted to available satellite data sets. The first set of algorithms implements the Penman-Monteith (P-M) formulation (Monteith, 1965) (e.g., Cleugh et al., 2007; Mu et al., 2011). The P-M formulation accounts for energy limitations, aerodynamic resistance, and stomatal conductance in its estimate of E_p , and parameterizes surface resistance based on VIs and surface humidity. The meteorological input requirements can be demanding for global implementation. The Priestley and Taylor (1972) (P-T) formulation is derived from the Penman-Monteith equations for a scenario with plentiful water so that the stomatal resistance is zero. P-T estimates of E_p are only based on insolation and temperature, which makes them more readily applicable to satellite measurements than the P-M methods. P-T applications must be combined with a way to estimate the reduction from the potential evaporation rate to account for hydrological or biophysical restrictions in water availability. Fisher et al. (2008) used estimates of water vapor pressure to parameterize water availability for soil evaporation, and VIs and air temperature to parameterize vegetation stress. This approach made use of the long satellite record of NDVI and net radiation to produce monthly ET estimates from 1984 to 2006 (PT-JPL). Another distinct approach to estimate evaporative stress is to combine P-T with a running-water-balance with inputs of precipitation and assimilation of soil moisture measurements (Miralles et al., 2011; Martens et al., 2017). The evaporative stress is subsequently parameterized based on prognostic model states, similar to methods employed by land surface models but with a more direct use of land surface remote sensing, see detailed description below (Section 5.3.1).

In contrast to these bottom-up approaches to estimating evaporative stress, energy balance approaches estimate actual evaporation directly from

the thermal fingerprint of the latent heat flux. This is the reason that EB approaches are regarded as more purely diagnostic in comparison to approaches that include prognostic information. EB approaches have a long legacy and have found wide application in agricultural studies that benefit from the high spatial resolution afforded by TIR-based imagers. All EB approaches solve for E as the residual of the surface energy balance (net radiation—ground heat flux—sensible heat flux). The first group of larger scale EB approaches treat evaporation as a single bulk flux that includes soil and vegetation sources, for example, SEBAL (Bastiaanssen et al., 1998), SEBS (Su, 2002), METRIC (Allen et al., 2007), and SSEB (Senay et al., 2016). They evaluate the energy balance at “dry” and “wet” extremes and estimate ET between these extremes based on the spatial variation of internally calibrated temperature within the scene of the satellite image. These EB implementations rely on accurate estimation of the temperature difference between surface and air for the estimation of sensible heat. This is challenging to apply to larger domains due to the inherent biases in the independent estimation of air and surface temperatures.

Two-source EB approaches consider soil and vegetation as separate “sources” for heat and water exchange. They partition LST and net radiation between soil and canopy components and use these to solve a set of physical equations that represent the turbulent flux exchanges between the soil, canopy, and atmosphere (Kustas and Norman, 1999; Norman et al., 1995). These early applications face the same challenge in estimating consistent surface and air temperatures over large areas as the one-source approaches. Regional applications of EB approaches are enabled when the impact of errors in the LST and air temperature boundary conditions are reduced. Anderson et al. (2007) achieved this by basing the physical retrieval of the two-source EB approach on the rate of change in surface temperature during the morning. This reduces the impact of errors in the absolute (instantaneous) LST and air temperature retrievals and forms the basis of a multiscale integrated approach to estimating ET that is detailed in Section 5.3.2.

5.3.1 GLEAM, a water balance approach to estimating evaporative stress

An example of a bottom-up approach to estimating evaporative stress is GLEAM: Global Land Evaporation, Amsterdam Methodology (Miralles et al., 2011; Martens et al., 2017). It contains an observation-driven LSM specifically tailored to estimate global ET for long-term climatological

analysis (e.g., [Miralles et al., 2014](#)). The LSM consists of a multilayer running-water-balance to estimate root zone water. Inputs to the water-balance are observed precipitation, and soil moisture observations (from PMW sensors). Central to this methodology is the use of P-T formulations to model potential evaporation based on insolation and temperature inputs (see [Section 5.1](#)).

The actual evaporation and transpiration are calculated as a fraction of E_p using parameterizations of evaporative stress. The stress is partly based on the modeled water availability in the surface layers which accounts for past precipitation, evaporation, and drainage. Estimates of evaporative stress for vegetation further account for vegetation water content through PMW measurements of vegetation optical depth. GLEAM includes separate stress functions and α for three dynamic surface components that contribute to ET: bare soil, short vegetation, tall vegetation.

GLEAM features the first global implementation of the Gash analytic model for the estimation of evaporation of intercepted rain water ([Gash, 1979](#); [Valente et al., 1997](#)). The volume of water that evaporates from the wet canopy during and immediately after a rain storm is estimated as a fraction of daily rainfall. The model parameters further account for canopy cover fraction, canopy storage, mean rainfall rates, and evaporation rates during wet canopy conditions ([Miralles et al., 2010](#)). A novel feature is the use of observed lightning frequency ([Cecil et al., 2014](#)) to distinguish synoptic from convective precipitation to account for the associated differences in rain rates.

Snow depth estimates from PMW observations are used to divert precipitation into a snowpack that is subject to sublimation before the eventual melt and entry into the soil water reservoir. The contribution of lakes and rivers is not modeled so that the total evaporation estimated by GLEAM only refers to the land fraction of the total surface area.

GLEAM is designed to be implemented for the entire duration of the modern satellite record and has been used to create daily ET records at 0.25-degree resolution from 1980 to present. These long-term ET records have been used in a series of recent hydrological and climate studies to study the impact of climate change and El Nino Southern oscillations on the water cycle, land-atmosphere feedbacks, hydrometeorological extremes, benchmarking and evaluating climate models ([Zhang et al., 2016](#); [Miralles et al., 2014](#)).

5.3.2 ALEXI: an integrated framework for two-source EB estimates of evaporation

The Atmosphere–Land Exchange Inverse (ALEXI) model (Anderson et al., 2007; Mecikalski et al., 1999) combines two-source energy balance models (Kustas and Norman, 1999; Norman et al., 1995) with atmospheric boundary layer (ABL) formulations for regional ET estimation. Model outputs include total ET, and estimates of soil evaporation and transpiration separately, with partitioning guided in part by the local vegetation cover fraction. ALEXI enables regional application of the two-source EB by basing the physical retrieval on the rate of change in surface temperature during the morning, reducing the impact of errors in the absolute (instantaneous) LST retrievals and in the air temperature boundary conditions.

The available energy is based on top-of-atmosphere shortwave and longwave radiances, albedo estimates, and longwave radiation calculated from LST according to Stefan–Boltzman’s law. Ground heat flux is estimated as a fixed percent of net radiation. LAI is used for partitioning incoming radiation (Anderson et al., 2007). A set of equations describes the energy balance for soil to atmosphere fluxes and vegetation to atmosphere.

The ABL model simulates the changes in air temperature between the time of the morning LST observation (ideally 1 hour after sunrise) and the midday observation (ideally 1 hour before solar noon). The ABL-modeled air temperature at a reference height above the canopy provides a boundary condition that is consistent with the surface fluxes generated by the EB model. P-T E_p serves as an initial estimate for canopy evaporation and is iteratively reduced until the closed energy balance produces soil evaporation that is nonnegative. This procedure is based on the assumption that no condensation occurs during clear-sky daytime hours (Kustas and Norman, 1999, 2000).

Although ALEXI was developed for geostationary sensors (Anderson et al., 2007), global implementations with MODIS-LST (Hain and Anderson, 2017; Holmes et al., 2018) are now routinely available through NASA’s Short-term Prediction Research and Transition (SPoRT). Combined with a long-term climatological record, the ratio of ALEXI ET over E_p is also used as an evaporative stress index to diagnose and monitor agricultural drought conditions (Anderson et al., 2011a). Because an EB-model like ALEXI does not model water availability it can be used

to identify neglected sources and sinks of water in LSM's, such as ground-water depth, irrigation extent, and tile drainage density (Yilmaz et al., 2014; Hain et al., 2015).

Importantly, ALEXI is part of an integrated framework of multiscale ET estimation (Anderson et al., 2011b) that also includes a flux disaggregation scheme (disALEXI: Norman et al., 2003; Anderson et al., 2004). DisALEXI utilizes higher resolution LST measurements (e.g., Landsat, or airborne platforms) to disaggregate the continental scale physical ALEXI retrievals of daily ET. On the days with high-resolution thermal observations this approach compares well with eddy-covariance measurements from flux towers. In a final step to the multiscale ET analysis framework, the Spatial and Temporal Adaptive Reflectance Fusion Model (STARFM) (Gao et al., 2006) is applied to generate a time-continuous, daily ET product at the fine spatial resolution of the disALEXI output. This ET fusion approach has been successfully demonstrated over rain-fed and irrigated cotton, corn, and soybean fields (Cammalleri et al., 2014; Yang et al., 2017), irrigated vineyards (Semmens et al., 2016), as well as forested landscapes (Yang et al., 2017).



5.4 New developments

Intermodel comparisons of global evaporation products show that they are able to capture important aspects of seasonality and spatial distribution related to climate regimes (Jimenez et al., 2011; Mueller et al., 2013; Michel et al., 2016; Miralles et al., 2016). However, these studies also reveal a lack of agreement between models in terms of the relative contribution of soil evaporation, plant transpiration, and evaporation of the intercepted water to the total evaporation at a global scale. This reflects the large uncertainties of the contribution of transpiration (Wei et al., 2017), but also the treatment of interception as a distinct process. In general, current LSMs are found to underestimate the transpiration contribution to global E compared to estimates from in situ data, satellite products, and isotope measurements (Schlesinger and Jasechko, 2014). These disagreements in the ratio of T to total ET are a significant contributor to uncertainty in long-term predictions of changes in the coupled carbon and water cycle. New measurements that can be used to better estimate

photosynthetic activity (Frankenberg et al., 2011), and thus water loss through transpiration, may allow for better observational constraints on the evaporation estimation.

Although surface energy balance approaches have a long legacy, long consistent records of global-scale ET estimates based on EB approach were not available until recently. This explains the lack of representation of EB approaches in the global evaporation comparisons discussed above, with SEBS as the lone exception. As was shown in Section 5.3.2, this situation is now changing and future assessments of global evaporation may be able to draw upon the full range of evaporation estimation approaches. Another development that will enhance the utility for EB approaches to climate science is in the application of more cloud-tolerant microwave observations to the estimation of LST (Holmes et al., 2009, 2016). This is intended to solve a central limitation of TIR-based LST, that no surface information penetrates clouds in the TIR frequency bands. This effectively limits (and biases) the temporal sampling of TIR-based approaches to clear conditions. The utility of microwave-based LST for EB estimates of evaporation has been demonstrated in the context of the ALEXI framework (Holmes et al., 2018). A full integration of PMW LST into the ALEXI framework will reduce the need for interpolation between days with clear-sky conditions and reduce uncertainty related to cloud filtering efficacy.

References

- Allen, R.G., Pereira, L.S., Raes, D., Smith, M., 1998. Crop evapotranspiration—Guidelines for computing crop water requirements—FAO Irrigation and drainage paper 56. FAO, Rome, 300 (9), D05109.
- Allen, R.G., Pereira, L.S., Howell, T.A., Jensen, M.E., 2011. Evapotranspiration information reporting: I. Factors governing measurement accuracy. *Agric. Water Manage.* 98 (6), 899–920.
- Allen, R.G., Tasumi, M., Trezza, R., 2007. Satellite-based energy balance for mapping evapotranspiration with internalized calibration (METRIC)—model. *J. Irrig. Drain. Eng.* 133 (4), 380–394.
- Anderson, M.C., Norman, J.M., Mecikalski, J.R., Torn, R.D., Kustas, W.P., Basara, J.B., 2004. A multiscale remote sensing model for disaggregating regional fluxes to micrometeorological scales. *J. Hydrometeorol.* 5 (2), 343–363.
- Anderson, M.C., Norman, J.M., Mecikalski, J.R., Otkin, J.A., Kustas, W.P., 2007. A climatological study of evapotranspiration and moisture stress across the continental United States based on thermal remote sensing: 2. Surface moisture climatology. *J. Geophys. Res. Atmosph.* 112 (D11).
- Anderson, M.C., Norman, J.M., Kustas, W.P., Houborg, R., Starks, P.J., Agam, N., 2008. A thermal-based remote sensing technique for routine mapping of land-surface carbon, water and energy fluxes from field to regional scales. *Remote Sens. Environ.* 112 (12), 4227–4241.

- Anderson, M.C., Hain, C., Wardlow, B., Pimstein, A., Mecikalski, J.R., Kustas, W.P., 2011a. Evaluation of drought indices based on thermal remote sensing of evapotranspiration over the continental United States. *J. Climate* 24 (8), 2025–2044.
- Anderson, M.C., Kustas, W.P., Norman, J.M., Hain, C.R., Mecikalski, J.R., Schultz, L., et al., 2011b. Mapping daily evapotranspiration at field to continental scales using geostationary and polar orbiting satellite imagery. *Hydrol. Earth Syst. Sci.* 15 (1), 223–239.
- Baldocchi, D., Falge, E., Gu, L., Olson, R., Hollinger, D., Running, S., et al., 2001. FLUXNET: a new tool to study the temporal and spatial variability of ecosystem-scale carbon dioxide, water vapor, and energy flux densities. *Bull. Am. Meteorol. Soc.* 82 (11), 2415–2434.
- Bastiaanssen, W.G., Menenti, M., Feddes, R.A., Holtslag, A.A.M., 1998. A remote sensing surface energy balance algorithm for land (SEBAL). 1. Formulation. *J. Hydrol.* 212, 198–212.
- Cammalleri, C., Anderson, M.C., Gao, F., Hain, C.R., Kustas, W.P., 2014. Mapping daily evapotranspiration at field scales over rainfed and irrigated agricultural areas using remote sensing data fusion. *Agric. Forest Meteorol.* 186, 1–11.
- Carlson, T.N., Ripley, D.A., 1997. On the relation between NDVI, fractional vegetation cover, and leaf area index. *Remote Sensing Environ.* 62 (3), 241–252.
- Cavero, J., Medina, E.T., Puig, M., Martínez-Cob, A., 2009. Sprinkler irrigation changes maize canopy microclimate and crop water status, transpiration, and temperature. *Agron. J.* 101 (4), 854–864.
- Cecil, D.J., Buechler, D.E., Blakeslee, R.J., 2014. Gridded lightning climatology from TRMM-LIS and OTD: dataset description. *Atmosph. Res.* 135, 404–414.
- Cleugh, H.A., Leuning, R., Mu, Q., Running, S.W., 2007. Regional evaporation estimates from flux tower and MODIS satellite data. *Remote Sens. Environ.* 106 (3), 285–304.
- Dorigo, W., Wagner, W., Albergel, C., Albrecht, F., Balsamo, G., Brocca, L., et al., 2017. ESA CCI Soil Moisture for improved Earth system understanding: state-of-the art and future directions. *Remote Sensing Environ.* 203, 185–215.
- Fisher, J.B., Tu, K.P., Baldocchi, D.D., 2008. Global estimates of the land–atmosphere water flux based on monthly AVHRR and ISLSCP-II data, validated at 16 FLUXNET sites. *Remote Sens. Environ.* 112 (3), 901–919.
- Frankenberg, C., Fisher, J.B., Worden, J., Badgley, G., Saatchi, S.S., Lee, J.E., et al., 2011. New global observations of the terrestrial carbon cycle from GOSAT: Patterns of plant fluorescence with gross primary productivity. *Geophys. Res. Lett.* 38 (17).
- Gao, F., Masek, J., Schwaller, M., Hall, F., 2006. On the blending of the Landsat and MODIS surface reflectance: predicting daily Landsat surface reflectance. *IEEE Trans. Geosci. Remote Sens.* 44 (8), 2207–2218.
- Gash, J.H.C., 1979. An analytical model of rainfall interception by forests. *Q J Roy Meteor. Soc.* 105 (443), 43–55.
- Hain, C.R., Anderson, M.C., 2017. Estimating morning change in land surface temperature from MODIS day/night observations: Applications for surface energy balance modeling. *Geophys. Res. Lett.* 44 (19), 9723–9733.
- Hain, C.R., Crow, W.T., Anderson, M.C., Yilmaz, M.T., 2015. Diagnosing neglected soil moisture source–sink processes via a thermal infrared–based two–source energy balance model. *J. Hydrometeorol.* 16 (3), 1070–1086.
- Holmes, T.R.H., De Jeu, R.A.M., Owe, M., Dolman, A.J., 2009. Land surface temperature from Ka band (37 GHz) passive microwave observations. *J. Geophys. Res. Atmosph.* 114 (D4).

- Holmes, T.R., Hain, C.R., Anderson, M.C., Crow, W.T., 2016. Cloud tolerance of remote-sensing technologies to measure land surface temperature. *Hydrol. Earth Syst. Sci.* 20 (8), 3263.
- Holmes, T.R.H., Hain, C.R., Crow, W.T., Anderson, M.C., Kustas, W.P., 2018. Microwave implementation of two-source energy balance approach for estimating evapotranspiration. *Hydrol. Earth Syst. Sci.* 22 (2), 1351.
- Jackson, D.L., Wick, G.A., Robertson, F.R., 2009. Improved multisensor approach to satellite-retrieved near-surface specific humidity observations. *J. Geophys. Res. Atmosph.* 114 (D16).
- Jasechko, S., Sharp, Z.D., Gibson, J.J., Birks, S.J., Yi, Y., Fawcett, P.J., 2013. Terrestrial water fluxes dominated by transpiration. *Nature* 49 (7445), 347.
- Jimenez, C., Prigent, C., Mueller, B., Seneviratne, S.I., McCabe, M.F., Wood, E.F., et al., 2011. Global intercomparison of 12 land surface heat flux estimates. *J. Geophys. Res. Atmosph.* 116 (D2).
- Jung, M., Reichstein, M., Ciais, P., Seneviratne, S.I., Sheffield, J., Goulden, M.L., et al., 2010. Recent decline in the global land evapotranspiration trend due to limited moisture supply. *Nature* 467 (7318), 951.
- Konings, A.G., Gentine, P., 2017. Global variations in ecosystem-scale isohydricity. *Global Change Biol.* 23 (2), 891–905.
- Konings, A.G., Williams, A.P., Gentine, P., 2017. Sensitivity of grassland productivity to aridity controlled by stomatal and xylem regulation. *Nat. Geosci.* 10 (4), 284.
- Kustas, W.P., Norman, J.M., 1999. Evaluation of soil and vegetation heat flux predictions using a simple two-source model with radiometric temperatures for partial canopy cover. *Agric. Forest Meteorol.* 94 (1), 13–29.
- Kustas, W.P., Norman, J.M., 2000. A two-source energy balance approach using directional radiometric temperature observations for sparse canopy covered surfaces. *Agron. J.* 92 (5), 847–854.
- Liu, Y.Y., Dijk, A.I., McCabe, M.F., Evans, J.P., Jeu, R.A., 2013. Global vegetation biomass change (1988–2008) and attribution to environmental and human drivers. *Global Ecol. Biogeogr.* 22 (6), 692–705.
- Martens, B., Gonzalez Miralles, D., Lievens, H., Van Der Schalie, R., De Jeu, R.A.M., Fernández-Prieto, D., et al., 2017. GLEAMv3: Satellite-based land evaporation and root-zone soil moisture. *Geosci. Model Dev* 10 (5), 1903–1925.
- Mecikalski, J.R., Diak, G.R., Anderson, M.C., Norman, J.M., 1999. Estimating fluxes on continental scales using remotely sensed data in an atmospheric-land exchange model. *J Appl. Meteorol.* 38 (9), 1352–1369.
- Michel, D., Jiménez, C., Miralles, D.G., Jung, M., Hirschi, M., Ershadi, A., et al., 2016. The WACMOS-ET project – part 1: tower-scale evaluation of four remote-sensing-based evapotranspiration algorithms. *Hydrol. Earth Syst. Sci.* 20 (2), 803–822. Available from: <https://doi.org/10.5194/hess-20-803-2016>.
- Miralles, D.G., Gash, J.H., Holmes, T.R.H., de Jeu, R.A.M., Dolman, A.J., 2010. Global canopy interception from satellite observations. *J. Geophys. Res.* 115 (D16), D16122. Available from: <https://doi.org/10.1029/2009JD013530>.
- Miralles, D.G., De Jeu, R.A.M., Gash, J.H., Holmes, T.R.H., Dolman, A.J., 2011. An application of GLEAM to estimating global evaporation. *Hydrol. Earth Syst. Sci. Discuss.* 8 (1).
- Miralles, D.G., Van Den Berg, M.J., Gash, J.H., Parinussa, R.M., De Jeu, R.A.M., Beck, H.E., et al., 2014. El Niño–La Niña cycle and recent trends in continental evaporation. *Nat. Clim. Change* 4 (2), 122.
- Miralles, D.G., Jiménez, C., Jung, M., Michel, D., Ershadi, A., McCabe, M.F., et al., 2016. The WACMOS-ET project, part 2: evaluation of global terrestrial evaporation data sets. *Hydrol. Earth Syst. Sci.* 20 (2), 823–842.

- Momen, M., Wood, J.D., Novick, K.A., Pangle, R., Pockman, W.T., McDowell, N.G., et al., 2017. Interacting effects of leaf water potential and biomass on vegetation optical depth. *J. Geophys. Res. Biogeo.* 122 (11), 3031–3046.
- Monteith, J.L., 1965. Evaporation and environment. *Symp. Soc. Exp. Biol.* 19 (205–23), 4.
- Mu, Q., Zhao, M., Running, S.W., 2011. Improvements to a MODIS global terrestrial evapotranspiration algorithm. *Remote Sens. Environ.* 115 (8), 1781–1800.
- Mueller, B., Hirschi, M., Jimenez, C., Ciais, P., Dirmeyer, P.A., Dolman, A.J., et al., 2013. Benchmark products for land evapotranspiration: LandFlux-EVAL multi-data set synthesis. *Hydrol Earth Syst. Sci.* Available from: <http://repository.kaust.edu.sa/kaust/handle/10754/334520>.
- Mueller, N.D., Butler, E.E., McKinnon, K.A., Rhines, A., Tingley, M., Holbrook, N.M., Huybers, P., 2016. Cooling of US Midwest summer temperature extremes from cropland intensification. *Nat. Clim. Change* 6 (3), 317.
- Norman, J.M., Kustas, W.P., Humes, K.S., 1995. Source approach for estimating soil and vegetation energy fluxes in observations of directional radiometric surface temperature. *Agric. For. Meteorol.* 77 (3–4), 263–293. Available from: [https://doi.org/10.1016/0168-1923\(95\)02265-Y](https://doi.org/10.1016/0168-1923(95)02265-Y).
- Norman, J.M., Anderson, M.C., Kustas, W.P., French, A.N., Mecikalski, J., Torn, R., et al., 2003. Remote sensing of surface energy fluxes at 101-m pixel resolutions. *Water Resour. Res.* 39 (8), 1221.
- Oki, T., Kanae, S., 2006. Global hydrological cycles and world water resources. *Science* 313 (5790), 1068–1072.
- Otkin, J.A., Anderson, M.C., Hain, C., Svoboda, M., Johnson, D., Mueller, R., et al., 2016. Assessing the evolution of soil moisture and vegetation conditions during the 2012 United States flash drought. *Agric. Forest Meteorol.* 218, 230–242.
- Owe, M., de Jeu, R., Holmes, T., 2008. Multisensor historical climatology of satellite-derived global land surface moisture. *J. Geophys. Res. Earth Surface* 113 (F1).
- Prigent, C., Jimenez, C., Aires, F., 2016. Toward “all weather,” long record, and real-time land surface temperature retrievals from microwave satellite observations. *J. Geophys. Res. Atmosph.* 121 (10), 5699–5717.
- Priestley, C.H.B., Taylor, R.J., 1972. On the assessment of surface heat flux and evaporation using large-scale parameters. *Mon. Weather Rev.* 100 (2), 81–92.
- Schlesinger, W.H., Jasechko, S., 2014. Transpiration in the global water cycle. *Agr. Forest Meteorol.* 189, 115–117.
- Semmens, K.A., Anderson, M.C., Kustas, W.P., Gao, F., Alfieri, J.G., McKee, L., et al., 2016. Monitoring daily evapotranspiration over two California vineyards using Landsat 8 in a multi-sensor data fusion approach. *Remote Sens. Environ.* 185, 155–170.
- Senay, G.B., Friedrichs, M.K., Singh, R.K., Velpuri, N.M., 2016. Evaluating landsat 8 evapotranspiration for water use mapping in the Colorado river basin. *Remote Sens. Environ.* 185, 171–185.
- Serbin, S.P., Singh, A., McNeil, B.E., Kingdon, C.C., Townsend, P.A., 2014. Spectroscopic determination of leaf morphological and biochemical traits for northern temperate and boreal tree species. *Ecol. Appl.* 24 (7), 1651–1669.
- Skofronick-Jackson, G., Petersen, W.A., Berg, W., Kidd, C., Stocker, E.F., Kirschbaum, D.B., et al., 2017. The global precipitation measurement (GPM) mission for science and society. *Bull. Am. Meteorol. Soc.* 98 (8), 1679–1695.
- Smith, E.A., Asrar, G., Furuhashi, Y., Ginati, A., Mugnai, A., Nakamura, K., et al., 2007. International global precipitation measurement (GPM) program and mission: an overview. In *Measuring Precipitation From Space*. Springer, Dordrecht, pp. 611–653.
- Su, Z., 2002. The Surface Energy Balance System (SEBS) for estimation of turbulent heat fluxes. *Hydrol. Earth Syst. Sci.* 6 (1), 85–100.

- Tomita, H., Hihara, T., Kubota, M., 2018. Improved satellite estimation of near-surface humidity using vertical water vapor profile information. *Geophys. Res. Lett.* 45 (2), 899–906.
- Valente, F., David, J.S., Gash, J.H.C., 1997. Modelling interception loss for two sparse eucalypt and pine forests in central portugal using reformulated rutter and gash analytical models. *J. Hydrol.* 190 (1–2), 141–162.
- Wei, Z., Yoshimura, K., Wang, L., Miralles, D.G., Jasechko, S., Lee, X., 2017. Revisiting the contribution of transpiration to global terrestrial evapotranspiration. *Geophys. Res. Lett.* 44 (6), 2792–2801.
- Wolfé, G.M., Kawa, S.R., Hanisco, T.F., Hannun, R.A., Newman, P.A., Swanson, A., et al., 2018. The NASA Carbon Airborne Flux Experiment (CARAFE): instrumentation and methodology. *Atmosph. Measurement Tech.* 11 (3), 1757.
- Yang, Y., Anderson, M.C., Gao, F., Hain, C.R., Semmens, K.A., Kustas, W.P., et al., 2017. Daily landsat-scale evapotranspiration estimation over a forested landscape in North Carolina, USA, using multi-satellite data fusion. *Hydrol. Earth Syst. Sci.* 21 (2), 1017–1037.
- Yilmaz, M.T., Anderson, M.C., Zaitchik, B., Hain, C.R., Crow, W.T., Ozdogan, M., et al., 2014. Comparison of prognostic and diagnostic surface flux modeling approaches over the Nile River basin. *Water Resour. Res.* 50 (1), 386–408.
- Zhang, Y., Peña-Arancibia, J.L., McVicar, T.R., Chiew, F.H.S., Vaze, J., Liu, C., et al., 2016. Multi-decadal trends in global terrestrial evapotranspiration and its components. *Sci. rep.* 6, 19124.

EXHIBIT 12



Use of remote sensing for evapotranspiration monitoring over land surfaces

W. P. KUSTAS & J. M. NORMAN

To cite this article: W. P. KUSTAS & J. M. NORMAN (1996) Use of remote sensing for evapotranspiration monitoring over land surfaces, Hydrological Sciences Journal, 41:4, 495-516, DOI: [10.1080/02626669609491522](https://doi.org/10.1080/02626669609491522)

To link to this article: <https://doi.org/10.1080/02626669609491522>



Published online: 24 Dec 2009.



Submit your article to this journal [↗](#)



Article views: 5798



View related articles [↗](#)



Citing articles: 48 View citing articles [↗](#)

Use of remote sensing for evapotranspiration monitoring over land surfaces

W. P. KUSTAS

USDA Agricultural Research Service, Hydrology Laboratory, Beltsville, Maryland 20750, USA

J. M. NORMAN

Department of Soil Science, University of Wisconsin, Madison, Wisconsin 53706, USA

Abstract Monitoring evapotranspiration (ET) at large scales is important for assessing climate and anthropogenic effects on natural and agricultural ecosystems. This paper describes techniques used in evaluating ET with remote sensing, which is the only technology that can efficiently and economically provide regional and global coverage. Some of the empirical/statistical techniques have been used operationally with satellite data for computing daily ET at regional scales. The more complex numerical simulation models require detailed input parameters that may limit their application to regions containing a large database of soils and vegetation properties. Current efforts are being directed towards simplifying the parameter requirements of these models. Essentially all energy balance models rely on an estimate of the available energy (net radiation less soil heat flux). Net radiation is not easily determined from space, although progress is being made. Simplified approaches for estimating soil heat flux appear promising for operational applications. In addition, most ET models utilize remote sensing data in the shortwave and thermal wavelengths to measure key boundary conditions. Differences between the radiometric surface temperature and aerodynamic temperature can be significant and progress in incorporating this effect is evident. Atmospheric effects on optical data are significant, and optical sensors cannot see through clouds. This has led some to use microwave observations as a surrogate for optical data to provide estimates of surface moisture and surface temperature; preliminary results are encouraging. The approaches that appear most promising use surface temperature and vegetation indices or a time rate of change in surface temperature coupled to an atmospheric boundary layer model. For many of these models, differences with ET observations can be as low as 20% from hourly to daily time scales, approaching the level of uncertainty in the measurement of ET and contradicting some recent pessimistic conclusions concerning the utility of remotely sensed radiometric surface temperature for determining the surface energy balance.

Utilisation de la télédétection pour le suivi de l'évapotranspiration sur les terres

Résumé Le suivi à grande échelle de l'évapotranspiration (ET) est important pour évaluer l'impact des effets climatiques et anthropiques sur les écosystèmes naturels ou agricoles. Cet article décrit les techniques

utilisées pour estimer l'ET grâce à la télédétection, qui est la seule technologie permettant de fournir une couverture régionale ou planétaire de façon efficace et économique. Certaines méthodes empiriques et/ou statistiques utilisant des données satellitaires ont été utilisées opérationnellement pour estimer l'ET quotidienne à l'échelle régionale. Les modèles de simulation numérique les plus complexes exigent l'introduction de paramètres détaillés qui peut limiter leur application aux régions pour lesquelles existe une importante base de données concernant les sols et la végétation. Les efforts actuels tendent à limiter les exigences en termes de paramètres de ces modèles. Fondamentalement, tous les modèles de bilan d'énergie s'appuient sur une estimation de l'énergie disponible (différence entre la radiation nette et le flux de chaleur dans le sol). Il n'est pas facile de mesurer la radiation nette à partir de l'espace, bien que des progrès aient été enregistrés. Des méthodes simplifiées d'estimation du flux de chaleur dans le sol semblent prometteuses pour les applications opérationnelles. De plus la plupart des modèles d'ET utilisent la télédétection dans la gamme des courtes longueurs d'onde et du rayonnement thermique pour mesurer les conditions aux limites les plus importantes. Les différences entre la température radiométrique de surface et la température aérodynamique peuvent être significatives et le gain à attendre de la prise en compte de cet effet est évident. Les effets de l'atmosphère sur les données optiques sont importants, et les capteurs optiques ne peuvent pas voir à travers les nuages. Ceci a conduit certains chercheurs à utiliser des observations dans la gamme des micro-ondes comme substitut aux données optiques afin de fournir des estimations de l'humidité des sols et de la température de surface; les résultats préliminaires sont encourageants. Les approches apparaissant comme les plus prometteuses consistent à utiliser la température de surface et des indices de végétation ou le taux de variation de la température de surface au cours du temps couplés à un modèle de couche limite atmosphérique. Pour beaucoup de ces modèles les différences entre le calcul et l'ET observée peuvent descendre à 20 % pour des échelles de temps allant de l'heure à la journée, qui sont de l'ordre de grandeur de l'incertitude sur la mesure de l'ET, ce qui contredit certains jugements pessimistes récents mettant en cause l'utilité de la mesure de la température radiométrique de surface par télédétection pour estimer le bilan d'énergie de surface.

INTRODUCTION

Monitoring evapotranspiration (ET) has important implications in modelling regional and global climate and the hydrological cycle as well as assessing environmental stress on natural and agricultural ecosystems. Results from climate models indicate that changes in available moisture released to the atmosphere can have significant feedback effects on cloud formation, which in turn greatly impacts the radiation budget and precipitation fields at global and continental scales (Wetherald & Manabe, 1988; Sato *et al.*, 1989). At the regional and mesoscale, modelling studies and observations indicate that the amount of ET or latent heat flux (LE) vs sensible heat flux (H) can affect atmospheric motions influencing local and regional weather via temperature and moisture advection and cloud formation (Rabin *et al.*, 1990; Segal & Arritt, 1992). While changes in precipitation have an obvious and direct impact on the hydrological budget, the antecedent soil moisture condition, which is largely

determined by the antecedent ET, can play a significant role in the amount of runoff at the watershed scale (Loague & Freeze, 1985). For many land surfaces, even those containing sparse vegetation cover, ET rates are closely related to the need of plants to assimilate carbon for their maintenance and growth (Montieth, 1988). As a result, significant deviation from a potential or optimal ET rate for different vegetated surfaces has been related to plant stress indicators, which in turn have been related to vegetation temperatures (Jackson, 1981).

Surface temperature describes the state of the surface and the partitioning of the available energy (the net radiation less the soil heat flux) into H and LE . Satellite remote sensing is the only technology that can provide radiometric surface temperature observations in a globally consistent and economically feasible manner. This has led to international research efforts using remotely sensed surface temperature and data in other wavelengths for quantifying ET (Sellers *et al.*, 1990). The use of optical data (i.e. wavelengths in the visible to thermal bands) requires cloud free conditions and correction for atmospheric effects. Remote sensing measurements in the microwave region can provide information about the surface through clouds and are not significantly affected by the atmosphere. These are certainly advantages since at any time 50% of the Earth's surface is cloud covered. Furthermore, a significant relationship appears to exist between passive microwave observations and surface temperature (MacFarland *et al.*, 1990), but to the authors' knowledge no attempts have been made to use a microwave-derived surface temperature for computing ET. In addition, the spatial resolution of passive microwave sensor data are one to two orders of magnitude larger (i.e. 10^1 to 10^2 km) than that which is available operationally from infrared sensors. Hence the application of passive microwave data for estimating ET may be restricted to regional and global scales. On the other hand, active microwave or radar observations have higher resolution (i.e. of the order of 10^1 m), but the backscatter is strongly affected by soil roughness, topography and canopy architecture, which makes it more difficult to extract surface soil moisture (Engman, 1991).

All the wavebands being used by satellite-based instruments are affected by multiple features of the landscape. Thus a remotely sensed signal is not uniquely related to a single surface property, and semi-empirical algorithms are required to convert the observed radiances into physical quantities useful in surface energy balance modelling. While satellite remote sensing can provide information critically needed for quantifying ET from field to global scales at acceptable temporal resolutions, the nonuniqueness in relating the observed radiances to landscape features makes it difficult to apply remote sensing techniques to different surfaces without ground truth data. As a result, major efforts in modelling and observational studies to derive useful algorithms for making the conversions to physical quantities in different climatic regions have been recently undertaken or completed (Kustas, 1995; Sellers *et al.*, 1995).

The techniques discussed in this paper, which are based on the use of remote sensing data, evaluate ET at an hourly to daily time frame; this is appropriate for atmospheric, hydrological and agricultural applications. For

climatological applications, several remote sensing methods (empirical in nature) that estimate ET on a monthly and annual basis have been developed (Choudhury, 1991), but are not discussed here. The methods vary in complexity from statistical/semi-empirical approaches to more physically-based analytical approaches and ultimately to numerical models that simulate the flow of heat and water through the soil, vegetation and atmosphere. There will also be a discussion of two methods that are conceptually quite different from the way in which remote sensing data have been traditionally used in predicting ET.

THE SURFACE BOUNDARY CONDITION: THE AVAILABLE ENERGY FOR ET

In computing ET, the surface energy balance equation is the primary boundary condition to be satisfied:

$$R_n + G + H + LE = 0 \quad (1)$$

where R_n is the net radiation, G is the soil heat flux, H is the sensible heat flux and LE is the latent heat flux, all in W m^{-2} . In equation (1), fluxes away from the surface are negative and towards the surface are positive. In this paper, ET will represent the vapour flux converted to mm of water per day (mm day^{-1}). In addition, when describing the magnitudes of the various components in equation (1), daytime conditions will be assumed, which typically means no horizontal advection and hence $R_n > 0$, G , H and $LE < 0$. For many of the approaches, the estimation of the available energy ($R_n + G$) that is partitioned between the turbulent fluxes H and LE has not been given as much attention as in the parameterizations used in predicting the turbulent fluxes. In many cases, R_n is the largest component in equation (1) while G can be from 5 to 50% of R_n depending on vegetation cover and soil moisture conditions (Brutsaert, 1982).

A number of approaches using remote sensing data from the GOES satellites have been developed for estimating the four components of R_n (Sellers *et al.*, 1990), namely:

$$R_n = (1 - \alpha)R_s + (1 - \epsilon_s)R_{ld} - \epsilon_s \sigma T_{sh}^4 \quad (2)$$

where R_s is the incoming shortwave solar radiation, R_{ld} is the incoming longwave radiation, α is the surface shortwave albedo, ϵ_s is the surface emissivity, σ is the Stefan-Boltzman constant ($5.67 \times 10^{-8} \text{ W m}^{-2} \text{ K}^{-4}$), T_{sh} is the hemispherical radiometric temperature as defined by Norman & Becker (1995), so that the quantity $\epsilon_s \sigma T_{sh}^4$ represents the upwelling longwave radiation flux, R_{lu} . The radiometric temperature measured by an infrared radiometer from a spaceborne platform, T_{rad} , is assumed to approximate T_{sh} .

Both R_s and α have been estimated from GOES using empirical/statistical and physically-based models (Pinker *et al.*, 1995). On a daily basis, the estimate of R_s from satellite data has an uncertainty of approximately 10%, but at shorter time scales, for example hourly, the uncertainty may be greater (probably on the

order of 20-30%, on average), especially for partly cloudy conditions (Pinker *et al.*, 1994). Validating R_s at hourly or shorter time scales under partly cloudy skies is especially difficult due to sampling problems associated with the limited-area network of ground-based measurements typically available from field experiments (Pinker *et al.*, 1994).

Satellite estimates of the contribution of the net longwave flux at the surface have been developed using sounding data (Darnell *et al.*, 1992). The Tiros Operational Vertical Sounder (TOVS) of the NOAA satellites contains infrared and microwave sensors that can be used for estimating both R_{ld} and T_{rad} . Other approaches have utilized meteorological data collected at screen level with semi-empirical relationships for estimating R_{ld} , and then use T_{rad} for calculating the upwelling longwave component (Jackson *et al.*, 1987).

Sellers *et al.* (1990) raise the concern that estimating the four components of R_n could lead to error accumulation, especially in estimating the net longwave flux because both R_{ld} and R_{lu} are large components, so the difference would be small and prone to significant uncertainty. This has led some to estimate surface R_n from top of the atmosphere (TOA) R_n (Pinker & Tarpley, 1988). While it has been shown that there is little correlation between surface and TOA net longwave flux (Harshvardhan *et al.*, 1990), there is a strong correlation between R_s and R_n at the surface. This has led to statistical approaches using slowly varying surface properties such as surface albedo and soil moisture with remotely sensed estimates of R_s for estimating R_n (Kustas *et al.*, 1994b). Other techniques use narrow band reflectance data and T_{rad} from aircraft and satellite-based platforms for estimating the upwelling components αR_s and R_{lu} and use meteorological data for estimating the downwelling components R_s and R_{ld} (e.g. Moran *et al.*, 1989; Daughtry *et al.*, 1990). Comparisons with ground-based observations at meteorological time scales (i.e. half-hourly to hourly) indicate that the differences are within the uncertainty in the measurements, namely 5-10%.

The soil heat flux can be solved as a function of the thermal conductivity of the soil and the vertical temperature gradient. This temperature gradient cannot be measured remotely, hence numerical models solve for G by having several soil layers (Campbell, 1985). This requires detailed information about soil properties. Models using routine weather data may provide satisfactory predictions of soil heat flux (e.g. Camillo, 1989). An alternative approach takes G/R_n as a constant under daytime conditions that varies as a function of the amount of vegetation cover or leaf area index (LAI), which can be estimated via remotely sensed vegetation indices, (VI) (Choudhury *et al.*, 1994). Several studies have shown that the value of G/R_n typically ranges between 0.4 for bare soil and 0.05 for full vegetation cover (Choudhury *et al.*, 1987). Observations (Clothier *et al.*, 1986; Kustas *et al.*, 1993a) indicate that a linear relationship between VI and G/R_n exists, although analytically it has been shown that the relationship should be nonlinear (Kustas *et al.*, 1993a).

The applicability of using the ratio G/R_n is somewhat limited due to the temporal variation in the ratio over the daytime and the effects of soil moisture

and soil properties on the G/R_n relationship (Brutsaert, 1982). Comparisons with observations at meteorological time scales suggest these simplified techniques can yield differences of 20-30% (Kustas *et al.*, 1993a).

DETERMINATION OF THE TURBULENT FLUXES H & LE

Atmospheric correction issues

For the approaches using T_{rad} and VIs , accounting for the attenuation of the radiances received by satellite-based sensors is not a trivial matter (Kaufman, 1989; Price, 1989). In correcting thermal-infrared data, whether using radiative transfer models or split-window techniques the uncertainty is 1° to 3°C over land surfaces (Becker & Li, 1990; Perry & Moran, 1994). Model sensitivity to such an uncertainty in T_{rad} can be significant, especially over large vegetation where errors can be $\sim 100\text{ W m}^{-2}$ for hourly to daily time scales (Norman *et al.*, 1995a). However, the 150 W m^{-2} uncertainty in estimating sensible heat flux from radiometric surface temperature observations suggested by Sellers *et al.* (1995) is in many cases two to three times larger than errors reported by many other researchers (Choudhury, 1994).

Empirical/statistical and semi-empirical approaches

These methods have mainly been developed to predict daily ET using instantaneous remote sensing observations and assumptions about the relationship between midday H and LE and $(R_n + G)$. Experimental observations analysed by Hall *et al.* (1992) suggest that the evaporative fraction ($EF = -LE/(R_n + G)$) remains fairly constant over the daytime period. Results using this empirical finding will be discussed later.

One of the most widely applied approaches, using a T_{rad} observation near midday, was pioneered by Jackson *et al.* (1977) whereby they observed that daily differences between ET and R_n could be approximated by the following linear expression:

$$R_{n,d} + LE_d = A + B(T_{rad,i} - T_{a,i}) \quad (3)$$

where the subscripts i and d represent instantaneous and daily values, respectively, A and B are statistical regression coefficients and T_a is the air temperature at screen height (i.e. around 2 m above the surface). A more general form of this expression was proposed by Seguin & Itier (1983) based on theoretical and experimental observations, namely:

$$R_{n,d} + LE_d = B(T_{rad,i} - T_{a,i})^n \quad (4)$$

where B is dependent on surface roughness and the value of n depends on stability ($n = 1$ for stable and 1.5 for unstable conditions). A variant of

equation (4) was introduced by Nieuwenhuis *et al.* (1985) who replaced $T_{a,i}$ and $R_{n,a}$ with a reference canopy temperature ($T_{c,i}$) corresponding to conditions of potential ET ($LE_{d,p}$). The linear form of equation (3) has been verified experimentally and theoretically (Carlson & Buffum, 1989; Lagouarde, 1991). Recently, Carlson *et al.* (1995) used a SVAT model to show that a systematic relationship exists between the B and n parameters in equation (4) and fractional cover, which can be estimated with remotely sensed data. Theoretical and experimental work by Lagouarde & McAneney (1992) resulted in the derivation of an equation for estimating daily sensible heat flux, (H_d) using T_{rad} measured around the time of the NOAA-AVHRR overpass (1400 local standard time) and maximum T_a . The equation is similar in form to Dalton's evaporation equation (see Brutsaert, 1982) and requires the determination of two empirical parameters relating instantaneous to daytime average values of wind speed and surface-air temperature differences. On a daily basis the above techniques appear to have an uncertainty of ± 1 mm day⁻¹ or 20-30%.

The approaches described above attempt to extrapolate "instantaneous" remote sensing observations of the derived fluxes to daily totals which are required for many hydrological and agricultural applications. Interest in daily fluxes led Jackson *et al.* (1983) to develop a procedure using the assumption that the temporal trend in LE would follow the course of solar radiation during the daylight period. They showed that for a clear day the ratio of daily to midday R_s (R_{sm}) could be approximated by an analytical expression:

$$R_{sd}/R_{sm} = 2N/[\pi \sin(\pi t/N)] \quad (5)$$

where N is the day length in hours, and t is the time starting at sunrise. Several studies have shown this technique can yield satisfactory estimates of ET (Brutsaert & Sugita, 1992).

With the assumption that EF remains nearly constant over the daytime period, an instantaneous estimate of the fluxes and hence EF from a remote sensing observation would have the potential to provide daily ET as long as one can estimate the daytime average available energy ($R_n + G$). Several studies have found this technique can give reasonable results with differences in daily ET of less than 1 mm day⁻¹ (Sugita & Brutsaert, 1991; Brutsaert & Sugita, 1992; Hall *et al.*, 1992; Kustas *et al.*, 1994a). The estimates of daily ET from either using equation (5) or assuming EF is constant, however, should be adjusted for the contribution of nighttime LE . Nighttime ET can be anywhere from 10% to 30% of the daily total (Owe & van de Griend, 1990). This percentage of the daily total will largely depend upon the climate and season. For temperate climates in the summer, 10-20% of the daily total is probably typical (Brutsaert & Sugita, 1992).

Recently, Zhang & Lemeur (1995) examined the underlying assumptions of both equation (5) and of EF being constant using the Penman-Monteith equation, and compared the results with measurements from a mixed agricultural and forested region during HAPEX-MOBILHY (Hydrological Atmospheric Pilot Experiment-Modelization du Bilan Hydrique; see e.g. André *et al.*,

1986) under clear skies. They found that EF is fairly constant for short vegetation, but may not be for forests. Furthermore, the midday values of EF tended to be smaller than the daytime average and the daytime total available energy is required to use this method. Therefore they felt that the Jackson *et al.* (1983) approach was more suitable since it required only one instantaneous estimate of LE and equation (5) to compute daily ET. However, equation (5) will only be suitable for clear day conditions whereas Sugita & Brutsaert (1991) and Kustas *et al.* (1994a) found that EF was reasonably constant under a wider variety of conditions.

Physically-based analytical approaches

Price (1980) proposed a model for obtaining daily-integrated fluxes directly by integrating equation (1) over a 24 hour period with some simplifying assumptions. The result is an analytical expression for computing daily ET. It requires as primary input a 24 hour max-min difference in T_{rad} and daily average climate data obtained by routine weather station observations (i.e. wind speed, air temperature and vapour pressure). This model readily lends itself to the NOAA-AVHRR series of satellites which provide day-night pairs of radiometric surface temperature. Further refinements to the technique were made by Price (1982) resulting in a prognostic model that appears to give appropriate ET values when compared to local estimates using standard meteorological and pan evaporation data. However, the amplitude of the max-min difference in T_{rad} is affected by more than surface soil moisture when vegetation is present and therefore it is less directly coupled to the relative magnitude of ET (Norman *et al.*, 1995a).

Other methods generally compute LE by evaluating R_n , G and H and solving for LE by residual in equation (1). At least one radiometric surface temperature observation is required. Unfortunately, most of these approaches that are described below provide only an "instantaneous" estimate of the fluxes because these models require T_{rad} , which means that only one estimate of LE can be computed during the daytime except when using T_{rad} observations from satellites such as GOES or METEOSAT.

With R_n and G estimated by the remote sensing methods described earlier, sensible heat flux is normally computed using the following expression:

$$H = \frac{-\rho C_p (T_{aero} - T_a)}{r_H} \quad (6)$$

where ρ is the air density, C_p is the specific heat of air at constant pressure, r_H is the resistance to heat transfer, T_{aero} is the surface aerodynamic temperature (Norman & Becker, 1995) and T_a is the air temperature either measured at screen height or the potential temperature in the mixed layer (Brutsaert & Sugita, 1991; Brutsaert *et al.*, 1993). The resistance to heat transfer is affected by windspeed, atmospheric stability and surface roughness (Brutsaert, 1982).

Since T_{aero} cannot be measured by remote sensing, it is usually replaced by T_{rad} . For uniform canopy cover, the difference between T_{aero} and T_{rad} is typically less than 2°C (Choudhury *et al.*, 1986; Huband & Monteith, 1986), but for partial vegetation cover the differences can reach 10°C (Kustas, 1990). This has forced many investigators to adjust r_H via empirical methods related to the scalar roughness for heat (Kustas *et al.*, 1989; Sugita & Brutsaert, 1990; Kohsiek *et al.*, 1993) or use of an additional resistance term (Stewart *et al.*, 1994). However, these adjustments to equation (6) are not generally applicable because they have not been related to physical quantities causing differences between momentum and scalar transport (McNaughton & Van den Hurk, 1995). This is supported by Sun & Mahrt (1995) who analysed T_{rad} observations collected over heterogeneous surfaces and found existing scalar roughness parameterizations for predicting reliable H fluxes with equation (6) were not generally applicable. Fortunately, methods are being developed with single-source (Troufleur *et al.*, 1995) and dual-source models (Norman *et al.*, 1995b; Lhomme *et al.*, 1994) to account for differences between T_{aero} and T_{rad} , and thus avoid the need for empirical adjustments to r_H . A recent study by Zhan *et al.* (1996) compared several different models for computing H with T_{rad} over different ecosystems. They showed that models containing the least empiricism to account for the differences between T_{rad} and T_{aero} gave the best results with differences less than 30%, on average. The model by Norman *et al.* (1995b) generally gave the smallest differences with measured H fluxes. The average difference was around 20%, which is considered the level of uncertainty in eddy correlation and Bowen ratio techniques for determining the surface fluxes in heterogeneous terrain (Nie *et al.*, 1992).

Another approach to solve this problem relates to performing detailed simulations using microclimate and radiative transfer models that can predict the relationship between T_{rad} and T_{aero} as a function of surface conditions such as vegetation cover or leaf area index and surface soil moisture, and solar zenith and azimuth angles (Prévot *et al.*, 1994). Some preliminary results from the simulations indicate that leaf area index is a major factor in determining the order of magnitude of the scalar roughness needed in equation (6) if T_{aero} is replaced by T_{rad} . A similar result using a Lagrangian approach was obtained by McNaughton & Van den Hurk (1995) who represented the difference between momentum and scalar transport using an excess resistance term. Further research with these approaches should be encouraged.

Numerical models

A significant number of numerical models has been developed over the past decade to simulate surface energy flux exchanges using remote sensing data (usually observations of T_{rad}) for updating the model parameters (Camillo *et al.*, 1983; Carlson *et al.*, 1981; Soer, 1980; Taconet *et al.*, 1986). The advantage of these approaches is that the temporal trace of the fluxes can be

simulated and periodically updated with the remote sensing data. Taconet *et al.* (1986) show the feasibility of using this approach with AVHRR data and more recently included the geostationary satellite data (METEOSAT) to increase the stability of the model inversion and atmospheric correction to the satellite observations (Taconet & Vidal-Madjar, 1988).

Unfortunately, these models require many input parameters related to soil and vegetation properties not readily available at regional scales. This need for a reduction in the number of parameters for operational purposes has prompted some to simplify numerical models in order that remote sensing could potentially be used to estimate most of them (Bougeault *et al.*, 1991). An extreme example of this is given by Brunet *et al.* (1991) who use an atmospheric boundary layer (ABL) model to calculate regional scale energy fluxes with a Penman-Montieth equation for parameterizing the energy transport across the soil-vegetation-atmosphere interface. The surface resistance is the main adjustable parameter, and is adjusted in order for the model to match the early afternoon infrared surface temperature observation from the NOAA-AVHRR satellite. Preliminary tests using observations under different moisture and crop conditions and surface temperatures from ground-based stations indicate the model adequately simulates the temporal trace and magnitudes of both the energy fluxes and surface temperature.

Numerical models have several advantages over the statistical/semi-empirical and analytical approaches. First, they typically contain more of the physics of energy transport in the soil-vegetation-atmosphere system. Second, with initial and boundary conditions, they can simulate the energy fluxes continuously. Yet many still require continuous weather data such as wind speed, air temperature and vapour pressure, or in the case of atmospheric models which can simulate the near-surface weather, they require radiation data. In practice, few of these models can be used at regional scales with remote sensing data because of the amount of vegetation and soils information required to evaluate the necessary parameters. Attempts at bridging this gap between having a physically-based robust model simulating the energy fluxes and remote sensing providing necessary information for determining key surface parameters in an operational mode have been successful to some degree (Sellers *et al.*, 1992; Crosson *et al.*, 1993). Two such approaches which appear to have great potential for estimating ET operationally are discussed below in some detail.

ALTERNATIVE APPROACHES IN USING REMOTE SENSING FOR ESTIMATING ET

Exploiting the VI/T_{rad} relationship

Numerous studies have found a significant negative correlation between $NDVI$ and T_{rad} over different surfaces (Goward *et al.*, 1985; Hope & McDowell, 1992; Nemani & Running, 1989; Nemani *et al.*, 1993). They suggest that this

relationship is related to the amount of available energy partitioned into LE which is driven by variation in transpiration or evaporative cooling. Hope *et al.* (1986) show theoretically that with VI and T_{rad} one can extract canopy resistance. However, this assumes complete canopy cover which does not usually exist in most natural ecosystems.

Nemani & Running (1989) used an ecological model for forested ecosystems and observed a nonlinear relationship between the slope of the $NDVI-T_{rad}$ curve and the canopy resistance. Goward & Hope (1989) also proposed that the slope was a measure of the surface resistance. These approaches will be difficult to apply to most landscapes with partial canopy cover since variabilities in fractional cover and surface soil moisture cause significant scatter in the VI/T_{rad} relationship. Furthermore, studies suggest that the relationship between surface resistance and the $NDVI/T_{rad}$ slope will vary significantly with vegetation type. Nemani *et al.* (1993) showed that the $NDVI/T_{rad}$ slope responded to changes in water status of forested areas, but not of grasslands. The variability in slope for grasslands appeared to be mainly caused by variation in fractional cover rather than in ET. Smith & Choudhury (1991) used a coupled dual-source soil-vegetation model to show that the $NDVI/T_{rad}$ slope largely depended on whether the drying soil surface is the source of the decline in ET or whether it is the vegetation. They also observed that the linear relationship between $NDVI$ and T_{rad} did not exist for forests but only for agricultural and native pastures.

Others have used an energy balance model for computing spatially distributed fluxes from the variability within the $NDVI/T_{rad}$ plot from a single scene (Price, 1990). Price (1990) used $NDVI$ to estimate the fraction of a pixel covered by vegetation. From the $NDVI/T_{rad}$ plot Price (1990) showed how one could derive bare soil and vegetation temperatures and, with enough spatial variation in surface moisture, estimate daily ET for the limits of full cover vegetation, dry and wet bare soils.

Following Price (1990), Carlson *et al.* (1990; 1994) combined an ABL model with a SVAT for mapping surface soil moisture, vegetation cover and surface fluxes. Model simulations are run for two conditions: 100% vegetative cover with the maximum $NDVI$ being known *a priori*, and with bare soil conditions knowing the minimum $NDVI$. Using ancillary data (including a morning sounding, vegetation and soil type information) root-zone and surface soil moisture are varied, respectively, until the modeled and measured T_{rad} are closely matched for both cases so that fractional vegetated cover and surface soil moisture are derived. Further refinements to this technique have been developed by Gillies & Carlson (1995) for potential incorporation into climate models. Comparisons between modelled-derived fluxes and observations have been made recently by Gillies *et al.* (1996) using high resolution aircraft-based remote sensing measurements from a grassland ecosystem during FIFE (First ISLSCP Field Experiment; see e.g. Sellers *et al.*, 1988) and from a semiarid rangeland ecosystem during Monsoon '90 (Kustas & Goodrich, 1994). Approximately 90% of the variance in the fluxes were captured by the model.

In a related approach, Moran *et al.* (1994) define theoretical boundaries in the $SAVI/(T_{rad} - T_a)$ two-dimensional space using the Penman-Monteith equation, where $SAVI$ is the soil-adjusted vegetation index proposed by Huete (1988). The boundaries define a trapezoid, which has at the upper two corners unstressed and stressed 100% vegetated cover and at the lower two corners, wet and dry bare soil conditions. In order to calculate the vertices of the trapezoid, measurements of R_n , vapour pressure, T_a , and wind speed are required as well as vegetation specific parameters; these include maximum and minimum $SAVI$ for the full cover and bare soil case, maximum leaf area index, and maximum and minimum stomatal resistance. Moran *et al.* (1994) analyse and discuss several of the assumptions underlying the model, especially those concerning the linearity between variations in canopy-air temperature and soil-air temperatures and transpiration and evaporation. Information about ET rates is derived from the location of the $SAVI/(T_{rad} - T_a)$ measurements within the date and time-specific trapezoid. This approach permits the technique to be used for both heterogeneous and uniform areas and thus does not require having a range of $NDVI$ and surface temperature in the scene of interest as required by Carlson *et al.* (1990) and Price (1990). Moran *et al.* (1994) have compared the method for estimating relative rates of ET with observations over agricultural fields and showed it could be used for irrigation scheduling purposes. More recently, Moran *et al.* (1995) have shown the technique has potential for computing ET over natural grassland ecosystems.

Humes *et al.* (1995) have shown that the relationship between $NDVI$ and T_{rad} for a semiarid rangeland landscape can show some of the same features seen over other surfaces when the data are acquired at extremely high resolution or small pixel size. Yet, at the resolution of satellite-based sensors, they show that the range of variability in $NDVI$ and T_{rad} can be significantly reduced making it more difficult to use $NDVI/T_{rad}$ approaches. Gillies & Carlson (1995), however, were able to use their approach with 1 km pixel data from the NOAA-AVHRR satellites. A significant correlation at regional scales between $NDVI$ and temporal changes in surface temperature was obtained by Diak *et al.* (1995) using NOAA-AVHRR and GOES (8 km resolution) data; but this correlation strongly depended on whether areas with predominately low $NDVI$ s or vegetation cover were included in the domain. Friedl & Davis (1994) used high resolution aircraft data from FIFE, similar to the type used by Gillies *et al.* (1995), and helicopter data with a soil-canopy-sensor model to interpret properly observed patterns in T_{rad} . They found that a significant amount of the variance in $NDVI$ and T_{rad} was related to landcover type, and more importantly that there was no observed relationship between the amount of vegetation cover and surface fluxes. Values of T_{rad} calculated using the soil-canopy-sensor model showed that the relationship between soil background temperature and variability in fractional vegetative cover is the dominant factor, not the energy flux partitioning between H and LE , causing the negative correlation between T_{rad} and $NDVI$. However, Friedl & Davis (1994) point out that this last result is dependent on the scale of the analysis. They indicate that for a much coarser resolution and for a much larger

satellite scene, as shown by Price (1990) using AVHRR data over the Great Plains of North America, variations in $NDVI$ and T_{rad} reflect agricultural practices and synoptic weather patterns (rainfall) rather than natural variability in canopy cover. Their main conclusion is that an invertible energy balance model using remotely sensed surface temperature must account for the effects of landcover type, soil moisture and soil background temperature effects on radiometric observations to obtain reliable ET estimates.

Time rate of change of T_{rad}

An important conceptual step in improving the procedure for estimating soil moisture and the surface energy balance came with the idea of using the time rate of change of T_{rad} from a geostationary satellite such as GOES with an atmospheric boundary layer model (Wetzel *et al.*, 1984). By using time rate of change of T_{rad} , one reduces the need for absolute accuracy in satellite sensing and atmospheric corrections, both major challenges. Diak (1990) improved this approach further with a method for partitioning the available energy ($R_n + G$) into H and LE by using the rate of rise of T_{rad} from the GOES satellite and ABL rise from the 1200 Greenwich Mean Time (GMT) synoptic sounding to the 0000 GMT sounding. The model is initialized with the 1200 GMT sounding of temperature, humidity and wind speed. Then the surface Bowen ratio (i.e. the ratio of the turbulent fluxes H/LE) and the "effective" surface roughness are varied until the predicted 12 hour rise in ABL height and T_{rad} match the observations. This "effective" surface roughness combines the effects of the surface aerodynamic roughness, viewing angle and fractional vegetative cover. Estimates of surface albedo and emissivity are required by the model.

Diak & Whipple (1993) further refined the model by including a procedure to account for the effects of horizontal and vertical temperature advection and vertical motions above the ABL. Sensitivity of the model to the determination of the surface energy balance and to the "effective" roughness was performed with a case study using data from the Midwest and Great Plains areas in the Continental USA. They also verified their model estimates of the surface energy balance with measurements from the FIFE site for two days. The model-derived ET values were within 10% of the measurements suggesting this technique may provide reliable ET estimates at regional scales. Additional comparisons of 12 hour averages of sensible heat flux with FIFE observations support the utility of their model (see Fig. 2 from Diak *et al.*, 1995). They also found that temperature advection usually does not significantly impact the surface energy balance estimates given by the model on a daily basis, although for areas which are routinely affected by advection the biasing could impact longer term averages of ET (i.e. at climate time scales).

In a related approach, Anderson *et al.* (1996) recently developed and tested a two-source surface energy balance model requiring measurements of the time rate of change of surface temperature and an early morning ABL

sounding. With this model, many of the problems associated with the use of radiometric surface temperature are avoided. The model accommodates the first order dependence of the radiometric surface temperature on view angle, avoids the need for atmospheric corrections and precise emissivity evaluation, and does not require *in situ* measurements of air temperature. The performance of the model was evaluated with experimental data from FIFE and Monsoon '90. The model yielded uncertainties in flux estimates comparable to models needing *in situ* air temperature observations and were comparable to the uncertainties in surface energy flux measurements.

Recognizing the fact that using T_{rad} requires detailed information on the characteristics of the surface and the structure of the overlying atmosphere, which is often incomplete for many regions, Diak *et al.* (1994) proposed a method that employs the High Resolution Interferometer-Sounder (HIS) for estimating the turbulent heat fluxes, H and LE . The premise is that the temporal changes in the radiances observed by HIS implicitly measure changes in the lower atmosphere, which are a measure of the absolute amount of energy added to the ABL. The HIS radiance changes were described by coefficients obtained by an eigenvalue decomposition procedure. These coefficients were in turn related to various components of the surface energy balance equation using multiple linear regression. Diak *et al.* (1994) provide convincing evidence that this method responds to temperature changes in the lower atmosphere as well as surface temperature changes. Consequently, this technique is equivalent to the method of Diak (1990), but without requiring any ancillary data, just two remote radiance measurements. However, even when HIS becomes operational, co-located flux measurements will be required to establish a data base to use the HIS technique. One possible solution is to identify sites that have sufficiently detailed surface information to permit some of the other techniques described above to be used to calibrate this procedure. In any event, the HIS technique offers tremendous potential since it can evaluate the surface energy balance relying only on remotely sensed data.

Techniques using microwave remote sensing

While most of these approaches use optical remote sensing, work should continue on trying to use microwave data for estimating T_{rad} (Njoku, 1994) and other important surface parameters because these data are not significantly affected by atmospheric attenuation and clouds. The possibility also exists for using relatively simple models with microwave data for computing the contribution of soil evaporation to daily ET (Kustas *et al.*, 1993b; Chanzy & Kustas, 1994). Moreover, compared to thermal-infrared observations, passive microwave data at low-frequencies (< 5 GHz) sample different depths in the soil, thereby providing information related to profile soil moisture (Jackson *et al.*, 1995). With active microwave or radar, low-frequency (~ 5 GHz) microwave backscatter data have been used with radiometric surface temperature observations for estimating soil surface and canopy temperatures, which are then used

in a dual-source model for computing the surface fluxes (Troufleau *et al.*, 1994). Preliminary results from field studies using active microwave measurements indicate that high frequency (~ 15 GHz) microwave backscatter is related to the *NDVI* while low-frequency microwave backscatter may be related to the quantity $(T_{rad} - T_a)$ (Moran *et al.*, 1996). These preliminary results with microwave observations indicate that the data can be very useful for interpreting T_{rad} observations over partial vegetation cover and in providing additional information that may improve estimates of input parameters used in ET models (Diak *et al.*, 1995). Nevertheless, the pixel resolution of passive microwave sensors are on the order of 10-100 km and thus may limit their use to regional and global scale applications, while better algorithms are needed to interpret backscatter signals from active microwave data.

SUMMARY

The methods reviewed in this paper for using remote sensing to estimate ET cover a broad range of complexity from empirical/statistical to numerical models simulating the heat and water flow through the soil-vegetation system to the overlying atmosphere. For agricultural and hydrological applications, relatively simple methods using one-time-of-day remote sensing observations for quantifying daily ET have been applied operationally (Seguin *et al.*, 1989; 1991), while the application of SVAT models with remote sensing observations in operational climate and hydrological models are being developed and tested (Ottlé & Vidal-Madjar, 1994; Gillies & Carlson, 1995).

Since the greatest value-added benefit of remote sensing is application at pixel-to-regional scales, this is emphasized in this summary. A series of issues has emerged as important for remote sensing of ET from measurement and modelling studies and theoretical considerations:

1. T_{rad} is not equal to T_{aero} .
2. Most models are sensitive to errors in $(T_{aero} - T_{air})$ and the measurement of T_{air} at the *time* and location of the T_{rad} observation is not typically available.
3. T_{rad} dependence on view angle cannot generally be neglected because differences in vegetation and soil temperatures can be significant depending on soil moisture conditions.
4. Thermal emissivity is only known approximately on the pixel scale.
5. Atmospheric corrections and satellite calibrations contribute significant errors in the measurement of T_{rad} that are not always known adequately.
6. Remote observations are instantaneous, while integrated fluxes are desired on hourly, daily or longer time scales.
7. Satellites with larger pixel sizes (1-4 km) can provide sufficiently frequent observations in time (i.e. GOES), but may have uncertainties related to the averaging over heterogeneous subpixel areas.
8. Continuous (hourly or daily) surface flux estimates are most useful and clouds cause remote observations to be intermittent.

Table 1 A summary of model types used to estimate ET at different temporal and spatial scales with remote sensing (see below for list of symbols)

Model type (model no.)	Main input variables	Main model parameters	Temporal scale of ET estimate	Spatial scale of ET estimate	References
Semi-Empir./Statistical (1)	$T_{rad,i}, T_{a,i}, R_{n,d}$	Z_{om}, B, n	daily	local to regional	Jackson <i>et al.</i> (1977) Segun & Iler (1983) Carlson <i>et al.</i> (1995)
Semi-Empir./Statistical (2)	$T_{rad,i}, u_d, T_{a,d}, e_{a,d}, R_{s,d}$	$T_p, h_c, B', LE_{p,d}$	daily	local to regional	Nieuwenhuis <i>et al.</i> (1985) Thunnissen & Nieuwenhuis (1983)
Phys./Analy. (3)	$T_{rad,i}(d), T_{rad,i}(n), T_{a,d}, u_{a,d}, e_{a,d}$	$\alpha, Z_{om}, \epsilon, M$	daily	regional	Price (1980; 1982)
Phys./Analy. Single-source (4)	$T_{rad,i}, u_i, T_{a,i}, e_{a,i}, R_{s,i}, VIS_i, NIR_i$	Z_{om}, z_{oh}, d_o	instant. to daily	local to regional	Jackson <i>et al.</i> (1987) Moran <i>et al.</i> (1989) Kustas <i>et al.</i> (1994a)
Phys./Analy. Single-source (5)	$\theta_{rad,i}, \theta_{a,i}, U_i, R_{n,i}, G_i$	Z_{om}, Z_{oh}, D_o	instant.	regional	Brutsaert & Sugita (1991) Brutsaert <i>et al.</i> (1993)
Phys./Analy. Dual-source (6)	$T_{rad,i}, T_{a,i}, u_i, R_{n,i}$	$Z_{om}, d_o, h_c, LAI, f_g$	instant.	local	Norman <i>et al.</i> (1995b)
Phys./Analy. (7)	$T_{rad,i}, T_{a,i}, u_i, e_{a,i}, R_{n,i}, G_i, VIS_i, NIR_i$	$Z_{om}, d_o, h_c, LAI, LAI_{max}, SAVI, r_{c, min}/max$	instant. to daily	local to regional	Moran <i>et al.</i> (1994)
Phys./Analy. (8)	$u_i, R_{n,i}, \Delta T_{rad}, \Delta T, \Delta \theta_{a,i}, \Delta z$	$Z_{om}, d_o, h_c, LAI, f_g$	instant. to daily	local to regional	Anderson <i>et al.</i> (1996)
Numerical (9)	$T_{rad,i}, T_{a,i}, u_i, e_{a,i}, R_{s,i}, sm_{s,i}, sm_{g,i}$	$Z_{om}, d_o, h_c, LAI, \lambda, r_c, r_{soil}$	instant. to daily	local	Soer (1980) Camillo <i>et al.</i> (1983)
Numerical (10)	$T_{rad,i}, \theta_{a,i}, sm_{s,i}, sm_{g,i}$	$x_{om}, LAI, h_c, P, r_c, r_{soil}$	instant. to daily	local to regional	Carlson <i>et al.</i> (1981) Taconet <i>et al.</i> (1986)
Numerical (11)	$T_{a,i}, u_i, e_{a,i}, R_{s,i}, sm_{s,i}, sm_{g,i}, VIS_i, NIR_i$	$Z_{om}, h_c, LAI, r_c, r_{soil}, \alpha$	instant. to daily	local to regional	Crosson <i>et al.</i> (1992) Sellers <i>et al.</i> (1992)
Numerical (12)	$T_{rad,i}, \theta_{a,i}, U_i, E_{a,i}, VIS_i, NIR_i$	$Z_{om}, z_{om}, h_c, NDVI, LAI, P, r_c, r_{soil}, \alpha$	instant. to daily	local to regional	Carlson <i>et al.</i> (1994) Gillies & Carlson (1995)

...continued

Table 1 continued

Numerical (13)	$\theta_{rad,i}$ $\theta_{a,i}$ $R_{s,i}$ $R_{L,i}$ $E_{a,i}$	z_{om} z_{oh} r_{surf} γ_θ	instant. to daily	regional	Brunet <i>et al.</i> (1991)
Numerical (14)	$\theta_{a,i}$ U_i $E_{a,i}$ $sm_{g,i}$ $\Delta T_{rad}/\Delta t$	z_{om} $P \propto \epsilon Bio$	instant. to daily	regional	Wetzel <i>et al.</i> (1984)
Numerical (15)	$\theta_{a,i}$ U_i $E_{a,i}$ $\Delta T_{rad}/\Delta t$ $\Delta H_{ABL}/\Delta t$	$\alpha \epsilon$	daily	regional	Diak (1990) Diak & Whipple (1993)
Phys./Stat. (16)	$\Delta \theta_d/\Delta t$	-	daily	regional	Diak <i>et al.</i> (1994)

Subscripts: i = instantaneous; d = daily; min = minimum; and max = maximum.

Abbreviations: Semi-Empir. = Semi-Empirical; Phys./Analy. = Physically based/Analytical; and Phys./Stat. = Physically based/Statistical.

Symbols:

T_{rad}	radiometric surface temperature	B	slope of equation (4) in text
T_p	surface temperature of a surface evaporating at the potential rate	n	exponent of equation (4) in text
T_a	near-surface air temperature	B'	modified slope of equation (4)
(d)	daytime observation at time of maximum surface temperature	M	diurnal heat capacity
(n)	nighttime observation at time of minimum surface temperature	P	thermal inertia
R_n	net radiation	LAI	leaf area index
G	soil heat flux	h_c	canopy height
R_s	incoming solar radiation	Bio	vegetation biomass
R_L	incoming atmospheric long wave radiation	VIS	visible reflectance
u	near-surface wind speed	NIR	near-infrared reflectance
e_a	near-surface vapour pressure	$NDVI$	normalized difference vegetation index
θ_{rad}	potential radiometric surface temperature	$SAVI$	soil adjusted vegetation index
θ_a	potential temperature in the atmospheric boundary layer (ABL)	t	time
U	wind speed in the ABL	f_g	fraction of green vegetation
E_a	vapour pressure/humidity in the ABL	H_{ABL}	height of the ABL
z_{om}, z_{om}^*	roughness length for momentum: local, regional	sm_g	soil moisture in root zone
z_{oh}, z_{oh}^*	roughness length for heat: local, regional	sm_s	near-surface soil moisture
d_{ov}, D_o	displacement height: local, regional	α	shortwave albedo
r_c	canopy resistance	ϵ	surface emissivity
r_{soil}	soil resistance	λ	soil thermal conductivity
r_{surf}	bulk surface resistance	γ_θ	gradient of potential temperature in the inversion layer

Table 1 contains a representative but not exhaustive list of models for using remote observations to estimate ET. Our attempt at characterizing which of the above eight issues each of these models addresses is contained in Table 2. Clearly, none of the models address all the important issues at the present time, but several of the models address the most critical issues (2 and 5) as well as some of the important issues (1, 3, 4 and 6). None of the models explicitly address the issue of subpixel averaging (7). Preliminary studies (Crosson *et al.*, 1993; Sellers *et al.*, 1992) and some in progress using FIFE data suggest that issue 7 may be a significant problem at the 1 km scale but may average out at the 10 km scale (Norman & Divakarla, 1995). None of the current models addresses the issue of continuous surface fluxes even with clouds, but studies are in progress to combine the thermal IR remote sensing approaches discussed in this paper with mesoscale models, synoptic surface observations and microwave observations. If issues 1 - 7 are addressed adequately, issue 8 will not limit remote estimation of regional ET fluxes.

Table 2 List of models from Table 1 and indication whether they address the eight issues identified in the Summary (+ in a column means that at the authors' level of understanding, the model addresses that issue for the value-added application of remote sensing to regional ET estimation; a blank means that the model is not interpreted to address that issue)

Model no./ Issue no.	1	2	3	4	5	6	7	8	9	10	11	12	13	14	15	16
1					+	+	+	+	+	+	+	+				
2					+			+		+		+	+	+	+	+
3						+		+								
4								+						+	+	+
5								+				+		+	+	+
6	+	+	+	+			+	+	+	+	+	+	+	+	+	+
7																
8																

Acknowledgements The authors acknowledge funding support from NASA under grant number NAGW-4138 through the Science Division of the Office of Mission to Planet Earth, and the support of the University of Wisconsin Agricultural Experiment Station. The authors would like to thank Drs T. N. Carlson, J. L. Hatfield and M. S. Moran for their comments on an early version of this manuscript.

REFERENCES

- Anderson, M. C., Norman, J. M., Diak, G. R., Kustas, W. P. & Mecikalski, J. R. (1996) A two-source time-integrated model for estimating surface fluxes from thermal infrared satellite observations. *Remote Sens. Environ.* (Accepted)
- André, J. C., Goutorbe, J. P. & Perrier, A. (1986) HAPEX-MOBILHY: A hydrologic atmospheric experiment for the study of water budget and evaporation flux at the climatic scale. *Bull. Am. Met. Soc.* **67**, 138-144.
- Becker, F. & Li, Z. L. (1990) Towards a local split window method over land surfaces, *Int. J. Remote Sens.* **11**, 369-393.
- Bougeault, P., Noilhan, J., Lacarrere, P. & Mascart, P. (1991) An experiment with an advanced surface parameterization in a mesobeta-scale model. Part I: Implementation. *Mon. Weath. Rev.* **119**, 2358-2373.
- Brunet, Y., Nunez, M. & Lagouarde, J.-P. (1991) A simple method for estimating regional evapotranspiration from infrared surface temperature data. *ISPRS J. Photogram. Remote Sens.* **46**, 311-327.
- Brutsaert, W. (1982) *Evaporation into the Atmosphere*. Reidel, Dordrecht, The Netherlands.
- Brutsaert, W. & Sugita, M. (1991) A bulk similarity approach in the atmospheric boundary layer using radiometric skin temperature to determine regional fluxes. *Boundary-Layer Meteor.* **55**, 1-23.
- Brutsaert, W. & Sugita, M. (1992) Application of self-preservation in the diurnal evolution of the surface energy budget to determine daily evaporation. *J. Geophys. Res.* **97**(D17), 18377-18382.
- Brutsaert, W., Hsu, A. Y. & Schmugge, T. J. (1993) Parameterization of surface heat fluxes above a forest with satellite thermal sensing and boundary layer soundings. *J. Appl. Met.* **32**, 909-917.
- Camillo, P. (1989) Estimating soil surface temperatures from profile temperature and flux measurements. *Soil Sci.* **148**, 233-243.
- Camillo, P. J., Gurney, R. J. & Schmugge, T. J. (1983) A soil and atmospheric boundary layer model for evapotranspiration and soil moisture studies. *Wat. Resour. Res.* **19**, 371-380.
- Campbell, G. S. (1985) *Soil Physics with Basic*. Elsevier, New York, USA.
- Carlson, T. N., Dodd, J. K., Benjamin, S. G. & Cooper, J. N. (1981) Satellite estimation of the surface energy balance, moisture availability and thermal inertial. *J. Appl. Met.* **20**, 67-87.
- Carlson, T. N. & Buffum, M. J. (1989) On estimating total daily evapotranspiration from remote surface measurements. *Remote Sens. Environ.* **29**, 197-207.
- Carlson, T. N., Perry, E. M. & Schmugge, T. J. (1990) Remote estimation of soil moisture availability and fractional vegetation cover for agricultural fields. *Agric. For. Met.* **52**, 45-69.
- Carlson, T. N., Gillies, R. R. & Perry, E. M. (1994) A method to make use of thermal infrared temperature and NDVI measurements to infer soil water content and fractional vegetation cover. *Remote Sens. Rev.* **52**, 45-59.
- Carlson, T. N., Capehart, W. J. & Gillies, R. R. (1995) A new look at the simplified method for remote sensing of daily evapotranspiration. *Remote Sens. Environ.* **54**, 161-167.
- Chanzy, A. & Kustas, W. P. (1994) Evaporation monitoring over land surface using microwave radiometry. In: *ESA/NASA International Workshop*, ed. B. J. Choudhury, Y. H. Kerr, E. G. Njoku & P. Pampaloni, 531-550. VSP, Utrecht, The Netherlands.
- Choudhury, B. J. (1991) Multispectral satellite data in the context of land surface heat balance. *Rev. Geophys.* **29**, 217-236.
- Choudhury, B. J. (1994) Synergism of multispectral satellite observations for estimating regional land surface evaporation. *Remote Sens. Environ.* **49**, 264-274.
- Choudhury, B. J., Reginato, J. R. & Idso, S. B. (1986) An analysis of infrared temperature observations over wheat and calculation of latent heat flux. *Agric. For. Met.* **37**, 75-88.
- Choudhury, B. J., Idso, S. B. & Reginato, J. R. (1987) Analysis of an empirical model for soil heat flux under a growing wheat crop for estimating evaporation by an infrared-temperature based energy balance equation. *Agric. For. Met.* **39**, 283-297.
- Choudhury, B. J., Ahmed, N. U., Idso, S. B., Reginato, R. J. & Daughtry, C. S. T. (1994) Relations between evaporation coefficients and vegetation indices studied by model simulations. *Remote Sens. Environ.* **50**, 1-17.
- Clothier, B. E., Clawson, K. L., Pinter, Jr., P. J., Moran, M. S., Reginato, R. J. & Jackson, R. D. (1986) Estimation of soil heat flux from net radiation during the growth of alfalfa. *Agr. Forest Met.* **37**, 319-329.
- Crosson, W. L., Smith, E. A. & Cooper, H. J. (1993) Estimation of surface heat and moisture fluxes over a prairie grassland. 4: Impact of satellite remote sensing of slow canopy variables on performance of a hybrid biosphere model. *J. Geophys. Res.* **98**(D3), 4979-4999.
- Darnell, W. L., Staylor, W. F., Gupta, S. K., Ritchey, N. A. & Wilber, A. C. (1992) Seasonal variation of surface radiation budget derived from International Satellite Cloud Climatology Project C1 data. *J. Geophys. Res.* **97**(15), 741-760.
- Daughtry, C. S. T., Kustas, W. P., Moran, M. S., Pinter, Jr., P. J., Jackson, R. D., Brown, P. W., Nichols, W. D. & Gay, L. W. (1990) Spectral estimates of net radiation and soil heat flux. *Remote Sens. Environ.* **32**, 111-124.
- Diak, G. R. (1990) Evaluation of heat flux, moisture flux and aerodynamic roughness at the land surface

- from knowledge of the PBL height and satellite-derived skin temperatures. *Agric. For. Met.* **52**, 181-198.
- Diak, G. R. & Whipple, M. A. (1993) Improvements to models and methods for evaluating the land-surface energy balance and "effective" roughness using radiosonde reports and satellite-measured "skin" temperatures. *Agric. For. Met.* **63**, 189-218.
- Diak, G. R., Scheuer, C. J., Whipple, M. S. & Smith, W. L. (1994) Remote sensing of land-surface energy balance using data from the high-resolution interferometer sounder (HIS): A simulation study. *Remote Sens. Environ.* **48**, 106-118.
- Diak, G. R., Rabin, R. M., Gallo, K. P. & Neale, C. M. (1995) Regional-scale comparisons of NDVI, soil moisture indices from surface and microwave data and surface energy budgets evaluated from satellite and in-situ data. *Remote Sens. Rev.* **12**, 355-382.
- Engman, E.T. (1991) Applications of microwave remote sensing of soil moisture for water resources and agriculture. *Remote Sens. Environ.* **35**, 213-226.
- Friedl, M. A. & Davis, F. W. (1994) Sources of variation in radiative surface temperature over a tall grass prairie. *Remote Sens. Environ.* **48**, 1-17.
- Gillies, R. R. & Carlson, T. N. (1995) Thermal remote sensing of surface soil water content with partial vegetation cover for incorporation into climate models. *J. Appl. Met.* **34**, 745-756.
- Gillies, R. R., Cui, J., Carlson, T. N., Kustas, W. P. & Humes, K. S. (1996) Verification of a method for obtaining surface soil water content and energy fluxes from remote measurements of NDVI and surface radiant temperature. *Int. J. Remote Sens.* (In review).
- Goward, S., Cruickshanks, G. D. & Hope, A. (1985) Observed relation between thermal emission and reflected spectral radiance of a complex vegetated landscape. *Remote Sens. Environ.* **18**, 137-146.
- Goward, S. N. & Hope, A. S. (1989) Evapotranspiration from combined reflected solar and emitted terrestrial radiation: Preliminary FIFE results from AVHRR data. *Adv. Space Res.* **9**, 239-249.
- Hall, F. G., Huemmrich, K. F., Geotz, S. J., Sellers, P. J. & Nickerson, J. E. (1992) Satellite remote sensing of surface energy balance: success, failures and unresolved issues in FIFE. *J. Geophys. Res.* **97**(D17), 19061-19090.
- Harshvardhan, Randall, D. A. & Dazlich, D. A. (1990) Relationship between the longwave cloud radiative forcing at the surface and the top of the atmosphere. *J. Clim.* **3**, 1435-1443.
- Hope, A. S., Petzold, D. E., Goward, S. N. & Ragan, R. M. (1986) Simulated relationships between spectral reflectance, thermal emissions, and evapotranspiration of a soybean canopy. *Wat. Resour. Bull.* **22**, 1011-1019.
- Hope, A. S. & McDowell, T. P. (1992) The relationship between surface temperature and a spectral vegetation index of a tallgrass prairie: effects of burning and other landscape controls. *Int. J. Remote Sens.* **13**, 2849-2863.
- Huband, N. D. S. & Monteith, J. L. (1986) Radiative surface temperature and energy balance of a wheat canopy. Part I: Comparison of radiative and aerodynamic canopy temperature. *Boundary-Layer Met.* **36**, 1-17.
- Huete, A. R. (1988) A soil-adjusted vegetation index (SAVI). *Remote Sens. Environ.* **27**, 47-57.
- Humes, K. S., Kustas, W. P. & Schmugge, T. J. (1995) Effects of soil moisture and spatial resolution on the surface temperature/vegetation index relationships for a semiarid watershed. In: *Preprints AMS Conf. on Hydrology*. (Dallas, Texas, USA), 147-151.
- Jackson, R. D. (1981) Canopy temperature and crop water stress. In: *Advances in Irrigation* ed. D. Hillel, Vol 1, 43-85. Academic Press, New York, USA.
- Jackson, R. D., Reginato, R. J. & Idso, S. B. (1977) Wheat canopy temperature: A practical tool for evaluating water requirements. *Wat. Resour. Res.* **13**, 651-656.
- Jackson, R. D., Hatfield, J. L., Reginato, R. J., Idso, S. B. & Pinter, Jr., P. J. (1983) Estimates of daily evapotranspiration from one time of day measurements. *Agr. Water Mgmt.* **7**, 351-362.
- Jackson, R. D., Moran, M. S. Gay, L. W. & Raymond, L. H. (1987) Evaluating evaporation from field crops using airborne radiometry and ground-based meteorological data. *Irrig. Sci.* **8**, 81-90.
- Jackson, T. J., O'Neill P. E., Kustas, W. P., Bennett, E. & Swift, C. T. (1995) Passive microwave observation of diurnal soil moisture at 1.4 and 2.65 Ghz. In: *Proc. 1995 Int. Geoscience and Remote Sensing Symp. IEEE*, Vol. I, 492-494.
- Kaufman, Y. J. (1989) The atmospheric effect on remote sensing and its corrections. In: *Theory and Applications of Optical Remote Sensing*, ed. G. Asrar. Wiley, New York, USA.
- Kohsiek, W., De Bruin, H. A. R., The, H. & van den Hurk, B. (1993) Estimation of the sensible heat flux of semi-arid area using surface radiative temperature measurements. *Boundary-Layer Meteor.* **63**, 213-230.
- Kustas, W. P. (1990) Estimates of evapotranspiration with a one- and two-layer model of heat transfer over partial canopy cover. *J. Appl. Met.* **29**, 704-715.
- Kustas, W. P. (1995) Recent advances associated with large scale field experiments in hydrology. *Rev. of Geophys. Suppl.*, 959-965.
- Kustas, W. P., Choudhury, B. J., Moran, M. S., Reginato, R. J., Jackson, R. D., Gay, L. W. & Weaver, H. L. (1989) Determination of sensible heat flux over sparse canopy using thermal infrared data. *Agric. For. Met.* **44**, 197-216.
- Kustas, W. P., Daughtry, C. S. T. & van Oevelen, P. J. (1993a) Analytical treatment of the relationships between soil heat flux/net radiation ratio and vegetation indices. *Remote Sens. Environ.* **46**, 319-330.
- Kustas, W. P., Schmugge, T. J., Humes, K. S., Jackson, T. J., Parry, R., Weltz, M. A. & Moran, M. S. (1993b) Relationships between evaporative fraction and remotely sensed vegetation index and

- microwave brightness temperature for semiarid rangelands. *J. Appl. Met.* **32**, 1781-1790.
- Kustas, W. P. & Goodrich, D. C. (1994) Preface to Monsoon '90 Special Section. *Wat. Resour. Res.* **30**, 1211-1225.
- Kustas, W. P., Perry, E. M., Doraiswamy, P. C. & Moran, M. S. (1994a) Using satellite remote sensing to extrapolate evapotranspiration estimates in time and space over a semiarid rangeland basin. *Remote Sens. Environ.* **49**, 275-286.
- Kustas, W. P., Pinker, R. T., Schmugge, T. J. & Humes, K. S. (1994b) Daytime net radiation estimated for a semiarid rangeland basin from remotely sensed data. *Agric. For. Met.* **71**, 337-357.
- Lagouarde, J.-P. (1991) Use of NOAA AVHRR data combined with an agrometeorological model for evaporation mapping. *Int. J. Remote Sens.* **12**, 1853-1864.
- Lagouarde, J.-P. & McAneney, K. J. (1992) Daily sensible heat flux estimation from a single measurement of surface temperature and maximum air temperature. *Boundary-Layer Meteor.* **59**, 341-362.
- Lhomme, J.-P., Monteny, B. & Amadou, M. (1994) Estimating sensible heat flux from radiometric temperature over sparse millet. *Agric. For. Met.* **68**, 77-91.
- Loague, K. M. & Freeze, R. A. (1985) A comparison of rainfall runoff modeling techniques on small upland watersheds. *Wat. Resour. Res.* **21**, 229-248.
- MacFarland, M. J., Miller, R. I. & Neale, C. M. U. (1990) Land surface temperature derived from SSM/I passive microwave brightness temperatures. *IEEE Trans. Geosci. Remote Sens.* **28**, 839-845.
- McNaughton, K. G. & Van den Hurk, B. J. J. M. (1995) A 'Lagrangian' revision of the resistors in the two-layer model for calculating the energy budget of a plant canopy. *Boundary-Layer Meteor.* **74**, 262-288.
- Monteith, J. L. (1988) Does transpiration limit the growth of vegetation or vice versa? *J. Hydrol.* **100**, 57-68.
- Moran, M. S., Jackson, R. D., Raymond, L. H., Gay, L. W. & Slater, P. N. (1989) Mapping surface energy balance components by combining LANDSAT Thematic Mapper and ground-based meteorological data. *Remote Sens. Environ.* **30**, 77-87.
- Moran, M. S., Clarke, T. R., Inoue, Y. & Vidal, A. (1994) Estimating crop water deficit using the relation between surface-air temperature and spectral vegetation index. *Remote Sens. Environ.* **49**, 246-263.
- Moran, M. S., Rahman, A. F., Washburne, J. C., Goodrich, D. C., Weltz, M. A. & Kustas, W. P. (1995) Combining Penman-Monteith equation with measurements of surface temperature and reflectance to estimate evaporation rates from semiarid grassland. Accepted *Agric. For. Met.*
- Moran, M. S., Vidal, A., Troufleau, D., Qi, J., Clarke, T. R., Pinter, P. J., Jr., Mitchell, T., Inoue, Y. & Neale, C. M. U. (1996) Combining multifrequency microwave and optical data for farm management. (In preparation).
- Nemani, R. R. & Running, S. W. (1989) Estimation of regional surface resistance to evapotranspiration from NDVI and thermal-IR AVHRR data. *J. Appl. Met.* **28**, 276-284.
- Nemani, R., Pierce, L., Running, S. & Goward, S. (1993) Developing satellite derived estimates of surface moisture status. *J. Appl. Met.* **32**, 548-557.
- Nie, D., Kanemasu, E. T., Fritschen, L. J., Weaver, H. L., Smith, E. A., Verma, S. B., Field, R. T., Kustas, W. P. & Stewart, J. B. (1992) An intercomparison of surface energy flux measurement systems during FIFE 1987. *J. Geophys. Res.* **97**(D17), 18715-18724.
- Nieuwenhuis, G. J. A., Schmidt, E. A. & Tunnissen, H. A. M. (1985) Estimation of regional evapotranspiration of arable crops from thermal infrared images. *Int. J. Remote Sens.* **6**, 1319-1334.
- Njoku, E. (1994) Surface temperature estimation over land using satellite microwave radiometry. In: *ESA/NASA International Workshop*, ed. B. J. Choudhury, Y. H. Kerr, E. G. Njoku & P. Pampaloni, 509-530. VSP, Utrecht, The Netherlands.
- Norman, J.M. & Becker, F. (1995) Terminology in thermal infrared remote sensing of natural surfaces. *Remote Sens. Rev.* **12**, 159-173.
- Norman, J. M. & Divakarla, M. (1995) Scaling carbon, water and energy fluxes from 30 m to 15 km. *Agronomy Abst.*, 22. Amer. Soc. Agronomy, Madison, Wisconsin, USA.
- Norman, J. M., Divakarla, M. & Goel, N. S. (1995a) Algorithms for extracting information from remote thermal-IR observations of the Earth's surface. *Remote Sens. Environ.* **51**, 157-168.
- Norman, J. M., Kustas, W. P. & Humes, K. S. (1995b) A two-source approach for estimating soil and vegetation energy fluxes from observations of directional radiometric surface temperature. *Agric. For. Met.* **77**, 263-293.
- Ottlé, C. & Vidal-Madjar, D. (1994) Assimilation of soil moisture inferred from infrared remote sensing in a hydrological model over the HAPEX-MOBILHY region. *J. Hydrol.* **158**, 241-264.
- Owe, M. & van de Griend, A. A. (1990) Daily surface moisture model for large area semiarid land application with limited climate data. *J. Hydrol.* **121**, 119-132.
- Perry, E. M. & Moran, M. S. (1994) An evaluation of atmospheric corrections of radiometric surface temperatures for a semiarid rangeland watershed. *Wat. Resour. Res.* **30**, 1261-1269.
- Pinker, R. T. & Tarpley, J. D. (1988) The relationship between the planetary and surface net radiation: an update. *J. Appl. Met.* **27**, 957-964.
- Pinker, R. T., Kustas, W. P., Laszlo, I., Moran, M. S. & Huete, A. R. (1994) Satellite surface radiation budgets on basin scale in semi-arid regions. *Wat. Resour. Res.* **30**, 1375-1386.
- Pinker, R. T., Frovin, R. & Li, Z. (1995) A review of satellite methods to derive surface shortwave irradiance. *Remote Sens. Environ.* **51**, 108-124.
- Prévoit, L., Brunet, K. T., Paw, U. & Seguin, B. (1994) Canopy modelling for estimating sensible heat flux from thermal infrared measurements. In: *Proc. Workshop on Thermal Remote Sensing of the Energy*

- and Water Balance over Vegetation in Conjunction with Other Sensors, (La Londe Les Maures, France), 17-26.
- Price, J. C. (1980) The potential of remotely sensed thermal infrared data to infer surface soil moisture and evaporation. *Wat. Resour. Res.* **16**, 787-795.
- Price, J. C. (1982) Estimation of regional scale evaporation through analysis of satellite thermal-infrared data. *IEEE Trans. Geosci. Remote Sens.* **GE-20**, 286-292.
- Price, J. C. (1989) Quantitative aspects of remote sensing in the thermal infrared. In: *Theory and Applications of Optical Remote Sensing*, ed. G. Asrar, 578-603. Wiley, New York, USA.
- Price, J. C. (1990) Using spatial context in satellite data to infer regional scale evapotranspiration. *IEEE Trans. Geosci. Remote Sens.* **GE-28**, 940-948.
- Rabin, R. M., Stadler, S., Wetzel, P. J., Stensrud, D. J. & Gregory, M. (1990) Observed effects of landscape variability on convective clouds. *Bull. Amer. Meteor. Soc.* **71**, 272-280.
- Sato, N., Sellers, P. J., Randall, E. K., Schneider, J., Shukla, J., Kinter III, J. L., Hou, Y.-T. & Albertazzi, E. (1989) Effects of implementing the simple biosphere model (Sib) in a general circulation model. *J. Atmos. Sci.* **46**(18), 2757-2782.
- Segal, M. & Arritt, R. W. (1992) Nonclassical mesoscale circulations caused by surface sensible heat-flux gradients. *Bull. Amer. Meteorol. Soc.* **73**, 1593-1604.
- Seguin, B. & Itier, B. (1983) Using midday surface temperature to estimate daily evaporation from satellite thermal IR data. *Int. J. Remote Sens.* **4**, 371-383.
- Seguin, B., Assad, E., Freaud, J. P., Imbernon, J., Kerr, Y. H. & Lagouarde, J. P. (1989) Use of meteorological satellites for rainfall and evaporation monitoring. *Int. J. Remote Sens.* **10**, 847-854.
- Seguin, B., Lagouarde, J.-P. & Saranc, M. (1991) The assessment of regional crop water conditions from meteorological satellite thermal infrared data. *Remote Sens. Environ.* **35**, 141-148.
- Sellers, P. J., Hall, F. G., Asrar, G., Strebel, D. E. & Murphy, R. E. (1988) The first ISLSCP field experiment (FIFE). *Bull. Am. Met. Soc.* **69**, 22-27.
- Sellers, P. J., Rasool, S. I. & Bolle, H.-J. (1990) A review of satellite data algorithms for studies of the land surface. *Bull. Amer. Meteorol. Soc.* **71**, 1429-1447.
- Sellers, P. J., Heiser, M. D. & Hall, F. G. (1992) Relations between surface conductance and spectral vegetation indices at intermediate (100 m² to 15 km²) length scales. *J. Geophys. Res.* **97**(D17), 19033-19059.
- Sellers, P. J., Meeson, B. W., Hall, F. G., Asrar, G., Murphy, R. E., Schiffer, R. A., Bretherton, F. P., Dickinson, R. E., Ellingson, R. G., Field, C. B., Huemmrich, K. F., Justice, C. O., Melack, J. M., Roulet, N. T., Schimel, D. S. & Try, P. D. (1995) Remote sensing of the land surface for studies of global change: Models – algorithms – experiments. *Remote Sens. Environ.* **51**, 1-17.
- Smith, R. C. G. & Choudhury, B. J. (1991) Analysis of normalized difference and surface temperature observations over southeastern Australia. *Int. J. Remote Sens.* **12**, 2021-2044.
- Soer, G. J. R. (1980) Estimation of regional evapotranspiration and soil moisture conditions using remotely sensed crop surface temperatures. *Remote Sens. Environ.* **9**, 27-45.
- Stewart, J. B., Kustas, W. P., Humes, K. S., Nichols, W. D., Moran, M. S. & de Bruin, H. A. R. (1994) Sensible heat flux-radiometric surface temperature relationship for eight semiarid areas. *J. Appl. Met.* **33**, 1110-1117.
- Sugita, M. & Brutsaert, W. (1990) Regional surface fluxes from remotely sensed skin temperature and lower boundary layer measurements. *Wat. Resour. Res.* **26**, 2937-2944.
- Sugita, M. & Brutsaert, W. (1991) Daily evaporation over a region from lower boundary layer profiles. *Wat. Resour. Res.* **27**, 747-752.
- Sun, J. & Mahrt, L. (1995) Determination of surface fluxes from the surface radiative temperature. *J. Atmos. Sci.* **52**, 1096-1106.
- Taconet, O., Carlson, T. Bernard, R. & Vidal-Madjar, D. (1986) Evaluation of a surface/vegetation parameterization using satellite measurements of surface temperature. *J. Clim. Appl. Met.* **25**, 1752-1767.
- Taconet, O. & Vidal-Madjar, D. (1988) Applications of a flux algorithm to a field - satellite campaign over vegetated area. *Remote Sens. Environ.* **26**, 227-239.
- Thunnissen, H. A. M. & Nieuwenhuis, G. J. A. (1990) A simplified method to estimate regional 24-h evapotranspiration from thermal infrared data. *Remote Sens. Environ.* **31**, 211-225.
- Troufleau, D., Vidal, A., Beaudoin, A., Moran, M. S., Weltz, M. A., Goodrich, D. C., Washburn, J. & Rahman, A. F. (1994) Using optical-microwave synergy for estimating surface energy fluxes over semi-arid rangeland. In: *Proc. Physical Measurements and Signatures in Remote Sensing*, (Val d'Isere, France), 1167-1174.
- Troufleau, D., Lhomme, J.-P., Monteny, B. & Vidal, A. (1995) Sensible heat flux and radiometric surface temperature over sparse Sahelian vegetation I: Is the kB⁻¹ a relevant parameter? *J. Hydrol.* (In press).
- Wetherald, R. T. & Manabe, S. (1988) Cloud feedback processes in a general circulation model. *J. Atmos. Sci.* **45**, 1397-1415.
- Wetzel, P. J., Atlas, D. & Woodward, R. (1984) Determining soil moisture from geosynchronous satellite infrared data: A feasibility study. *J. Clim. Appl. Met.* **23**, 375-391.
- Zhan, X., Kustas, W. P. & Humes, K. S. (1995) An intercomparison study on models of sensible heat flux over partial canopy surfaces with remotely sensed surface temperature. *Remote Sens. Environ.* (In press).
- Zhang, L. & Lemeur, R. (1995) Evaluation of daily evapotranspiration estimates from instantaneous measurements. *Agric. For. Met.* **74**, 139-154.

EXHIBIT 13

Eldridge, Melissa

From: Eldridge, Melissa <MEldridge@bhfs.com>

Sent: Wednesday, February 28, 2024 10:00 AM

To: Watermaster@mojavewater.org

Cc: Leland P. McElhaney <lmcelhaney@bmklawplc.com>; rcwagner@wbecorp.com; Hastings, Stephanie <SHastings@bhfs.com>; Carlson, Mack <mcarlson@bhfs.com>

Subject: Agenda Item 7 - Revised Comments on Watermaster's Production Safe Yield Update

On behalf of Golden State Water Company (GSWC), attached are revised comments related to the Mojave Basin Area (Basin) Watermaster's evaluation and update of the Production Safe Yield for each Subarea of the Basin. Please disregard the prior letter.

Melissa A. Eldridge

Legal Practice Assistant

Brownstein Hyatt Farber Schreck, LLP

1021 Anacapa Street, 2nd Floor

Santa Barbara, CA 93101

805.882.1482 tel

MEldridge@bhfs.com

Brownstein - we're all in.

February 28, 2024

Stephanie Osler Hastings
Attorney at Law
805.882.1415 direct
shastings@bhfs.com

VIA EMAIL TO: WATERMASTER@MOJAVEWATER.ORG

Board of Directors
Mojave Basin Area Watermaster
Mojave Water Agency
13846 Conference Center Drive
Apple Valley, CA 92307-4377

RE: Agenda Item 7 - Comments on Watermaster's Production Safe Yield Update (REVISED)

Dear Board of Directors:

On behalf of Golden State Water Company (GSWC), we submit the following revised comments related to the Mojave Basin Area (Basin) Watermaster's evaluation and update of the Production Safe Yield (or PSY) for each Subarea of the Basin.¹ We request that the Watermaster review our comments and consider the attached technical analysis by aquilogic, Inc. (aquilogic) as the Watermaster continues to refine its update of the PSY for each Subarea—specifically Watermaster's estimate of flow across the Transition Zone—and issues its Free Production Allowance for Water Year 2024-25 and Annual Report for 2023-24 required by the Mojave Basin Judgment.

I. Statement of Interest

GSWC, formerly Southern California Water Company and a party to the Judgment, is a division of American States Water Company, a "Class A" utility regulated by the California Public Utilities Commission, provides water service to approximately 260,000 customers throughout California. GSWC's Mountain Desert District operates water systems within three of the Mojave Basin Subareas—Alto, Este, and Centro—and provides water service to 15,275 water service connections and a population of approximately 50,400 in and around the cities and communities of Barstow, Apple Valley, and Lucerne Valley. GSWC has adjudicated Base Annual Production² rights of 1,940 acre-feet per year (AFY) in the Alto Subarea, 178 AFY in the Este Subarea, and 14,407 AFY in the Centro Subarea. Groundwater produced from 29 wells located in these Subareas provides GSWC's sole source of supply for its Mountain Desert District customers. Accordingly, GSWC has a significant interest in

¹ This February 28, 2024 revised comment letter clarifies statements in our prior February 27, 2024 comment letter and supersedes it. The clarifications are in Section V of this letter.

² All capitalized terms not defined herein have the same meaning as set forth in the Judgment.

implementation of the Judgment and management of the Basin, and in particular the sustainability of those Subareas in which GSWC operates—especially in the Centro Subarea.

II. Importance of the Accuracy of the Calculation of PSY

The accuracy of the PSY for each Subarea is critical to implement the Physical Solution imposed by the Judgment. Based on the PSY, Watermaster adjusts the Free Production Allowance (or FPA) for each Subarea. Given the importance of the calculation of PSY and FPA under the Judgment and its corresponding effects on Producers' rights, the Watermaster has the obligation to use the best available records and data, and install, operate, and maintain measurement devices to monitor streamflow and groundwater levels.³

III. Water Levels in the Centro Subarea Continue to Decline

Since entry of the Judgment in 1996, water levels in the Centro Subarea have remained the same or continued to decline, despite Centro Subarea Producers reducing pumping consistent with the FPAs and Alta Subarea Producers purportedly meeting their Minimum Subarea Obligations, as Watermaster has reported in its Annual Reports.⁴ Falling water levels became particularly pronounced beginning in late 2017 near the City of Barstow and Lenwood and Hodge Recharge Sites resulting in water quality impacts to GSWC's Bradshaw Wellfield which consists of eleven active production wells. At the same time, nitrate levels in four of the production wells increased to levels exceeding the Nitrate MCL of 10 mg/l. GSWC was forced to take these wells out of service and to construct a \$5 million dollar nitrate treatment facility to treat and contain the nitrate impacted supply. The on-going operation and maintenance cost of the nitrate system is on the order of \$2 million per year. Nitrate impacts are continuing to expand to additional wells at the Bradshaw Wellfield and expansion of the newly constructed treatment facility may be necessary.

IV. Concern with Accuracy of Watermaster's Estimate of Flow Across the Transition Zone and the Resulting Impact on Watermaster's Calculation of PSY

GSWC has reviewed the Watermaster Engineer's presentation to the Watermaster Board on January 24, 2024 and also the memorandum from Robert C. Wagner regarding the Transition Zone Water Balance memorandum, dated February 28, 2024, and recently posted to the Watermaster website. GSWC is concerned that the Watermaster's calculation of PSY and FPA do not accurately reflect observed conditions in the Centro subarea and that further study is required to ensure adequate and

³ Judgment, ¶¶ 24(e), (w), see also Judgment, Ex. G, ¶ 2(b), 6 (requiring installation of monitoring wells in the Transition Zone and at Subarea boundaries).

⁴ See, e.g., Watermaster, 2021-2022 Twenty-ninth Annual Report, p. 28, Fig. 3-15 (May 1, 2023) available at https://www.mojavewater.org/wp-content/uploads/2023/10/29AR2122_Revised.pdf (acknowledging some seasonal variability in water levels but noting continuing decline in water levels for at least the past 10 years).

sustainable supplies to GSWC's Barstow System. The accuracy of the Watermaster's calculation of flow across the Transition Zone is of critical importance to the Watermaster's calculation of the PSY and FPAs for each Subarea.⁵

V. GSWC Commissioned an Independent Analysis of Flow Across the Transition Zone

In anticipation of the Watermaster's update of the PSY, GSWC asked aquilogic to analyze inflows into the Centro Subarea from the Transition Zone. Aquilogic's analysis, presented in the enclosed memorandum dated February 23, 2024 and titled "Progress Report and Mojave Basin Transition Zone Water Budget" (hereafter, "aquilogic memorandum") concludes that surface water inflow into the Centro Subarea may be overestimated because the Watermaster's assumption that all inflows into the Transition Zone at the Lower Narrows gage, adjusted by an estimated Transition Zone water balance, are equal to inflows into the Centro Subarea is likely incorrect.

The aquilogic memorandum describes the available stream gages along the Mojave River in the vicinity of the Transition Zone. It identifies that Lower Narrows gage provides a long-term dataset at the upstream boundary of the Transition Zone (adjacent to the Alto Subarea), but no similar long-term downstream gage exists at the Transition Zone boundary with the Centro Subarea.⁶ Aquilogic, however, identifies that the Wild Crossing gage historically existed near the Centro Subarea and Transition Zone boundary between March 1966 through October 1970.⁷ The Wild Crossing gage provides the best available data that show the potential change in surface flows in the Mojave River across the Transition Zone by comparing flow rates at the Lower Narrows and Wild Crossing gages.⁸ Based on the data available, surface water flows at the Wild Crossing gage, when operational, were significantly lower than those at the Lower Narrows gage, suggesting that the Mojave River recharges groundwater in the Transition Zone rather than flowing into the Centro Subarea, as Watermaster assumes.⁹

Further, aquilogic identified that the average annual net stream recharge within the Transition Zone between Water Year 1966-1970 was approximately 59,500 AFY.¹⁰ When compared to the Judgment's estimate of 2,000 AFY of Subsurface Flow between the Transition Zone and the Centro Subarea, it is

⁵ The Judgment requires that the Watermaster rely on pertinent hydrologic data and estimates, including the factors and criteria identified in Exhibits C and H of the Judgment, to calculate the PSY and FPAs. (See Judgment, ¶¶ 2(a), 24(o), (w), Exes. C & H.) For example, Exhibit C to the Judgment explains the process to establish the Base Flow and Storm Flow in the Mojave River at the Lower Narrows (Transition Zone boundary with the Alto Subarea) to estimate inflows into the Centro Subarea that inform the calculation of PSY and FPA. (See Judgment, Ex. C, ¶ B(1).)

⁶ The aquilogic memorandum identifies that closest gages to the Centro Subarea and Transition Zone boundary are the Barstow gage and the recently established Hodge/Hinkley gage, which are more than eight miles from the boundary and have significant limitations due to the width of the river channel at these locations. (aquilogic memorandum, p. 2.)

⁷ *Id.* at p. 2.

⁸ *Id.* at p. 3.

⁹ See *id.* at p. 3, Fig. 2.

¹⁰ See *id.* at pp. 3-4, Fig. 3.

unclear without additional analysis what happens to this additional recharge.¹¹ Based on available well information, the aquilologic memorandum finds that it is reasonable to conclude that groundwater pumping within the Transition Zone, along with environmental uses, remove the additional stream recharge from the Transition Zone.¹² In sum, the assumption that Centro Subarea stream inflow equals stream discharge measure at the Lower Narrows gage, adjusted by an estimated Transition Zone water balance, may not be accurate.¹³

The aquilologic memorandum further analysis to estimate the PSY and FPA for the Centro Subarea more accurately, including:

- preparation of a more detailed Transition Zone water budget based on U.S. Geological Survey modeling and other data sources;¹⁴
- expansion of the model domain used for the PSY to include all of the Transition Zone, Centro and Baja Subareas; and
- preparation of a written draft report for stakeholder review and comment prior to submission to the court.¹⁵

Given the impacts of falling water levels in the Centro Subarea on GSWC operations and facilities, coupled with aquilologic's analysis and recommendations presented in the attached memorandum, GSWC believes additional analysis of flow across the Transition Zone is warranted to support implementation of the Judgment.

VI. GSWC Request for Further Analysis of the Transition Zone as Part of the PSY Update

GSWC respectfully requests that the Watermaster consider these comments and the aquilologic memorandum before completing its update of PSY for each Subarea and before issuing its Free Production Allowance for Water Year 2024-25 and Annual Report for 2023-24. In addition, should the recommended analysis show the need for additional subsurface and surface monitoring to evaluate hydrogeologic conditions with the Transition Zone, especially at the Centro Subarea boundary, GSWC asks Watermaster to commit to install, operate, and maintain appropriate monitoring equipment to address data gaps.

¹¹ *Id.* at p. 4; Judgment, Ex. G, ¶ 1(e).

¹² aquilologic memorandum, p. 5.

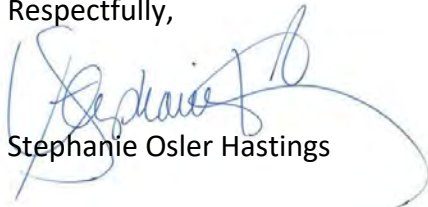
¹³ The aquilologic memorandum also notes that 15,095 AF of treated wastewater was discharged in the Transition Zone downstream of the Lower Narrows gage in Water Year 2022, suggesting that Watermaster's assumptions for the Transition Zone require further review based on current conditions as well. (aquilologic memorandum, p. 5.)

¹⁴ See *id.* at pp. 6-7.

¹⁵ The February 28, 2024 Watermaster memorandum does not appear to include the recommended analyses.

Thank you for your consideration of these comments. GSWC appreciates the Watermaster's commitment to further evaluate Basin conditions as required by and as necessary to implement the Judgment effectively.

Respectfully,

A handwritten signature in blue ink, appearing to read "Stephanie Osler Hastings", is written over a large, light blue circular scribble.

Stephanie Osler Hastings

cc: Leland McElhaney, Brunick, McElhaney & Kennedy
Robert Wagner, Watermaster Engineer

Attached: aquilogic, Inc. memorandum, dated February 23, 2024

27288210.8

MEMORANDUM

To: Stephanie Hastings, Shareholder, Brownstein, Farber, Hyatt, Schreck, LLP
From: Anthony Brown, Principal-in-Charge, aquilologic, Inc.
Robert H. Abrams, Ph.D., P.G., CHg., Senior Principal Consultant, aquilologic, Inc.
Date: February 23, 2024
Subject: Progress Report and Mojave Basin Transition Zone Water Budget
Project No.: 018-10

Aquilologic, Inc. (**aquilologic**) has prepared this memorandum for two purposes. First, the memorandum documents preliminary work performed for the Golden State Water Company in the Mojave Basin pertaining to water outflow from the Transition Zone, which represents inflow to the Centro Subarea (**Figure 1**). Preliminary work indicates this outflow may be overestimated by the Mojave Basin Watermaster (Watermaster). Consequently, inflow to the Centro Subarea may also be overestimated. Second, the memorandum outlines an approach to provide further assessment of this outflow/inflow, to be supported by data and analyses.

The Mojave Basin is subject to a Stipulated Judgment (Judgment) of water rights.¹ The Judgment stipulates that Alto Subarea Producers have an obligation to deliver 23,000 acre-feet per year (AFY) of Subsurface Flow² and Base Flow³ to the Transition Zone. Watermaster appears to assume that surface water inflow to the Transition Zone provides the basis for estimating surface water inflow to the Centro Subarea.⁴ However, there is no direct evidence to support this assumption. In fact, there is direct evidence that this assumption may be incorrect.

BACKGROUND

The Transition Zone is defined in the Judgment as part of the Alto Subarea. Watermaster assumes that the Alto Subarea Producers' obligation to the Transition Zone is satisfied by inflow to the Transition Zone from upstream portions of the Alto Subarea.⁵ This inflow is comprised of Subsurface Flow and Base Flow. The obligation to the Transition Zone appears to be considered by Watermaster to also satisfy an obligation to the Centro Subarea. For example, the first annual report notes, "[s]uch discharge records are used in the calculations of compliance by Alto

¹ Riverside (1996). Judgment after Trial, Mojave Basin Area Adjudication. City of Barstow et al. v. City of Adelanto et al. Riverside County Superior Court Case No. 208568. January 10.

² Subsurface Flow is defined in the Judgment as, "Groundwater which flows beneath the earth's surface."

³ Base Flow is defined in the Judgment as, "That portion of the total surface flow measured Annually at Lower Narrows which remains after subtracting Storm Flow."

⁴ After accounting for estimated gains/losses in the Transition Zone, such as sewage treatment plant outfall and estimated consumptive use, as stated or implied in multiple annual reports.

⁵ Watermaster (1995). First annual report of the Mojave Basin Area Watermaster, 1993-1994, City of Barstow et al. v. City of Adelanto et al. Riverside County Superior Court Case No. 208568, Riverside County. February 28.

*Subarea Producers with their obligation to the Centro Subarea.*⁶ Subsequent annual reports contain similar statements.

The Judgment specifies that 2,000 AFY of the Alto Producers' obligation to the Transition Zone is satisfied by Subsurface Flow. Watermaster assumes that groundwater inflow to the Centro Subarea from the Transition Zone is also 2,000 AFY.^{7,8} Therefore, Watermaster appears to assume that 21,000 AFY of the obligation to the Centro Subarea must be satisfied by Base Flow from the Transition Zone.

Watermaster states that the change of groundwater storage in the Transition Zone is zero because water levels in key piezometers near both the upstream and downstream boundaries of the Transition Zone are relatively constant.⁹ Because of this, Watermaster assumes Mojave River discharge measured at the Lower Narrows gage, adjusted by an estimated Transition Zone water balance, is essentially equivalent to Mojave River discharge entering the Centro Subarea¹⁰ (**Figure 1**). However, there is no active stream gage at the upstream boundary of the Centro Subarea. Therefore, Watermaster's assumption regarding inflow to the Centro Subarea cannot be evaluated directly.

STREAM DISCHARGE

There are no stream gages in most of the Transition Zone. However, there is one long-term gage (i.e., water year [WY] 1931 to present) located at the upstream boundary of the Transition Zone (Lower Narrows gage) (**Figure 1**). Another long-term stream gage is located near the Centro Subarea-Baja Subarea boundary (Barstow gage). A stream gage has recently been re-established approximately eight miles downstream of the Transition Zone-Centro Subarea boundary (Hodge/Hinkley gage).

The Hodge/Hinkley and Barstow gages measure discharge across an ephemeral Mojave River channel that can be over 0.25 miles wide. Discharge is generally limited at these gages to Storm Flow (i.e., very little, if any, Base Flow is measured by these gages).¹¹ The wide channel leads to uncertainty in the stream discharge measurements from these gages because Storm Flows may

⁶ Watermaster (1995). First annual report of the Mojave Basin Area Watermaster, 1993-1994, City of Barstow et al. v. City of Adelanto et al. Riverside County Superior Court Case No. 208568, Riverside County. February 28.

⁷ As stated or implied in multiple annual reports.

⁸ However, it should be noted that the cross-sectional area for groundwater flow between the Transition Zone and the Centro Subarea potentially expands and contracts with varying volumes of Transition Zone recharge, which may increase or decrease the assumed 2,000 AFY of Subsurface Flow. Studies to understand the geometry of this potentially dynamic cross-sectional area are warranted but have not yet been undertaken by Watermaster.

⁹ As stated or implied in multiple annual reports

¹⁰ The Lower Narrows gage is located at the upstream boundary of the Transition Zone.

¹¹ Storm Flow is defined in the Judgment as *"That portion of the total surface flow originating from precipitation and runoff without having first percolated to Groundwater storage in the zone of saturation and passing a particular point of reckoning, as determined annually by the Watermaster."*

not always fill the entire width of the channel or may flow in parts of the channel away from the gage. Nevertheless, discharge measurements from these gages are the best available data.

From WY 1931 through WY 2023, Mojave River discharge at the Lower Narrows gage averaged 46,100 AFY. Discharge decreased by an average of 341 AFY over that period. From WY 1994 through WY 2023, Mojave River discharge at the Lower Narrows gage averaged 28,300 AFY. The decrease in average annual discharge over this period increased to 521 AFY.

As noted, there is no active stream gage at or adjacent to the Centro Subarea's upstream boundary. However, there was such a gage from March 1966 through WY 1970: the Wild Crossing gage (**Figure 1**).

DATA ANALYSIS

The Wild Crossing gage was discontinued because of unstable controls and changing stage-discharge relations that did not allow for acceptable discharge records.¹² However, stream discharge measured at the Wild Crossing gage is the best data available that can show the potential change in discharge between the upstream boundary of the Transition Zone and the upstream boundary of the Centro Subarea, despite its shortcomings and relatively short period of record. It should be noted that the Hodge/Hinkley gage was also discontinued two different times since 1932 because of unstable controls and changing stage-discharge relations. However, it was reestablished in 2022, which suggests high-quality data can be gathered at gage locations previously deemed problematic.

Stream Recharge to Groundwater

Figure 2 shows the annual discharge at the Lower Narrows gage, the Wild Crossing gage, and the Barstow gage for the period WY 1966 through WY 1970.¹³ For the purposes of this analysis, net stream recharge to groundwater is approximated as the difference in discharge between successive gages.¹⁴ Discharge at the Wild Crossing gage was lower than discharge at the Lower Narrows gage every year during this period. WY 1969 is particularly striking because annual stream discharge at the Wild Crossing gage (156,000 AF) was 135,000 AF lower than discharge at the Lower Narrows gage (291,000 AF), a decrease of approximately 46 percent.¹⁵

¹² Lines, G.C. (1996). Ground-water and surface-water relations along the Mojave River, Southern California: U.S. Geological Survey Water-Resources Investigations Report 95-4189, 43 p.

¹³ The Wild Crossing gage was not active until March 1, 1966, thus may underestimate the annual discharge for WY 1966.

¹⁴ This is a reasonable approximation, even though it ignores Base Flow and evapotranspiration, because most of the flow measured at the Wild Crossing gage and the Barstow gage are from episodic storm events. However, evapotranspiration along the stream course may require further evaluation.

¹⁵ WY 1969 represents the largest amount of discharge on record for the Lower Narrows, Wild Crossing, and Barstow gages.

The consistent pattern of lower stream discharge at the Wild Crossing gage compared to the Lower Narrows gage during this period indicates that stream discharge at the Lower Narrows gage was more likely than not significantly greater than stream discharge entering the Centro Subarea. Furthermore, the consistent pattern indicates that significant net stream recharge to groundwater from the Mojave River likely occurred in the Transition Zone.

Figure 3 shows that the average annual stream discharge for WY 1966-1970 decreased substantially between the Lower Narrows and Wild Crossing gages (i.e., by approximately 51,500 AFY). The total average annual net stream recharge between the Lower Narrows gage and the Barstow gage for the WY 1966-1970 period was approximately 59,500 AFY (**Figure 3**). Thus, 86 percent of the total net stream recharge between the Lower Narrows and Barstow gages occurred between the Lower Narrows gage and the Wild Crossing gage, i.e., in the Transition Zone (**Figure 3**). Net stream recharge between the Wild Crossing gage and the Barstow gage (i.e., the Centro Subarea) represents only 14 percent of the total net stream recharge between the Lower Narrows and Barstow gages.

As noted, net stream recharge in the Transition Zone averaged approximately 51,500 AFY for WY 1966-1970. Also as noted, the Judgment specifies that Subsurface Flow into the Centro Subarea from the Transition Zone is 2,000 AFY. Thus, the fate of the Transition Zone net stream recharge is unclear without further analysis, which is discussed below.

Groundwater Extractions

Groundwater extraction data were obtained for 1951-1973 and WY 1994-2022 from the Mojave Water Agency (MWA).¹⁶ Data were analyzed for 1966-1970 and WY 1994-2022 to determine annual groundwater extractions in the Transition Zone. Data from the earlier period were scanned from hard copy and digitized. Data from the later period were provided digitally.

Figures 4 and **5** show the wells for which extractions were reported for the 1966-1970 and WY 1994-2022 periods, respectively. Groundwater extractions were compared to stream recharge to assess if extractions may account for the fate of the Transition Zone stream recharge.

The upper panel of **Figure 6** compares the annual stream recharge in the Transition Zone to the annual reported groundwater extractions. As noted, the WY 1969 stream discharge and recharge were anomalously high. They are statistical outliers, which may cause the average value of stream recharge for WY 1966-1970 to be skewed high when compared to average groundwater extractions, which typically do not have extreme changes year to year.

Rather than comparing average values for this period, the median values of annual stream recharge (33,234 AFY) and annual groundwater extractions (30,287 AFY) for the 1966-1970 period were compared. The median values suggest that most of the Mojave River net stream

¹⁶ Jeff Ruesch, Mojave Water Agency, email communications, July 2023.

recharge to groundwater in the Transition Zone during the 1966-1970 period was extracted by the approximately 260 wells completed in the Transition Zone at that time (**Figures 4 and 6**).

Transition Zone groundwater extractions in the 1966-1970 period may have facilitated higher net stream recharge by sufficiently changing the hydraulic gradient between the River and groundwater enough to induce stream recharge. This could occur even while water levels in key piezometers remain relatively constant. If so, the water-level data may appear to show that the change in groundwater storage in the Transition Zone is zero, when in fact the groundwater flow system is highly dynamic and may include significant net stream recharge.

The lower panel of **Figure 6** shows groundwater extractions in the Transition Zone for the 1966-1970 and WY 1994-2022 periods. The median value for 1966-1970 was 30,287 AFY. The median value for WY 1994-2022 was 11,522 AFY. This is a significant decrease in pumping, likely due to implementation of the Judgment. This decrease may suggest that recent and current net stream recharge in the Transition Zone is minimal compared to the WY 1966-1970 period.

However, a reasonable hypothesis is that significant net stream recharge continued to occur proportionately in the Transition Zone in the recent past and is currently occurring. The analysis described above suggests that groundwater extractions, on average, may remove an equivalent volume of net stream recharge from the Transition Zone. If so, surface water inflow to the Centro Subarea may be overestimated when based on the adjusted stream discharge measured at the Lower Narrows gage, because there may be unaccounted stream losses in the Transition Zone.

Additionally, the occurrence of Transition Zone stream losses and the effect of groundwater extractions and phreatophytes on streamflow losses and stream discharge in the Mojave Basin has been noted in previous reports prepared by others.^{17,18} Furthermore, it should be noted that 15,095 AF of treated wastewater was discharged to the Transition Zone downstream of the Lower Narrows stream gage during WY 2022.¹⁹

OUTLINE OF PROPOSED WORK TO FURTHER EVALUATE THE TRANSITION ZONE WATER BUDGET

Watermaster was directed by the Court in 2022 to re-evaluate the Production Safe Yield (PSY) for each Subarea. **Aquilologic** believes a rigorous reevaluation must include a detailed

¹⁷ Stamos, C.L., Martin, P., Nishikawa, T., and Cox, B.F. (2001). Simulation of ground-water flow in the Mojave River Basin, California. U.S. Geologic Survey Water-Resources Investigations Report 01-4002 Version 1.1.

¹⁸ Todd Engineers (2013). Final report: Conceptual hydrogeologic model and assessment of water supply and demand for the Centro and Baja Management Subareas, Mojave River Groundwater Basin. Prepared by Todd Engineers and Kennedy/Jenks Consultants for the Mojave Water Agency. July.

¹⁹ Watermaster (2023). Twenty-ninth annual report of the Mojave Basin Area Watermaster, water year 2021-2022, City of Barstow et al. v. City of Adelanto et al. Riverside County Superior Court Case No. 208568, Riverside County. May 1.

redetermination of the Transition Zone water budget. Material presented to date by Watermaster does not appear to have included a redetermined Transition Zone water budget.²⁰

The analyses performed to date by **aquilogic** and others suggest that groundwater flow dynamics and the Transition Zone water budget are complex. The analyses provide a foundation for deeper evaluation of the Transition Zone water budget and its evolution through time. For example, the **aquilogic** analyses reported here can form components of an overall water budget evaluation. The objective of such an evaluation would be to provide an in-depth analysis of the volume of water that flows into the Centro Subarea annually.

A complete water budget would include all inflows, outflows, and the change of groundwater storage over time. Previous work by others can be leveraged to support development of a complete water budget. For example, the Judgment specifies that 2,000 AFY of groundwater flows into the Centro Subarea from the Transition Zone. This flow rate was specified before in-depth modeling was conducted by the U.S. Geological Survey (USGS) or MWA. A deeper analysis may reveal that this specified flow rate is too low or too high.

Groundwater flow into the Centro Subarea occurs in the Mojave River alluvium, in deeper horizons across the Helendale Fault, and other areas along the Transition Zone-Centro Subarea boundary (**Figure 1**). This flow rate is difficult to assess without using a groundwater flow model. A groundwater model can be used to contribute to a complete water budget evaluation by calculating the transient change in groundwater storage and groundwater flow rates that cannot otherwise be determined due to lack of data in key locations. **Aquilogic** strongly recommends that the current Mojave Basin groundwater flow model used by Watermaster be updated to include the entire basin, as soon as possible. In its current form, it is premature to use the model for any analyses involving the Transition Zone.

The water budget for the Transition Zone should be developed with sufficient detail and rigor to at least meet Sustainable Groundwater Management Act (SGMA) regulations for historic and current water budgets. A preliminary list of tasks to be performed includes, but may not be limited to, the following:

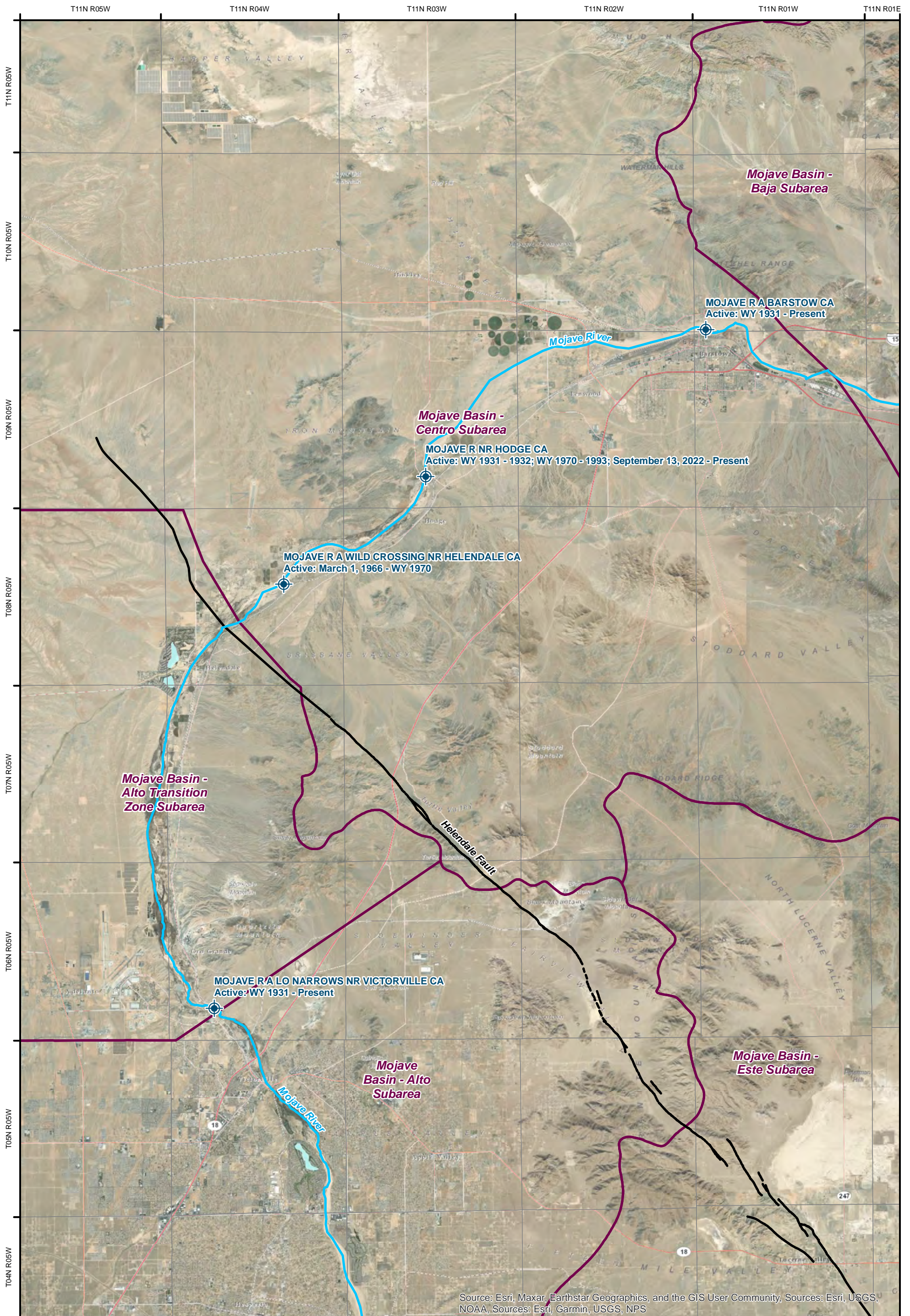
- Compile and review available previous work by others on groundwater flow and water budgets in the Alto and Centro Subareas, including the Transition Zone
- Evaluate the usefulness of the USGS Basin Characterization Model (BCM)²¹ and the Parameter-elevation Regressions on Independent Slopes Model (PRISM)²² dataset for application to the Transition Zone water budget





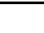
²⁰ Watermaster (2024). Groundwater Model and Production Safe Yield Update. Watermaster presentation prepared by Wagner and Bonsignore, Consulting Civil Engineers. Mojave Water Agency / Watermaster Board Meeting, January 24, 2024.

²¹ https://ca.water.usgs.gov/projects/reg_hydro/basin-characterization-model.html

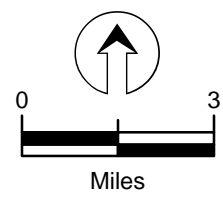
²² <https://prism.oregonstate.edu/>


- Evaluate groundwater levels in the Transition Zone from WY 1931-present, with particular focus on the WY 1966-1970 and WY 1994-2022 periods to support the analyses described above
 - Estimate evapotranspiration by standard methods, including the use of satellite and areal images, and compare with previous studies
 - Compile all available water level data for the Transition Zone
 - Evaluate the water level data in terms of changes in well hydrographs and spatial water-level distributions over time
 - Determine if groundwater levels increased, decreased, or remained the same during the WY 1966-1970 period
- Use the USGS model and the updated MWA model (if and when available) to further evaluate the WY 1966-1970 period
 - Update the USGS model as needed, including groundwater extractions and potentially extending the model in time
 - Evaluate Transition Zone changes in groundwater storage, stream recharge, effects of evapotranspiration, groundwater extractions, and surface and groundwater flow into the Centro Subarea
- Critically evaluate results and available previous work to determine the best estimate of the Transition Zone water budget
- Identify data gaps and limitations in the analyses
- Effectively communicate the results to stakeholders
- Thoroughly document the analyses and prepare both draft and final reports



-  Stream Gages
-  Helendale Fault
-  Mojave River
-  Adjudicated Areas
-  Township/Range

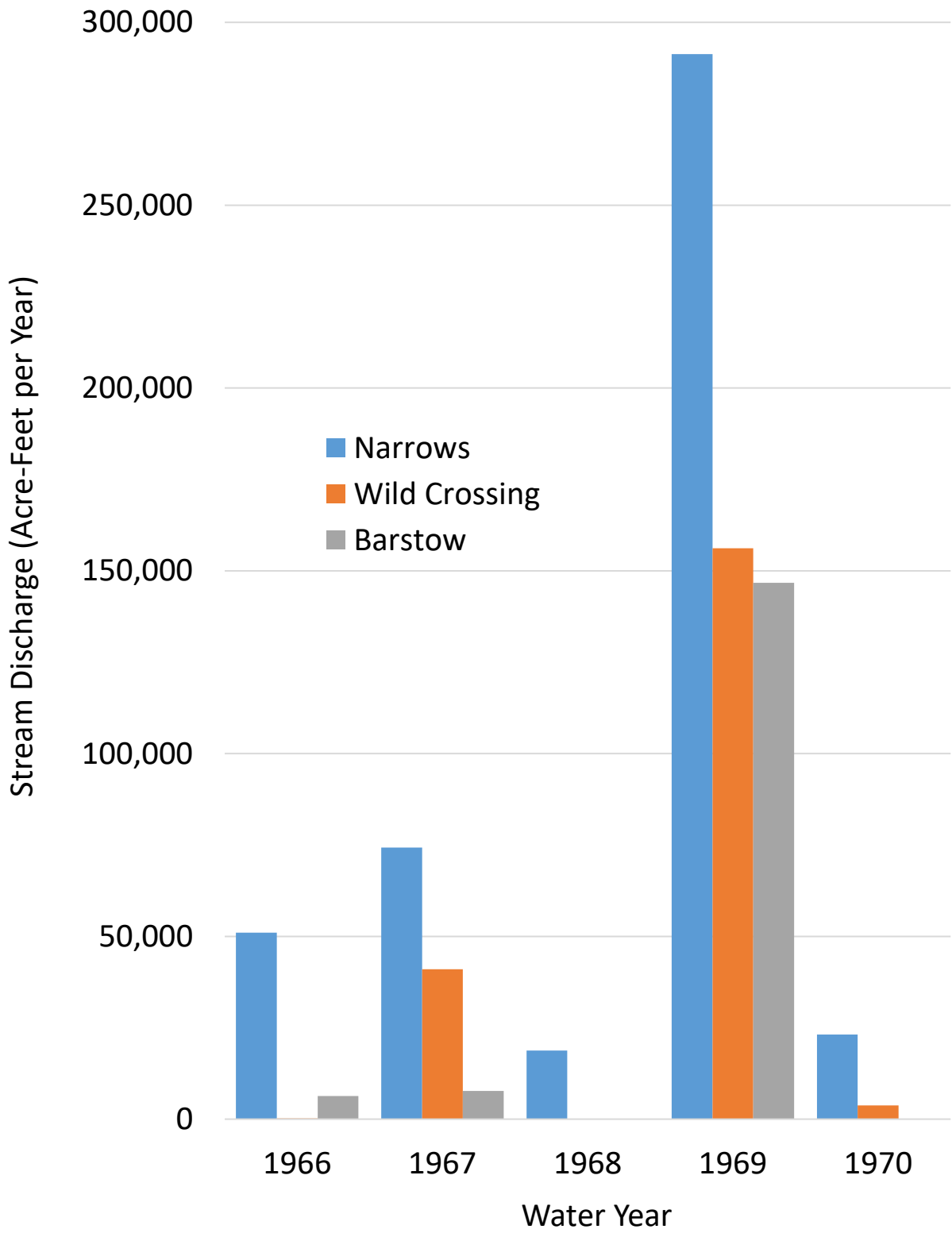
Notes:
 All locations approximate.
 WY: Water Year

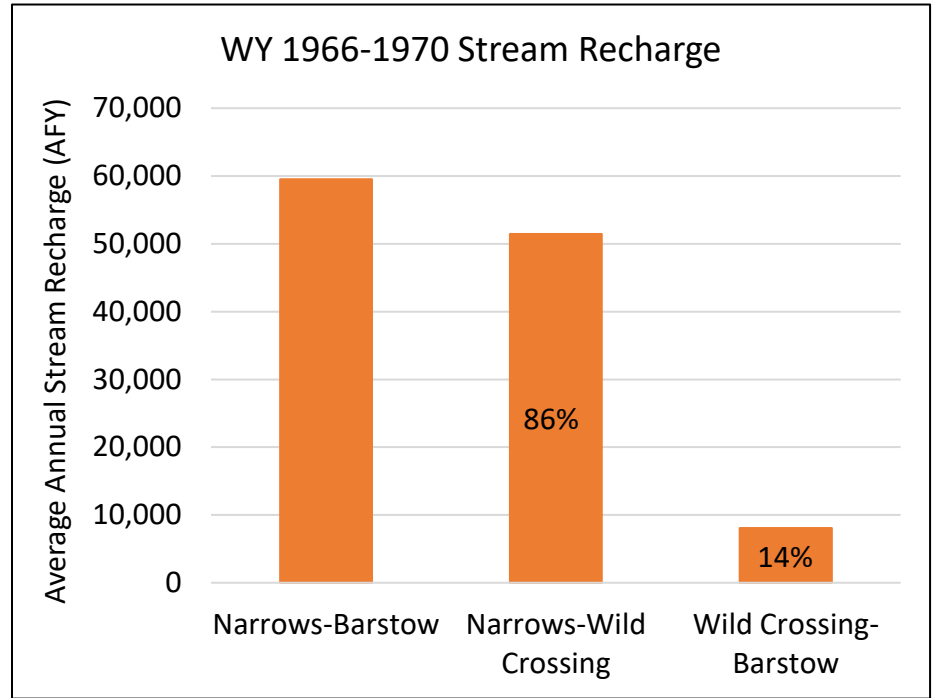
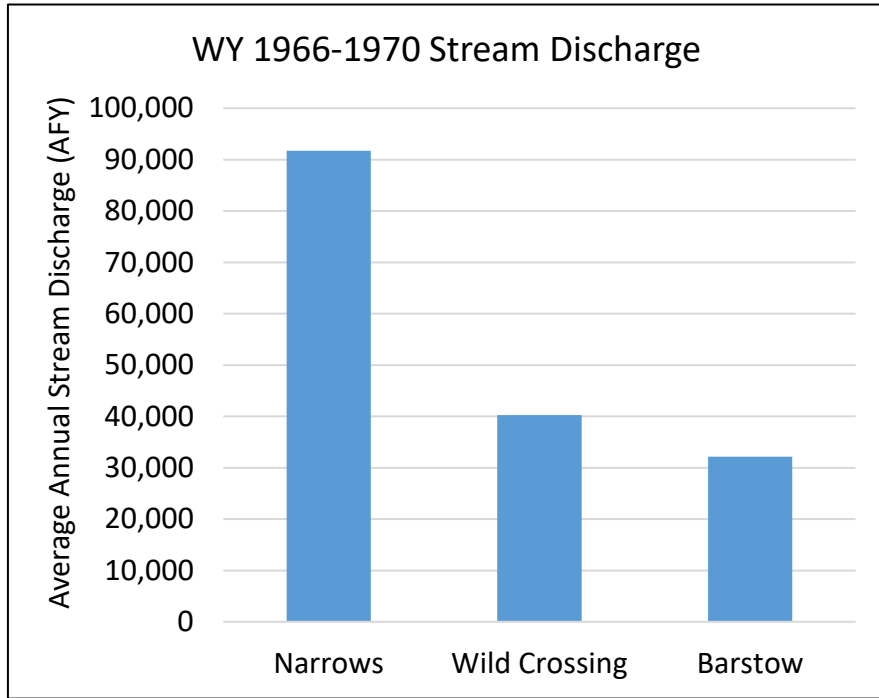


 aquilologic, Inc. BHFS - GSWC Mojave

Key Features in the Mojave Basin

Date: 10/18/2023	Project #: 018-10	Figure 1
------------------	-------------------	-----------------





AFY: Acre-Feet per Year
 WY: Water Year

aquilogic, Inc.

BHFS- GSWC Mojave

Stream Discharge and Recharge

Date: 2/23/2024

Project #: 018-10

Figure 3

GSWC 0962

T08N R05W

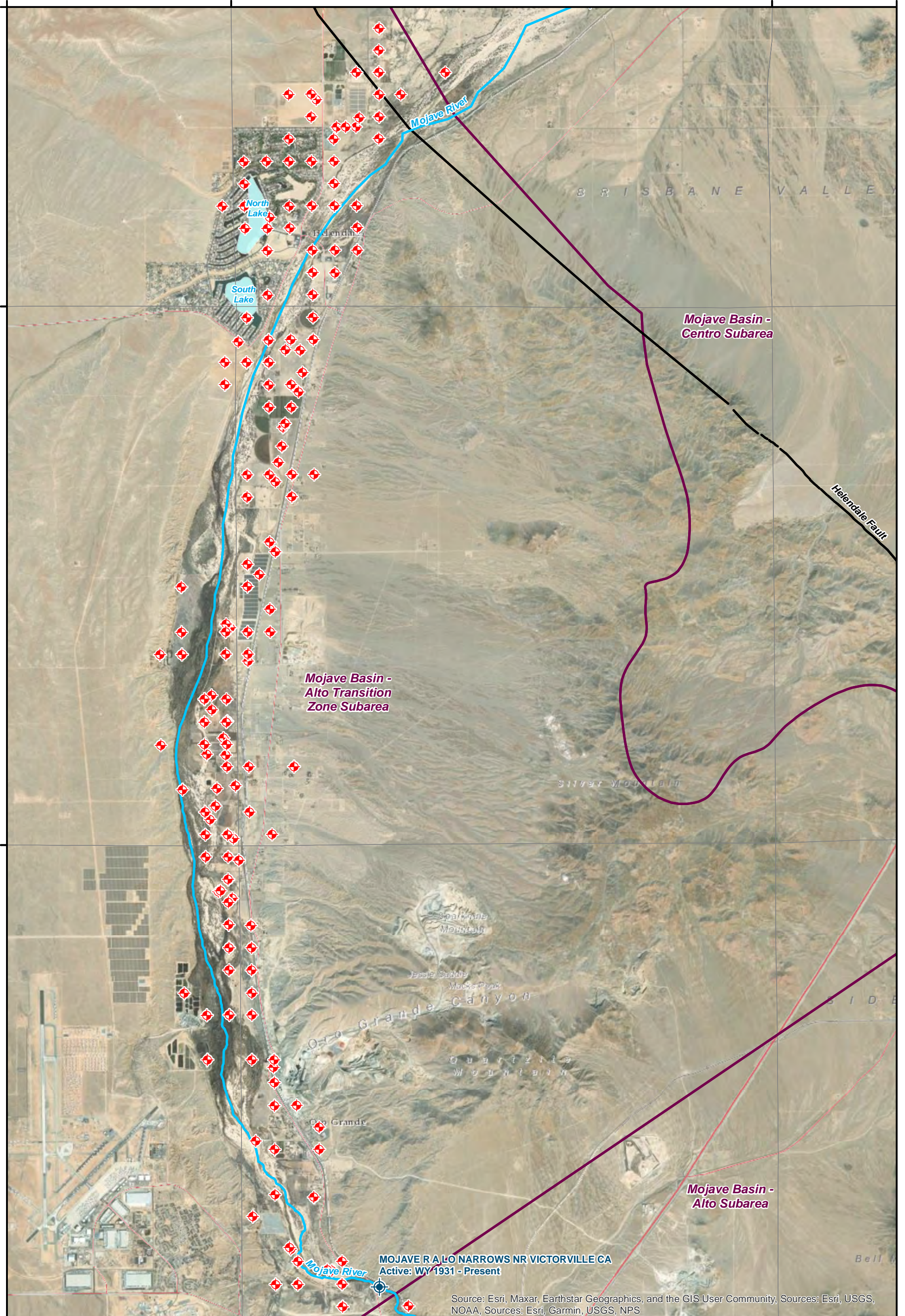
T08N R04W

T08N R03W

T08N R05W

T07N R05W

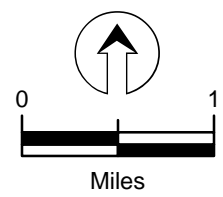
T06N R05W



MOJAVE R & LO NARROWS NR VICTORVILLE CA
 Active: WY 1931 - Present

Source: Esri, Maxar, Earthstar Geographics, and the GIS User Community, Sources: Esri, USGS, NOAA, Sources: Esri, Garmin, USGS, NPS

- ◆ Production Well Locations
 - Stream Gages
 - Helendale Fault
 - Mojave River
 - Adjudicated Areas
 - Township/Range
- Notes:**
 All locations approximate.



aquilogic, Inc. BHFS - GSWC Mojave

**Transition Zone Production Wells
 1966-1970**

Date: 10/18/2023	Project #: 018-10	Figure 4
------------------	-------------------	-----------------

GSWC 0963

T08N R05W

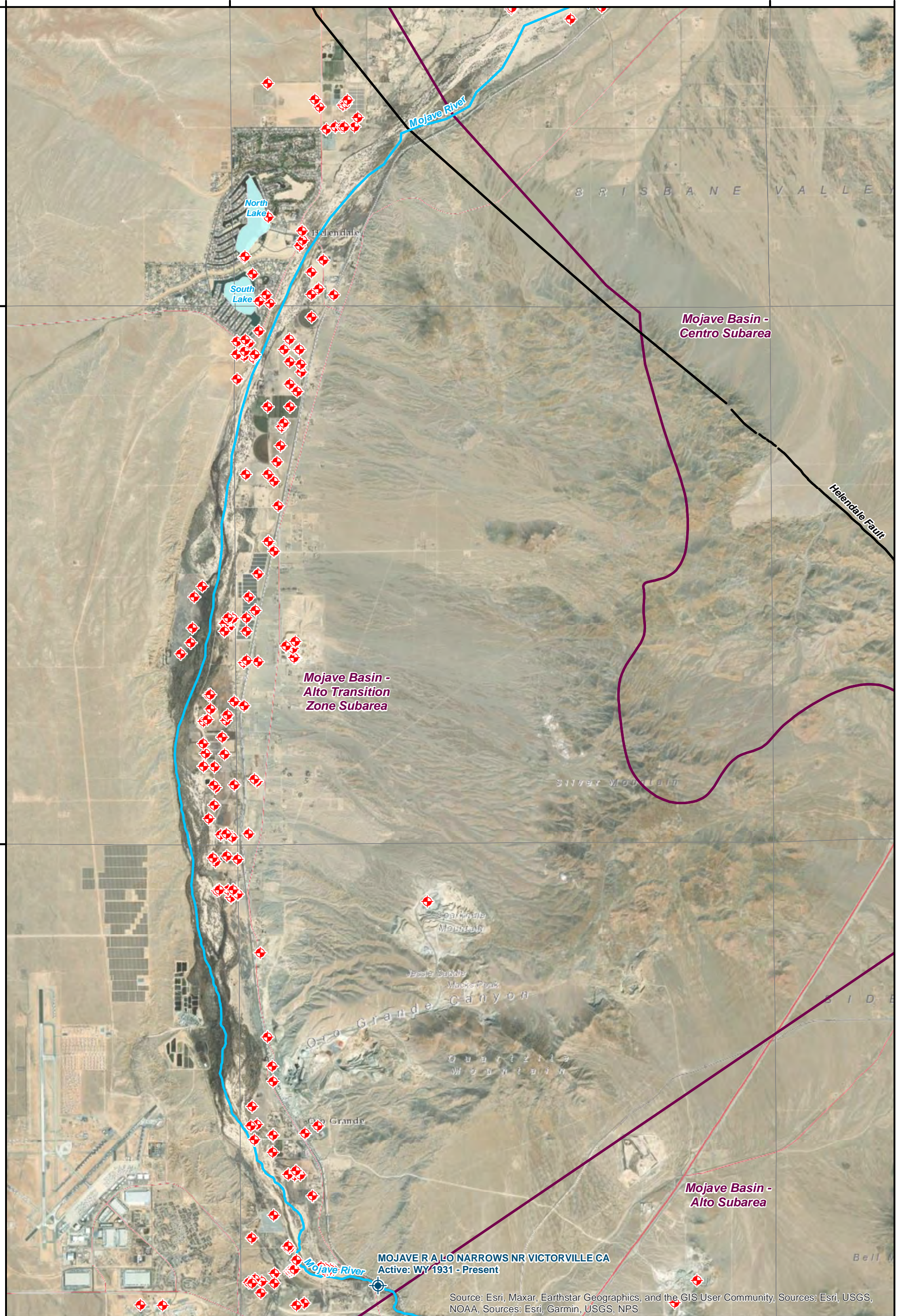
T08N R04W

T08N R03W

T08N R05W

T07N R05W

T06N R05W

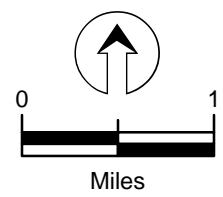


MOJAVE R & LO NARROWS NR VICTORVILLE CA
Active: WY 1931 - Present

Source: Esri, Maxar, Earthstar Geographics, and the GIS User Community, Sources: Esri, USGS, NOAA, Sources: Esri, Garmin, USGS, NPS

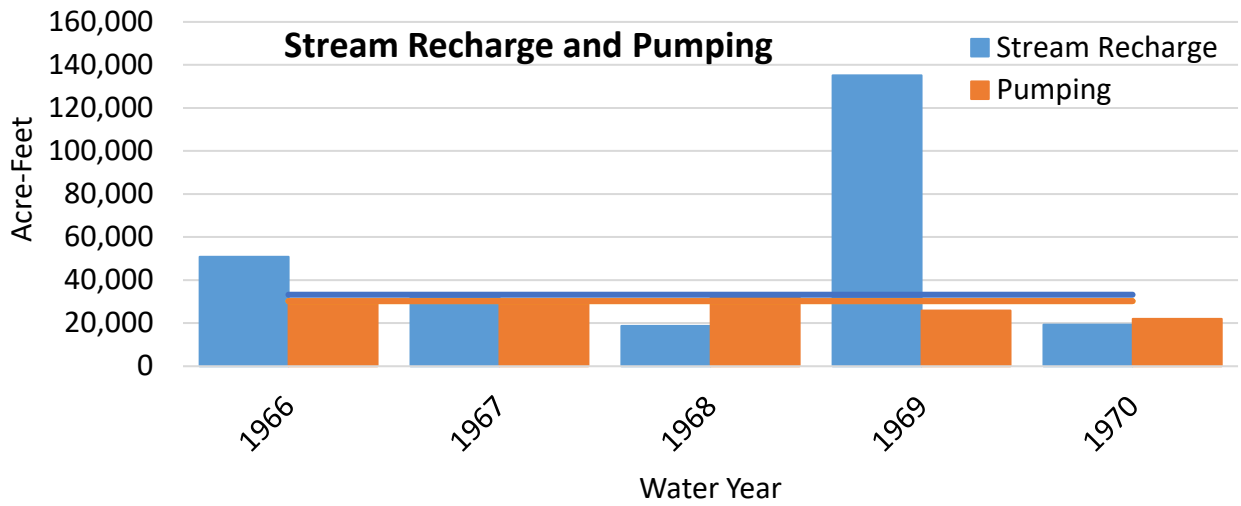
- ◆ Production Well Locations
- Stream Gages
- Helendale Fault
- Mojave River
- Adjudicated Areas
- Township/Range

Notes:
All locations approximate.
WY: Water Year

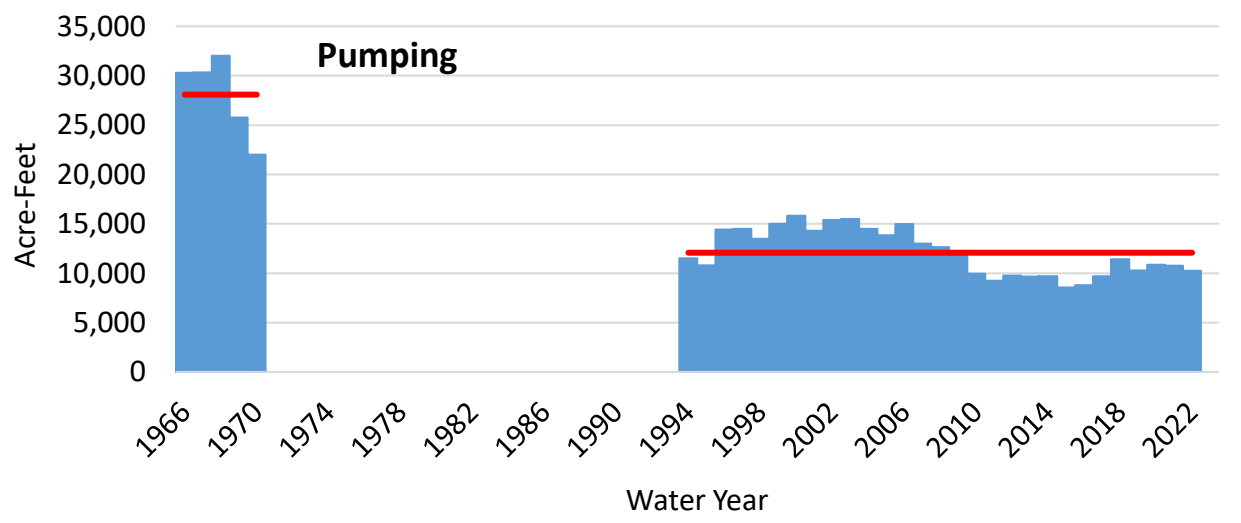


aquilogic, Inc.		BHFS - GSWC Mojave
Transition Zone Production Wells		
WY 1994 - 2022		
Date: 10/18/2023	Project #: 018-10	Figure 5

GSWC 0964



1966-1970
 Median Stream Recharge = 33,234 AFY
 1966-1970
 Median Pumping = 30,287 AFY



1966-1970
 Median = 30,287 AFY

1994-2022
 Median = 11,522 AFY

EXHIBIT 14

March 27, 2024

VIA EMAIL TO: WATERMASTER@MOJAVEWATER.ORG

Stephanie Osler Hastings
Attorney at Law
805.882.1415 direct
shastings@bhfs.com

Board of Directors
Mojave Basin Area Watermaster
Mojave Water Agency
13846 Conference Center Drive
Apple Valley, CA 92307-4377

RE: Agenda Items 7 & 9 - Comments on Watermaster's Production Safe Yield Update (February 2024), proposed recommendation for Free Production Allowance for Water Year 2024-25, Watermaster Annual Report for Water Year 2022-23

Dear Board of Directors:

This letter follows my letter dated February 28, 2024 on behalf of Golden State Water Company (GSWC) related to the Mojave Basin Area (Basin) Watermaster's evaluation and update of the Production Safe Yield (PSY) for each Subarea of the Basin—specifically Watermaster's estimate of flow across the Transition Zone. GSWC is a party to the Mojave Basin Judgment and a producer in three of the Mojave Basin Subareas—Alto, Este, and Centro.

Despite the significant concerns raised by my February 28, 2024 letter, which included a technical analysis by aquilogic, Inc. regarding the accuracy of the Watermaster's calculation of flow across the Transition Zone, and the potential resulting impacts on Watermaster's calculation of the Production Safe Yield and Free Production Allowances for each Subarea, to date, GSWC has not received any response from the Watermaster.¹

At the Watermaster's February 28 meeting, the Watermaster Engineer's presentation² included some information not previously shared that may represent an attempt to assess streamflow losses (i.e., groundwater recharge) in the Transition Zone, although the purpose is unclear.³ To the extent that this information implies that most streamflow loss between the Lower Narrows gage and the Barstow gage

¹ The minutes of the Watermaster's February 28, 2024 meeting reflect Director Limbaugh's direction to the Mojave Water Agency or the Watermaster to respond to GSWC February 28, 2024 comment letter.

² Watermaster Agenda, February 28, 2024, Item 7 Presentation: Production Safe Yield Update and Proposed Free Production Allowance (2024-2025), available at:
https://mojavewater.granicus.com/Viewer.php?view_id=2&clip_id=1336&meta_id=107549

³ Watermaster Agenda, February 28, 2024, Item 7 Presentation: Production Safe Yield Update and Proposed Free Production Allowance (2024-2025), slides 24 and 25. The March 27, 2024 presentation on the same topic does not include this information. (See generally, Watermaster Agenda, March 27, 2024, Item 7 Presentation: Production Safe Yield Update and Proposed Free Production Allowance (2024-2025).)

occurs in the downstream half of the Centro Subarea, it contradicts the analysis conducted by aquilogic, which points to the conclusion that most streamflow loss between the Lower Narrows gage and the Barstow gage may occur in the Transition Zone—before it reaches the Centro Subarea. Given that groundwater extraction patterns, and perhaps other factors, have changed over the last 50+ years, this apparent contradiction can only be resolved through further, in-depth analysis, preferably with a well-calibrated groundwater flow model, which to date has not occurred.

Accordingly, GSWC reiterates its prior request that the Watermaster consider and respond to its comments and recommendations, inclusive of those contained in the aquilogic memorandum, before completing its update of PSY for each Subarea and before issuing its Free Production Allowance for Water Year 2024-25 and Annual Report for 2023-24. In addition, should the recommended analysis show the need for additional subsurface and surface monitoring to evaluate hydrogeologic conditions with the Transition Zone, especially at the Centro Subarea boundary, GSWC asks Watermaster to commit to install, operate, and maintain appropriate monitoring equipment to address data gaps.

If helpful, GSWC would be pleased to discuss its concerns in more detail with Watermaster Staff and Engineer.

Respectfully,



Stephanie Osler Hastings

cc: Leland McElhaney, Brunick, McElhaney & Kennedy
Robert Wagner, Watermaster Engineer
Toby Moore, Golden State Water Co.
Bob Abrams, aquilogic, Inc.

EXHIBIT 15

Nicholas F. Bonsignore, P.E.
Robert C. Wagner, P.E.
Paula J. Whealen

Martin Berber, P.E.
Patrick W. Ervin, P.E.
David P. Lounsbury, P.E.
Vincent Maples, P.E.
Leah Orloff, Ph.D, P.E.
David H. Peterson, C.E.G., C.H.G.
Ryan E. Stolfus

MEMORANDUM

To: Mr. Lee McElhaney
Attorney, Mojave Basin Area Watermaster
Brunick, McElhaney & Kennedy
lmcelhaney@bmklawplc.com

From: Robert Wagner, P.E., A. Leonardo Urrego-Vallowe

Date: April 12, 2024

Re: **Response to comments on Transition Zone Water Balance memorandum, dated February 28, 2024.**

This memorandum responds to comments on the Mojave Basin Area Watermaster’s update to the Production Safe Yield (PSY) for the Alto and Centro subareas that was presented by Watermaster Engineer to the Watermaster Board on January 24, 2024 and on the Watermaster memorandum titled “Production Safe Yield & Consumptive Use Update” dated February 28, 2024.

The comments Ms. Stephanie Hastings, Attorney transmitted on behalf of Golden State Water Company (GSWC) highlight the importance of accuracy in the calculation of the Free Production Allowance (FPA) as required by the Judgment. The comments indicated that GSWC has concerns that the calculation of the of PSY and FPA do not accurately represent observed conditions in the Centro subarea. Watermaster understands that GSWC concern is based on decline in groundwater levels in its wells within the Centro subarea, water quality impacts associated with this decline and the operational costs associated with these issues.

The comments included a technical analysis prepared by Aquilogic titled “Progress Report and Mojave Basin Transition Zone Water Budget” (referred to as the “aquilogic memorandum”). The aquilogic memorandum concludes that Watermaster has overestimated the streamflow recharge into the Centro subarea because the Watermaster incorrectly assumed that all inflows into the Transition Zone (TZ) are equal to the inflows to the Centro subarea. The aquilogic memorandum states that Watermaster assumption of the change in storage for the TZ is zero may be incorrect given that there is no direct measurement of stream flows at the upstream boundary of the Centro subarea.

Mr. Lee McElhaney

April 12, 2024

Page 2

The aquilologic memorandum explains that the USGS Wild Crossing gage was in operation for a relatively short period of time (March 1966 to September 1970). A stream flow analysis of the Wild Crossing gage relative to the Lower Narrows gage during the period of record indicated that most of the Mojave River recharge occurred along the TZ rather than within the Centro subarea and therefore, the assumption regarding the change in storage for the TZ appears to be incorrect.

In addition, the aquilologic memorandum states that “the Wild Crossing gage was discontinued because of unstable controls and changing stage-discharge relations that did not allow for acceptable discharge records.” Watermaster does not believe the data recorded at the Wild Crossing gage is representative enough to include in the current calculation of return flows into the TZ and neither in the calculation of the PSY and FPA. This is because stream flows at the Wild Crossing gage were recorded for a short period of time (only four complete water years) and because operations at this gage were discontinued due to inaccuracy issues as mentioned in the aquilologic memorandum.

Watermaster assumption of no change in storage for the TZ is supported by the consistent decrease in groundwater pumping within the TZ. Historic groundwater production in the TZ is shown below (**Figure 1**). The average pumping between 1951-2020 and 2001-2020 declined about 40.7%.

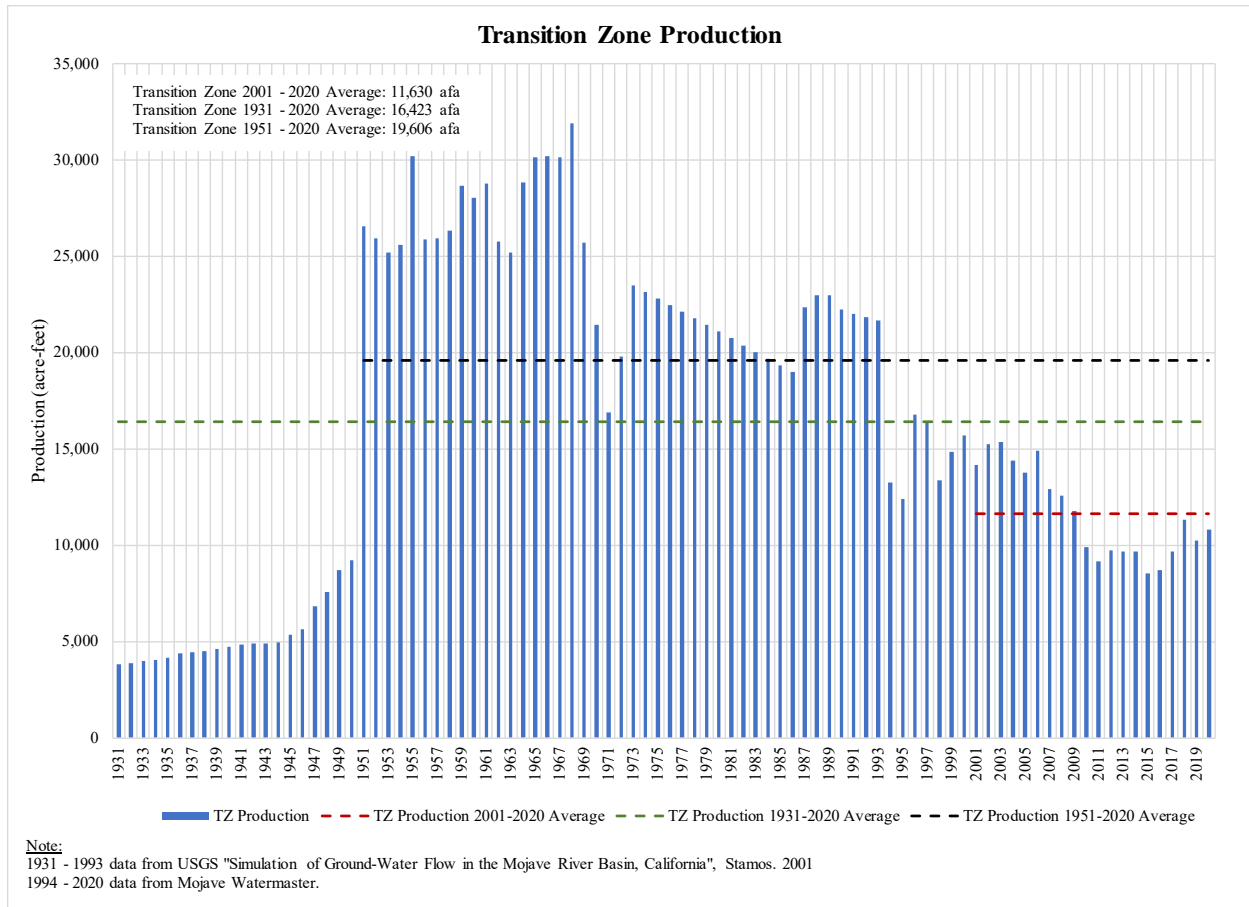


Figure 1. Historic groundwater pumping in the Transition Zone.

In September 2022, USGS initiated operations of the streamflow gage #10262000 Mojave River near Hodge. In water year (WY) 2023, total annual stream flow at the Lower Narrows was 96,606 acre-feet (AF) and total stream flow at the Hodge gage was 84,351 AF. The difference between these two gages was about 12,203 AF. Total discharge from VVWRA into the Mojave River was 14,274 AF. Neglecting stream flow losses due to evaporation, net stream change between Lower Narrows and the Hodge gage was about 24% (or 26,529 AF during 2023). The reach between the Lower Narrows gage and the Hodge gage is nearly 23.5 miles; and the distance between the Lower Narrows gage and the Helendale Fault is about 13 miles. Hence, we expect that only 13% (or 14,675 AF) of the net stream change would have occurred along the TZ. This is consistent with the historical record of losses between Lower Narrows and the Helendale Fault.

As explained in the Watermaster Annual Report for Water Year 2022-23 (Annual Report), the elements of use from the TZ are: 1) Groundwater extractions (pumping), and 2) Consumptive use by native vegetation (phreatophytes). The verified production during WY 2023 was 10,039 AF. Total consumptive use for phreatophytes was calculated to be about 5,702 AF. Return flows from pumping during 2023 was 3,180 AF. Thus, total use from the TZ during WY 2023

was 12,561 AF (production plus phreatophytes use minus return flows) which is close to the net change in stream flows in the TZ estimated above (14,675 AF). In other words, the net streamflow loss is accounted for by the groundwater pumping, return flow and water demand for phreatophytes.

We prepared an estimated surface water balance for the TZ for WY 2023 for purposes of calculating the outflow to Centro subarea for WY 2023 as shown on **Table 1**.

Table 1. Transition Zone Water Balance for WY 2023 (all values are provided in units of AF).

WATER SUPPLY	
Surface Water Inflow	
Lower Narrows	96,606
VWVRA	14,274
Ungaged (Runoff from Precipitation)	745
Subsurface Inflow	2,000
Return Flow from Production ⁽¹⁾	3,180
Imports	0
Total Inflows	116,806
CONSUMPTIVE USE AND OUTFLOW	
Surface Water Outflow	
Gaged	0
Ungaged	99,064
Subsurface Outflow	2,000
Production	10,039
Phreatophytes	5,702
Imports	0
Total Outflows	116,806
<u>Notes:</u>	
⁽¹⁾ Return flows are calculated as total production (10,039 AF) minus consumptive use (6,859 AF).	

Hydrographs showing historical groundwater levels within the TZ (Figure 3-13 of the Annual Report) indicate that groundwater levels have been stable for most of the wells since at least 1993. This supports our assumption that average change in storage in the TZ historically has been nearly zero. If a positive change in groundwater storage had occurred as suggested by Aquilogic, we would expect to see evidence of an increase in the groundwater elevations.

Watermaster also understands the concern presented on behalf of GSWC regarding the declining water levels in the Centro subarea and the impacts to the GSWC operations and facilities.

Watermaster is implementing groundwater modeling tools to improve the understanding of water supply, use and disposal for the Centro subarea. Watermaster has developed a groundwater model for the Alto subarea and used model outputs to update PSY and FPA for the Alto subarea as described in the Watermaster memorandum. Watermaster is in the process of extending the model to include Centro and the other subareas and future PSY and FPA updates will incorporate output from model results.

According to the aquilogic memorandum, average annual streamflow between the Lower Narrows and Wild Crossing gage was decreased by approximately 51,500 AFY (acre-feet per year) during WY 1966 to 1970. This would suggest that about 51,500 AFY is net recharge into the TZ via percolation. However, the historic pumping during the 1960s was remarkably higher than present conditions (see **Figure 1**). Historic production in the TZ, during the five years evaluated by Aquilogic is summarized in **Table 2**. Average total pumping in the TZ during the 1966-70 period was 27,885 AF.

Table 2. Historical groundwater pumping in the Transition Zone during WY 1966-1970

WY	Total Pumping
1966	30,208
1967	30,138
1968	31,893
1969	25,727
1970	21,460
Average 1966-70	27,885

Watermaster expects that losses from the surface water supply within the TZ correspond to pumping rather than recharge. As noted on the Watermaster memorandum, we updated the hydrologic base period for purposes of establishing PSY for Alto and Centro; the average pumping in the TZ during the updated hydrologic base period (2001-2020) was 11,630 AF. Total verified production during 2023 was 10,039 AF. Therefore, the average pumping of the base period and the pumping during 2023 were roughly 60% lower than the average total pumping during the 1966-70 period.

A historic aerial imagery comparison between 1969 and 2022 is provided in **Figure 2** (1969 aerial imagery) and **Figure 3** (2022). The 1969 aerial imagery shows the extent of agricultural development along the Mojave River between the Helendale Fault and the Hodge gage, including the vicinity of the Wild Crossing gage (near Indian Trail). The 1969 aerial imagery indicates the significant irrigation within the area of interest. The 2022 aerial imagery evidences the change in land use with most irrigation areas being fallowed over time. The change in groundwater pumping since the 1960s has changed the behavior of the river relative to recharge within the TZ.

Watermaster concludes that the decrease in annual stream flows during 1966-1970 between the Lower Narrows and the Wild Crossing gage was likely due to the high groundwater extractions downstream of the TZ rather than significant net stream recharge within the TZ.

Total annual stream flow at the Mojave River at Barstow gage was 8,687 AF during WY 2023 (as reported on the Annual Report). The net stream change between the Hodge gage and the Barstow gage was 75,664 AF during WY 2023 (i.e., difference between 84,351 and 8,687 AF). The distance between the Hodge gage and the Barstow gage is nearly 12 miles. Watermaster

estimates that groundwater recharge from surface supply between these gages was about 90% of the total flow at Hodge.

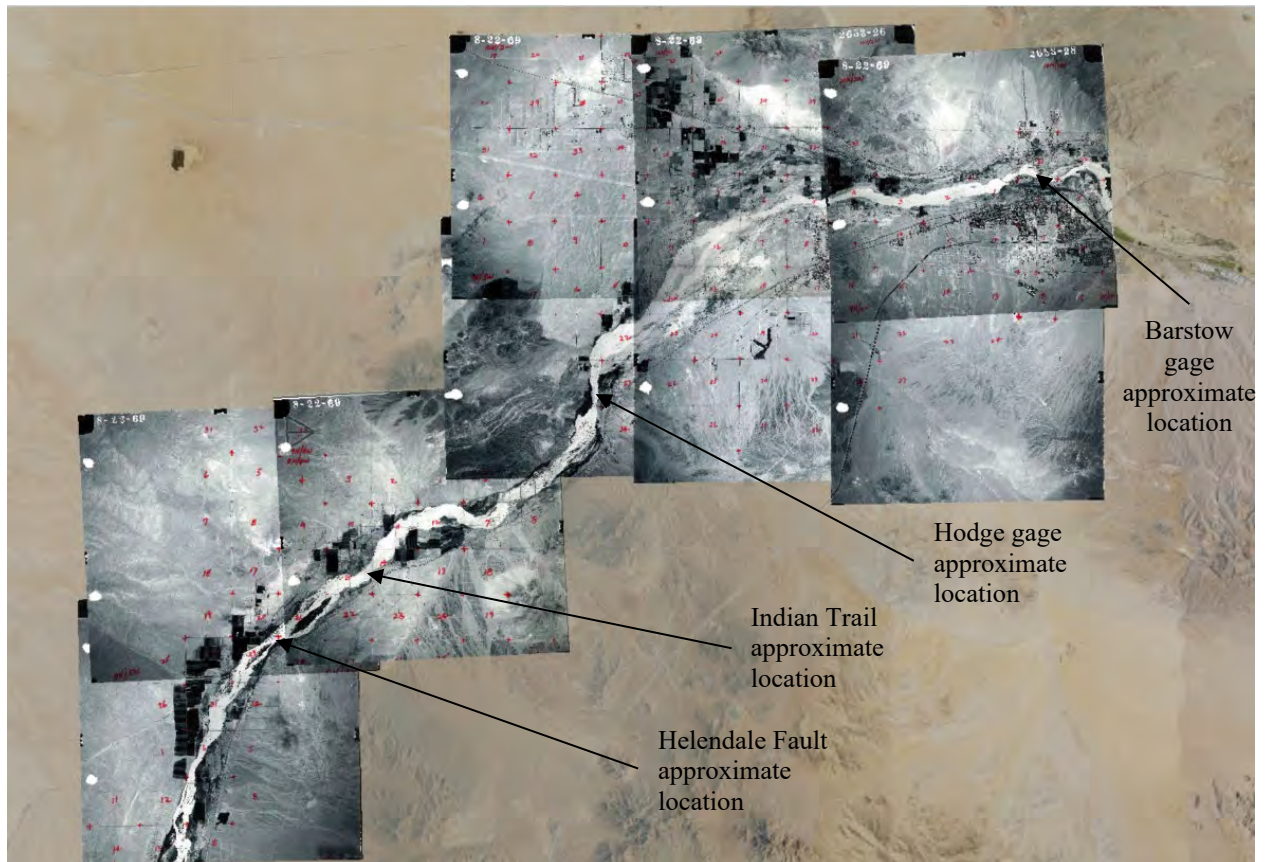


Figure 2. Aerial imagery of the area of interest taken in 1969 with the 2022 background image.

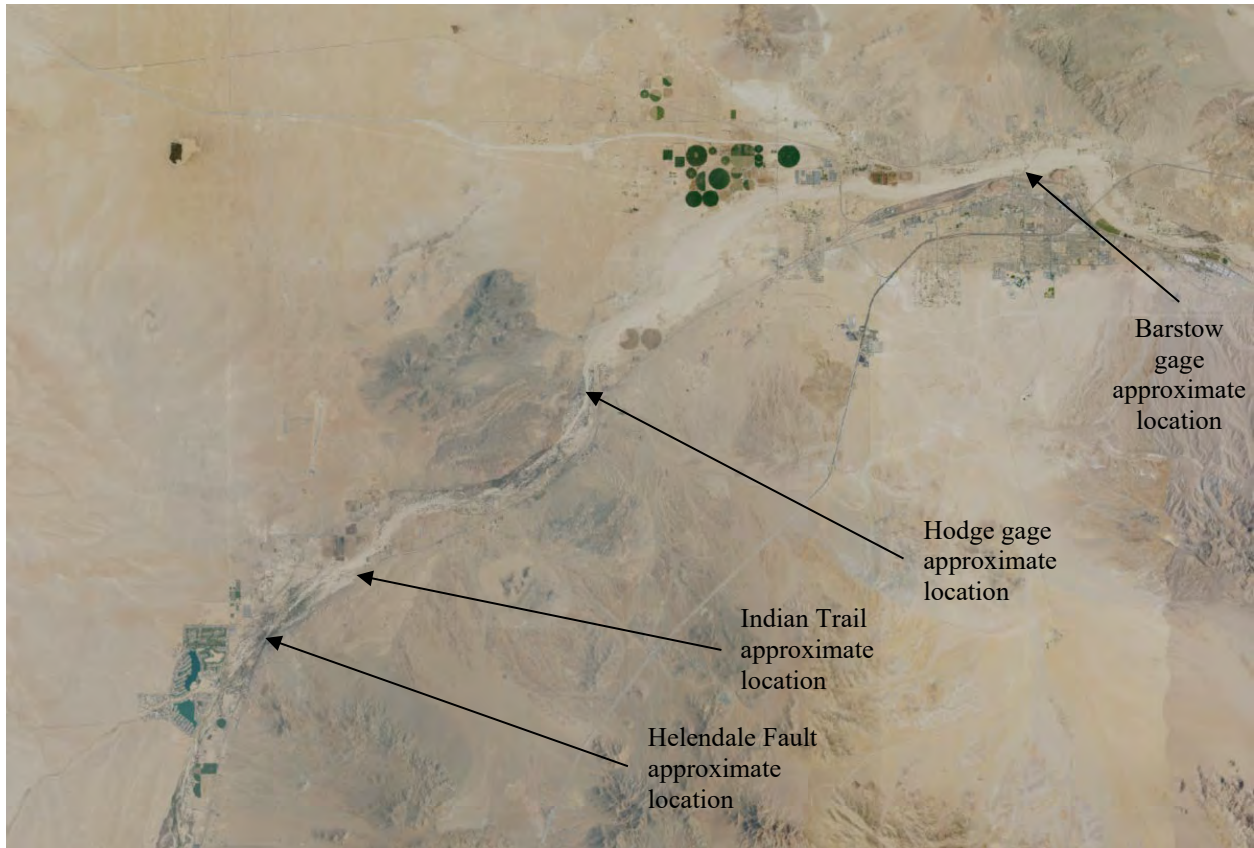


Figure 3. Aerial imagery of the area of interest taken in 2022.

Attached to this memorandum is the excerpts from “Exhibit A, Area of Influence of the Mohave River and it’s 20 subareas” prepared by Edward Fitzgerald Dibble, Consulting Engineer (Dibble, 1973) showing the total annual extractions as reported by the Mojave Water Agency. Section 8 of the excerpts corresponds to the area between the Helendale Fault and Lenwood (Centro subarea). Total annual production for Section 8 during the years 1951 to 1973 is summarized in **Table 3**.

Table 3. Total annual extractions within Section 8 for the years 1951-1973.

Year	Total Production	Year	Total Production
1951	8,686	1963	8,344
1952	9,002	1964	8,648
1953	10,105	1965	7,458
1954	10,547	1966	7,327
1955	10,338	1967	8,638
1956	11,600	1968	11,437
1957	9,868	1969	7,873
1958	10,108	1970	8,888
1959	10,485	1971	7,408
1960	12,911	1972	6,197
1961	12,028	1973	5,389
1962	11,983	Average 1951-73	9,359

The output from the groundwater flow model by the USGS (Stamos, 2001) provides simulated streamflow at various locations of the Mojave River (see **Figure 4**). The long-term flow average at Vista Road (at Helendale) is the approximate discharge from the TZ. The 1951-1999 average of 35,819 AF is close to the total average surface flow to Centro subarea (37,205AF) for the 1991-2023 period.¹ Average annual surface outflow from Alto to Centro during 1936-61 was estimated to be 35,500 AF (California Department of Water Resources, 1967). Thus, surface flows from the TZ into Centro subarea, as estimated at Helendale Fault have not changed significantly.

Figure 5 shows the long-term average discharge at Lower Narrows (USGS gage) plus the discharge from VVWRA to be 49,028 AF for the period 1951 to 1990 (VVWRA data started in 1986). The recent long-term average of 1991 to 2023 was 48,899 AF. Therefore, long-term inflow to the TZ has also been historically consistent.

¹ Calculated from the water balance at the TZ to be the average surface outflow (34,900 AF for 1991-2023) plus the average makeup purchases (2,305 AF for 1995-2023).

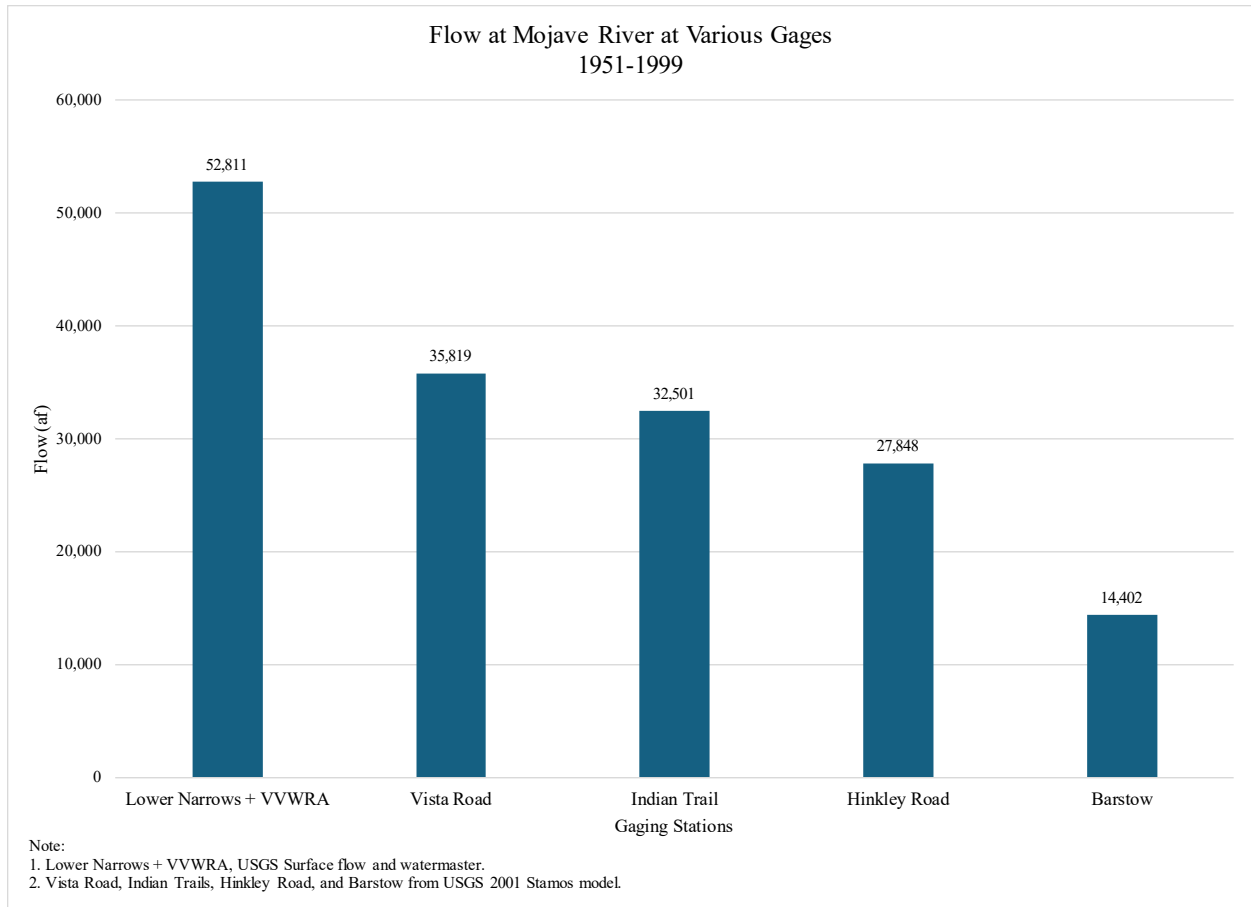


Figure 4. Simulated long-term average stream flows at the Mojave River from the USGS model.

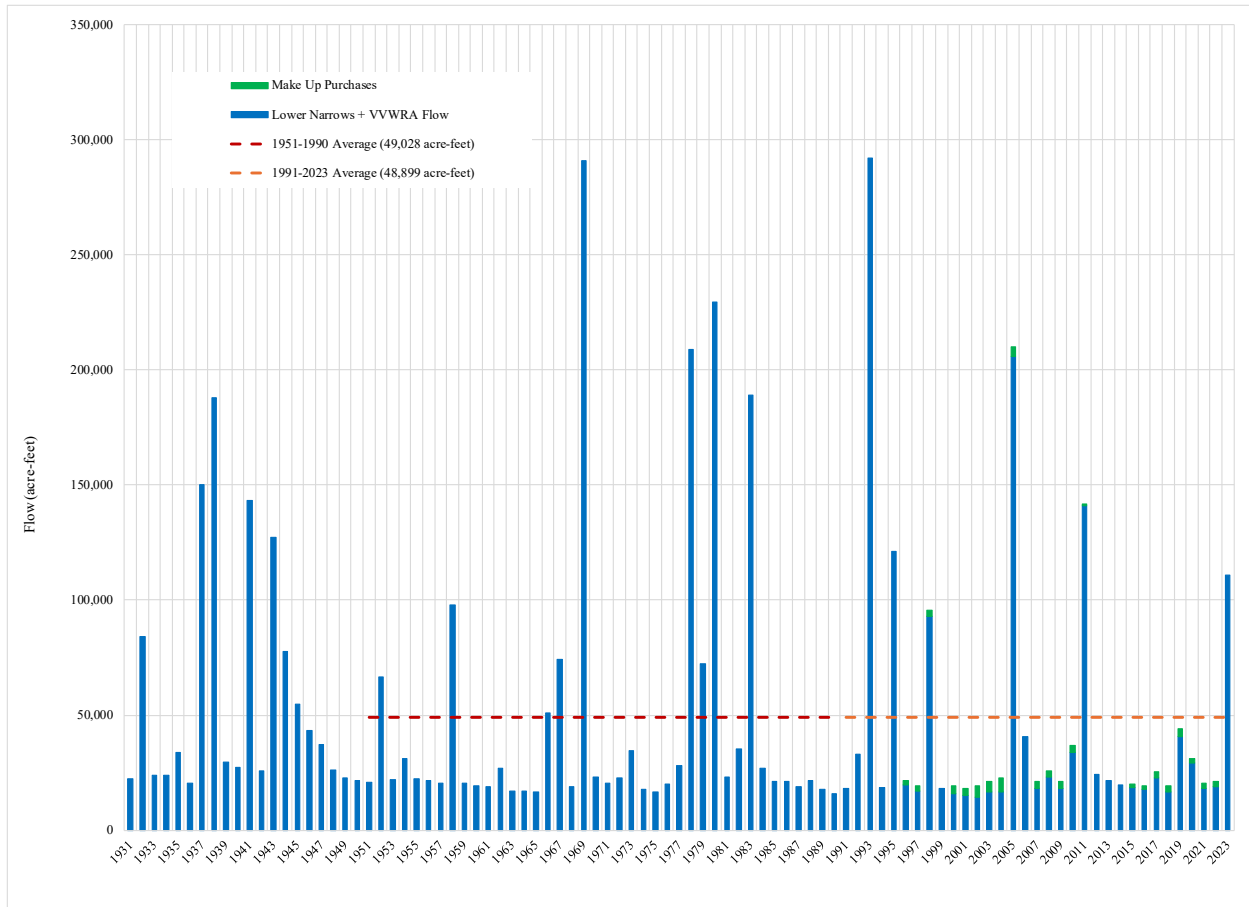


Figure 5. Total stream flows at Lower Narrows + VVWRA

In addition, the net change in simulated average stream flows between the reach of the Lower Narrows and the Vista Road (at Helendale) was 16,992 AF (difference between 52,811 and 35,819 AF from **Figure 4**). According to the historical groundwater production in the TZ shown on **Figure 1**, the average pumping during the period of 1951-1999 was 22,940 AF. Irrigation return flows to the TZ are in the order of 50-percent of the pumping.² Thus, we expect that average consumptive use from 1951-1999 to be about 11,470 AF. The USGS study by Lines and Bilhorn reported that the consumptive use by riparian vegetation was estimated to be about 6,000 AF along the TZ and this amount is representative of “normal” hydrologic conditions along the Mojave River (Lines & Bilhorn, 1996). The net change in stream flows along the TZ (16,992 AF) can be attributed to consumptive use by phreatophytes (6,000 AF) and consumptive use by pumping (11,470) rather than groundwater recharge from stream flows.

² From Hardt (1971) page 48, and Stamos (2001) page 32.

Requirements from the Judgment

The Judgment states that Alto subarea producers have a surface and subsurface flow obligation to the Transition Zone consisting of 21,000 AF of surface base flow (excluding storm flow) and 2,000 AF of subsurface flow. The obligation is calculated annually and maintained by assessing the Alto producers a Make Up Obligation based on a calculation outlined in Exhibit G, of the Judgment and included in the Watermaster Annual Reports as Tables 4-2 and 4-3. Exhibit G (e) provides “Alto Subarea Producers--an average Annual combined Subsurface Flow and Base Flow of 23,000 acre-feet per Year to the Transition Zone. For the purposes of Paragraph 6 of this Exhibit G, the Subsurface Flow component shall be deemed to be 2,000 acre-feet per Year. In any Year Alto Subarea Producers shall have an obligation to provide to the Transition Zone a minimum combined Subsurface Flow and Base Flow...” The Alto subarea obligation to the Transition Zone has been met every year.

Closing

Brownstein Hyatt Farber Schreck, LLP provided comments on behalf of Golden State Water Company suggesting that Watermaster assumption of the change in storage for the TZ is zero may be incorrect. Brownstein included a technical analysis prepared by Aquilogic which concluded that Watermaster has overestimated the streamflow recharge into the Centro subarea because the Watermaster incorrectly assumed that all inflows into the TZ are equal to the inflows to the Centro subarea.

In response to the comments provided by Brownstein, Watermaster evaluated the historical data to support our assumption that the average change in storage within the TZ has been nearly zero. Watermaster concludes that loss in stream flows observed along the TZ during the 1960s was attributed to consumptive uses in the TZ rather than groundwater recharge from stream flows.

Measured water levels in the TZ (Figure 3-13 of the Annual Report) have been historically stable which supports the accuracy of Watermaster assumption of no change in storage in the TZ. The historic decline in pumping and the change in the land use in the TZ since the 1960s has contributed to the water level stability observed in the TZ. The analysis of long-term historical data suggests that surface inflows (including VVWRA discharges) to the TZ and surface outflows from the TZ into Centro subarea have not changed significantly over time.

Enclosures:

Excerpts from “Exhibit A, Area of Influence of the Mohave River and it’s 20 subareas” prepared by Edward Fitzgerald Dibble, Consulting Engineer (1973).

Mr. Lee McElhaney

April 12, 2024

Page 12

References

California Department of Water Resources. (1967). *Bulletin No. 84 Mojave River Ground Water Basins Investigation*. California Department of Water Resources.

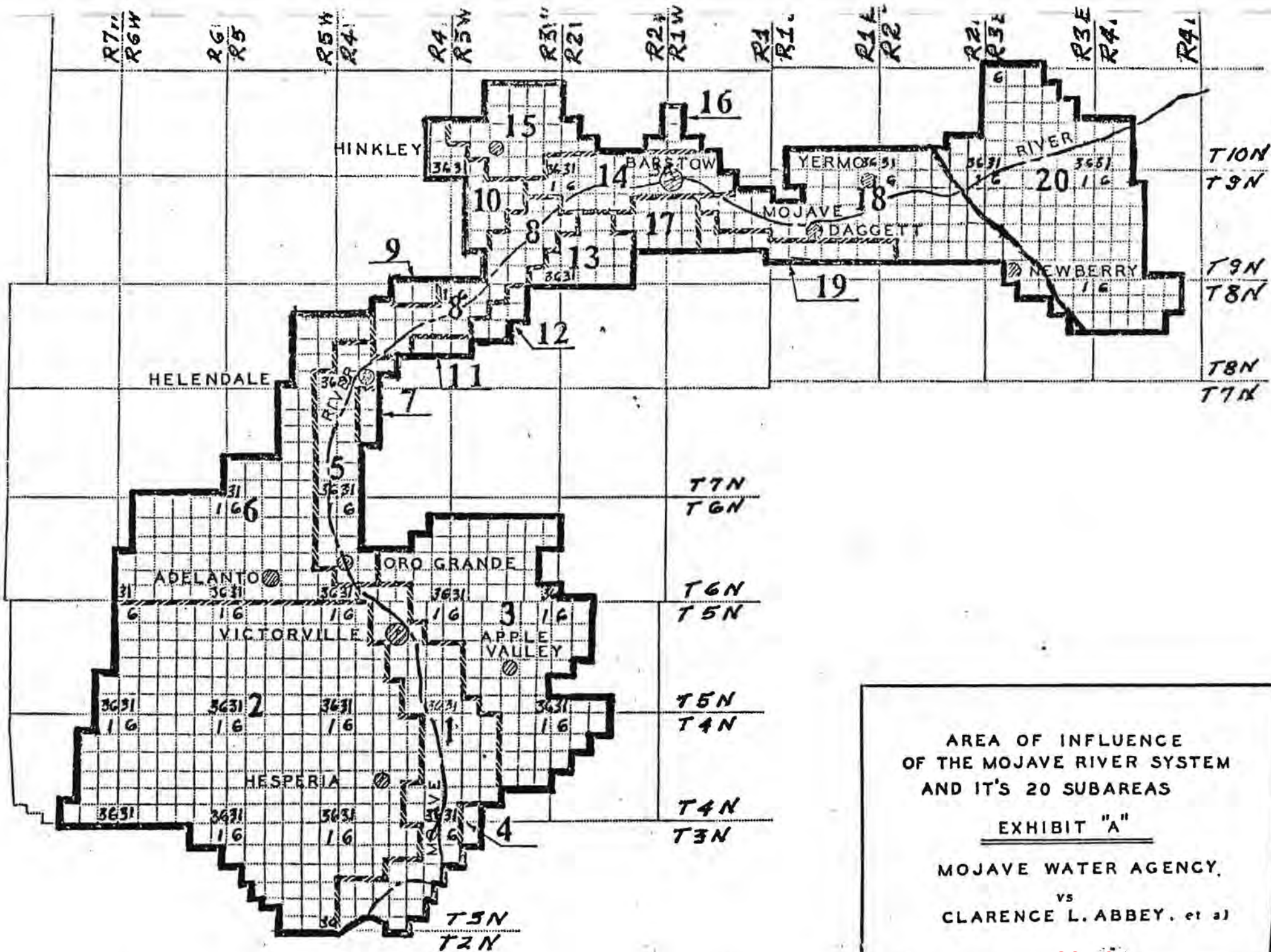
Dibble, E. F. (1973). *Water Production Verification Program*.

Hardt, W. F. (1971). *Hydrologic analysis of Mojave River Basin, California, using electric analog model*. USGS.

Lines, G. C., & Bilhorn, T. W. (1996). *Riparian Vegetation and Its Water Use During 1995 Along the Mojave River, Southern California*. U.S. Geological Survey.

Stamos, C. L. (2001). *Simulation of ground-water flow in the Mojave River Basin, California*. United States Geological Survey.

ENCLOSURES



AREA OF INFLUENCE
 OF THE MOJAVE RIVER SYSTEM
 AND IT'S 20 SUBAREAS
EXHIBIT "A"
 MOJAVE WATER AGENCY,
 vs
 CLARENCE L. ABBEY, et al

SUB AREA	NO. OF WELLS	NO. OF DEWELERS	ANNUAL TOTALS FOR SUBAREAS 1 THROUGH 19 WITH PROD. RIGHTS															PRODUCTION RIGHTS		
			1951	1952	1953	1954	1955	1956	1957	1958	1959	1960	1961	1962	1963	1964	1965	5-YR AVG	MAX YR	LMTD
	3	2	6,663	6,761	6,759	6,757	6,755	6,733	6,508	7,166	6,194	5,223	4,262	3,292	2,128	1,040	6,760	6,760	6,760	
01	270	111	63,811	75,566	73,380	72,052	69,953	59,716	59,626	65,291	68,316	67,135	69,601	66,047	69,945	71,383	103,720	118,109	20,246	
02	22	8	1,780	2,273	2,932	1,711	1,613	960	816	1,292	1,500	2,156	2,475	1,916	3,342	3,342	4,090	5,809	1,481	
03	67	41	2,244	3,146	4,456	4,547	4,201	5,135	3,610	5,058	5,082	5,304	4,039	3,268	3,811	3,811	6,725	8,781	2,734	
05	246	78	26,129	25,549	24,827	25,452	29,081	25,503	25,293	26,019	28,475	28,657	25,119	25,656	30,081	28,008	38,472	44,510	8,342	
06	6	4	306	281	255	242	291	379	512	379	105	127	84	103	61	22	356	613	285	
08	146	53	8,686	9,002	10,105	10,547	10,338	9,868	11,600	10,108	10,485	12,028	11,983	8,344	7,458	15,506	19,919	5,814		
10	3	2	0	0	0	0	3	4	8	11	10	18	16	21	22	22	33	33	0	
13	10	4	159	156	166	158	201	193	202	193	203	206	203	293	669	705	652	736	1	
14	171	86	16,350	16,455	17,125	18,176	18,138	17,874	17,983	18,139	18,349	18,278	18,461	18,042	18,394	19,003	25,004	29,547	6,608	
15	148	61	13,523	13,601	15,506	13,779	13,210	11,097	11,537	10,117	11,203	10,044	9,290	8,750	8,270	6,989	17,166	20,770	8,440	
16	4	1	15	20	25	30	35	46	45	43	40	42	40	53	49	64	34	49	64	
17	2	2	24	29	29	34	39	26	43	21	32	0	0	0	0	0	26	32	26	
18	172	79	11,022	12,193	14,419	15,920	16,902	14,166	13,511	16,629	18,729	20,226	20,524	21,305	24,633	20,622	26,576	32,352	3,506	
TOTALS	1,270	532	150,712	165,032	169,984	169,405	170,760	151,479	151,515	160,344	160,723	168,481	162,473	159,832	167,871	164,464	244,997	288,035	64,244	

MUJAVE WATER AGENCY

ANNUAL TOTALS FOR SUBAREAS 1 THROUGH 19 WITH PROD. RIGHTS

4/23/10

SUB AREA	NO. OF WELLS	NO. OF OWNERS	1966	1967	1968	1969	1970	1971	1972	1973
	3	2	0	1,488	2,522	4,218	0	0	0	
01	270	111	70,664	70,216	67,863	74,099	57,929	54,773	51,042	58,316
02	22	8	3,799	3,749	4,438	4,246	4,733	4,369	4,855	5,563
03	67	41	3,257	3,145	4,011	3,270	4,075	4,011	4,450	4,606
05	246	78	30,210	30,080	31,696	25,477	21,617	17,020	19,629	22,763
06	6	4	21	196	302	257	275	219	161	122
08	146	53	7,327	8,638	11,437	7,873	8,888	7,408	6,197	5,389
10	3	2	22	27	22	32	24	24	18	16
13	10	4	536	501	477	547	465	419	324	388
14	171	86	20,106	20,506	20,763	17,275	19,168	23,447	25,779	23,605
15	148	61	6,810	6,619	6,054	5,720	6,185	5,269	4,511	4,654
16	4	1	41	43	60	62	87	78	68	55
17	2	2	0	0	0	0	0	0	0	
18	172	79	20,910	21,741	21,104	19,320	24,017	25,150	25,301	24,930
TOTALS	1,270	532	163,703	166,957	170,749	162,396	147,463	142,187	142,335	150,407

EXHIBIT 16

Golden State Water Company Pumping Well Data Files

Two Excel files containing data from 20 wells operated by Golden State Water Company within the Centro Subarea are here:

<https://bhfs.sharefile.com/share/view/sc4bbae97dcb44d288d59e7da82922368>.

One file (Mountain Desert Production Data v4 Barstow only.xlsx) contains pumping data collected from GSWC wells by staff between 1996 through June 2024. The other file (Mountain Desert Water Levels v2 Barstow.xlsx) contains static and pumping water level data collected from GSWC wells by staff between 1996 through June 2024.

Should you have any issues accessing these files, please contact Mack Carlson at mcarlson@bhfs.com or (805) 963-7000 for assistance.

PROOF OF SERVICE

I am over the age of eighteen years and not a party to the within-entitled action. I am employed in Santa Barbara County, California. My business address is Brownstein Hyatt Farber Schreck, LLP, 1021 Anacapa Street, 2nd Floor, Santa Barbara, California 93101-2711. My electronic service address is Meldridge@bhfs.com. On September 5, 2024, I served a copy of the following document(s):

GOLDEN STATE WATER COMPANY'S EVIDENCE IN SUPPORT OF MOTION TO ENFORCE JUDGMENT - VOLUME 3

X BY E-MAIL OR ELECTRONIC TRANSMISSION: I caused a copy of the document(s) listed above to be sent to the persons at the e-mail addresses listed below

William J. Brunick, Esq.
Leland P. McElhaney, Esq.
Brunick, McElhaney & Kennedy, PLC
P. O. Box 13130
San Bernardino, CA 92423-3130
Email: bbrunick@bmklawplc.com
lmcelhaney@bmklawplc.com

Attorneys for Defendant/Cross-Complainant
Mojave Water Agency

Valerie Wiegenstein
Jeffrey D. Ruesch
Watermaster Services Managers
Mojave Basin Area Watermaster
Mojave Water Agency
13846 Conference Center Drive
Apple Valley, CA 92307
Email: vwiegenstein@MojaveWater.org
jruesch@mojavewater.org

Mojave Basin Area Watermaster

I declare under penalty of perjury under the laws of the State of California that the above is true and correct. Executed on September 5, 2024, at Santa Barbara, California.


Melissa Eldridge

PROOF OF SERVICE

**STATE OF CALIFORNIA }
COUNTY OF SAN BERNARDINO}**

I am employed in the County of the San Bernardino, State of California. I am over the age of 18 and not a party to the within action; my business address is 13846 Conference Center Drive, Apple Valley, California 92307.

On September 6, 2024, the document(s) described below were served pursuant to the Mojave Basin Area Watermaster’s Rules and Regulations paragraph 8.B.2 which provides for service by electronic mail upon election by the Party or paragraph 10.D, which provides that Watermaster shall mail a postcard describing each document being served, to each Party or its designee according to the official service list, a copy of which is attached hereto, and which shall be maintained by the Mojave Basin Area Watermaster pursuant to Paragraph 37 of the Judgment. Served documents will be posted to and maintained on the Mojave Water Agency’s internet website for printing and/or download by Parties wishing to do so.

Document(s) filed with the court and served herein are described as follows:

**GOLDEN STATE WATER COMPANY’S EVIDENCE IN SUPPORT OF
MOTION TO ENFORCE JUDGMENT – VOLUME 3
(Pages GSWC 0801 - GSWC 0987)**

 X (STATE) I declare under penalty of perjury under the laws of the State of California that the above is true and correct.

Executed on September 6, 2024 at Apple Valley, California.



Jeffrey D. Ruesch

Mojave Basin Area Watermaster Service List as of September 06, 2024

Attn: Roberto Munoz
35250 Yermo, LLC
11273 Palms Blvd., Ste. D.
Los Angeles, CA 90066-2122

Attn: John McCallum
Abshire, David V.
PO Box # 2059
Lucerne Valley, CA 92356-2059

Attn: Dwayne Oros
Adelanto, City Of
11600 Air Expressway
Adelanto, CA 92301-1914

(adesdevon@gmail.com)
Ades, John and Devon (via email)

Attn: Pedro Dumaua
(pdumaua@ducommun.com)
Aerochem, Inc. (via email)
4001 El Mirage Rd.
Adelanto, CA 92301-9489

Attn: Lori Clifton (lclifton@robar.com)
Agcon, Inc. (via email)
17671 Bear Valley Road
Hesperia, CA 92345-4902

Attn: Chun Soo and Wha Ja Ahn
(chunsooahn@naver.com)
Ahn Revocable Living Trust (via email)
P. O. Box 45
Apple Valley, CA 92307-0001

Attn: Simon Ahn (ssahn58@gmail.com)
Ahn Revocable Trust (via email)
29775 Hunter Road
Murrieta, CA 92563-6710

Attn: Chun Soo Ahn
(davidahnmd@gmail.com,
chunsooahn@naver.com;
davidahn0511@gmail.com)
Ahn, Chun Soo and David (via email)
P. O. Box 45
Apple Valley, CA 92307-0001

Attn: Chun Soo Ahn
(chunsooahn@naver.com)
Ahn, Chun Soo and Wha Ja (via email)
P. O. Box 45
Apple Valley, CA 92307-0001

Ake, Charles J. and Marjorie M.
2301 Muriel Drive, Apt. 67
Barstow, CA 92311-6757

Attn: Paul Tsai (paul@ezzlife.com)
America United Development, LLC (via
email)
19625 Shelyn Drive
Rowland Heights, CA 91748-3246

Attn: Ana Chavez
American States Water Company
160 Via Verde, Ste. 100
San Dimas, CA 91773-5121

Anderson, Ross C. and Betty J.
13853 Oakmont Dr.
Victorville, CA 92395-4832

Attn: Daniel B. Smith (avfwd@gmail.com)
Apple Valley Foothill County Water District
(via email)
22545 Del Oro Road
Apple Valley, CA 92308-8206

Attn: Matthew Patterson
Apple Valley Heights County Water District
P. O. Box 938
Apple Valley, CA 92308-0938

Attn: Matthew Schulenberg
Apple Valley Unified School District
12555 Navajo Road
Apple Valley, CA 92308-7256

Attn: Emely and Joe Saltmeris
Apple Valley View Mutual Water Company
P. O. Box 3680
Apple Valley, CA 92307-0072

Attn: Tina Kuhns
Apple Valley, Town Of
14955 Dale Evans Parkway
Apple Valley, CA 92307-3061

(ArchibekFarms@gmail.com;
Sandi.Archibek@gmail.com)
Archibek, Eric (via email)
41717 Silver Valley Road
Newberry Springs, CA 92365-9517

Avila, Angel and Evalia
1523 S. Visalia
Compton, CA 90220-3946

Attn: Sheré R. Bailey
(LegalPeopleService@gmail.com)
Bailey 2007 Living Revocable Trust, Sheré R.
(via email)
10428 National Blvd
Los Angeles, CA 90034-4664

Attn: Daniel Shaw (barhwater@gmail.com)
Bar H Mutual Water Company (via email)
P. O. Box 844
Lucerne Valley, CA 92356-0844

Barber, James B.
43774 Cottonwood Road
Newberry Springs, CA 92365

Attn: John Munoz
(barlenwater@hotmail.com);
Bar-Len Mutual Water Company (via email)
P. O. Box 77
Barstow, CA 92312-0077

Attn: Curtis Palmer
Baron, Susan and Palmer, Curtis
141 Road 2390
Aztec, NM 87410-9322

Attn: Jennifer Riley (hriley@barstowca.org)
Barstow, City of (via email)
220 East Mountain View Street -Suite A
Barstow, CA 92311

Mojave Basin Area Watermaster Service List as of September 06, 2024

Bartels, Gwendolyn J.
156 W 100 N
Jerome, ID 83338-5256

Attn: Barbara Davisson
Bass Trust, Newton T.
14924 Chamber Lane
Apple Valley, CA 92307-4912

Attn: Remo E. Bastianon
Bastianon Revocable Trust
9484 Iroquois Rd.
Apple Valley, CA 92308-9151

Attn: Mike Beinschroth
(Beinschroth@gmail.com)
Beinschroth Family Trust (via email)
18794 Sentenac Road
Apple Valley, CA 92307-5342

Beinschroth, Andy Eric
6719 Deep Creek Road
Apple Valley, CA 92308-8711

Attn: Chuck Bell (Chuckb193@outlook.com;
Chuckb193@outlook.com)
Bell, Charles H. Trust dated March 7, 2014
(via email)
P. O. Box 193
Lucerne Valley, CA 92356-0193

Best, Byron L.
21461 Camino Trebol
Lake Forest, CA 92630-2011

Attn: Deborah Stephenson
(stephenson@dmsnaturalresources.com;
Jason.Murray@bnsf.com;
Blaine.Bilderback@bnsf.com)
BNSF Railway Company (via email)
602 S. Ferguson Avenue, Suite 2
Bozeman, MT 59718-

Attn: Deborah Stephenson
(stephenson@dmsnaturalresources.com)
BNSF Railway Company (via email)
602 S. Ferguson Avenue, Suite 2
Bozeman, MT 59718-6483

Borja, Leonil T. and Tital L.
20784 Iris Canyon Road
Riverside, CA 92508-

Box, Geary S. and Laura
P. O. Box 402564
Hesperia, CA 92340-2564

Attn: Marvin Brommer
Brommer House Trust
9435 Strathmore Lane
Riverside, CA 92509-0941

Attn: Valeria Brown
Brown Family Trust Dated August 11, 1999
26776 Vista Road
Helendale, CA 92342-9789

Brown, Jennifer
10001 Choiceana Ave.
Hesperia, CA 92345

Bruneau, Karen
19575 Bear Valley Rd.
Apple Valley, CA 92308-5104

(irim@aol.com)
Bryant, Ian (via email)
15434 Sequoia Avenue - Office
Hesperia, CA 92345-1667

(bubierbear@msn.com)
Bubier, Diane Gail (via email)
46263 Bedford Rd.
Newberry Springs, CA 92365-9819

Attn: Noah Furie
Budget Finance Company
PO BOX 641339
Los Angeles, CA 90064-6339

Bunnell, Dick
8589 Volga River Circle
Fountain Valley, CA 92708-5536

(kjbco@yahoo.com)
Bush, Kevin (via email)
7768 Sterling Ave.
San Bernardino, CA 92410-4741

Attn: Kristie Wright
(Kristie.Wright@associa.us)
Calico Lakes Homeowners Association (via
email)
11860 Pierce Street, Suite 100
Riverside, CA 92505-5178

Attn: William DeCoursey
(michael.lemke@dot.ca.gov;
William.Decoursey@dot.ca.gov)
California Department Of Transportation (via
email)
175 W. Cluster
San Bernardino, CA 92408-1310

Attn: Robert W. Bowcock
CalMat Company
405 N. Indian Hill Blvd.
Claremont, CA 91711-4614

Attn: Catalina Fernandez-Moores
(celias@calportland.com)
CalPortland Company - Agriculture (via
email)
P. O. Box 146
Oro Grande, CA 92368-0146

Attn: Catalina Fernandez-Moores
(cfernandez@calportland.com)
CalPortland Company - Oro Grande Plant (via
email)
P. O. Box 146
Oro Grande, CA 92368-0146

Attn: Tony Camanga
Camanga, Tony and Marietta
2309 Highland Heights Lane
Carrollton, TX 75007-2033

Attn: Myron Campbell II
Campbell, M. A. and Dianne
19327 Cliveden Ave
Carson, CA 90746-2716

Mojave Basin Area Watermaster Service List as of September 06, 2024

Carlton, Susan
445 Via Colusa
Torrance, CA 90505-

Attn: Denise Parra
Casa Colina Foundation
P.O. Box 1760
Lucerne Valley, CA 92356

Attn: Danielle Stewart
(danielle.stewart@wildlife.ca.gov;
Richard.Kim@wildlife.ca.gov;
Alisa.Ellsworth@wildlife.ca.gov)
CDFW - Camp Cady (via email)
4775 Bird Farm Road
Chino Hills, CA 91709-3175

Attn: Jared Beyeler
CDFW - Mojave Narrows Regional Park
222 W. Hospitality Lane, 2nd Floor
San Bernardino, CA 92415-0023

Attn: Paco Cabral
(paco.cabral@wildlife.ca.gov;
askregion6@wildlife.ca.gov;
aaron.johnson@wildlife.ca.gov)
CDFW - Mojave River Fish Hatchery (via
email)
12550 Jacaranda Avenue
Victorville, CA 92395-5183

Attn: Environmental
(valorie.moore@cemex.com)
Cemex, Inc. (via email)
16888 North E. Street
Victorville, CA 92394-2999

Attn: Jennifer Cutler
Center Water Company
P. O. Box 616
Lucerne Valley, CA 92356-0616

Attn: Nancy Ryman
Chamisal Mutual Water Company
P. O. Box 1444
Adelanto, CA 92301-2779

Attn: Carl Pugh (talk2betty@aol.com;
cpugh3@aol.com)
Cheyenne Lake, Inc. (via email)
44658 Valley Center Rd.
Newberry Springs, CA 92365-

Attn: Micahel Chisram
Chisram, et al.
414 S. Lincoln Ave.
Monterey Park, CA 91775-3323

Choi, Yong Il and Joung Ae
34424 Mountain View Road
Hinkley, CA 92347-9412

(joan.chong7@gmail.com;
joancksp@hotmail.com)
Chong, Joan (via email)
10392 Shady Ridge Drive
Santa Ana, CA 92705-7509

Christison, Joel
P. O. Box 2635
Big River, CA 92242-2635

Attn: Hwa-Yong Chung
Chung, et al.
11446 Midway Ave.
Lucerne Valley, CA 92356-8792

Clark, Arthur
P. O. Box 4513
Blue Jay, CA 92317-4513

Attn: Manoucher Sarbaz
Club View Partners
9903 Santa Monica Blvd., PMB #541
Beverly Hills, CA 90212-1671

Attn: Jaehwan Lee
Come Mission, Inc.
9965 Baker Road
Lucerne Valley, CA 92365-8490

Conner, William H.
11535 Mint Canyon Rd.
Agua Dulce, CA 91390-4577

Contratto, Ersula
13504 Choco Road
Apple Valley, CA 92308-4550

Attn: George Starke
Corbridge, Linda S.
8743 Vivero St
Rancho Cucamonga, CA 91730-

Cross, Sharon I.
P. O. Box 922
Lucerne Valley, CA 92356

Attn: Jay Hooper (jayho123@gmail.com)
Crown Cambria, LLC (via email)
9860 Gidley St.
El Monte, CA 91731-1110

Attn: Alessia Morris
Crystal Lakes Property Owners Association
P. O. Box 351
Yermo, CA 92398-0351

(dacostadean@gmail.com)
DaCosta, Dean Edward (via email)
32307 Foothill Road
Lucerne Valley, CA 92356-8526

Attn: Shanna Mitchell (daggettcsd@aol.com;
daggettcsd@outlook.com;
daggettwater427@gmail.com)
Daggett Community Services District (via
email)
P. O. Box 308
Daggett, CA 92327-0308

Attn: Steve and Dana Rivett
Daggett Ranch, LLC
P. O. Box 112
Daggett, CA 92327-0112

Attn: James Kelly
(James.Kelly@clearwayenergy.com)
Daggett Solar Power 3 LLC (via email)
5780 Fleet Street, Suite 130
Carlsbad, CA 92008-4715

Mojave Basin Area Watermaster Service List as of September 06, 2024

(ron@dadcopowerandlights.com)
Dahlquist, George R. (via email)
8535 Vine Valley Drive
Sun Valley, CA 91352-

Darr, James S.
40716 Highway 395
Boron, CA 93516

Attn: Alan L. De Jong
De Jong Family Trust
46561 Fairview Road
Newberry Springs, CA 92365-9230

Attn: Randy Wagner
Dennison, Quentin D. - Clegg, Frizell and Joke
44579 Temescal Street
Newberry Springs, CA 92365

Attn: Marie McDaniel
Desert Dawn Mutual Water Company
P. O. Box 392
Lucerne Valley, CA 92356-0392

Attn: Penny Zaritsky
(pennyzaritsky2000@yahoo.com)
Desert Girlz LLC (via email)
P. O. Box 709
Lucerne Valley, CA 92356-0709

Attn: Denise Courtney
Desert Springs Mutual Water Company
P. O. Box 396
Lucerne Valley, CA 92356-0396

Attn: Debby Wyatt
DLW Revocable Trust
13830 Choco Rd.
Apple Valley, CA 92307-5525

Attn: Judith Dolch-Partridge, Trustee
Dolch Living Trust Robert and Judith
4181 Kramer Lane
Bellingham, WA 98226-7145

Donaldson, Jerry and Beverly
16736 B Road
Delta, CO 81416-8501

Attn: Jeffery Lidman
Dora Land, Inc.
P. O. Box 1405
Apple Valley, CA 92307-0026

Attn: David Dorrance
Dorrance, David W. and Tamela L.
118 River Road Circle
Wimberley, TX 78676-5060

Attn: David Looper
Douglass, Tina
P.O. Box 1730
Lucerne Valley, CA 92356-

Dowell, Leonard
345 E Carson St.
Carson, CA 90745-2709

Evenson, Edwin H. and Joycelaine C.
P. O. Box 66
Oro Grande, CA 92368-0066

Attn: Stephanie L. Evert
(severt2166@aol.com)
Evert Family Trust (via email)
19201 Parker Circle
Villa Park, CA 92861-1302

Attn: David Dittenmore
(d2dittenmore@bop.gov; rslayman@bop.gov)
Federal Bureau of Prisons, Victorville (via email)
P. O. Box 5400
Adelanto, CA 92301-5400

Fejfar, Monica Kay
34080 Ord Street
Newberry Springs, CA 92365-9791

(wwcc0626@gmail.com)
Feng, Jinbao (via email)
33979 Fremont Road
Newberry Springs, CA 92365-9136

(afc30@yahoo.com)
Fernandez, Arturo (via email)
28 Calle Fortuna
Rancho Santa Margarita, CA 92688-2627

Ferro, Dennis and Norma
1311 1st Ave. N
Jacksonville Beach, FL 32250-3512

(ropingmom3@yahoo.com)
Finch, Jenifer (via email)
9797 Lewis Lane
Apple Valley, CA 92308-8357

Attn: Alex and Jerrica Liu
(alexliu1950@gmail.com; alexroseanneliu@yahoo.com)
First CPA LLC (via email)
46669 Valley Center Rd
Newberry Springs, CA 92365-

Attn: Mike Fischer
(carlsfischer@hotmail.com; fischer@fischercompanies.com)
Fischer Revocable Living Trust (via email)
1372 West 26th St.
San Bernardino, CA 92405-3029

Attn: Paul Johnson
Fisher Trust, Jerome R.
7603 Hazeltine Ave
Van Nuys, CA 91405-1423

Attn: Daisy Cruz
Foothill Estates MHP, LLC
9454 Wilshire Blvd., Ste. 920
Beverly Hills, CA 90212-2925

(cfrates@renewablegroup.com)
Frates, D. Cole (via email)
113 S La Brea Ave., 3rd Floor
Los Angeles, CA 90036-2998

Attn: Deborah A. Friend
Friend, Joseph and Deborah
P. O. Box 253
Barstow, CA 92312-0253

Attn: Mark Asay (bettybrock@ironwood.org; waltbrock@ironwood.org)
Fundamental Christian Endeavors, Inc. (via email)
49191 Cherokee Road
Newberry Springs, CA 92365

Gabrych, Eugene
2006 Old Highway 395
Fallbrook, CA 92028

Mojave Basin Area Watermaster Service List as of September 06, 2024

Gabrych, Eugene
2006 Old Highway 395
Fallbrook, CA 92028-8816

Gaeta, Miguel and Maria
9366 Joshua Avenue
Lucerne Valley, CA 92356-8273

Attn: Jay Storer
Gaeta, Trinidad
10551 Dallas Avenue
Lucerne Valley, CA 92356

Garcia, Daniel
223 Rabbit Trail
Lake Jackson, TX 77566-3728

Attn: Sang Hwal Kim
Gardena Mission Church, Inc.
P. O. Box 304
Lucerne Valley, CA 92356-0304

Garg, Om P.
358 Chorus
Irvine, CA 92618-1414

Attn: Brent Peterson
Gayjikian, Samuel and Hazel
34534 Granite Road
Lucerne Valley, CA 92356-

Attn: Jeffrey Edwards
(jedwards@fbremediation.com)
GenOn California South, LP (via email)
P. O. Box 337
Daggett, CA 92327-0337

(Nereida.Gonzalez@gswater.com,
ana.chavez@gswater.com)
Golden State Water Company (via email)
160 Via Verde, Ste. 100
San Dimas, CA 91773-5121

Attn: Nereida Gonzalez
(ana.chavez@gswater.com,
Nereida.Gonzalez@gswater.com)
Golden State Water Company (via email)
160 Via Verde, Ste. 100
San Dimas, CA 91773-5121

Attn: Scot Gasper
Gordon Acres Water Company
P. O. Box 1035
Lucerne Valley, CA 92356-1035

Gray, George F. and Betty E.
975 Bryant
Calimesa, CA 92320-1301

Attn: Brian E. Bolin
Green Acres Estates
P. O. Box 29
Apple Valley, CA 92307-0001

Attn: Eric Archibek
Green Hay Packers LLC
41717 Silver Valley Road
Newberry Springs, CA 92365-9517

Attn: Nick Grill (terawatt@juno.com)
Grill, Nicholas P. and Millie D. (via email)
35350 Mountain View Rd
Hinkley, CA 92347-9613

Gubler, Hans
P. O. Box 3100
Landers, CA 92285

Attn: Tamara J Skoglund
(TamaraMcKenzie@aol.com)
Gulbranson, Merlin (via email)
511 Minnesota Ave W
Gilbert, MN 55741-

Gutierrez, Jose and Gloria
24116 Santa Fe
Hinkley, CA 92347

Attn: Bryan C. Haas and Mary H. Hinkle
(resrvc4you@aol.com)
Haas, Bryan C. and Hinkle, Mary H. (via
email)
14730 Tigertail Road
Apple Valley, CA 92307-5249

(hackbarthoffice@gmail.com)
Hackbarth, Edward E. (via email)
12221 Poplar Street, Unit #3
Hesperia, CA, CA 92344-9287

Attn: Doug and Cheryl Hamilton
Hamilton Family Trust
19945 Round Up Way
Apple Valley, CA 92308-8338

Attn: William Handrinos
Handrinos, Nicole A.
1140 Parkdale Rd.
Adelanto, CA 92301-9308

Hang, Phu Quang
645 S. Shasta Street
West Covina, CA 91791-2818

Attn: Donald F. Hanify
Hanify, Michael D., dba - White Bear Ranch
PO BOX 1021
Yermo, CA 92398-1021

Attn: Matt Wood
(Matthew.wood@martinmarietta.com)
Hanson Aggregates WRP, Inc. (via email)
P. O. Box 1115
Corona, CA 92878-1115

Attn: Mary Jane Hareson
Hareson, Nicholas and Mary
1737 Anza Avenue
Vista, CA 92084-3236

Attn: Kenny Harmsen (harmscow@aol.com)
Harmsen Family Trust (via email)
23920 Community Blvd.
Hinkley, CA 92347-9721

Harter, Joe and Sue
10902 Swan Lake Road
Klamath Falls, OR 97603-9676

(harvey1.92356@gmail.com)
Harvey, Lisa M. (via email)
P. O. Box 1187
Lucerne Valley, CA 92356-

Haskins, James J.
11352 Hesperia Road, #2
Hesperia, CA 92345-2165

Mojave Basin Area Watermaster Service List as of September 06, 2024

Hass, Pauline L.
P. O. Box 273
Newberry Springs, CA 92365-

Attn: Craig Carlson (kcox@helendalecsd.org;
ccarlson@helendalecsd.org)
Helendale Community Services District (via
email)
P. O. Box 359
Helendale, CA 92342-0359

Attn: Joshua Maze
Helendale School District
P. O. Box 249
Helendale, CA 92342-0249

Attn: Jeff Gallistel
Hendley, Rick and Barbara
P. O. Box 972
Yermo, CA 92398-0972

Hensley, Mark P.
35523 Mountain View Rd
Hinkley, CA 92347-9613

Attn: Jeremy McDonald
(jmcdonald@cityofhesperia.us)
Hesperia - Golf Course, City of (via email)
9700 Seventh Avenue
Hesperia, CA 92345-3493

Attn: Janie Martines
(janiemartines@gmail.com)
Hesperia Venture I, LLC (via email)
10 Western Road
Wheatland, WY 82201-8936

Attn: Jeremy McDonald
(jmcdonald@cityofhesperia.us)
Hesperia Water District (via email)
9700 7th Avenue
Hesperia, CA 92345-3493

Attn: Jeremy McDonald
(tsouza@cityofhesperia.us)
Hesperia, City of (via email)
9700 Seventh Avenue
Hesperia, CA 92345-3493

Attn: Carabeth Carter ()
Hettinga Revocable Trust (via email)
P. O. Box 455
Ehrenberg, AZ 84334-0455

Attn: Lisset Sardeson
Hi Desert Mutual Water Company
23667 Gazana Street
Barstow, CA 92311

(leehiett@hotmail.com)
Hiett, Harry L. (via email)
P. O. Box 272
Daggett, CA 92327-0272

Attn: Robert W. Bowcock
High Desert Associates, Inc.
405 North Indian Hill Blvd.
Claremont, CA 91711-4614

Attn: Lori Clifton (lclifton@robar.com)
Hi-Grade Materials Company (via email)
17671 Bear Valley Rd
Hesperia, CA 92345-4902

Attn: Lori Clifton (lclifton@robar.com)
Hi-Grade Materials Company (via email)
17671 Bear Valley Road
Hesperia, CA 92345-4902

Attn: Frank Hilarides
Hilarides 1998 Revocable Family Trust
37404 Harvard Road
Newberry Springs, CA 92365

Attn: Katherine Hill (Khill9@comcast.net)
Hill Family Trust and Hill's Ranch, Inc. (via
email)
84 Dewey Street
Ashland, OR 97520-

Attn: Anne Roark
Hitchin Lucerne, Inc.
P. O. Box 749
Lucerne Valley, CA 92356-0749

Ho, Ting-Seng and Ah-Git
P.O. Box 20001
Bakersfield, CA 93390-0001

Attn: Joan Rohrer
Hollister, Robert H. and Ruth M.
22832 Buendia
Mission Viejo, CA 92691-

Attn: Jeffrey R Holway and Patricia Gage
(patricia.gage@yahoo.com)
Holway Jeffrey R and Patricia Gage (via
email)
1401 Wewatta St. #1105
Denver, CO 80202-1348

Holway, Jeffrey R
1401 Wewatta St. #1105
Denver, CO 80202-1348

Attn: Katherine K. Hsu
Holy Heavenly Lake, LLC
1261 S. Lincoln Ave.
Monterey Park, CA 91755-5017

Attn: Paul Hong
Hong, Paul B. and May
P. O. Box #1432
Covina, CA 91722-0432

Attn: Sandra D. Hood
Hood Family Trust
2142 W Paseo Del Mar
San Pedro, CA 90732-4557

Attn: Barry Horton
Horton Family Trust
47716 Fairview Road
Newberry Springs, CA 92365-9258

Attn: Ester Hubbard
Hubbard, Ester and Mizuno, Arlean
47722 Kiloran St.
Newberry Springs, CA 92365-9529

Attn: Paul Johnson
Huerta, Hector
25684 Community Blvd
Barstow, CA 92311-

(hconnie630@gmail.com)
Hunt, Connie (via email)
39392 Burnside Loop
Astoria, OR 97103-8248

Attn: Ralph Hunt
Hunt, Ralph M. and Lillian F.
P. O. Box 603
Yermo, CA 92398-0603

Mojave Basin Area Watermaster Service List as of September 06, 2024

Attn: Daniel and Karen Gray
(calivolunteer@verizon.net)
Hyatt, James and Brenda (via email)
31726 Fremont Road
Newberry Springs, CA 92365

(econorx@yahoo.com)
Im, Nicholas Nak-Kyun (via email)
23329 Almarosa Ave.
Torrance, CA 90505-3121

Irvin, Bertrand W.
3224 West 111th Street
Inglewood, CA 90303-

Attn: James Jackson Jr.
Jackson, James N. Jr Revocable Living Trust
1245 S. Arlington Avenue
Los Angeles, CA 90019-3517

Attn: Lawrence Dean
Jackson, Ray Revocable Trust No. 45801
P.O. Box 8250
Redlands, CA 92375-1450

Attn: Audrey Goller
(audrey.goller@newportpacific.com)
Jamboree Housing Corporation (via email)
15940 Stoddard Wells Rd - Office
Victorville, CA 92395-2800

Attn: Gary A. Ledford
(gleddream@gmail.com)
Jess Ranch Water Company (via email)
906 Old Ranch Road
Florissant, CO 80816-

Attn: Cynthia Mahoney
(cyndisue87@yahoo.com)
Johnson, Carlean F. Trust Dated 10/29/2004
(via email)
8626 Deep Creek Road
Apple Valley, CA 92308-8769

Attn: Paul Johnson
(johnsonfarming@gmail.com)
Johnson, Paul - Industrial (via email)
10456 Deep Creek Road
Apple Valley, CA 92308-8330

Johnson, Ronald
1156 Clovis Circle
Dammeron Valley, UT 84783-5211

Attn: Lawrence W. Johnston
Johnston, Harriet and Johnston, Lawrence W.
P. O. Box 401472
Hesperia, CA 92340-1472

Attn: Magdalena Jones
(mygoldenbiz9@gmail.com)
Jones Trust dated March 16, 2002 (via email)
35424 Old Woman Springs Road
Lucerne Valley, CA 92356-7237

Attn: Paul Jordan
Jordan Family Trust
1650 Silver Saddle Drive
Barstow, CA 92311-2057

Attn: Ray Gagné
Jubilee Mutual Water Company
P. O. Box 1016
Lucerne Valley, CA 92356

Attn: Lee Logsdon
Juniper Riviera County Water District
P. O. Box 618
Lucerne Valley, CA 92356-0618

Attn: Ash Karimi
Karimi, Hooshang
1254 Holmby Ave
Los Angeles, CA 90024-

Attn: Robert R. Kasner
(Robertkasner@aol.com)
Kasner Family Limited Partnership (via email)
11584 East End Avenue
Chino, CA 91710-

(Robertkasner@aol.com)
Kasner, Robert (via email)
11584 East End Avenue
Chino, CA 91710-1555

Attn: Martin A and Mercedes Katcher
Katcher, August M. and Marceline
12928 Hyperion Lane
Apple Valley, CA 92308-4565

Kemp, Robert and Rose
48441 National Trails Highway
Newberry Springs, CA 92365

Attn: Peggy Shaughnessy
Kemper Campbell Ranch
10 Kemper Campbell Ranch Road - Office
Victorville, CA 92395-3357

Kim, Jin S. and Hyun H.
6205 E Garnet Circle
Anaheim, CA 92807-4857

Attn: Alan and Annette De Jong
Kim, Joon Ho and Mal Boon Revocable Trust
46561 Fairview Road
Newberry Springs, CA 92365-9230

(juskim67@yahoo.com)
Kim, Ju Sang (via email)
1225 Crestview Dr
Fullerton, CA 92833-2206

Kim, Seon Ja
34981 Piute Road
Newberry Springs, CA 92365-9548

Attn: Richard Koering
Koering, Richard and Koering, Donna
40909 Mountain View Road
Newberry Springs, CA 92365-9414

Attn: Catherine Cerri
(ccerri@lakearrowheadcsd.com)
Lake Arrowhead Community Services District
(via email)
P. O. Box 700
Lake Arrowhead, CA 92352-0700

Mojave Basin Area Watermaster Service List as of September 06, 2024

Attn: Claire Cabrey
(HandleWithClaire@aol.com;
mjaynes@mac.com)
Lake Jodie Property Owners Association (via
email)
8581 Santa Monica Blvd., #18
West Hollywood, CA 90069-4120

(PhillipLam99@Yahoo.com)
Lam, Phillip (via email)
864 Sapphire Court
Pomona, CA 91766-5171

Attn: Robert Lawrence Jr.
Lawrence, William W.
P. O. Box 98
Newberry Springs, CA 92365

Lee, Doo Hwan
P. O. Box 556
Lucerne Valley, CA 92356-0556

Attn: Virginia Janovsky
(virginiajanovsky@yahoo.com)
Lem, Hoy (via email)
17241 Bullock St.
Encino, CA 91316-1473

Attn: Billy Liang
Liang, Yuan - I and Tzu - Mei Chen
4192 Biscayne St
Chino, CA 91710-3196

Attn: Manshan Gan
Lo, et al.
5535 N Muscatel Ave
San Gabriel, CA 91776-1724

(lowgo.dean@gmail.com)
Low, Dean (via email)
3 Panther Creek Ct.
Henderson, NV 89052-

Attn: Manoucher Sarbaz
Lucerne Valley Partners
9903 Santa Monica Blvd., PMB #541
Beverly Hills, CA 90212-1671

Attn: Nancy Lan
Lake Waikiki
230 Hillcrest Drive
La Puente, CA 91744-4816

(jlanglej@kurschgroup.com)
Langley, James (via email)
12277 Apple Valley Road, Ste. #120
Apple Valley, CA 92308-1701

Lawson, Ernest and Barbara
20277 Rock Springs Road
Apple Valley, CA 92308-8740

Attn: Sepoong & Woo Poong Lee
Lee, et al., Sepoong and Woo Poong
#6 Ensueno East
Irvine, CA 92620-

Lenhart, Ronald and Toni
4474 W. Cheyenne Drive
Eloy, AZ 85131-3410

Attn: Eric Larsen
(eric.larsen@libertyutilities.com;
tony.pena@libertyutilities.com)
Liberty Utilities (Apple Valley Ranchos
Water) Corp. (via email)
P. O. Box 7005
Apple Valley, CA 92307

Attn: Neal Davies (ndavies@terra-gen.com;
dkelly@terra-gen.com)
Lockhart Land Holding, LLC (via email)
43880 Harper Lake Road
Hinkley, CA 92347-

Lua, Michael T. and Donna S.
18838 Aldridge Place
Rowland Heights, CA 91748-4890

Attn: Marian Walent
(LVVMC677@gmail.com)
Lucerne Vista Mutual Water Company (via
email)
P. O. Box 677
Lucerne Valley, CA 92356-0677

Attn: c/o J.C. UPMC, Inc. Lori Rodgers
(ljm9252@aol.com;
timrohmbuilding@gmail.com)
Lake Wainani Owners Association (via email)
2812 Walnut Avenue, Suite A
Tustin, CA 92780-7053

Attn: Vanessa Laosy
Lavanh, et al.
18203 Yucca St.
Hesperia, CA 92345-

Attn: Anna K. Lee (aklee219@gmail.com)
Lee, Anna K. and Eshban K. (via email)
10979 Satsuma St
Loma Linda, CA 92354-6113

Lee, Vin Jang T.
42727 Holcomb Trl
Newberry Springs, CA 92365

Attn: Brad Francke
LHC Alligator, LLC
P. O. Box 670
Upland, CA 91785-0670

Attn: James Lin
Lin, Kuan Jung and Chung, Der-Bing
2026 Turnball Canyon
Hacienda Heights, CA 91745-

Attn: Patricia Miranda
Lopez, Baltazar
12318 Post Office Rd
Lucerne Valley, CA 92356-

Attn: Gwen L. Bedics
Lucerne Valley Mutual Water Company
P. O. Box 1311
Lucerne Valley, CA 92356

Attn: Eugene R. & Vickie R. Bird
M Bird Construction
1613 State Street, Ste. 10
Barstow, CA 92311-4162

Mojave Basin Area Watermaster Service List as of September 06, 2024

Attn: Maria Martinez
M.B. Landscaping and Nursery, Inc.
6831 Lime Avenue
Long Beach, CA 90805-1423

Attn: Robert Saidi
Mahjoubi, Afsar S.
46622 Fairview Road
Newberry Springs, CA 92365

Attn: Jimmy Berry
Manning, Sharon S.
19332 Balan Road
Rowland Heights, CA 91748-4017

Attn: Allen Marcroft
Marcroft, James A. and Joan
P. O. Box 519
Newberry Springs, CA 92365

Attn: James M. Hansen, Jr. (gm@mrcwd.org;
gmmrcwd@gmail.com)
Mariana Ranchos County Water District (via
email)
9600 Manzanita Street
Apple Valley, CA 92308-8605

Marshall, Charles
32455 Lakeview Road
Newberry Springs, CA 92365-9482

Martin, Michael D. and Arlene D.
32942 Paseo Mira Flores
San Juan Capistrano, CA 92675

Attn: Rod Sexton
McCollum, Charles L.
15074 Spruce St
Hesperia, CA 92345-2950

McKinney, Paula
144 East 72nd
Tacoma, WA 98404-1060

Attn: Olivia L. Mead
Mead Family Trust
31314 Clay River Road
Barstow, CA 92311-2057

Attn: David I. Milbrat
Milbrat, Irving H.
P. O. Box 487
Newberry Springs, CA 92365-0487

Attn: Donna Miller
Miller Living Trust
6124 Parsonage Circle
Milton, FL 32570-8930

Attn: Freddy Garmo (freddy@garmolaw.com)
Minn15 LLC (via email)
5464 Grossmont Center Drive, #300
La Mesa, CA 91942-3035

Attn: David Riddle
(driddle@mitsubishicement.com)
Mitsubishi Cement Corporation (via email)
5808 State Highway 18
Lucerne Valley, CA 92356-8179

Attn: Philip Mizrahie
Mizrahie, et al.
4105 W. Jefferson Blvd.
Los Angeles, CA 90048-

Attn: Thomas A. Hrubik (tahgolf@aol.com)
MLH, LLC (via email)
P. O. Box 2611
Apple Valley, CA 92307-0049

Attn: Sarah Bliss
Mojave Desert Land Trust
60124 29 Palms Highway
Joshua Tree, CA 92252-4130

Attn: Mahnaz Ghamati
(mahnaz.ghamati@atlantica.com)
Mojave Solar, LLC (via email)
42134 Harper Lake Road
Hinkley, CA 92347-9305

Attn: Doug Kerns
(aanabtawi@mojavewater.org)
Mojave Water Agency (via email)
13846 Conference Center Drive
Apple Valley, CA 92307-4377

Attn: Doug Kerns
(tmccarthy@mojavewater.org)
Mojave Water Agency (via email)
13846 Conference Center Drive
Apple Valley, CA 92307-4377

Attn: Manoucher Sarbaz
Monaco Investment Company
9903 Santa Monica Blvd., PMB #541
Beverly Hills, CA 90212-1671

Attn: Ken Elliot (Billie@ElliotPlace.com)
Morris Trust, Julia V. (via email)
7649 Cypress Dr.
Lanexa, VA 23089-9320

Moss, Lawrence W. and Helen J.
38338 Old Woman Springs Road Spc# 56
Lucerne Valley, CA 92356-8116

Attn: Bradford Ray Most
Most Family Trust
39 Sundance Circle
Durango, CO 81303-8131

Attn: Dennis Hills
Mulligan, Robert and Inez
35575 Jakobi Street
Saint Helens, OR 97051-1194

Murphy, Jean
46126 Old National Trails Highway
Newberry Springs, CA 92365-9025

(z.music5909@gmail.com;
zajomusic@gmail.com)
Music, Zajo (via email)
43830 Cottonwood Rd
Newberry Springs, CA 92365-8510

Attn: James Hansen
(gm@marianaranchoswd.org)
Navajo Mutual Water Company (via email)
21724 Hercules St.
Apple Valley, CA 92308-8490

Attn: Billy Liang (flossdaily@hotmail.com;
asaliking@yahoo.com)
New Springs Limited Partnership (via email)
4192 Biscayne St.
Chino, CA 91710-3196

Attn: Jodi Howard
Newberry Community Services District
P. O. Box 220
Newberry Springs, CA 92365-0220

Mojave Basin Area Watermaster Service List as of September 06, 2024

Attn: Jeff Gaastra (jeffgaastra@gmail.com)
Newberry Springs Recreational Lakes
Association (via email)
32935 Dune Road, Space 10
Newberry Springs, CA 92365-

Attn: Mary Ann Norris
Norris Trust, Mary Ann
29611 Exeter Street
Lucerne Valley, CA 92356-8261

Attn: Kenton Eatherton
(keatherton@verizon.net)
NSSL, Inc. (via email)
9876 Moon River Circle
Fountain Valley, CA 92708-7312

Núñez, Luis Segundo
9154 Golden Seal Court
Hesperia, CA 92345-0197

Attn: Pearl or Gail Nunn
Nunn Family Trust
P. O. Box 545
Apple Valley, CA 92307-0010

Attn: Jeff Gaastra (jeffgaastra@gmail.com;
andy@seesmachine.com;
bbswift4044@cox.net)
O. F. D. L., Inc. (via email)
32935 Dune Road, #10
Newberry Springs, CA 92365-9175

Attn: Chun Soo Ahn
(chunsooahn@naver.com)
Oasis World Mission (via email)
P. O. Box 45
Apple Valley, CA 92307-0001

Attn: Kody Tompkins
(ktompkins@barstowca.org)
Odessa Water District (via email)
220 E. Mountain View Street, Suite A
Barstow, CA 92311-2888

Attn: Dorothy Ohai
Ohai, Reynolds and Dorothy
13450 Monte Vista
Chino, CA 91710-5149

Attn: Craig Maetzold
(craig.maetzold@omya.com)
Omya California, Inc. (via email)
7225 Crystal Creek Rd
Lucerne Valley, CA 92356-8646

Attn: John P. Oostdam
Oostdam Family Trust, John P. and Margie K.
24953 Three Springs Road
Hemet, CA 92545-2246

Attn: Nick Higgs
Oro Grande School District
P. O. Box 386
Oro Grande, CA 92368-0386

Attn: Taghi Shoraka
P and H Engineering and Development
Corporation
1423 South Beverly Glen Blvd. Apt. A
Los Angeles, CA 90024-6171

Attn: Jessica Bails (J4Dx@pge.com)
Pacific Gas and Electric Company (via email)
22999 Community Blvd.
Hinkley, CA 92347-9592

Pak, Kae Soo and Myong Hui Kang
P. O. Box 1835
Lucerne Valley, CA 92356-1835

Patino, José
3914 W. 105th Street
Inglewood, CA 90303-1815

(wndrvr@aol.com)
Paustell, Joan Beinschroth (via email)
10275 Mockingbird Ave.
Apple Valley, CA 92308-8303

Pearce, Craig L.
127 Columbus Dr
Punxsutawney, PA 15767-1270

Perko, Bert K.
P. O. Box 762
Yermo, CA 92398-0762

Pettigrew, Dan
285 N Old Hill Road
Fallbrook, CA 92028-2571

Attn: Sean Wright (swright@pphcsd.org;
dbartz@pphcsd.org; llowrance@pphcsd.org)
Phelan Piñon Hills Community Services
District (via email)
4176 Warbler Road
Phelan, CA 92371-8819

Attn: John Poland
Poland, John R. and Kathleen A.
5511 Tenderfoot Drive
Fontana, CA 92336-1156

Polich, Donna
75 3rd Avenue #4
Chula Vista, CA 91910-1714

Porter, Timothy M.
34673 Little Dirt Road
Newberry Springs, CA 92365-9646

Attn: Carin McKay
Precision Investments Services, LLC
791 Price Street, #160
Pismo Beach, CA 93449-2529

Price, Donald and Ruth
933 E. Virginia Way
Barstow, CA 92311-4027

Pruett, Andrea
P. O. Box 37
Newberry Springs, CA 92365

(s_quakenbush@yahoo.com)
Quakenbush, Samuel R. (via email)
236 Iris Drive
Martinsburg, WV 25404-1338

Attn: Ron Herrmann
Quiros, Fransisco J. and Herrmann, Ronald
35969 Newberry Rd
Newberry Springs, CA 92365-9438

Attn: Elizabeth Murena
(waterboy7F8@msn.com; etminav@aol.com)
Rancheritos Mutual Water Company (via
email)
P. O. Box 348
Apple Valley, CA 92307

Mojave Basin Area Watermaster Service List as of September 06, 2024

Reed, Mike
9864 Donaldson Road
Lucerne Valley, CA 92356-8105

Attn: Brian C. Vail (bvail@river-west.com)
Reido Farms, LLC (via email)
2410 Fair Oaks Blvd., Suite 110
Sacramento, CA 95825-7666

(LucerneJujubeFarm@hotmail.com)
Rhee, Andrew N. (via email)
11717 Fairlane Rd, #989
Lucerne Valley, CA 92356-8829

Attn: Kelly Rice
Rice, Henry C. and Diana
31823 Fort Cady Rd.
Newberry Springs, CA 92365-

Attn: Ian Bryant
Rim Properties, A General Partnership
15434 Sequoia Road
Hesperia, CA 92345-1667

Attn: Josie Rios
Rios, Mariano V.
P. O. Box 1864
Barstow, CA 92312-1864

Rivero, Fidel V.
612 Wellesley Drive
Corona, CA 92879-0825

(RayRizvi@Yahoo.com)
Rizvi, S.R Ali (via email)
4054 Allyson Terrace
Freemont, CA 94538-4186

Attn: Bill Taylor or Property Mngr
(billt@rrmca.com)
Robertson's Ready Mix (via email)
200 S. Main Street, Suite 200
Corona, CA 92882-2212

Attn: Susan Sommers (sommerssqz@aol.com)
Rossi Family Trust, James Lawrence Rossi
and Naomi (via email)
P. O. Box 120
Templeton, CA 93465-0120

Attn: Robert Vega
Royal Way
2632 Wilshire Blvd., #480
Santa Monica, CA 90403-4623

Attn: Sam Marich
Rue Ranch, Inc.
P. O. Box 133109
Big Bear Lake, CA 92315-8915

Attn: Dale W. Ruisch
Ruisch Trust, Dale W. and Nellie H.
10807 Green Valley Road
Apple Valley, CA 92308-3690

Attn: Sherwin Shoraka
S and B Brothers, LLC
1423 S. Beverly Glen Blvd., Ste. A
Los Angeles, CA 90024-6171

Attn: Jafar Rashid
(jr123realestate@gmail.com)
S and E 786 Enterprises, LLC (via email)
3300 S. La Cienega Blvd.
Los Angeles, CA 90016-3115

Attn: Sara Fortuna (sarajfortuna@gmail.com;
fourteengkids@aol.com)
Saba Family Trust dated July 24, 2018 (via
email)
212 Avenida Barcelona
San Clemente, CA 92672-5468

Attn: Kanoë Barker
(kanoebarker@yahoo.com)
Sagabean-Barker, Kanoëlolokelani L. (via
email)
42224 Valley Center Rd
Newberry Springs, CA 92365

(BILLU711@Yahoo.com)
Samra, Jagtar S. (via email)
10415 Edgebrook Way
Northridge, CA 91326-3952

San Bernardino Co Barstow - Daggett Airport
268 W. Hospitality Lane, Suite 302
San Bernardino, CA 92415-0831

Attn: Jared Beyeler
(waterquality@sdd.sbcounty.gov)
San Bernardino County - High Desert
Detention Center (via email)
222 W. Hospitality Lane, 2nd Floor - SDW
San Bernardino, CA 92415-0415

Attn: Trevor Leja
(trevor.leja@sdd.sbcounty.gov)
San Bernardino County Service Area 29 (via
email)
222 W. Hospitality Lane, 2nd Floor (Spec
San Bernardino, CA 92415-0450

Attn: Jared Beyeler
(ssamaras@sdd.sbcounty.gov;
jbeyeler@sdd.sbcounty.gov;
waterquality@sdd.sbcounty.gov)
San Bernardino County Service Area 42 (via
email)
222 W. Hospitality Lane, 2nd Floor - SDW
San Bernardino, CA 92415-0450

Attn: Jared Beyeler
(ssamaras@sdd.sbcounty.gov;
jbeyeler@sdd.sbcounty.gov;
waterquality@sdd.sbcounty.gov)
San Bernardino County Service Area 64 (via
email)
222 W. Hospitality Lane, 2nd Floor - SDW
San Bernardino, CA 92415-0450

Attn: Jared Beyeler
(ssamaras@sdd.sbcounty.gov;
jbeyeler@sdd.sbcounty.gov;
waterquality@sdd.sbcounty.gov)
San Bernardino County Service Area 70J (via
email)
222 W. Hospitality Lane, 2nd Floor - SDW
San Bernardino, CA 92415-0450

Attn: Michelle Scray (mcsctray@gmail.com)
Scray, Michelle A. Trust (via email)
16869 State Highway 173
Hesperia, CA 92345-9381

Attn: Rod Sexton
Sexton, Rodney A. and Sexton, Derek R.
P.O. Box 155
Rim Forest, CA 92378-

Attn: Joseph Tapia
Sheep Creek Water Company
P. O. Box 291820
Phelan, CA 92329-1820

Mojave Basin Area Watermaster Service List as of September 06, 2024

Sheng, Jen
5349 S Sir Richard Dr
Las Vegas, NV 89110-0100

(gloriasheppard14@gmail.com)
Sheppard, Thomas and Gloria (via email)
33571 Fremont Road
Newberry Springs, CA 92365-9520

Short, Jerome E.
P. O. Box 1104
Barstow, CA 92312-1104

Attn: Carlos Banuelos
(maint@silverlakesassociation.com;
fibarra@silverlakesassociation.com)
Silver Lakes Association (via email)
P. O. Box 179
Helendale, CA 92342-0179

Attn: Nepal Singh (NepalSingh@yahoo.com)
Singh, et al. (via email)
4972 Yearling Avenue
Irvine, CA 92604-2956

Attn: Denise Smith
Smith, Denise dba Amerequine Beauty, Inc
P. O. Box 188
Newberry Springs, CA 92365-0188

Smith, Porter and Anita
8443 Torrell Way
San Diego, CA 92126-1254

Attn: Steve Kim (stevekim1026@gmail.com)
Snowball Development, Inc. (via email)
P. O. Box 2926
Victorville, CA 92393-2926

Attn: Chan Kyun Son
Son's Ranch
P. O. Box 1767
Lucerne Valley, CA 92356

Attn: Erika Clement
(Shannon.Oldenburger@SCE.com;
erika.clement@sce.com)
Southern California Edison Company (via
email)
2 Innovation Way, 2nd Floor
Pomona, CA 91768-2560

Attn: Maria de Lara Cruz
(maria.delaracruz@mineralstech.com)
Specialty Minerals, Inc. (via email)
P. O. Box 558
Lucerne Valley, CA 92356-0558

Sperry, Wesley
P. O. Box 303
Newberry Springs, CA 92365-0303

Spillman, James R. and Nancy J.
12132 Wilshire
Lucerne Valley, CA 92356-8834

Attn: Eric Miller (emiller@svla.com;
alogan@svla.com;)
Spring Valley Lake Association (via email)
SVL Box 7001
Victorville, CA 92395-5107

Attn: Joe Trombino
Spring Valley Lake Country Club
7070 SVL Box
Victorville, CA 92395-5152

Attn: Father Sarapamon
St. Antony Coptic Orthodox Monastery
P. O. Box 100
Barstow, CA 92311-0100

(chiefgs@verizon.net)
Starke, George A. and Jayne E. (via email)
8743 Vivero Street
Rancho Cucamonga, CA 91730-1152

Storm, Randall
51432 130th Street
Byars, OK 74831-7357

Sudmeier, Glenn W.
14253 Highway 138
Hesperia, CA 92345-9422

Attn: Alexandra Lioanag
(sandra@halannagroup.com)
Summit Valley Ranch, LLC (via email)
220 Montgomery Street, Suite PH-10
San Francisco, CA 94104-3433

Attn: Alex Vienna
Sundown Lakes, Inc.
P. O. Box 364
Newberry Springs, CA 92365-0364

Attn: Stephen H. Douglas
(sdouglas@centaurusenergy.com;
mdoublesin@centcap.net;
cre.notices@clenera.com)
Sunray Land Company, LLC (via email)
1717 West Loop South, Suite 1800
Houston, TX 77027-3049

Attn: Venny Vasquez (lbaroldi@synagro.com)
Synagro-WWT, Inc. (dba Nursury Products,
LLC) (via email)
P. O. Box 1439
Helendale, CA 92342-

Attn: Russell Szykowski
Szykowski, Ruth J.
46750 Riverside Rd.
Newberry Springs, CA 92365-9738

Attn: Bill and Elizabeth Tallakson
(billtallakson@sbcglobal.net)
Tallakson Family Revocable Trust (via email)
11100 Alto Drive
Oak View, CA 93022-9535

Tapie, Raymond L.
73270 Desert Greens Dr N
Palm Desert, CA 92260-1206

Taylor, Sharon L.
14141 State Hwy 138
Hesperia, CA 92345-9339

Mojave Basin Area Watermaster Service List as of September 06, 2024

(jerryteisan@gmail.com)
Teisan, Jerry (via email)
P. O. Box 2089
Befair, WA 98528-2089

Attn: Daryl or Lucinda Lazenby
Thayer, Sharon
P. O. Box 845
Luceren Valley, CA 92356-

Attn: Stephen Thomas
Thomas, Stephen and Lori
4890 Topanga Canyon Bl.
Woodland Hills, CA 91364-4229

Attn: Lynnette L. Thompson
Thompson Living Trust, James A. and Sula B.
22815 Del Oro Road
Apple Valley, CA 92308

Attn: Rodger Thompson
Thompson Living Trust, R.L. and R.A.
9141 Deep Creek Road
Apple Valley, CA 92308-8351

Thrasher, Gary
14024 Sunflower Lane
Oro Grande, CA 92368-9617

Attn: Doug Heinrichs
Thunderbird County Water District
P. O. Box 1105
Apple Valley, CA 92307-1105

Attn: Jim Hoover
Triple H Partnership
35870 Fir Ave
Yucaipa, CA 92399-9635

Attn: Mike Troeger (mjtroeger@yahoo.com)
Troeger Family Trust, Richard H. (via email)
P. O. Box 24
Wrightwood, CA 92397

Turner, Terry
726 Arthur Lane
Santa Maria, CA, CA 93455-7403

Attn: Aurelio Ibarra (aibarra@up.com;
powen@up.com)
Union Pacific Railroad Company (via email)
HC1 Box 33
Kelso, CA 92309-

(druppall@aicdent.com)
Uppal, Gagan (via email)
220 S Owens Drive
Anaheim, CA 92808-1327

(gagevaage23@gmail.com)
Vaage, Gage V. (via email)
47150 Black Butte Road
Newberry Springs, CA 92365-9698

Vaca, Andy and Teresita S.
5550 Avenue Juan Bautista
Riverside, CA 92509-5613

Attn: Dean Van Bastelaar
Van Bastelaar, Alphonse
45475 Martin Road
Newberry Springs, CA 92365-9625

Attn: Glen and Jennifer Van Dam
(gvandam@verizon.net)
Van Dam Family Trust, Glen and Jennifer
(via email)
3190 Cottonwood Avenue
San Jacinto, CA 92582-4741

Attn: Jacob Bootsma
Van Leeuwen Trust, John A. and Ietie
44128 Silver Valley Road
Newberry Springs, CA 92365-9588

Attn: John Driscoll
Vernola Trust, Pat and Mary Ann
P. O. Box 2190
Temecula, CA 92593-2190

Attn: John Nahlen
Victor Valley Community College District
18422 Bear Valley Road, Bldg 10
Victorville, CA 92395-5850

Attn: Jade Kiphen
Victor Valley Memorial Park
17150 C Street
Victorville, CA 92395-3330

Attn: Arnold Villarreal
(avillarreal@victorvilleca.gov;
ccun@victorvilleca.gov)
Victorville Water District, ID#1 (via email)
P. O. Box 5001
Victorville, CA 92393-5001

Attn: Arnold Villarreal
(avillarreal@victorvilleca.gov;
kmetzler@victorvilleca.gov;
snawaz@victorvilleca.gov)
Victorville Water District, ID#1 (via email)
P. O. Box 5001
Victorville, CA 92393-5001

Attn: Arnold Villarreal
(sashton@victorvilleca.gov;
avillarreal@victorvilleca.gov;
dmathews@victorvilleca.gov)
Victorville Water District, ID#2 (via email)
PO Box 5001
Victorville, CA 92393-5001

Vogler, Albert H.
17612 Danbury Ave.
Hesperia, CA 92345-7073

Attn: Joan Wagner
Wagner Living Trust
22530 Calvert Street
Woodland Hills, CA 91367-1704

Attn: Christian Joseph Wakula
Wakula Family Trust
11741 Ardis Drive
Garden Grove, CA 92841-2423

(Jlow3367@gmail.com)
Wang, Steven (via email)
2551 Paljay Avenue
Rosemead, CA 91770-3204

Mojave Basin Area Watermaster Service List as of September 06, 2024

Ward, Raymond
P. O. Box 358
Newberry Springs, CA 92365-0358

Weems, Lizzie
9157 Veranda Court
Las Vegas, NV 89149-0480

Weerasinghe, Maithri N.
P. O. Box 487
Barstow, CA 92312-0487

(andrewwerner11@gmail.com)
Werner, Andrew J. (via email)
1718 N Sierra Bonita Ave
Los Angeles, CA 90046-2231

Attn: James Woody
West End Mutual Water Company
P. O. Box 1732
Lucerne Valley, CA 92356

West, Howard and Suzy
9185 Loma Vista Road
Apple Valley, CA 92308-0557

West, Jimmie E.
P. O. Box 98
Oro Grande, CA 92368-0098

Attn: Nick Gatti ()
Western Development and Storage, LLC (via email)
5701 Truxtun Avenue, Ste. 201
Bakersfield, CA 93309-0402

Attn: Chung Cho Gong
Western Horizon Associates, Inc.
P. O. Box 397
Five Points, CA 93624-0397

Attn: Genaro Zapata
Westland Industries, Inc.
520 W. Willow St.
Long Beach, CA 90806-2800

Attn: Thomas G. Ferruzzo
(tferruzzo@ferruzzo.com)
Wet Set, Inc. (via email)
44505 Silver Valley Road, Lot #05
Newberry Springs, CA 92365-9565

Wiener, Melvin and Mariam S.
1626 N. Wilcox Avenue
Los Angeles, CA 90028-6234

Attn: Manoucher Sarbaz
Wilshire Road Partners
9903 Santa Monica Blvd., PMB #541
Beverly Hills, CA 90212-1671

Attn: Connie Tapie
(praisethelord77777@yahoo.com)
Withey, Connie (via email)
P. O. Box 3513
Victorville, CA 92393-3513

Witte, E. Daniel and Marcia
31911 Martino Drive
Daggett, CA 92327-9752

Attn: Mark J. Cluff
WLSR, Inc.
3507 N 307th Drive
Buckeye, AZ 85396-6746

Attn: David A. Worsley
Worsley, Joseph A. and Revae
P. O. Box 422
Newberry Springs, CA 92365-0422

(thechelseaco@yahoo.com)
Yang, Zilan (via email)
428 S. Atlantic Blvd #205
Monterey Park, CA 91754-3228

Attn: Christine M. Carson, Esq.
(ccarson@awattorneys.com)
Aleshire & Wynder, LLP (via email)
3880 Lemon Street
Suite 520
Riverside, CA 92501-

Attn: Robert Hensley, Esq.
(rhensley@awattorneys.com)
Aleshire & Wynder, LLP (via email)
3880 Lemon Street
Suite 520
Riverside, CA 92501-

Attn: Pam Lee, Esq. (plee@awattorneys.com)
Aleshire & Wynder, LLP (via email)
3880 Lemon Street
Suite 520
Riverside, CA 92501-

Attn: Alison Paap (apaap@agloan.com)
American AgCredit (via email)
42429 Winchester Road
Temecula, CA 92590-2504

Attn: Wesley A. Miliband, Esq.
(wes.miliband@aalr.com)
Atkinson, Andelson, Loya, Ruud & Romo
(via email)
2151 River Plaza Drive
Suite 300
Sacramento, CA 95833-

Attn: W.W. Miller, Esq. (bmiller@aalr.com)
Atkinson, Andelson, Loya-Ruud & Romo (via email)
3612 Mission Inn Avenue, Upper Level
Riverside, CA 92501

Attn: Christopher L. Campbell, Esq.
Baker, Manock & Jensen
5260 N. Palm Avenue, 4th Floor
Fresno, CA 93704-2209

Attn: Aloson Toivola, Esq.
(alison.toivola@bbkllaw.com)
Best, Best & Krieger LLP (via email)
300 South Grand Avenue
25th Floor
Los Angeles, CA 90071

Attn: Eric L. Garner, Esq.
(eric.garner@bbkllaw.com)
Best, Best & Krieger LLP (via email)
3750 University Avenue
3rd Floor
Riverside, CA 92502-1028

Mojave Basin Area Watermaster Service List as of September 06, 2024

Attn: Piero C. Dallarda, Esq.
(piero.dallarda@bbklaw.com)
Best, Best & Krieger LLP (via email)
P.O. Box 1028
Riverside, CA 92502-

Attn: Christopher Pisano, Esq.
(christopher.pisano@bbklaw.com)
Best, Best & Krieger LLP (via email)
300 South Grand Avenue
25th Floor
Los Angeles, CA 90071

Attn: Stephanie Osler Hastings, Esq.
(SHastings@bhfs.com; mcarlson@bhfs.com)
Brownstein Hyatt Farber Schreck, LLP (via email)
1021 Anacapa Street, 2nd Floor
Santa Barbara, CA 93101-2102

Attn: William J. Brunick, Esq.
(wbrunick@bmklawplc.com)
Brunick, McElhaney & Kennedy PLC (via email)
1839 Commercenter West
P.O. Box 13130
San Bernardino, CA 92423-3130

Attn: Terry Caldwell, Esq.
Caldwell & Kennedy
15476 West Sand Street
Victorville, CA 92392

Attn: Stephen Puccini
(stephen.puccini@wildlife.ca.gov)
California Department of Fish and Wildlife
(via email)

Attn: Alexander Devorkin, Esq.
California Department of Transportation
100 South Main Street, Suite 1300
Los Angeles, CA 90012-3702

Attn: Nancy McDonough
California Farm Bureau Federation
2300 River Plaza Drive
Sacramento, CA 95833

Attn: Jeffery L. Caufield, Esq.
(Jeff@caufieldjames.com)
Caufield & James, LLP (via email)
2851 Camino Del Rio South, Suite 410
San Diego, CA 92108-

Attn: Andrew L. Jared, Esq.
(ajared@chwlaw.us)
Colantuono, Highsmith & Whatley, PC (via email)
790 E. Colorado Blvd., Suite 850
Pasadena, CA 91101-2109

Attn: Matthew T. Summers, Esq.
(msummers@chwlaw.us)
Colantuono, Highsmith & Whatley, PC (via email)
790 E. Colorado Blvd., Suite 850
Pasadena, CA 91101-2109

Attn: Maria Insixiengmay
(Maria.Insxiengmay@cc.sbcounty.gov)
County of San Bernardino, County Counsel
(via email)
385 N. Arrowhead Avenue, 4th Floor
San Bernardino, CA 92415-0140

Attn: Robert E. Dougherty, Esq.
Covington & Crowe
1131 West 6th Street
Suite 300
Ontario, CA 91762

Attn: Ed Dygert, Esq.
Cox, Castle & Nicholson
3121 Michelson Drive, Ste. 200
Irvine, CA 92612-

Attn: Noah GoldenKrasner, Dep
(Noah.GoldenKrasner@doj.ca.gov)
Department of Justice (via email)
300 S. Spring Street, Suite 1700
Los Angeles, CA 90013

Attn: Marilyn Levin, Dep
(Marilyn.Levin@doj.ca.gov)
Department of Justice (via email)
300 S. Spring Street, Suite 1702
Los Angeles, CA 90013

Attn: Diana Carloni, Esq.
(diana@carlonilaw.com)
Diana J. Carloni (via email)
21001 N. Tatum Blvd.
Suite 1630-455
Phoenix, AZ 85050-

Attn: James S. Heiser, Esq.
Ducommun, Inc.
23301 S. Wilmington Avenue
Carson, CA 90745

Attn: Michele Hinton, Ms.
(mhinton@fennemorelaw.com)
Fennemore LLP (via email)
8080 N Palm Ave, Third Floor
Fresno, CA 93711-

Attn: Kelly Ridenour, Ms.
(kridenour@fennemorelaw.com)
Fennemore LLP (via email)
550 East Hospitality Lane
Suite 350
San Bernardino, CA 92408-4206

Attn: Marlene Allen Murray, Esq.
(mallenmurray@fennemorelaw.com)
Fennemore LLP (via email)
550 East Hospitality Lane
Suite 350
San Bernardino, CA 92408-4206

Attn: Derek Hoffman, Esq.
(dhoffman@fennemorelaw.com)
Fennemore LLP (via email)
550 East Hospitality Lane
Suite 350
San Bernardino, CA 92408-4206

Attn: Thomas G. Ferruzzo, Esq.
(tferruzzo@ferruzzo.com)
Ferruzzo & Ferruzzo, LLP (via email)
3737 Birch Street, Suite 400
Newport Beach, CA 92660

Attn: Toby Moore, PhD, PG, CHG
(TobyMoore@gswater.com)
Golden State Water Company (via email)
160 W. Via Verde, Suite 100
San Dimas, CA 91773-

Attn: Andre de Bortnowsky, Esq.
(andre@gblawoffices.com)
Green de Bortnowsky, LLP (via email)
30077 Agoura Court, Suite 210
Agoura Hills, CA 91301-2713

Attn: Michelle McCarron, Esq.
(mmccarron@gdblwoffices.com;
andre@gdblwoffices.com)
Green de Bortnowsky, LLP (via email)
30077 Agoura Court, Suite 210
Agoura Hills, CA 91301-2713

Attn: Calvin R. House, Esq.
Gutierrez, Preciado & House
3020 E. Colorado BLVD
Pasadena, CA 91107-3840

Mojave Basin Area Watermaster Service List as of September 06, 2024

Attn: Curtis Ballantyne, Esq.
Hill, Farrer & Burrill
300 S. Grand Avenue, 37th Floor
1 California Plaza
Los Angeles, CA 90071

Attn: Thomas S. Bunn, Esq.
(TomBunn@lagerlof.com)
Lagerlof, Senecal, Gosney & Kruse, LLP (via email)
301 N. Lake Avenue, 10th Floor
Pasadena, CA 91101-5123

Attn: Robert C. Hawkins, Esq.
Law Offices of Robert C. Hawkins
14 Corporate Plaza, Suite 120
Newport, CA 92660

Attn: Adnan Anabtawi
(aanabtawi@mojavewater.org)
Mojave Water Agency (via email)
13846 Conference Center Drive
Apple Valley, CA 92307

Attn: Betsy Brunswick (bmb7@pge.com)
Pacific Gas and Electric Company (via email)
77 Beale Street, B28P
San Francisco, CA 94105-1814

Attn: Todd O. Maiden, Esq.
(TMaiden@ReedSmith.com)
Reed Smith LLP (via email)
101 Second Street
Suite 1800
San Francisco, CA 94105-

Attn: Randall R. Morrow, Esq.
Sempra Energy Law Department
Office of the General Counsel
555 West Fifth Street, Suite 1400
Los Angeles, CA 90013-1011

Attn: Rick Ewaniszyk, Esq.
The Hegner Law Firm
14350 Cive Drive
Suite 270
Victorville, CA 92392

Attn: Michael Turner, Esq.
(mturner@kasdandclaw.com)
Kasdan, LippSmith Weber Turner, LLP (via email)
19900 MacArthur Blvd., Suite 850
Irvine, CA 92612-

Attn: Peter J. Kiel, Esq.
(pkiel@cawaterlaw.com)
Law Office of Peter Kiel PC (via email)
PO Box 422
Petaluma, CA 94953-0422

Attn: Arthur G. Kidman, Esq.
McCormick, Kidman & Behrens
695 Town Center Drive, Suite 400
Costa Mesa, CA 92626-7187

Attn: Frederic A. Fudacz, Esq.
(ffudacz@nossaman.com)
Nossaman LLP (via email)
777 South Figueroa Street, 34th Floor
Los Angeles, CA 90017-

Attn: Joesfina M. Luna, Esq.
(fluna@redwineandsherrill.com)
Redwine and Sherrill (via email)
3890 Eleventh Street
Suite 207
Riverside, CA 92501-

Attn: James L. Markman, Esq.
Richards, Watson & Gershon
1 Civic Center Circle
P.O. Box 1059
Brea, CA 92822-1059

Attn: Shannon Oldenburg, Esq.
(shannon.oldenburg@sce.com)
Southern California Edison Company
Legal Department (via email)
P.O. Box 800
Rosemead, CA 91770

Attn: Agnes Vander Dussen Koetsier
(beppeau@aol.com)
Vander Dussen Trust, Agnes & Edward (via email)
P.O. Box 5338
Blue Jay, CA 92317-

Attn: Mitchell Kaufman, Esq.
(mitch@kmlp.com)
Kaufman McAndrew LLP (via email)
16633 Ventura Blvd., Ste. 500
Encino, CA 91436-1835

Attn: Fred J. Knez, Esq.
Law Offices of Fred J. Knez
6780 Indiana Ave, Ste 150
Riverside, CA 92506-4253

Attn: Jeffrey D Ruesch
(watermaster@mojavewater.org)
Mojave Basin Area Watermaster (via email)
13846 Conference Center Drive
Apple Valley, CA 92307

Attn: Kieth Lemieux
(KLemieux@omlowlaw.com)
Olivarez Madruga Lemieux O'Neill, LLP (via email)
500 South Grand Avenue, 12th Floor
Los Angeles, CA 90071-2609

Attn: Steven B. Abbott, Esq.
(sabbott@redwineandsherrill.com;
fluna@redwineandsherrill.com)
Redwine and Sherrill (via email)
3890 Eleventh Street
Suite 207
Riverside, CA 92501-

Attn: Elizabeth Hanna, Esq.
Rutan & Tucker
P.O. Box 1950
Costa Mesa, CA 92626

Attn: ()
Southern California Gas Company
Transmission Environmental Consultant (via email)

Attn: Robert C. Wagner, P.E.
(rcwagner@wbecorp.com)
Wagner & Bonsignore
Consulting Civil Engineers (via email)
2151 River Plaza Drive, Suite 100
Sacramento, CA 95833-4133